

LIQUID LIQUID EXTRACTION STUDIES
IN A PILOT SCALE AGITATED COLUMN

by

AMAR NATH KHANDELWAL

A thesis submitted to the University
of Aston in Birmingham for the degree
of Doctor of Philosophy

Department of Chemical Engineering,
University of Aston in Birmingham

June 1978

660.28424 KHA

27 JUN 1977 232478

STATE UNIVERSITY OF NEW YORK
SUNY BINGHAMTON

LIBRARY

STATE UNIVERSITY OF NEW YORK
SUNY BINGHAMTON
LIBRARY

May 1978



SUMMARY

LIQUID-LIQUID EXTRACTION STUDIES IN A PILOT SCALE COLUMN

AMAR NATH KHANDELWAL

Ph.D.

1978

A study has been made of the hydrodynamics and mass transfer characteristics of the Rotating Disc Contactor.

The literature relating to this extractor and relevant phenomena, e.g. droplet break-up and coalescence, single drop mass transfer, axial mixing and phase inversion/flooding, has been reviewed.

A 450 mm. diameter, fourteen compartment R.D.C. was designed and operated with the system kerosene-acetone-water over a range of practical rotor speeds. The results were compared with those from a modified, existing 101 mm. diameter R.D.C.

The time to reach steady state varied with operating parameters and was approximately equal to the time taken for a total flow of two and a half times the column volume. Hold-up of dispersed phase varied in an axial as well as a radial direction. Nearly equal drop sizes were generated at equal energy per unit volume in the two columns. Flooding rather than phase inversion defined the limiting capacities with the chosen system in both columns. Mass transfer efficiency was expressed in terms of overall coefficients. Drop size increased with mass transfer from kerosene-acetone (dispersed) to water (continuous) phase in both columns.

Mathematical models were derived to determine -

- (a) Column diameter, and hence geometry, from data obtained on a pilot scale using a similar system, or from data with any system.
- (b) Column height, for large columns from data obtained on a pilot scale.

These models were incorporated into a recommended design procedure.

Key words: Rotating Disc Contactor,
Liquid-liquid extraction.

ACKNOWLEDGEMENTS

The author wishes to thank the following:

Professor G.V. Jeffreys,

for his encouragement and supervision and for providing the facilities for research.

Dr. C.J. Mumford,

for his continual help, supervision and constructive criticism.

The Technical Staff of the Department of Chemical Engineering,
for their assistance in fabricating the equipment and in photographic work.

Miss N.P. Freeman,

for her diligence in typing the thesis.

The Science Research Council,

for financial support during this study.

CONTENTS

	<u>Page No.</u>
1. INTRODUCTION	1
2. LIQUID-LIQUID EXTRACTION EQUIPMENT	6
2.1 Equipment Classification	6
2.2 Selection of Equipment	8
2.3 The Rotating Disc Contactor - Advantages and Applications	14
2.3.1 Advantages of the R.D.C. over Other Extraction Devices	16
2.3.2 Application of R.D.C.	17
3. THE DESIGN AND SCALE-UP OF THE ROTATING DISC CONTACTOR	20
3.1 Fundamentals	20
3.1.1 Flow Patterns in an R.D.C.	22
3.1.2 Power Requirements of the R.D.C.	25
3.1.3 Internal Geometry	27
3.2 Hydrodynamics	28
3.2.1 Hold-up	28
3.2.1.1 Hold-up Profile	34
3.2.2 Limiting Capacity of the R.D.C.	39
3.3 Column Diameter	44
3.3.1 Calculation on the Basis of Physical Properties	45
3.3.2 Determination by Scale-up of Pilot Plant Data	47
3.4 Column Height	47
3.4.1 Height of the Coalescence Section	49

	<u>Page No</u>
3.4.2 Height of the Bottom Section (h_s)	49
3.4.3 Effective Extractor Height	50
3.5 Scale Up of Rotating Disc Contactor	55
4. DROPLET PHENOMENA	60
4.1 Drop Formation	61
4.1.1 Surface Area of the Drop During Formation	70
4.2 Droplet Break-up	73
4.3 Drop Size Distribution	84
4.4 Coalescence Processes	94
4.4.1 Coalescence Fundamentals	95
4.4.2 Interdrop Coalescence in the Agitated Zone	95
4.4.3 Flocculation and Coalescence in the Phase Separation Zone	99
5. MASS TRANSFER FUNDAMENTALS	104
5.1 Mass Transfer During Drop Formation	104
5.1.1 Mass Transfer at Different Rates of Formation	109
5.2 Mass Transfer During Droplet Release	111
5.3 Mass Transfer Within Droplets	111
5.3.1 The Rigid Drop	113
5.3.2 The Non-rigid Drop	114
5.3.2.1 Oscillating Drops	117
5.4 Mass Transfer in the Continuous Phase	120
5.4.1 From and to 'Rigid' Drops	121
5.4.2 From and to 'Non-rigid' Drops	121

	<u>Page No.</u>
5.5 Mass Transfer During Coalescence	125
5.6 Overall Coefficient of Mass Transfer	127
5.7 Miscellaneous Phenomena	128
5.7.1 Mass Transfer and Interfacial Instability	128
5.7.2 Effect of Surface Active Agent	133
5.7.3 Wall Effects	134
5.8 Applicability of Single Drop Mass Transfer Models for the Design of Agitated Columns	136
6. AXIAL MIXING	139
6.1 Models Describing the Performance of an Extraction Column	140
6.1.1 Plug Flow Model	140
6.1.2 Stage Model	144
6.1.3 Back-flow Model	147
6.1.4 Diffusion Model	148
6.1.5 Combined Model with Forward Mixing	150
6.2 Application to R.D.C.	151
7. THE ROTATING DISC CONTACTOR -OPERATING EXPERIENCE	165
7.1 Wetting Effects	165
7.2 Phase Inversion	171
7.3 Limitation of R.D.C. Scale-up Method	177
8. DESIGN OF EXPERIMENTS	180
8.1 Objectives	180
8.2 Design of Equipment	180
8.2.1 450 mm diameter R.D.C. column	185

	<u>Page No.</u>
8.2.1.1. Ancilliary Equipment	191
8.2.2 101 mm diameter small R.D.C. column	194
8.3 Selection of Liquid-liquid System	198
8.4 Experimental Techniques	199
8.4.1 Cleaning Procedure	199
8.4.2 System Purity Checks	199
8.4.3 Measurement and Calibration	200
Techniques	
8.4.4 Determination of Equilibrium	202
Distribution Diagrams	
8.4.5 Photography and Associated	203
Techniques	
8.4.6 Operating Procedure and Ranges	204
9. EXPERIMENTAL PROCEDURE AND RESULTS	206
9.1 Non-mass Transfer Studies	206
9.1.1 Flooding Phenomena	206
9.1.2 Drop Size Distributions	208
9.1.3 Hold-up	214
9.1.3.1 Axial hold-up in the Two	220
Columns	
9.1.3.2 Radial Hold-up in the 450	224
mm. diameter column	
9.1.3.3 Average hold-up Studies in	230
the Two Columns	
9.1.4 Drop Size Produced at the Distributor	231
9.2 Mass Transfer Studies	240
9.2.1 Hold-up	240
9.2.2 Interfacial Area Estimation	240

	<u>Page No.</u>
9.2.3 Mass Transfer Experiments	241
9.2.3.1 Procedure	247
9.2.3.2 Time to Reach Steady State	248
9.2.3.3 Results	250
10. MATHEMATICAL MODELS	253
10.1 Scale-up of Column Diameter	253
10.1.1 Special Case for Identical Systems for Two Different Scales of Operation	253
10.1.2 Scale up of Column Diameter - General Case - Dissimilar Systems	263
10.2 Scale-up of Column Height	267
10.3 Verification of Column Diameter Model	272
10.3.1 Special Case - Identical Systems	272
10.3.2 Tentative Verification of General Case - Dissimilar Systems	274
11. DISCUSSION OF RESULTS	280
11.1 Non-mass Transfer Studies	280
11.1.1 Hold-up	280
11.1.2 Flooding	285
11.1.3 Drop Size	289
11.2 Mass Transfer Studies	294
11.2.1 Hold-up	294
11.2.2 Drop Size	295
11.2.3 Mass Transfer Calculation	296
12. CONCLUSIONS	298
12.1 General Conclusions	298
12.2 Recommended Design Procedure	303

	<u>Page No.</u>
12.2.1 Column Diameter	304
12.2.2 Internal Geometry	305
12.2.3 Design Procedure for the Distributor	305
12.2.4 Column Height	306
Recommendations for the Future Work	311
Appendices	314
Nomenclature	322
References	339

1. INTRODUCTION

Liquid-liquid extraction involves the separation of a liquid mixture by means of a solvent in which one or more of the components is preferentially soluble. The process has been used increasingly for separations because of the rapid world-wide development of the chemical industry, and the increasing importance of petrochemical, wet metallurgy and synthetic fibre processes.

Extraction has been used in the working up of coal tar liquors, and in recent years separation of hydrocarbons in the petroleum industry (1). The separation of aromatics from paraffinic and naphthenic hydrocarbons by use of liquid sulphur dioxide in the Edeleanu process represents one example (2). It is also widely used in the purification of products in the organic and inorganic chemical industries (3).

Liquid-liquid extraction is often used to separate a liquid mixture when it is impracticable, or inconvenient, to obtain the desired components by distillation. Normally distillation is the most efficient method of separating a mixture into its constituents, but extraction may be preferred under the following circumstances:

- (i) When valuable components would be destroyed, or damaged, by the temperature required for separation by distillation;

- (ii) When the required component is present in the feed liquor in very small quantities;
- (iii) When the feed is non-volatile;
- (iv) When a large number of constituents in the feed have similar volatilities or form azeotropes; and/or
- (v) When one component only, of intermediate volatility, is required from a mixture composed of a very large number of components.

Whilst distillation exploits differences in the volatilities of the components, in extraction use is made of differences in their solubilities in a selected solvent. Following extraction it is necessary to recover the solute and solvent and this often entails fractional distillation. For example the recovery of acetic acid by extraction with a solvent, such as ethyl acetate, is followed by distillation of the extract obtained. This two-stage process offers a considerable saving in energy, compared with direct distillation of a very weak acetic acid.

Any extraction process involves:

- (a) Bringing the solvent and solution into intimate contact;
- (b) Separation of the two resulting phases; and
- (c) Removal and recovery of solute and solvent.

A wide variety of equipment can be used to carry out

steps (a) and (b) in either a continuous or stagewise manner. The equipment, their applications and advantages are discussed fully in Chapter 2.

In order to provide intimate contact between the phases in all practical extractors one phase is dispersed as droplets. The rate of solute transfer N , can then be expressed as the product of an overall mass transfer coefficient K , the interfacial area A , and the concentration driving force ΔC ,

$$N = KA \Delta C \quad (1.1)$$

The overall coefficient K is made up of a series of resistances to diffusion, inside the drop, outside the drop, and at the interface. Neglecting the latter,

$$\frac{1}{K} = \frac{1}{k_d} + \frac{1}{mk_c} \quad (1.2)$$

where m is the distribution coefficient. To maximise the rate of mass transfer in equation 1.1, an attempt is generally made to maximise A . The total interfacial area depends on the drop size and dispersed phase hold up x , in the contactor. Assuming that the drops are spherical and their diameter can be represented by a mean value d_{vs} ,

$$A = \frac{6x}{d_{vs}} \quad (1.3)$$

where x is the dispersed phase hold-up.

The resistance to mass transfer inside the drop

depends on the motion of the fluid particles and widely different magnitudes of resistance have been reported (4, 5, 6), dependent on whether the fluid is stagnant circulating or oscillating. The different coefficients for each mode of transfer are reviewed in Chapter 5.

In recent years agitated columns involving internal pulsing or rotary agitation, giving rise to increased turbulence, have found wide application. Generally they offer the advantage of flexibility, high efficiency and reasonable volumetric capacity. The most common is the Rotating Disc Contactor, which was invented by Reman in 1951. Design is traditionally from data obtained on a small scale, with the efficiency and capacity measured in terms of heights of a transfer unit and flooding flow rates respectively. However, there are several limitations in this method. For example, the efficiency of a column decreases with the increase in column diameter due to increased axial mixing. Wall effects may also be significant in small columns, because droplet break up, coalescence and flow in an unrestricted continuous phase differ from those in the vicinity of the wall. Literature pertaining to the R.D.C. is reviewed in chapter 3; axial mixing effects are described in Chapter 6, and wall effects in Chapter 5.

The design of industrial scale R.D.C.s has been the subject of many studies (7, 8, 9, 10). However, the

principles are still not well understood. Therefore the present work comprises a study of the factors to be considered in the scale up of the R.D.C. from pilot plant data. Consideration is also given to phase inversion phenomena, which has recently been used to define limiting volumetric capacity with certain systems. The main objective is to provide a reliable method for the design of the R.D.C. or other industrial agitated columns, from data obtained on a small scale.

2. LIQUID-LIQUID EXTRACTION EQUIPMENT

2.1 Equipment Classification

Liquid-liquid extraction operations may be performed in either:

- (a) Equipment in which the liquids are mixed, extracted and separated in discrete stages. This class includes the mixer settler range of equipment and also perforated plate columns. Or
- (b) Equipment in which continuous counter-current contact is established between the immiscible phases to give the equivalent of any desired number of stages. These may be categorised as,
 - A. Gravity Operated Extractors
 - (1) Non-mechanical dispersion
 - (a) Spray column
 - (b) Baffle plate column
 - (c) Packed columns.
 - (2) Mechanically Agitated Columns
 - (a) Pulsed columns
 - (b) Rotary agitated columns.
 - B. Centrifugal Extractors.

Recently equipment has been classified on the basis of energy input as in Fig. 2.1 (11).

A complete description of all the continuous counter

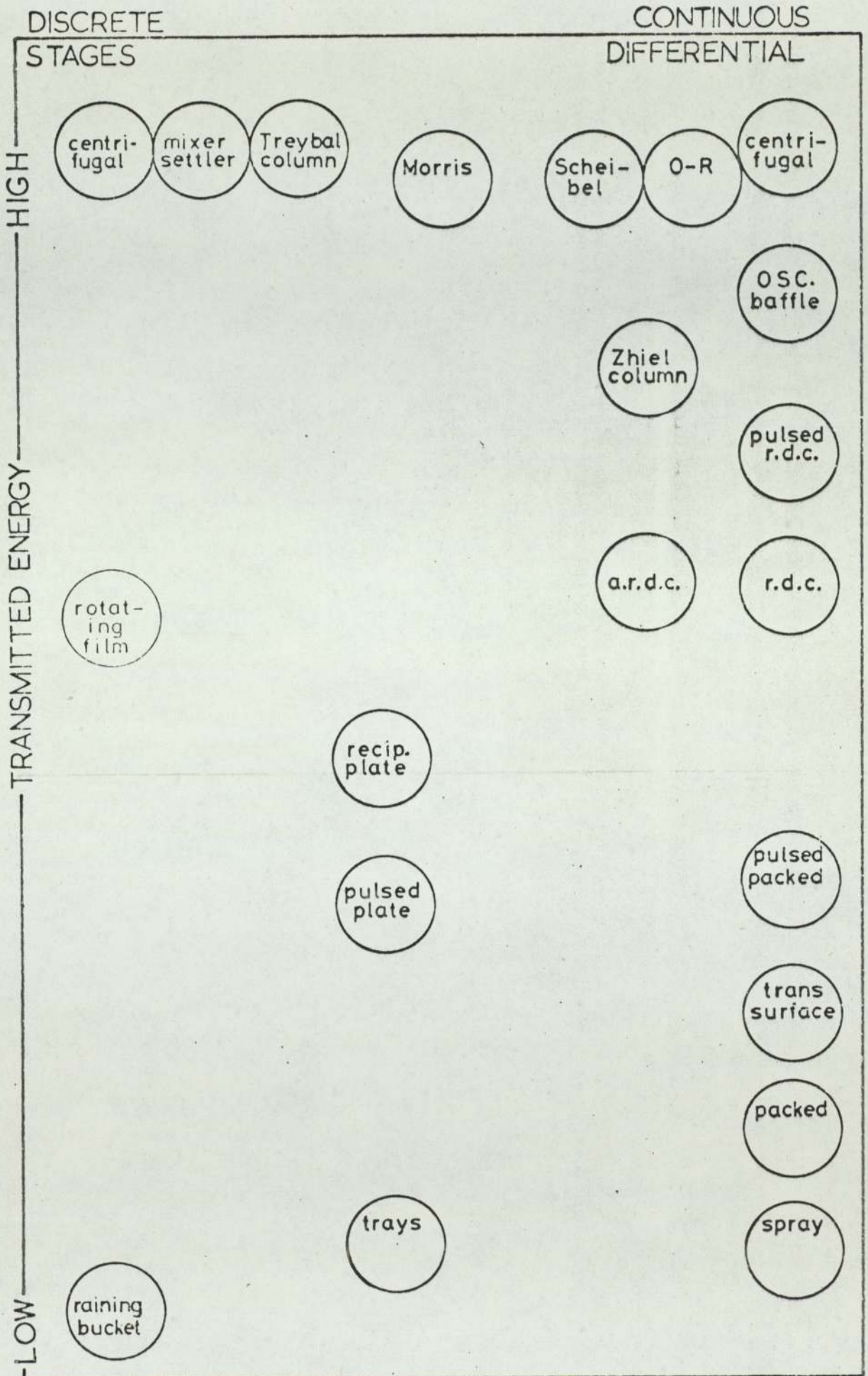


Fig. 2.1 CLASSIFICATION OF INDUSTRIAL CONTACTORS ON THE BASIS OF ENERGY INPUT.

current extractors shown in Fig. 2.1. is outside the scope of this work. However, a summary of the agitated column designs is given in Table 2.1.

2.2 Selection of Equipment

The choice of an extractor for any particular application is largely based on experience. Continuous contactors are generally preferable to mixer settlers when large throughputs are to be handled since they offer economies in agitation and power equipment cost, floor space and solvent inventory. They operate with relatively small amounts of hold up of raffinate and extract. This is important when processing radio active, flammable, expensive or low stability materials. In extraction processes it is necessary as a final step, or in multi-contact stagewise equipment, at intermediate steps, to separate the two phases. Rapid coalescence is desirable otherwise an excessive residence time is required or some of the continuous phase will be removed with the 'bulk' dispersed phase, resulting in reduced efficiency, capacity and loss of solvent. Hence the contactor which gives the most rapid solute transfer is not necessarily the most economic.

Continuous columns without mechanical agitation are unsuitable for use with systems of high interfacial tension since adequate dispersion cannot be achieved throughout the continuous phase. Mixer settlers are commonly used where only a few contact stages are required. They can handle

TABLE 2.1

CONTINUOUS DIFFERENTIAL CONTACTORS

CONTACTOR	TYPE	COMMENT
<p>1. R.D.C. (12)</p>	<p>Axially located discs driven in compartments separated by stator rings by a central shaft.</p>	<p>Operation reasonably flexible; efficiency not much affected by phase flow ratio; H.E.T.S. is remarkably low, around 20 per cent of that for a simple packed tower. Hydrodynamics and mass transfer characteristics are partially known.</p>
<p>2. A.R.D.C. (13, 14)</p>	<p>Similar to the R.D.C. except that the rotor is off-set from the column axis; separation of phases takes place in a shielded transfer section.</p>	<p>Mixing and separation zones claimed to reduce backmixing; but phase entrainment does occur in settling zone reducing overall efficiency (15). No special advantages over R.D.C.</p>
<p>3. Oldshue Rushton (16)</p>	<p>Vertical column divided into compartments by horizontal stator rings with vertical baffles in each compartment. Turbine in each compartment driven by a central shaft.</p>	<p>Coalescence-redispersion is predominant. Stage efficiencies obtained by Oldshue and Rushton varied from 40 to 90%. H.E.T.S. was nearly half that of a simple packed tower of same diameter.</p>
<p>4. Ziel Extractor (17)</p>	<p>Vertical column terminating at top and bottom in large vessels to assist settling. The stirring mechanism consists of a shaft fitted with a number of star-shaped impellers. Vertical, reciprocal, as well as rotary motion, is imposed on the impellers for effective mixing.</p>	<p>Theoretical efficiencies claimed to have been attained in the manufacture of phenol formaldehyde resin (17). No mass transfer data is available.</p>

Table 2.1 (continued)

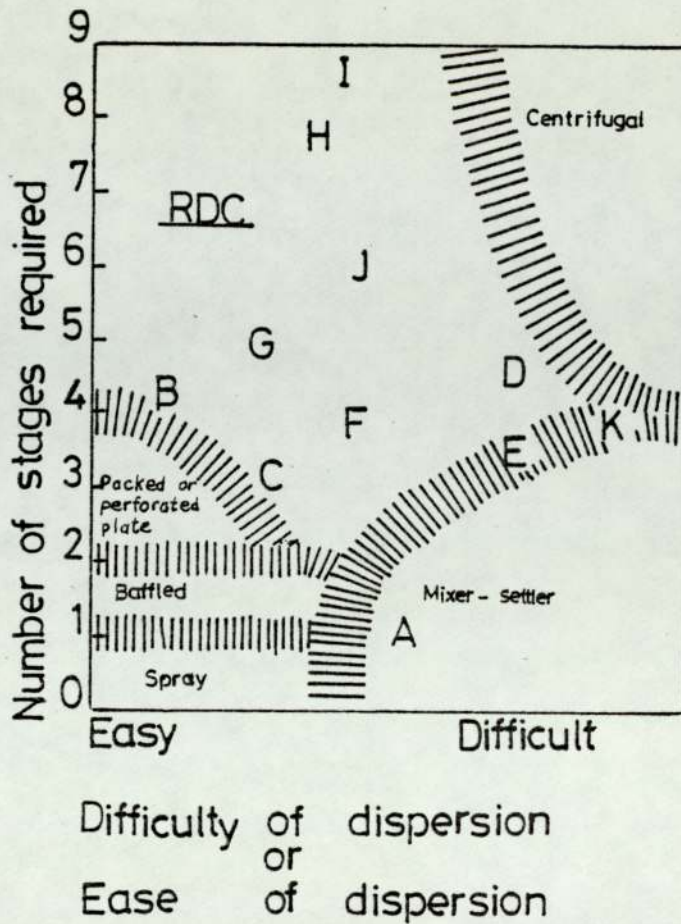
CONTACTOR	TYPE	COMMENT
<p>5. Scheibel Column (18)</p>	<p>Consists of alternate fully-baffled mixing sections and packed sections. Agitation is provided by centrally located impellers.</p>	<p>Coalescence-redispersion is predominant. Mass transfer coefficient is related by,</p> $Ka = C \left(\frac{\Delta\rho}{\sigma}\right)^{1.5}.$ <p>Capacity is limited by the permissible flow rate through the packing.</p>
<p>6. Khuni Extractor (19)</p>	<p>Incorporates the principles of R.D.C., Oldshue Rushton and sieve plate columns. Divided into compartments by plates perforated only at the centre so that flow from one compartment to the next is directed towards the agitator. Each compartment has four vertical baffles. Impeller agitator is provided. End sections are large for effective settling.</p>	<p>Published mass transfer data are limited. Capacity and scale-up are expressed by,</p> $\frac{d}{D} = C.Re^{0.61} . We^{0.6} . Fr^{0.05} .$ <p>The design allows for only low throughputs. Modified designs have found limited application (19).</p>
<p>7. Pulsed Columns (20)</p>	<p>Phases are interdispersed by inducing a pulsating motion either by means of diaphragm pump or a valveless piston. A variety of internal packing or baffles may be used. In one design the plates are pulsed.</p>	<p>Commercial application is limited. Employed in the extraction of metals from radio-active solutions. Power requirements are high. No published information is available for scale-up. Mass transfer data have been reported by various authors. (21, 22).</p>

mixtures of liquids containing suspended solids better than most other contactors, with the exception of certain rotary agitated types (23).

Centrifugal extractors have relatively high capital and operating costs and the number of stages which can be accommodated in a single unit is limited. Nevertheless, they are superior to all other contactors for processes requiring a low hold up, or low contact time, or if there is a low density difference between the phases.

Table 2.2 is a useful 'rule of thumb' method for a preliminary narrowing of the choice between the various types of extractor (24). The ratings are unsuitable - 0, Poor - 1, Fair - 2, Adequate - 3, Good - 4, and outstanding - 5. Not all the features in the table can be equated and, as will be discussed, special process factors often govern extractor selection. Equipment installed and operating costs are of primary importance. On this basis, and dependent on the number of stages for a given application, and the ease of phase dispersion/separation, an extractor selection chart can be drawn for any given feed rate range.

In general the choice of equipment for a given separation should be based on the minimum annual cost for the complete plant, i.e. extractor and ancillary equipment, as well as on operating and solvent loss costs. For a given feed rate range, Todd (24) has developed an extractor



Key to Fig. 2.2

Processes denoted by Letters:

- | | |
|--------------------------------|--------------------------------|
| A : Disulphide Wash | G : Lube oil - furfural |
| B : SO ₂ - Kerosene | H : Phenol recovery |
| C : Propane deasphalting | I : Rare Earths |
| D : Heavy naptha solutizer | J : Chlorohydrin extraction |
| E : Gasoline solutizer | K : CAA - butadiene extraction |
| F : Gas oil extraction | |

FIG. 2.2 RANGE OF APPLICABILITY OF VARIOUS EXTRACTORS

TABLE 2.2
ADVANTAGES AND DISADVANTAGES OF VARIOUS CONTACTORS (24)

Type	Capital cost	Operating and maintenance costs	Efficiency	Total capacity	Flexibility	Volumetric efficiency	Space Vertical	Floor	Ability to handle systems that emulsify
Spray tower	5	5	1	2	2	1	0	5	3
Baffle plate tower	4	5	2	4	2	3	1	5	3
Packed tower	4	5	2	2	2	2	1	5	3
R.D.C.	3	4	4	3	5	4	3	5	3
Pulsed plate column	3	3	4	3	4	4	3	5	1
Mixer-settler	2	2	3	4	3	3	5	1	0
Centrifugal	1	2	5	3	5	5	5	5	5

selection chart, as shown in Fig. 2.2. The governing consideration in the chart is the cost of installation and operation. Many of the extractors will operate outside their allocated regions but at higher cost. The abscissa and the border lines within the chart are necessarily approximate.

Fig. 2.2 also illustrates the theoretical stage dispersibility requirements for several commercially important systems. In general a system becomes more difficult to disperse as interfacial tension and density difference increase. For some systems, the abscissa could be more appropriately 'ease of phase separation' than difficulty of dispersion.

It is evident from Fig. 2.2. that for intermediate dispersable systems, mechanically aided extractors, such as the R.D.C., are appropriate for any process requiring more than two stages.

Recently Logsdail (25) has described the various design considerations and process parameters to be considered in arriving at a decision on solvent extraction equipment. The various factors and choice of extractors are outlined in Table 2.3.

2.3 The Rotating Disc Contactor - Advantages and Applications

As indicated by Table 2.2, 2.3 and Fig. 2.2 the Rotating Disc Contactor possesses several inherent advantages over

TABLE 2.3

FACTORS DETERMINING THE CHOICE OF AN EXTRACTOR (25)

FACTOR	CONTACTOR
1. Number of stages required: (i) few (2-3) stages (ii) (10-20) stages	All types Mixer-settler Cascade, Agitated columns.
2. Volumetric capacity. (i) Intermediate to high (ii) Low	Spray or packed columns R.D.C., Oldshue Rushton column, pulsed, mixer-settlers.
3. Residence time. (i) Short (ii) Long	Centrifugal types. Mixer-settler, differential contactors.
4. Phase ratio. (i) Large (ii) Moderate to low	Mixer-settler Other types.
5. Physical properties (i) Small $\frac{\sigma}{\Delta\rho}$ (ii) Large $\frac{\sigma}{\Delta\rho}$ (iii) High viscosities	Non-agitated contactors Mechanically agitated contactors Mechanically agitated contactors
6. Direction of mass transfer (i) From dispersed to continuous phase. (ii) From continuous to dispersed phase	Mechanically agitated contactor Little information is available.
7. Phase dispersion and Hold-Up. (i) If the phase of the highest throughput is to be dispersed. (ii) If a low hold-up of one phase is required.	Difficulties may be encountered in column contactors due to flooding and phase inversion. Centrifugal contactors
8. Presence of solids in one or both feeds.	Mixer columns e.g. Oldshue Rushton contactor.

other extractors. Hence its use is wide spread in industry. The various advantages of the R.D.C. and its application are outlined in this section.

2.3.1 Advantages of the R.D.C. Over Other Extraction Devices

The main advantages of an R.D.C. may be summarised as (12, 26, 27, 28),

- (i) High efficiency, measured as low H.T.U. or H.E.T.S. values.
- (ii) The ability to maintain this efficiency over a large capacity range. This is practicable because, by variation of rotor speed, the flow conditions in the contactor can be maintained at the optimum for any particular feed conditions.
- (iii) It is cheap and simple to build and operate. Figures quoted (29) for an early R.D.C. give cost at 50% hold-up as 10%, and solvent losses as 30%, of equivalent figures for a comparable mixer settler system. The low hold-up facilitates a rapid change from one product to another and hence the plant is more flexible. The power consumption of an R.D.C. is low and the bearing wear less in comparison with the pumps of an equivalent mixer settler, because lower motor speeds are required.

Reman (27) compared the performance of an R.D.C. with a packed column, for purification of synthetic detergent

and found that a single R.D.C. of 4ft. 9 inches in diameter and a total height of 17 feet could replace two packed columns, each 4 feet in diameter, and 70 feet high for processing 75 tons/day of crude detergent solution. The erected cost of the contactor was also 45% of that for the two packed columns.

Misek (30) compared the R.D.C. against a sieve plate extractor and found that for dephenolisation of 68 cubic metre/hr of ammoniacal water with benzene, use of an R.D.C. saved 74% (81 tons) of material of construction and reduced operating cost by 72%. There were additional savings due to the decrease in cost of pumps, supports and piping foundations. From the same study it was reported that, compared with previous results using a packed column for dephenolisation of 320 cubic metres/hr of water by means of butyl acetate, the R.D.C. gave savings in material of approximately 64% (2×10^5 Sterling pounds) and in operating cost of 2×10^4 Sterling pounds per year.

Unfortunately there are inadequate data in the literature for such comparisons. However, the information provided in Tables 2.2, 2.3 and Figure 2.2 provides guidelines for equipment selection.

2.3.2 Application of R.D.C.

There are numerous examples of the use of the R.D.C. in industry. Some examples of where it has been used

extensively are,

(a) Furfural Extraction of Lube Oil

This is the earliest R.D.C. extraction reported and has been very successful for the past 20 years (29, 31, 32, 33).

(b) Extraction of Oxygen Compounds From Fruit Juices With Alcohol

Although this is the most difficult extraction to carry out in a mixer-settler unit, due to a tendency to emulsify; it can be satisfactorily performed in an R.D.C. using low rotor speeds (33).

(c) Solutizer Extraction of Mercaptans

This can be performed satisfactorily with an R.D.C. (33).

(d) Propane Deasphalting

The use of an R.D.C. not only improves the yield of propane, but also gives better quality asphalt than the earlier mixer settler processes (28, 34, 35).

(e) Phenol Recovery

An R.D.C. gives much improved efficiency over the traditional tray columns (30).

(f) Extraction of Caprolactam

Use of the R.D.C. enhances efficiency, (26). It is also claimed that the R.D.C. is more economic than

centrifugal extractors and superior in flexibility of operation and insensitivity to solid phase impurities.

3. THE DESIGN AND SCALE-UP OF THE ROTATING DISC CONTACTOR

3.1 Fundamentals

In its simplest form, as shown in Fig. 3.1, an R.D.C. consists of a vertical cylindrical column, divided by stator rings into a series of similar equi-sized compartments. Each compartment contains a smooth, rotating disc centrally located between a pair of stators and, supported on a central shaft. The diameter of the rotating disc is always less than the diameter of the opening in the stator discs. This enables the equipment to be assembled easily.

The lighter liquid enters the contactor at the bottom and flows upwards counter-currently to the descending heavier liquid, which enters at the top. In modern designs, (37, 38), one of the liquids is dispersed at either the top or bottom of the column by means of a distributor. This has been found to provide a saving in the effective column height (39). The requisite size of droplets in the effective length of the contactor is maintained by variation of the rotor speed. Interstage settling and re-dispersion is not normally practised. However, some work (37, 40, 41) has been done in this area to improve the efficiency and capacity of the contactor. This is discussed in detail in Chapter 7. Flat rotor discs and stator rings without any protrusion are used, since they create uniform shearing conditions and assist in obtaining a small spread in droplet sizes.

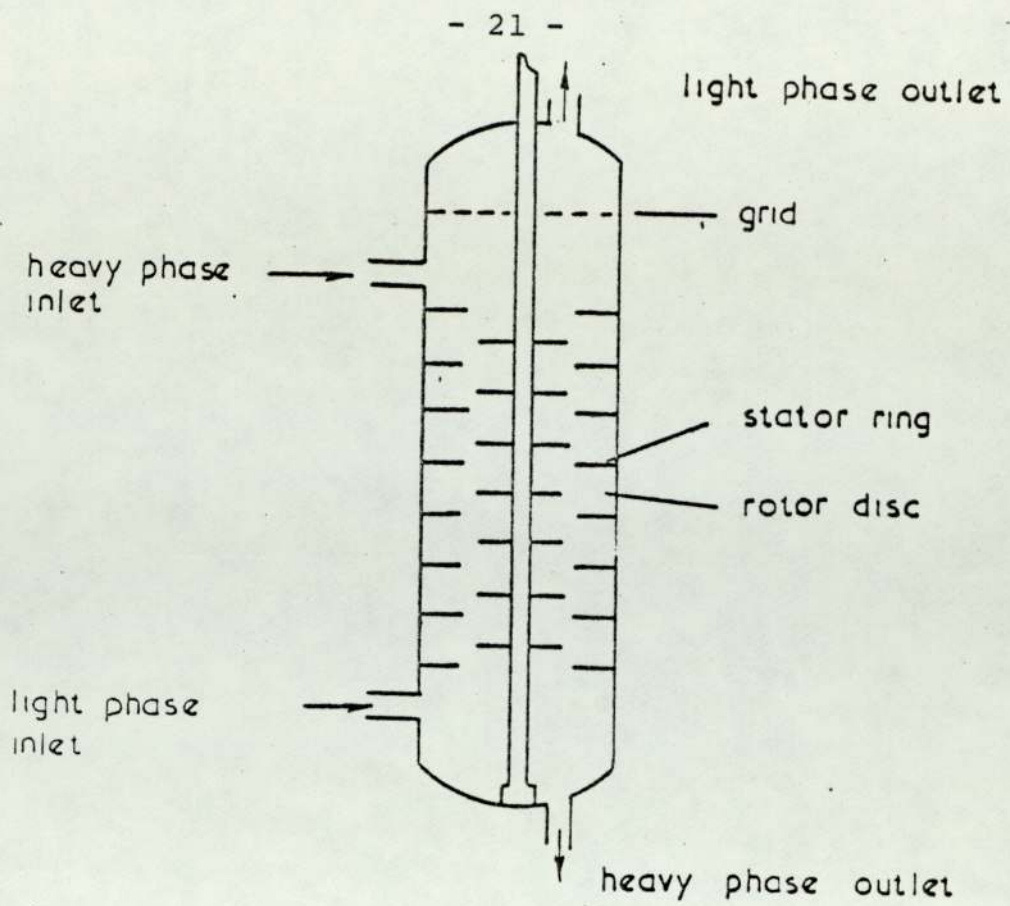


Fig. 3.1. Rotating disc contactor (31)

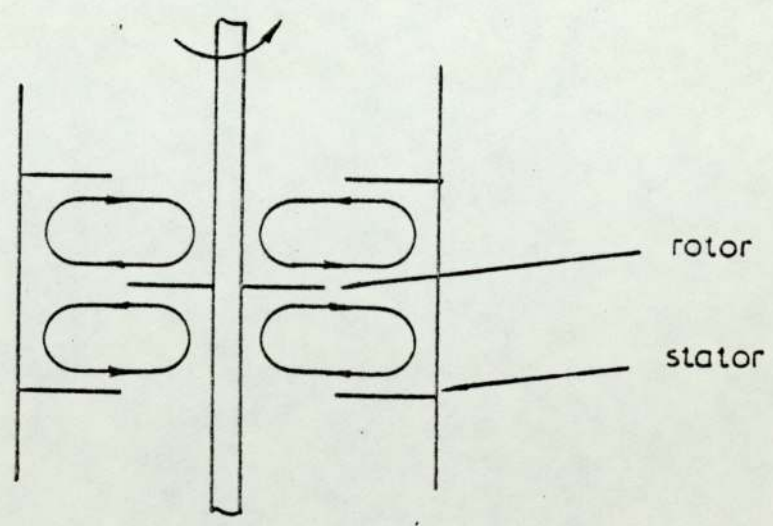


Fig. 3.2. Idealised flow pattern in a rotating disc contactor (12)

3.1.1 Flow Patterns in an R.D.C.

Four forces act on the liquid in an R.D.C., namely,

- (i) A rotation of the entire bulk about the shaft caused by the disc's motion.
- (ii) A slower movement caused by centrifugal force. This moves liquid from the shaft to the wall in the vicinity of the rotors and from the wall back to the shaft in the vicinity of the stators.
- (iii) Buoyancy, causing the light liquid to rise and the denser liquid to fall through each compartment, and
- (iv) Swirl due to tangential inlets. This method of introduction of the phases is now being replaced by injection via a distributor.

Thus in each compartment the interaction of two vortices and bulk axial flow produces complex mixing patterns resembling a rotating ring vortex (12, 7, 33, 27, 42).

In the absence of a distributor, the disperse phase enters the column as a continuous stream, which is rapidly broken down into droplets near the discs. If the drops are small enough they follow the vortex patterns but if they are large, they tend to move axially (9). Reman et al (27), proposed several flow patterns of the type shown in Fig. 3.2. Kung et al (43) later observed that the flow of the droplets followed the two general patterns illustrated

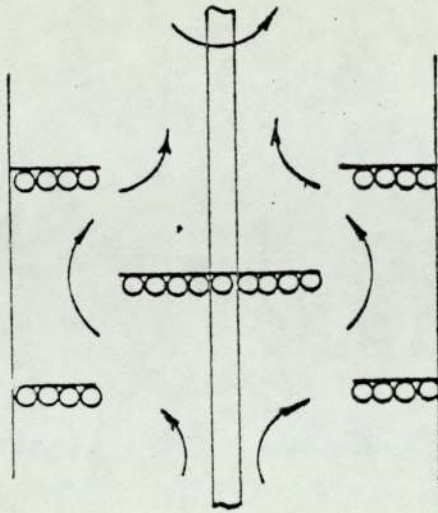


Fig. 3.3. Dispersed phase flow pattern
< 300 ft/min. peripheral speed (43)
R.D.C. system toluene - water

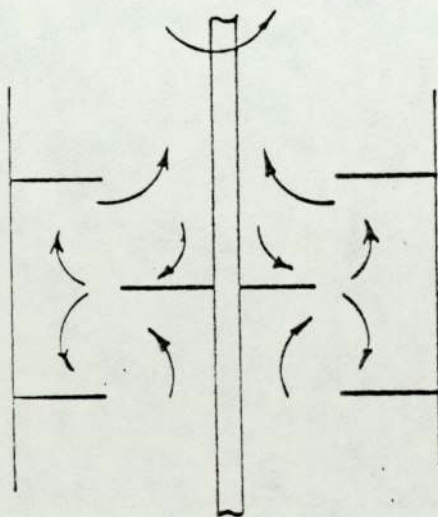


Fig. 3.4. Dispersed phase flow pattern
< 300 ft/min peripheral speed (43)
R.D.C. system toluene - water

in Figs. 3.3 and 3.4. In general at all rotor speeds less than 300 ft/min., except at the vicinity of the flood point, the flow of the liquid was counter-current with a rotation of the whole liquid mass around the rotor shaft. The movement of the liquid from the shaft towards the wall of the column in the vicinity of the rotor discs, and from the wall back towards the shaft in the vicinity of the stator rings, was not present under these conditions, and there was very little back mixing. This explains the absence from Fig. 3.3 of the recirculation loops, which appeared in Fig. 3.2. Also, as indicated in Fig. 3.3, for all runs at rotor peripheral speeds less than 300 ft/min. layers of dispersed phase droplets were generally observed to be trapped beneath the stator rings and/or rotor discs. However, the extent of droplet entrapment, was a function of the column geometry, the rotor speed and the liquid flow rates.

At rotor peripheral speeds higher than 300 ft/min. and/or at the vicinity of the flood points a similar flow pattern to that described by Reman (44) was observed, and back mixing became generally prominent. The severity of back mixing was a function of the column geometry, the rotor speed, and phase flow rates. Fig. 3.4 is similar to Fig. 3.2, except that the former underscored the difference in quantity which recirculated and the main body of the flow of the liquid. However at the vicinity

of the flood point the flow pattern of the dispersed phase approached that represented by Fig. 3.2.

3.1.2 Power Requirements of the R.D.C.

Although the power consumption of an R.D.C. may be relatively small in terms of total extraction processing costs, the correct sizing of the drive motor is important so that the rotor speed can be controlled to give maximum extraction efficiency under all conditions.

Reman et al (33) considered power requirements on the basis of mixing. They were able to correlate for any system and any R.D.C., the power number $N_p = \frac{P}{\rho_m N^3 R^5}$ with the disc Reynolds number, $Re_m = \frac{\rho NR^2}{\mu}$. Using this correlation the power requirements for a full size extractor could be found from pilot plant work.

Later Misek (45) analysed the results of previous authors and obtained,

$$N_p = B Re^A \quad (3.1)$$

Exponents A and B were determined experimentally as,

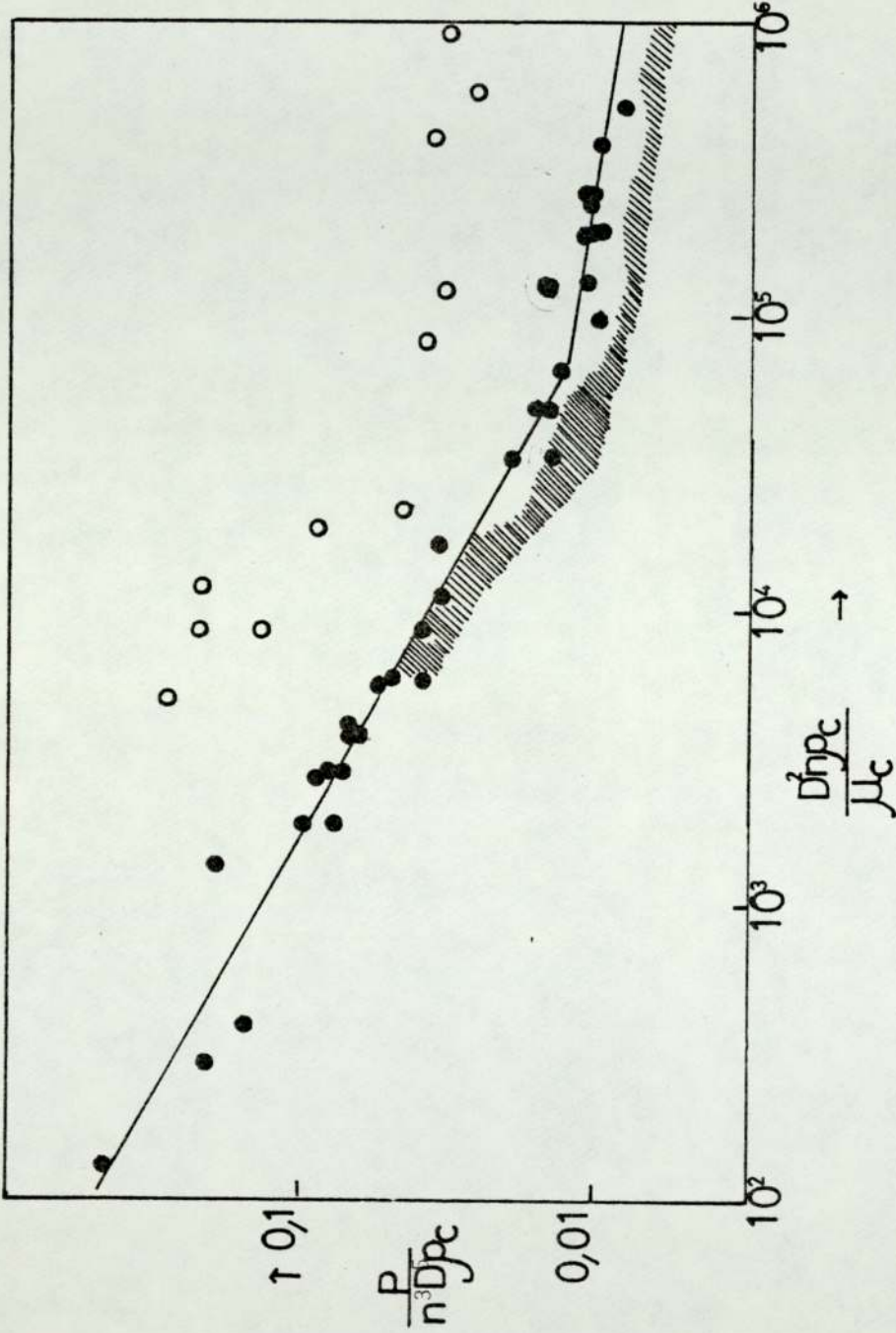
(i) In the laminar region,

$$A = - 0.568 ; \quad B = 6.78 \quad (3.2)$$

(ii) In the turbulent region,

$$A = - 0.155 ; \quad B = 0.069 \quad (3.3)$$

Misek (45) compared the results with those of Reman (33);



o Solid marks Misek data; empty marks Reman's data. Hatched section represents the data of Kempf and Schmidt with disc constructed of both hydrophylic and hydrophobic materials.

FIG. 3.5 POWER REQUIRED FOR AGITATION IN AN R.D.C. (45).

the power required was only one third of that predicted by Reman. This was explained on the basis that the results obtained by Reman were on a full scale plant and probably included all power losses due to friction and bearings, whereas Misek's results were on a pilot plant. The results obtained by Misek are shown in Fig. 3.5.

3.1.3 Internal Geometry

The inside geometry of the R.D.C. is determined by the diameter of the rotating disc, the stator opening and the height of the compartment, i.e. the distance between the successive stator rings or rotating discs.

Proper column geometry is of great significance since it affects both the column capacity and efficiency (8, 10, 27, 32, 46). Thus the column efficiency (27, 32) was found to increase with,

- (a) increase in the diameter of rotor discs,
- (b) decrease in the size of the stator opening, and
- (c) decrease in the height of the compartments.

Opposite effects generally apply for the capacity. Thus the need arises for optimisation between efficiency and capacity. The geometry therefore selected depends upon, whether,

- (a) the system is easily extractable, or
- (b) high efficiency-low capacity, or a low efficiency but high capacity is required for a particular application and system.

In general (8, 9, 10, 27, 43, 46) for optimum design, the column dimensions should have the following ratios,

$$\frac{\text{Stator diameter (S)}}{\text{Column diameter (D)}} = 0.66 \text{ to } 0.75$$

$$\frac{\text{Disc diameter (R)}}{\text{Column diameter (D)}} = 0.5 \text{ to } 0.66$$

$$\frac{\text{Compartment height (H)}}{\text{Column diameter (D)}} = 0.33 \text{ to } 0.5$$

Misek (10) has presented a nomograph for the determination of column dimensions. The results obtained from this nomograph, which is reproduced in Fig. 3.6, generally fall within the range mentioned above.

3.2 Hydrodynamics

3.2.1 Hold-up

In mass transfer calculations using equation 1.1 and 1.2, the interfacial area is estimated as the product of drop surface area and the total number of drops in the column. Hence it is necessary to predict either the drop residence times in the extractor, or the fraction of the column volume occupied by the dispersed phase. Since in extractors of complex geometry the droplet velocity is difficult to estimate, it is probably easier to determine the fractional hold up of the dispersed phase. Clearly the fractional hold-up for any system at a given phase flow rate will be characteristic of the extraction equipment. Thus in calculations for mass transfer and limiting flows of phases in counter current extractors,

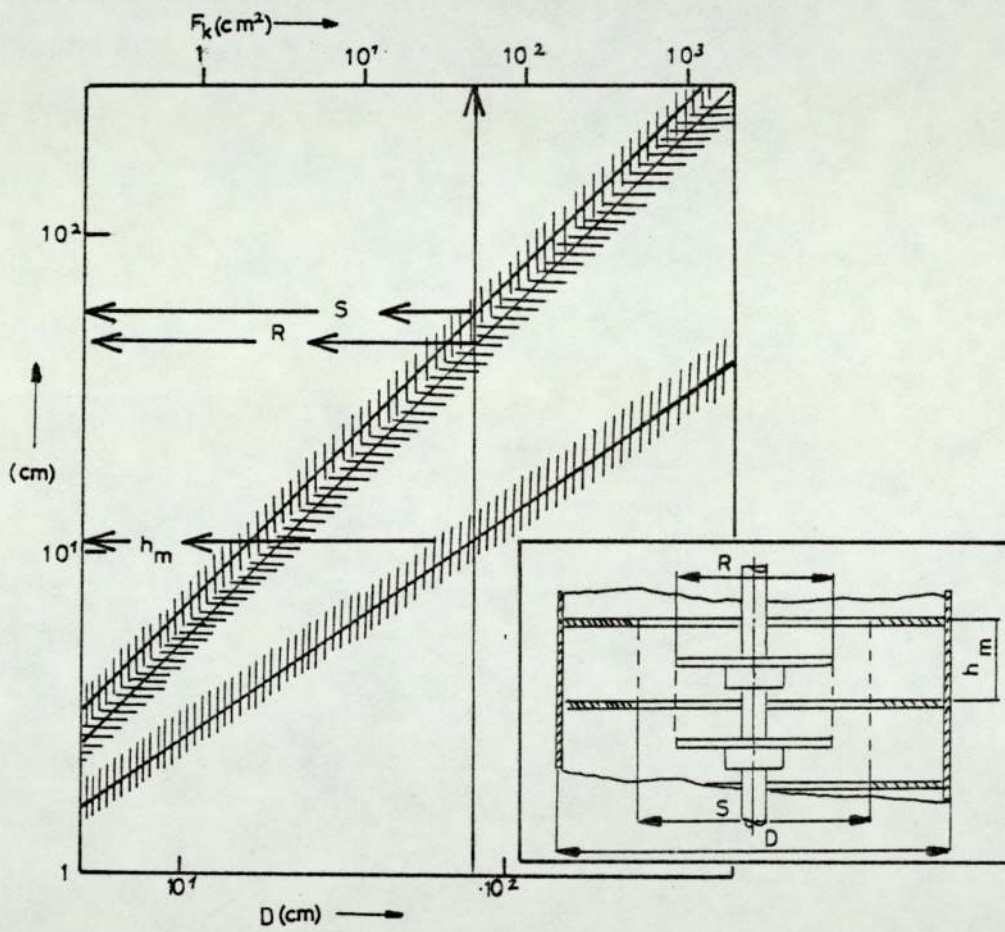


FIG. 3.6. NOMOGRAPH FOR THE DETERMINATION OF COLUMN GEOMETRY (10).

it is usually assumed that the hold up of the dispersed phase is constant along the column length. Experimental measurements of hold up profiles in mechanically agitated columns have shown however, that the hold up varies with the column height and often exhibits a rather sharp maximum in the middle of the column. Such hold up profiles occur especially in Rotating Disc Contactors of industrial size and have been described by Strand (8) and Rozkos (30).

Figs. 3.7 and 3.8 show typical hold up profiles in industrial R.D.C.'s extracting phenol with butylacetate and for furfural raffination of mineral oils (39). In each case, the hold up shows a maximum which increases with rotor speed. From an investigation into the efficiency of extractors, Rozkos (30) found that such a profile corresponded with the optimal operating conditions.

Logsdail, Thornton and Pratt (9) were the first to introduce the concept of dispersed phase hold up for the characterisation of column hydrodynamics and thus the empirical approach to the column design. These authors modified the concept of relating the slip velocity V_s of the dispersed phase to the hold-up, in a two phase system (47, 48, 49), by,

$$V_s = \frac{V_d}{X_d} + \frac{V_c}{1-X_d} \quad (3.4)$$

to
$$\bar{V}_N(1-X_d) = \frac{V_d}{X_d} + \frac{V_c}{1-X_d} \quad (3.5)$$

fural $q_c = 24 \text{ m}^3/\text{hr}$
oil $q_d = 118 \text{ m}^3/\text{hr}$

water $q_c = 45 \text{ m}^3/\text{hr}$
butylacetate $q_d = 45 \text{ m}^3/\text{hr}$
 $D_c = 2000 \text{ mm}$ $h_c = 9500 \text{ mm}$

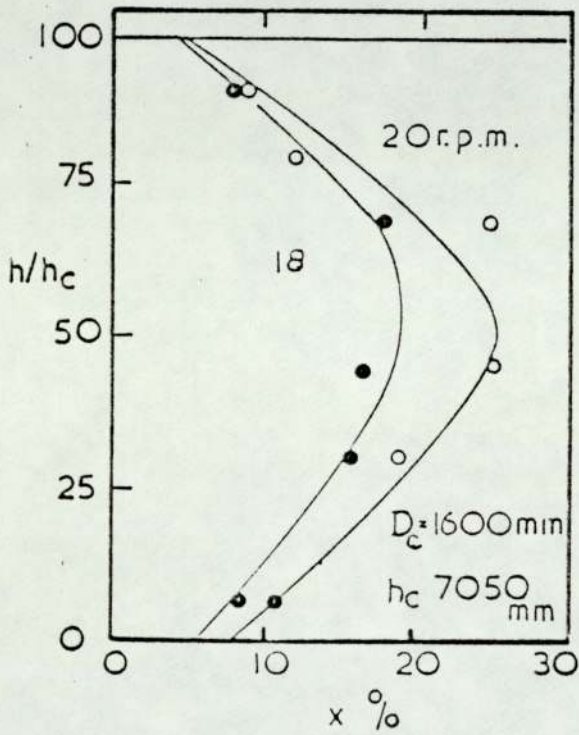


Fig. 3.7

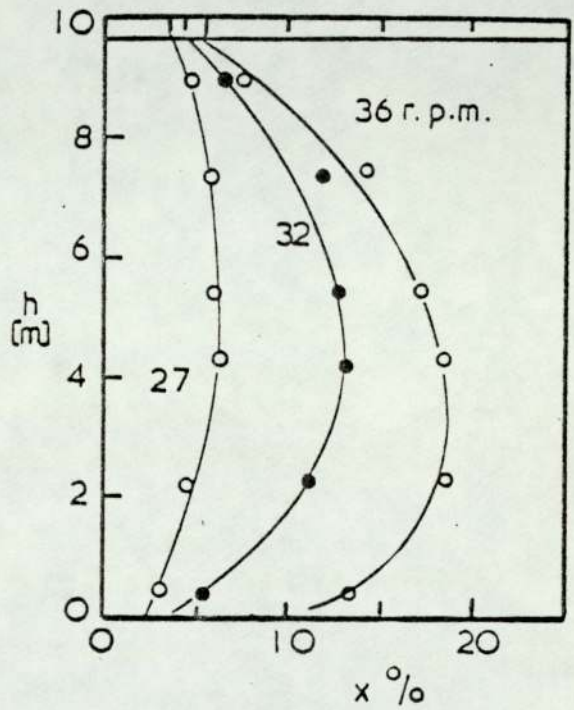


Fig. 3.8

Hold - up profile in an R.D.C. (39)

They defined \bar{V}_N as the mean relative velocity of the drop-lets extrapolated to essentially zero flowrates at a fixed rotor speed. They derived a correlation for \bar{V}_N from dimensional analysis considerations and calculated it using data obtained in a 3 inch dia. R.D.C. with the systems water/toluene, water/benzene, water/white spirit, water/butyl acetate and water/iso octane with variable rotor speed and column geometry.

The correlation is expressed as

$$\frac{\bar{V}_N \mu_c}{\gamma} = 0.012 \left(\frac{\Delta\rho}{\rho_c}\right)^{0.90} \left(\frac{g}{RN^2}\right)^{1.0} \left(\frac{S}{R}\right)^{2.3} \left(\frac{h}{R}\right)^{0.90} \left(\frac{R}{D}\right)^{2.7} \quad (3.6)$$

where the symbols have their usual significance as defined in the Nomenclature.

Kung and Beckman (43) studied the effect of column geometry and flow condition upon the dispersed phase hold up in an R.D.C. They varied stator opening disc, diameter, compartment height, rotor speed, and flowrates of the two phases. It was observed that at zero continuous phase flowrate hold-up increased with decreasing stator opening and compartment height and increasing disc diameter and rotor speed.

Their most important observation was that for a particular column geometry experimental data was well correlated by equation 3.5, whereas for the other set the data would not fit well, because of the effect of the

continuous phase flowrate. They therefore modified equation 3.5 to give,

$$\frac{V_d}{x} + \frac{K_1 V_C}{(1-x)} = \bar{V}_N (1-x) \quad (3.7)$$

where $K_1 = 2.1$ at $\frac{S-R}{D} \leq \frac{1}{24}$ and 1.0 at $\frac{S-R}{D} > \frac{1}{24}$.

Kung and Bechman also modified equation 3.6 using data from their study, and that of Reman and Olney (27), to give,

$$\frac{\bar{V}_N \mu_c}{\gamma} = K_1 \left(\frac{\Delta\rho}{\rho_c}\right)^{0.90} \left(\frac{g}{RN^2}\right)^{1.0} \left(\frac{S}{R}\right)^{2.3} \left(\frac{h}{R}\right)^{0.9} \left(\frac{R}{D}\right)^{2.6} \quad (3.8)$$

Equation 3.8 in fact differs from equation 3.6 only in that the exponent on $\frac{R}{D}$ is 2.6 instead of 2.7.

However, calculation of hold up by means of equation 3.7 or 3.5 does not consider coalescence and break-up of droplets in the R.D.C. This will affect the hold-up through changes in back-mixing and droplet velocity. Hence Misek (50) proposed that the hold up in an R.D.C. could be correlated by the relation,

$$\frac{U_d}{X} + \frac{U_c}{1-x} = \bar{U}_0 (1-x) \exp\left(\frac{Z}{\alpha} - 4.1\right) X \quad (3.9)$$

In equation 3.9, Z is a factor to correct for coalescence and is a function of column diameter, drop size and the physical properties of the phases, Thus,

$$Z = 1.59 \times 10^{-2} \left| \frac{D_k}{\mu_c} \left(\frac{\gamma}{\rho_c d_o} \right)^{\frac{1}{2}} \right|^{\frac{1}{2}}$$

Where μ_c is the kinematic viscosity of the continuous phase and γ is the interfacial tension.

The factor α corrects for back-mixing and is related to droplet Reynolds number.

3.2.1.1 Hold-up Profile

The variation of hold up along the length of an R.D.C. has been noted by Stainthorpe and Suddal (51) and by Olney (52). Suddal applied a correction factor to the dispersed phase hold up. This was found necessary in order to obtain an adjusted response curve which satisfied both the peak ordinate and abscissa criteria for back-mixing simultaneously. It was justified by the observation that, in agreement with the findings of Strand, et al, dispersed phase hold up varied along the column length, so that a model assuming a constant hold up was inapplicable.

Olney (52) also reported a distribution of drop size throughout the column and that drops of different size behaved differently, resulting in a wide distribution of residence times. The drop size distribution was bounded by an upper limit, or maximum stable size, and a lower limit, or minimum stable size, dependent on droplet interaction, i.e. break up and coalescence. Hence if a large range of drop size exists in a column the drop size

distribution $f(d_p)$ may need to be included in the design or analysis of the equipment. Furthermore, if drop size distribution is the result of droplet interaction it would be expected to be some function of hold-up and the degree of agitation.

Davies (41) was unable in fact to detect coalescence of droplets in an R.D.C. at hold-up's up to about 10% whereas Misek (53) claimed that at high hold up, of the order of 18%, drop to drop coalescence occurred. This has been confirmed by Mumford (54) who found that, in the absence of mass transfer, drop to drop coalescence was only appreciable at very high hold-up's and disc speed of the order of 1000 r.p.m.; conditions approaching flooding. Therefore, under normal R.D.C. operating conditions the U.L.D. (upper limit distribution) will be determined by the size of the nozzles in the droplet distributor plate at the dispersed phase entrance, and the L.L.D. (lower limit distribution) will be a function of the disc speed and the physical properties of the system undergoing extraction. This suggests that there will be a progressive decrease in drop size in an R.D.C. as the dispersed phase passes through it until at some plane in the column the surface energy of the drop just balances the drag and kinetic energy transmitted from the agitator. Drop to drop coalescence will tend to reduce the range of drop sizes but this will only become significant at high hold-up, usually in excess of 20%. Furthermore, as the drop

size if reduced, so will the drop tend to be influenced more by the local velocity of the agitator and less by buoyancy with the result that recirculation of the drops within a compartment of the extractor will increase; that is, hold up will be expected to increase along the column from the dispersed phase entry section.

Strand et al found a variation in hold up in a radial as well as an axial direction, using a toluene-water system in 6 inch and 42 inch diameter R.D.C.'s. Typical data for 42 inch column are reproduced in Fig. 3.9 and 3.10. The results obtained at other flow rates were qualitatively similar. Similar results were obtained in the 6 inch unit except that the radial profiles were more erratic, as a result of the small dimensions. However, the same authors found that $(x)_{av}$ did not differ significantly from $(x)_{max}$ except at very low rotor speeds, when the drops tended to be trapped beneath the rotors and stators, as described earlier.

Recently Rod (39) explained the rise of hold up to a maximum with the increase in rotor speed by considering two mechanisms to influence hold up, namely, the break up of drops in the mixed section of the extractor and the longitudinal mixing of the dispersion.

To derive a mathematical model it was assumed that the dispersed phase entering the mixed section of the column is distributed into drops of equal size d_1 . While

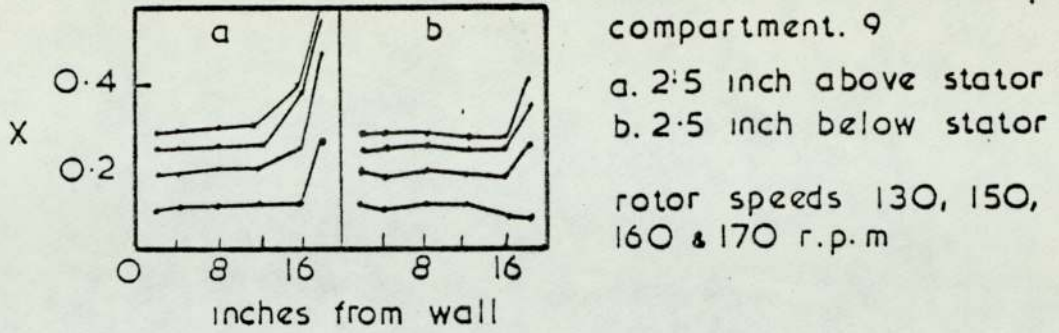


Fig. 3.9 Radial profile of hold-up
42. inch. R.D.C. system water - toluene(8)

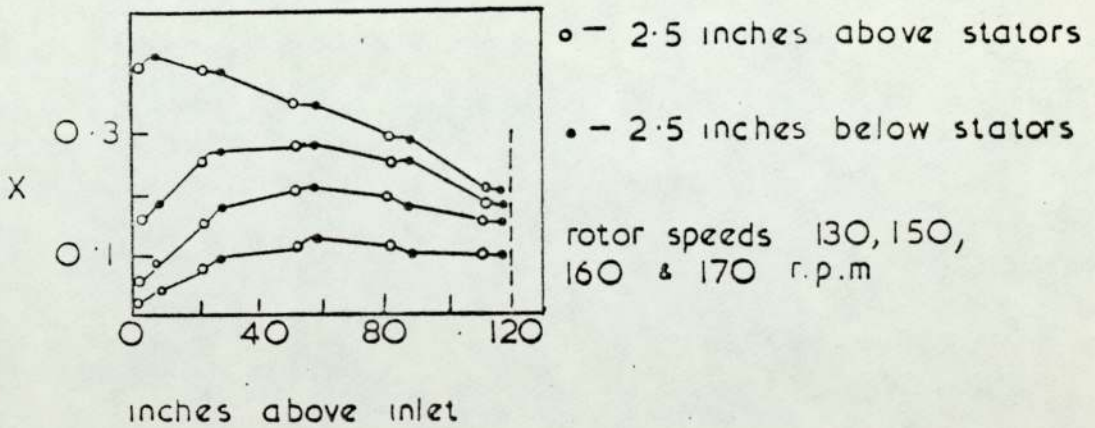


Fig. 3.10 Axial profile of hold-up (8)
42 inch R.D.C system water-toluene

passing through this section these drops break up into smaller drops of diameter d_1 at a rate proportional to their concentration in the dispersion. A diffusion model was used to describe the longitudinal mixing in the column and values of dispersion coefficient were assumed to be equal for both sizes of drops. The hold up profile was then described as the sum of two hold ups, one of large size X_1 , and the other of small size X_2 . Thus,

$$X = X_1 + X_2 \quad (3.11)$$

$$\text{where } X_1 = X_1^0 (C_1 e^{\lambda_1 Z} + C_2 e^{\lambda_2 Z}) \quad (3.12)$$

$$\begin{aligned} \text{and } X_2 = X_1^0 \left(\frac{P_2}{P_1} \right) & \left(1 - \frac{P_1 \lambda_1 - 1}{P_2 \lambda_2 - 1} C_1 e^{\lambda_1 Z} \right. \\ & \left. - \frac{P_1 \lambda_2 - 1}{P_2 \lambda_2 - 1} C_2 e^{\lambda_2 Z} + C_3 e^{-(1-Z)/P_2} \right) \end{aligned} \quad (3.13)$$

where constants $\lambda_{1,2}$, C_1 , C_2 and C_3 are given by

$$\lambda_{1,2} = 1 \pm \frac{(1+4 P_1 N)^{\frac{1}{2}}}{2 P_1} \quad (3.14)$$

$$C_1 = \frac{1 - P_1 \lambda_2^{-\beta}}{(1 - P_1 \lambda_1) (1 - P_1 \lambda_2^{-\beta}) - (1 - P_1 \lambda_2) (1 - P_1 \lambda_1^{-\beta}) e^{\lambda_1 - \lambda_2}} \quad (3.15)$$

$$C_2 = \frac{1 - C_1 (1 - P_1 \lambda_1)}{1 - P_1 \lambda_2} \quad (3.16)$$

$$\begin{aligned} C_3 = \frac{1}{\beta} \left| 1 - \beta - \frac{(P_1 \lambda_1 - 1) (1 - P_2 \lambda_1^{-\beta})}{P_2 \lambda_1 - 1} e^{\lambda_1} \right. \\ \left. - \frac{(P_1 \lambda_2 - 1) (1 - P_2 \lambda_2^{-\beta})}{P_2 \lambda_2 - 1} C_2 e^{X_2} \right| \end{aligned} \quad (3.17)$$

In the same study Rod suggested that equalisation of hold up profile to its maximum value, could increase interfacial area by more than 60% without approaching flooding conditions. This could be obtained by

- (1) using an efficient distributor producing a dispersion in which the mean size of the drops does not decrease while passing through the mixed section, and
- (2) a proper reduction of the free cross-section at the outlet boundary, by, for example, making the internal opening of the last stator ring smaller, to decrease the superficial outlet velocities of drops.

This should compensate for the escape of drops from the mixed section, caused by longitudinal mixing, thus preventing a hold up decrease at the outlet part of the section. However, this proposal is open to question, since maximum efficiency need not necessarily correlate with maximum hold up, because small drops have a lower mass transfer coefficient (37).

3.2.2 Limiting Capacity of the R.D.C.

In the design of the R.D.C. it is necessary to predict the column cross-sectional area for a specific loading. One approach used is based on the existence of a maximum flowrate of dispersed phase for a particular flowrate of the continuous phase at a certain rotor speed.

The maximum permissible throughput occurs just before flooding.

Flooding is one of the characteristics of counter-current flow devices, such that for each velocity of flow for one of the liquids there is a maximum possible velocity of the other. This is governed by the liquid properties, the design of the device, and the rotor speed. At a fixed flowrate of one liquid, if an attempt is made to exceed the maximum velocity for the second liquid, one of the liquids will be rejected by the equipment, which is then described as 'flooded'. For a given volumetric rate of flow of the two liquids, the cross-sectional area for flow must therefore be sufficiently large to avoid velocities that result in flooding.

Logsdail, Thornton and Pratt (9) derived a relation between the dispersed phase flowrate, the continuous phase flowrate and flooding hold ups, by asserting that at the flood points the flowrates reach a maximum. Introduction of this condition into equation 3.5, followed by differentiation and setting $(\frac{dV_d}{dx_d})$ and $(\frac{dV_c}{dx_d})$ equal to zero, results in,

$$V_{d(f)} = 2\bar{V}_N X_f^2 (1-x_f) \quad (3.18)$$

$$V_{c(f)} = \bar{V}_N (1-x_f)^2 (1-2x_f) \quad (3.19)$$

Equation 3.18 and 3.19 relate the phase flowrates at

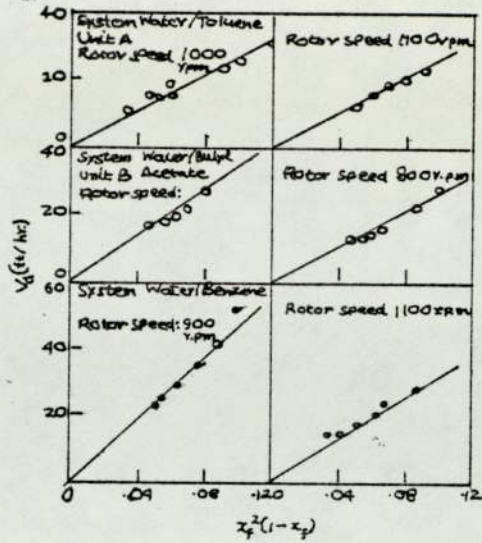


FIG. 3.11 DETERMINATION OF CHARACTERISTIC VELOCITY FROM THE FLOODING DATA, NON-MASS TRANSFER OPERATION.

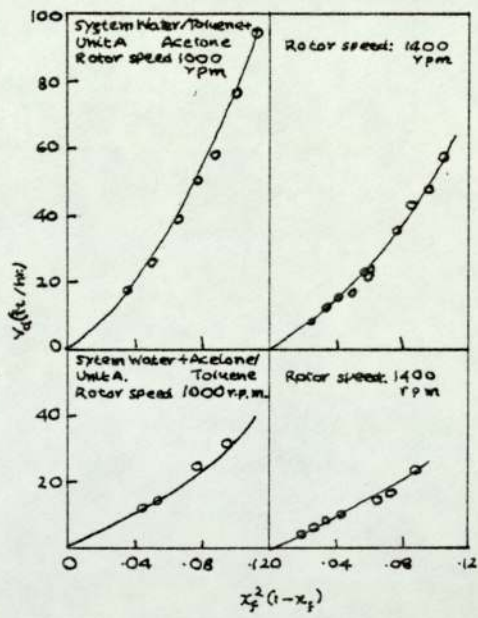


FIG. 3.12 DETERMINATION OF CHARACTERISTIC VELOCITY FROM THE FLOODING DATA (9), MASS TRANSFER OPERATION.

flooding to the corresponding hold-up, x_f . A relation between x_f and the flow ratio $V_{d(f)}/V_{c(f)}$ was then obtained by eliminating \bar{V}_N between equations 3.18 and 3.19 thus,

$$x_f = \frac{(L + 8L)^{0.5} - 3L}{4(1-L)} \quad (3.20)$$

where

$$L = \frac{V_{d(f)}}{V_{c(f)}} \quad (3.21)$$

\bar{V}_N was evaluated from experimental data under the condition of flooding, by substituting $V_{d(f)}$ and $V_{d(f)}$ into Equation 3.21 to give x_f for each determination and plotting $V_{d(f)}$ against $x_f^2(1-x_f)$ in accordance with equation 3.18. In the majority of cases, excellent straight lines were obtained which could be extrapolated through the origin. Values of \bar{V}_N were obtained from the slopes of these lines, equal to $2\bar{V}_N$. Typical results are shown in Fig. 3.11.

However, this method of treatment is applicable only when the mean droplet size, and, hence \bar{V}_N , remains constant over the entire hold up regime involved. This was not the case when acetone was initially present in the solvent phase; the droplets were noticeably larger and consequently had a greater mean velocity of ascent. Flooding rates were increased by 100-200% in this case. Conversely when the acetone was initially present in the aqueous phase, there was no noticeable change in the droplet size compared with non-mass transfer runs, but the flooding rates decreased by 10-15%. These effects

are demonstrated in Fig. 3.12. Clearly with acetone present in the solvent phase, the graph of $V_{d(f)}$ against $x_f^2(1-x_f)$ is no longer linear and the slope increases with hold up. This implies that \bar{V}_N , and hence the mean droplet diameter, also increases with hold-up. Conversely, when the acetone was present in the aqueous phase the plot is more nearly linear.

Misek (50) also calculated the limiting values of hold up using a similar procedure to that of Logsdail et al . After elimination of the characteristic velocity the final expression obtained was,

$$\frac{V_{d(f)}}{V_{c(f)}} = \frac{2x_f^2 |1-x_f+(Z-4.1)(x_f-x_f^2/2-\frac{1}{2})|}{(1-x_f)^2 |1-2x_f+(Z-4.1)(x_f-x_f^2)|} \quad (3.22)$$

Strand (8), found the procedure used by Thornton and co-workers satisfactory when a constriction factor C_R was introduced into the analysis. The constriction factor C_R is the minimum of the three area ratios $(\frac{S}{D})^2$, $|1-(\frac{R}{D})^2|$, $(\frac{S+R}{D})\sqrt{\frac{(S-R)^2}{D} + (\frac{H}{D})^2}$. They concluded that the method is valid for most scale up problems, provided that pilot data including drop hold up measurements, are obtained using a small R.D.C. of suitable design, and that a sufficient range of rotor speed is specified for the commercial design.

The method is not strictly applicable to real

separations involving mass transfer and pilot scale data may be essential. This arises because the characteristic drop size may depend quite strongly upon the transfer process. The change in interfacial properties with mass transfer may strongly inhibit drop coalescence in some cases, promote coalescence in others, and cause almost spontaneous emulsification in still other cases. Such observations are now well documented (55, 56). These effects, when they occur, are generally functions of the solute concentration so that hold up measurements may have to be made at several points along the length of the contactor when mass transfer is occurring.

Recently, under certain conditions of operation, the limiting capacity of the R.D.C. and Old-shue Rushton columns have also been defined by phase inversion (11,37,38). When this phenomena occurs the normal operation of a counter-current device is no longer possible, due to phase reversal. The phenomena is of importance to design because under certain conditions of operation phase inversion occurs before flooding. Phase inversion is therefore discussed in detail in Chapter 7.

3.3 Column Diameter

Two different methods are used to determine the column diameter. The first method is applicable when no experimental data is available and is based on the systems physical properties. The second method is used to scale up from pilot

plant data to full scale.

3.3.1 Calculation on the Basis of Physical Properties

Misek (10) proposed a method of calculation based on the simple rearrangement of equation 3.9, to give the column diameter as,

$$D = \left| \frac{4}{\pi \bar{V}_N} \text{Exp} \left\{ \left(4.1 - \frac{Z}{\alpha} \right) x \right\} \left\{ \frac{Q_d}{x(1-x)} + \frac{Q_c}{(1-x)^Z} \right\} \right|^{0.5} \quad (3.23)$$

Determination of column diameter from this equation requires the estimation of Z , α , and \bar{V}_N and hold up of dispersed phase. Misek (10) proposed a theoretical approach for calculation of these coefficients using the system properties and the correlation, which itself requires knowledge of the column diameter. The method therefore involves trial and error. Moreover the correlations proposed for the determination of coalescence coefficient Z , and velocity exponent α , (10) require the prediction of drop size.

Misek identified three regimes for the calculation of drop size. In the turbulent regime, when Re. No. $> 5.74 \times 10^4$, the following correlation is applicable

$$\frac{d_o N^2 R^2 \rho_c}{\sigma_i \text{Exp}(0.0887x\Delta R)} = 16.3 \left(\frac{h_m}{D} \right)^{0.46} \quad (3.24)$$

On diminishing the mixing intensity below a critical value of Reynolds No.,

$$(\text{Reynolds No})_{\text{Crit.}} = \frac{R^2 N \rho_c}{\mu_c} \text{Crit.} = 5.74 \times 10^4 \quad (3.25)$$

the break-up of drops occurs within a transitive region. Here the formula,

$$\frac{d_o N^2 R^2 \rho_c}{\sigma_i \text{Exp}(.0887\Delta R)} = 1.345 \times 10^{-6} \left| \frac{R^2 N \rho_c}{\mu_c} \right|^{1.42} \quad (3.26)$$

is valid. Further decrease in the mixing intensity causes the break up to take place in the laminar region (Re. No. $< 10^4$) where the formula,

$$d_o = 0.38 \sqrt{\frac{\sigma_i}{\Delta \rho g}} \quad (3.27)$$

is applicable.

The widespread application of these correlations is open to criticism, because different drop break up mechanisms exist in laboratory and industrial extractors. Moreover, the correlation takes no account of the effect of hold up on drop size and the variation of drop size with height.

Jeffreys (57) proposed a method for determination of column diameter using the physical properties of the system in a similar way to Misek (18). The method involves an initial assumption of column diameter, which is then rechecked by further calculations. The reliability of the method depends upon a number of correlations derived under different operating conditions with differing limits of accuracies. However, use can be made of this method if no pilot plant data is available.

3.3.2 Determination on the Basis of Scale-up of Pilot

Plant Data

Reman (7,27) proposed a method for the determination of the diameter of an industrial contactor on the assumption that limiting flowrates are proportional to the power input per unit volume. They may therefore be expressed by the graphical function,

$$\frac{V_c + V_d}{C_R} = f\left(\frac{N^3 R^5}{HD^2}\right) \quad (3.28)$$

where C_R is the minimum of $\left(\frac{S}{D}\right)^2$ or $\frac{D^2 - R^2}{S^2}$. Application of this approach is illustrated in Fig. 3.13 in which data for columns with different internal structures fall on a straight line (27). However, it is only applicable when the phase ratio $\frac{V_d}{V_c}$ is less than 3 and the two units under consideration are geometrically similar. As pointed out by Misek (10), such a requirement could reduce the efficiency of an industrial column because of the need to reduce the relative height of compartments, increase the rotor diameter and reduce the stator opening in an industrial unit to achieve the same degree of mixing, and thus efficiency, as on the small scale.

3.4 Column Height

The total height of an R.D.C. can be expressed as,

$$H = h_{\text{eff}} + h_c + h_s \quad (3.29)$$

where h_{eff} is the height of the effective column section

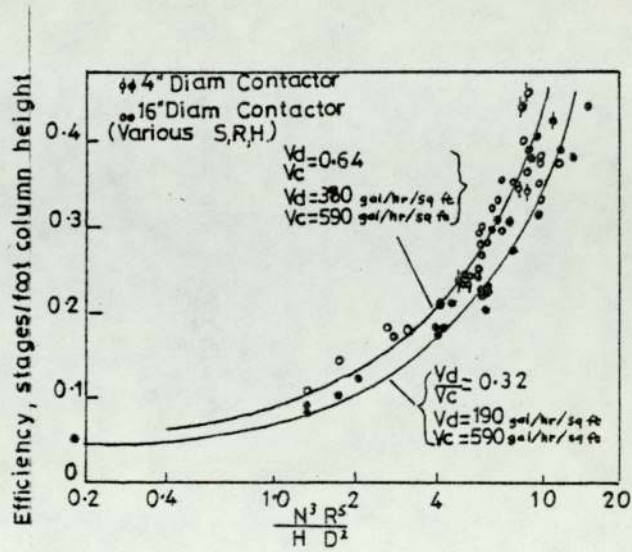


FIG. 3.14 EFFICIENCY vs $\frac{N^3 R^5}{H D^2}$ (7)

System water-kerosene-Butylamine, water as dispersed.

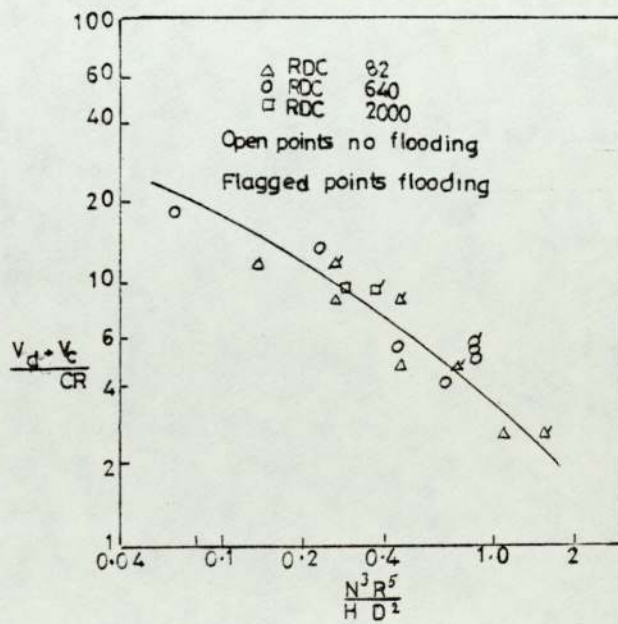


FIG. 3.13 CAPACITY CORRELATION (7)

in which the bulk of the mass transfer occurs, h_c is the height of the coalescence section and h_s is the height of the section where the entrained drops of the dispersed phase separate from the continuous liquid.

3.4.1 Height of the Coalescence Section

The height of the coalescence section is generally estimated using drop coalescence time correlations. Such correlations provide the time for droplets to coalesce on the interface from a knowledge of system properties and drop sizes. The correlations and their range of applicability is discussed in detail in chapter 4. The height of the settling section is,

$$h_c = t_{\text{coal}} \times V_d \quad (3.30)$$

3.4.2 Height of the Bottom Section (h_s)

It is necessary to avoid the continuous phase entraining and carrying the dispersed phase droplets with it, when discharging from the column. Therefore a sufficient height must be provided for disentrainment. The height of this section is calculated on the basis that, making due allowance for the existence of a drop size distribution in the R.D.C., droplets will be carried away by the continuous phase when its velocity exceeds their falling or rising velocity. This is a function of drop diameter. From an analysis of published data Misek (10) found that drops having a diameter $d_{32}/20$ do not exceed 1% by volume. Small drops obey Stokes law (10) so that

their velocities may be determined from,

$$(V_o)_{ST} = \frac{gd^2\Delta\rho}{18\mu_c} \quad (3.31)$$

If $V_c > (V_o)_{ST}$ entrainment of these drops will occur without any regard to the height of the settling section.

However, the small drops settling rate relationship could be used in several ways according to the nature of the problem:

- (a) The continuous and dispersed phase velocities may be selected to give,

$$V_c < (V_o)_{ST} 1\% \text{ or } V_c < (V_o)_{ST} 5\% \quad \text{or}$$

- (b) The diameter of the settling section may be enlarged to satisfy the above conditions, or
- (c) A separate settling tank may be installed. The tank is designed to prevent any entrainment; that is the dimensions of the settling tanks are selected so that $V_c < (V_o)_{ST} 1\%$.

3.4.3 Effective Extractor Height

In the past the effective column height has been determined using the concept,

$$h_{eff} = H.T.U. \times N.T.U. \quad (3.32)$$

where H.T.U. and N.T.U., for example for raffinite phase (20) are defined in a simplified case as,

$$H.T.U. = \frac{V_D}{K_D a} \quad (3.33)$$

$$N.T.U. = \frac{\ln \left| \left(\frac{x_{R1} - x_{E2}/m}{x_{R2} - x_{E2}/m} \right) \left(1 - \frac{1}{\epsilon} \right) + \frac{1}{\epsilon} \right|}{1 - \frac{1}{\epsilon}} \quad (3.34)$$

In general there are no reliable methods of estimating these variables from the system properties and operating parameters in an R.D.C. because,

- (a) Height of transfer Unit has been found to vary with the rotor speed (7,27). It tends to increase with an increase in rotor speed up to a maximum and then to decrease. This is due to the competing effects of the increase in surface area, but a change in the mode of mass transfer, and increased axial mixing, as smaller drops are produced at high rotor speeds, and
- (b) The geometrical parameters influence the efficiency of the extractor in different ways.

Two regions have been distinguished in an R.D.C. (7, 32), namely a turbulent region and a laminar region. Scale-up in the turbulent region has been based on an approximate relation defined by means of the height equivalent of a theoretical stage,

$$H_S \doteq \frac{d_{32}}{6K_F} \frac{G_F}{x_d} R^{-0.5} \quad (3.35)$$

Provided h_m/H_S is lower than 0.3, on the assumption that the mass transfer coefficient and the drop size may be

expressed as a function of power input per unit mass, efficiency can be correlated by plotting the function $\frac{1}{H_s}$ against $\frac{N^3 R^5}{HD^2}$. An example (7) of such a plot for the system water-butylamine and kerosene, extracted in columns of various diameters in the range 100 to 400 mm and with different internal geometries is shown in Fig. 3.14. The results, for a given phase ratio fall on the straight line. The results of Fig. 3.14 were expressed by,

$$H_s \doteq \left(\frac{N^3 R^5}{HD^2} \right)^{-0.7} \quad (3.35)$$

This method is only applicable when the power input per unit mass $\left(\frac{N^3 R^5}{HD^2} \right)$ is greater than $1000 \text{ cm}^2/\text{sec}^3$.

The analogous expression written for H.T.U. is

$$(H_p)_{OF} = \frac{d_{32} G_F}{6K_F x_d} \quad (3.36)$$

This expression does not include the extraction factor R. In a similar way to H.E.T.S. (H_s), the H.T.U.'s plotted against $\frac{N^3 R^5}{HD^2}$ fall on the single line irrespective of phase ratio.

For $\frac{N^3 R^5}{HD^2}$ below $1000 \text{ cm}^2/\text{sec}^3$, i.e. in the laminar region, the efficiency is independent of the rotor speed. Scale-up can then be achieved by,

$$H_s \doteq D^{-0.15} \quad (3.37)$$

Logsdail et al (9) also proposed a method for scale-up using the concept that the mass transfer coefficients

or H.T.U.'s were a function of the rising drop velocity. The H.T.U.'s were thus correlated by,

$$\left| \frac{(\text{H.T.U.})_{oc}}{V_c} \left(\frac{g^2 \rho_c}{\mu_c} \right)^{1/3} \right|_x = \left| \frac{x}{K_{oc}^a} \left(\frac{g^2 \rho_c}{\mu_c} \right)^{1/3} \right|$$

$$= K \left(\frac{\mu_c g}{\bar{V}_N^3 (1-x)^3 \rho_c} \right)^{2m/3} \left(\frac{\Delta \rho}{\rho_c} \right)^{2(m-1)/3} \quad (3.38)$$

Use of this expression requires evaluation of the constant K exponential m , and the characteristic velocity \bar{V}_N . These may be determined from tests with the specific system in a small scale laboratory column. However the derivation of the model testifies to the better applicability of this correlation in the laminar region (10).

Strand et al (8) and later Jeffreys (57) suggested the use of single drop mass transfer models for the determination of column heights. However application of this approach is limited because of the difficulty of predicting accurately which mode of mass transfer would be most applicable in a poly dispersed environment. The situation is further complicated in industrial systems where traces of impurities and surface active agents make the prediction even more difficult.

The different single drop mass transfer models, their applicability to industrial R.D.C. design and their limitations are discussed in detail in Chapter 5.

The applicability of equations 3.33 and 3.34 for the determination of effective column height is limited to cases where axial mixing effects are negligible. Otherwise an extra column height must be added to the height calculated from equation 3.33, 3.34 and 3.32. Axial mixing, and methods for allowing for it, are discussed in chapter 6.

Sleicher (58) has provided a solution for calculation of true mass transfer coefficients from the mass transfer with eddy diffusion in both phases. Assuming that the axial diffusivities may be used as the eddy diffusivities the solution for condition $\psi_p = \psi$ is approximately correlated by

$$\frac{T}{T_p} = \frac{N_{Pe_f} N_{Pe_s}}{N_{Pe_f} N_{Pe_s}^{-T_p} \left[a N_{Pe_b} + b N_{Pe_s} + c \sqrt{N_{Pe_f} N_{Pe_s}} \right]} - d \sqrt{N_{Pe_f} + N_{Pe_s}} + f (N_{Pe_f} - N_{Pe_s}) e^{-gT} \quad (3.39)$$

The overall number of transfer units for plug flow conditions is calculated from

$$T_p = \frac{1}{F-1} \ln \frac{1 - \psi_p}{1 - \psi} \quad (3.40)$$

The coefficients a, b, c, d, e, f, g , in equation 3.39 were provided in a tabulated form, as a function of the extraction factor F . The overall Peclet numbers for the dispersed feed phase are,

$$N_{Pe_f} = \frac{V_d H}{h E_a} \frac{L}{H}, \quad N_{Pe_s} = \frac{V_c H}{(1-h) E_a} \frac{L}{H} \quad (3.41)$$

and for a dispersed solvent phase are,

$$N_{Pe_f} = \frac{V_d H}{(1-h) E_a} \frac{L}{H}, \quad N_{Pe_s} = \frac{V_d H}{h E_a} \frac{L}{H} \quad (3.42)$$

A trial and error procedure is required to determine T from Equation 3.39 because, it also appears on the right hand side in the term e^{-gT} .

It is clear from the above that for any reliable design of an R.D.C., some hydrodynamic and mass transfer data must first be obtained in a pilot scale apparatus using the same system as that to be used in the industrial unit.

3.5 Scale-Up of Rotating Disc Contactors

As already described pilot plant studies should form the basis of design of industrial extractors. However, problems remain in extrapolating the results from a laboratory to a plant scale. The problems usually encountered are,

- (a) The operating conditions in industrial units are usually different from the operating conditions in the laboratory scale column.
- (b) The assumptions made to simplify the mathematical modelling may be justified on a laboratory scale, but have a greater impact on size enlargement. The prime example is the plug flow model of the extractor.
- (c) The flow structure in the industrial contactor might differ from the laboratory scale due to

change in materials of construction. The laboratory scale columns are usually made of glass, for flow visualisation, whereas industrial columns are invariably made of metal. The difference in wetting characteristics in the two columns may result in different break up and coalescence mechanisms, and hence in differences in capacity and efficiency of the two columns.

- (d) The principles of geometric, kinematic and dynamic similarity, whilst useful, are difficult to apply due to conflicting demands. For example dynamic similarity cannot be maintained since equal Reynolds numbers ($dV\rho/\mu$), which control mass transfer, and Weber numbers ($dV^2\rho/\gamma$), which control drop sizes and their distribution, are obviously impossible on two scales.
- (e) Mixing is usually poor in an industrial contactors.
- (f) In practice the efficiency of a full scale plant compared with the laboratory demonstrates a weakness in scale up. If the dynamical criterion is the same in the model and the full scale, the efficiency should be similar, but this is seldom the case. In general, the efficiency has been found to decrease with the increase in the column diameter. Hence extreme caution is needed when designing industrial units on the basis of model plant efficiency results.

The main reasons for encountering difficulty in scale-up arise from the combined effects of two phenomena, namely wall effect on the small scale and axial mixing on the large scale. The effects may result in very great errors. For example in scaling up data for furfural lube oil extraction, for the same amount of extraction, R.D.C. height had to be doubled for a diameter scale-up ratio of 30 (42). An even greater discrepancy was observed when scaling up an R.D.C. for solutizer extraction of mercaptans from naphthas. In this extraction, which was carried out with one volume of solvent (solutizer solution) to four volumes of naphtha, two modes of operation were applied; either the solutizer solution or the naphtha was chosen as the dispersed phase. The results in Table 3.1 show that the best efficiency was obtained on the small scale when the naphtha was dispersed. However, scaling up caused such a sharp deterioration for this mode of operation that on the large scale the solutizer dispersed condition gave the highest efficiency.

TABLE 3.1
SOLUTIZER EXTRACTION DATA (42)

Apparent height of transfer unit, H.T.U. in

	<u>R.D.C. DIAMETER</u>	
	<u>3 inch</u>	<u>25 inch</u>
Naptha dispersed	12	57
Solutizer dispersed	30	50

This observation was tentatively explained on the basis of the large residence time of the slowly flowing solutizer when naphtha was dispersed. More intense axial mixing in larger R.D.C.'s would then reduce the concentration gradient in the solutizer phase and thus decrease the overall mass transfer efficiency.

The use of similarity principles have been discussed by Johnstone and Thring (59) and Nagata (60). There are three similarity criteria - geometric, dynamic and kinematic. In considering dynamic similarity four groups of forces are important. These are the inertia force from the mixer and the fluid forces of viscosity, surface tension and gravity. Since it is impossible to keep the ratio of each of the individual fluid forces constant in scale-up with the same liquid, it is necessary to select those which are most important.

Recently Rosen and Krylov (61, 62) have also proposed a theory of scaling up and the use of hydrodynamic modelling. They claim that the hydrodynamic nature of the scaling effect allows industrial equipment to be designed by means of hydrodynamic model experiments, without using pilot plant tests. The hydrodynamic nature of the scaling effects, i.e. decrease in efficiency of mass transfer columns with increasing dimensions, is shown to result either from non-uniformity of the distribution of hydrodynamic flows over the cross section of an industrial

column or from an increase, due to scaling up, in the characteristic dimensions responsible for longitudinal mixing. The change of the flow structure caused by an increase in dimensions in the course of transition from laboratory apparatus to industrial equipment gives rise to the scaling effect.

Assuming that the transverse non-uniformity may be neglected in a laboratory column, the contribution of this non-uniformity to the effective longitudinal mixing coefficient being proportional to the square of the column diameter, the scaling effect in the continuous phase can be given as,

$$\Delta D = H(1 - l_{lab}) W_{eff} + f_o d_a^2 \frac{(\Delta W)^2}{HlW_{eff}} \quad (3.43)$$

where l is the characteristic dimension. This is defined for an R.D.C. as $h_m \left(\frac{R}{D}\right)^{2/3} \left(\frac{S}{D}\right)^2$; W_{eff} is the peripheral velocity of the rotor, f_o is a coefficient dependent on the geometry and H is a numerical coefficient. A similar expression could also be derived for the dispersed phase. No evidence as to the applicability of this method is given in their paper. Hence the validity is unproven.

In conclusion, although in some cases the scale-up of Rotating Disc Contactors has been achieved successfully the methods to use are still far from clear. Therefore there is a need for further investigation in this area.

4. DROPLET PHENOMENA

In continuous counter-current equipment, the light phase may be introduced into the continuous phase via a distributor plate in an attempt to obtain a uniform initial drop size distribution. However, despite careful design of the distributor plate, with equi-sized sharp-edged perforations, all sizes of drops are observed in an agitated Counter Current Contactor. This distribution of drop sizes results from the coalescence-redispersion mechanism arising from the application of external energy. Since droplet size is an important factor influencing both the mass transfer process in terms of, the interfacial area and diffusion mechanism, and the volumetric capacity systematic design should be from droplet analysis considerations.

In general, the distribution of drop sizes produced in agitated systems represent an equilibrium between the competing effects of break-up and coalescence. Coalescence rates are related to inter-droplet distance, i.e. hold-up, but vary with position in both agitated tanks and columns. Therefore, although many models have been developed to predict the mean drop size it can only be accurately determined experimentally (54, 63). In addition, because mass transfer is enhanced by coalescence and re-dispersion, discrete drop mass transfer rate data cannot easily be applied to the real situation in a column. However, in work with a variety of organic liquids dispersed

in water in a pilot scale R.D.C section, it was found that, in the absence of mass transfer, interdrop coalescence was negligible, until flowrates approached the flood point (54). Hence in the absence of any special interfacial effects associated with mass transfer, the column appears to function as a discrete drop contacting device. However, both the break up and formation mechanisms and interdroplet coalescence phenomena merit consideration since they are fundamental to the understanding of how columns operate.

4.1 Drop Formation

The rate of mass transfer in any liquid-liquid system is affected by the rate of formation of the droplets, their rate of passage through the continuous phase and finally their rate of coalescence.

In agitated columns, since the regime of formation is not dependent on agitator speed or hold up, but only on the linear velocity of dispersed phase through the distributor, some small discrepancy might be expected when correlating column mass transfer efficiency with operating parameters.

Recent work (64) has indeed shown that the rate of mass transfer of solute during drop formation in a spray column is large, and that 10% of the extraction occurs in the formation period. However, the majority of the

extraction is accomplished during passage of the drops through the continuous phase, and the rate of mass transfer during this period depends more on the fluid dynamics inside and outside the drops than on their distance of travel.

Hayworth and Treybal (65) and Null and Johnson (66) measured the drop volume produced from a nozzle. Treybal et al proposed the following correlation from theoretical considerations,

$$V_F + 4.11(10^{-4}) V_F^{2/3} \left(\frac{\rho_D V^2}{\Delta\rho} \right) = 21(10^{-4}) \left(\frac{\sigma_D}{\Delta\rho} \right) + 1.069(10^{-2}) \left(\frac{D_N^{0.747} V^{0.365} \mu_c^{0.186}}{\Delta\rho} \right)^{3/2} \quad (4.1)$$

where the symbols are defined in the nomenclature. Equation 4.1 is also presented in their paper in the form of a graph from which the drop diameter can be estimated without trial and error. However, an important limitation of their study was the use of surfactant to study the effect of interfacial tension on the drop diameter, since the effect of surfactant cannot be characterised solely by the resultant equilibrium lowering of interfacial tension. Scheele and Meister (67) first pointed out the drawback of using a synthetic wetting agent for the lowering of interfacial tension. They concluded that the effect cannot be

characterised simply by the resultant equilibrium interfacial tension lowering, because for a given surfactant concentration the interfacial tension increases with increasing velocity through the nozzle as a result of the slow diffusion of surfactant to the interface. This causes a much greater increase in the drop volume, with increasing nozzle velocity than is observed for pure liquids. Thus the allowance for interfacial tension dependency proposed by Hayworth and Treybal will cause appreciable error if the correlation is applied to pure systems with low interfacial tensions.

Null and Johnson presented an empirical correlation based on experimental observation of the drop geometry (66). Their results were presented in the form, of a correlation which included Froude, Laplace and Weber numbers. Both groups of workers based their analyses on photographs which illustrated the drop formation process.

Harkins and Brown (68) derived a correlation for the drop volume by equating the buoyancy forces acting to detach the drop from the nozzle with the interfacial force. Their analysis also included a constant F , the Harkins and Brown coefficient, for the liquid portion left at the tip of the nozzle, after a drop had broken away from it. The correlation is,

$$V_o = \frac{\pi D_N \gamma}{\Delta \rho g} F \quad (4.2)$$

where F is a function of $\phi/2a$ and,

$$a = \left(\frac{2\gamma}{\Delta\rho g} \right)^{\frac{1}{2}} \quad (4.3)$$

Ryan (69) presented a semi-empirical correlation based upon a wide range of experiments. This is,

$$V = V_o \left[1 + 1.38 \frac{g\Delta\rho D_F}{\gamma_F} \frac{D_N U_N}{2U_T} - 2.3 \frac{\rho_D D_N U_N^2}{2\gamma_F} \right] \quad (4.4)$$

where U_T is the drop terminal velocity which can be estimated from the Hu-Kintner correlation. The constants in Equation 4.4 were obtained by a statistical treatment of the experimental results.

Rao et al (70) criticised the semi-empirical equation of Hayworth and Treybal, which was based on a force balance in which the various forces acting on the drop were expressed as fractions of the total drop volume, since the exact instant at which the forces act is not known nor is their quantitative contribution to the total volume. They also pointed out that the model of Null and Johnson neglected the viscosity of the continuous phase, which plays an important role in the model proposed by Hayworth and Treybal. Hence they developed a 'two stage' model; the stages being the static drop stage, when only inflation of the drop takes place, and the detachment stage when the drop rises and detaches from the capillary. Two models were actually proposed for the 2nd stage. Static drop volume was given by,

$$V_s = \frac{2\pi R\gamma\phi (R/V^{1/3})}{(\rho_c - \rho_d)g} \quad (4.5)$$

where $\phi (R/V^{1/3})$ was a correction factor suggested by Harkin and Brown. For the final volume of the drop the expression proposed was,

$$V_F = V_S + V_D \quad (4.6)$$

where V_D was the volume added to the drop, during the detachment stage, due to the continuous pumping of the dispersed phase. V_D was then calculated from the volumetric flow rate and an estimation of the time of detachment.

The first model proposed for the 2nd stage was applicable to liquids of low viscosity and gave velocity v of the drop as,

$$v = \frac{C}{A} + B\left(\frac{t}{A} - \frac{1}{A^2}\right) + \left(\frac{B}{A^2} - \frac{C}{A}\right)C\exp(-At) \quad (4.7)$$

where

$$A = \frac{6\pi r\mu}{m}$$

$$B = \frac{\theta(\rho_c - \rho_d)g}{m}$$

and

$$C = \frac{\theta V_c \rho_d}{m}$$

The second applies to very viscous liquids and is given as

$$A \cdot D_S = \frac{Bt^2}{2} \quad (4.8)$$

where $t = \left(\frac{2AD_S}{B}\right)^{\frac{1}{2}}$ (4.9)

As in Hayworth and Treybal's work the effect of interfacial tension was predicted from the results of experiments using a surface active agent.

Recently Heertjes and De Nie (71) proposed a model for drop volume based on two stage formation. The first stage involves pure growth of the drop ending with equilibrium forces and the second stage is the period of release. Models have been developed for essential variables, which are the forces acting upon a drop, the way the dispersed phase enters the drop, the necking of the drop as a function of time and finally the velocity of rise of the neck. The drop volume released was given by,

$$V_F = V_{eg} + V_{re} \quad (4.10)$$

where $V_{eg} = FV$.

The value of V can be obtained from a balance of forces.

$$\text{Also } V_{re} = 2 T_g t_{rl} \quad (4.11)$$

in which time t_{rl} follows from,

$$T_2 t_{rl}^2 + (T_8 - T_9) t_{rl} - T_7 = 0 \quad (4.12)$$

where the terms T_2 , T_7 , T_8 and T_9 are the mathematical expressions given in the paper. There are several expressions to evaluate the T terms depending on the flow rate. The correlation predicted drop volume within an accuracy of 15% at all flowrates below jetting velocity. The correlations could be applied for $\mu_c < \approx 200$ C.P. and $0.025 \text{ cm} < d_1 < 0.6 \text{ cm}$. Deviation may arise from surface active agents and critical conditions such as extremely small density differences.

Scheele and Meisler (67) working with Newtonian liquids at low velocities proposed a correlation for the drop volume on the basis of a two stage model. The final correlation was,

$$V_D = F \left| \frac{\pi \sigma D_N}{g \Delta \rho} + \frac{20 \mu Q D_N}{D_F^2 g \Delta \rho} - \frac{4 \rho_d U_N}{3 g \Delta \rho} + 4.5 \left(\frac{Q^2 D_N \rho_d^2 \sigma}{(g \Delta \rho)^2} \right)^{1/3} \right| \quad (4.13)$$

where the constants were obtained only from data in which the dispersed phase was less dense than the continuous phase. The theoretical analysis should also be valid in the reverse situation provided injection is vertical. The only difference between the two situations is the direction of the pressure gradient in the continuous phase relative to the direction of dispersed phase injection.

These authors also plotted F vs. $D_N (F/V_F)^{1/3}$. The quantity $D_N (F/V_F)^{1/3}$ can be calculated directly when the drag term is negligible. For a continuous phase viscosity > 10 centipoise the drag term is no longer negligible and it is necessary to employ a trial and error solution.

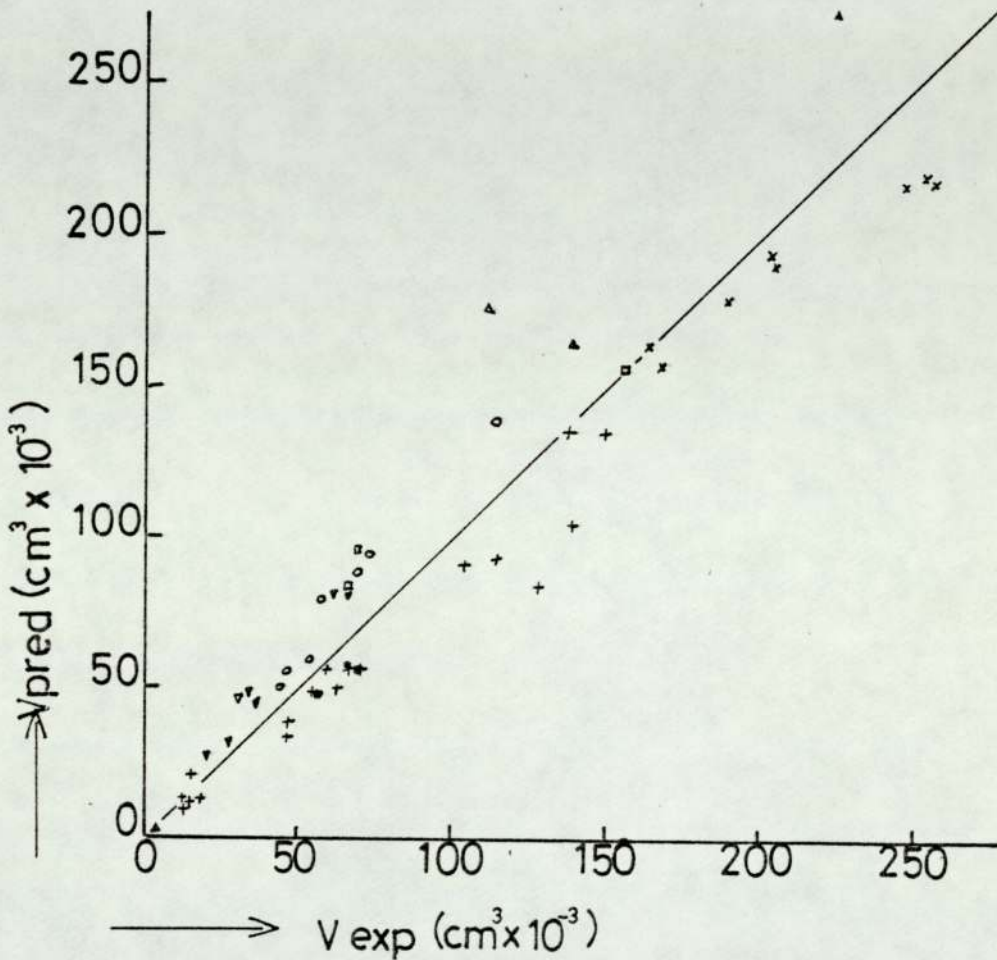
In all the recent publications on drop formation, theoretical consideration has been given to the relations for the prediction of drop volumes with all the studies distinguishing between two periods during drop formation. The correlation given by Null and Johnson (66) was based



on experiments with 34 systems, with the advantage that none of the experiments involved the use of surface active agents.

Narsinga Rao, et al (70) used the volume formed at infinitely slow formation as the basis for drop formation until the beginning of release and added a volume ϕ_{tre} . This model has limitations since the volume V_{eq} is certainly influenced by the speed of formation and the introduction of two different models for growth during the second period has no connection with the experimental observation. Furthermore, the criteria for release, such as velocity of rise being equal to $\frac{1}{2} \mu_c$, or the length of the neck being equal to the diameter of the drop certainly do not hold at high or low speeds of formation.

Scheele and Meister (67) used an elaborate application of force balances to predict the drop volume at the nozzle. Like others, they presented an expression fitting their own experimental observations. As shown in Fig. 4.1 this is open to some criticism. In addition, the Harkins and Brown correction factor was applied for non-static conditions to any drop volume and no consideration was taken of the interfacial tension changes during release. Ryan's analysis is also based on experimental data. Unfortunately, the accuracies of prediction by the various correlations are uncertain. For example significantly different experimental values have been presented by



Symbol Used	Author	System No.	Dispersed phase	Reference
X	Meister	10 - 12	Paraffine oil-heptane Different ratios	67 "
⊙	id	13	Benzene	"
▲	id	7	Butanol	"
+	id	1, 3 - 6	Heptane	"
○	Ryan	-	Cyclohexanol	69
△	id	-	Benzene	"
▽	id	-	MIK	"
◻	id	-	Hexane	"
▽	id	-	Phenetol	"

Continuous phase in water except for the systems 3 - 6 where a glycerol-water mixture has been used in different ratios.

FIG. 4.1 COMPARISON BETWEEN PREDICTED DROP VOLUME (V_{pred}) AND EXPERIMENTS (V_{exp}) FROM DIFFERENT AUTHORS.

different workers for benzene drops in water. Also Fig. 4.1 shows the results of Meister and Scheele and Ryan on different sides of the diagonal indicating that deviations between $V_{\text{pred.}}$ and $V_{\text{exp.}}$ were probably due to inaccuracies in experimentation or in the physical constants, mainly interfacial tension, used.

In conclusion, Scheele and Meister's method of prediction of drop volume has certain advantages over the other methods since,

- (i) It is based on a sound momentum balance.
- (ii) It covers a wide range of conditions of drop formation, from infinitely slow to the formation by the break up of jets, and
- (iii) predicted volumes agree with those determined experimentally within the accuracy limits shown in Fig. 4.1.

The only drawback of their model is the need for trial and error solution for the drop volume at higher viscosities. However, since the majority of systems encountered in liquid extraction practice have a viscosity less than 10 cp. Equation 4.13 can be solved analytically, by neglecting the drag term.

4.1.2 The Surface Area of the Drop During Formation

Until recently drop surface area was commonly determined by considering the drop as a perfect sphere.

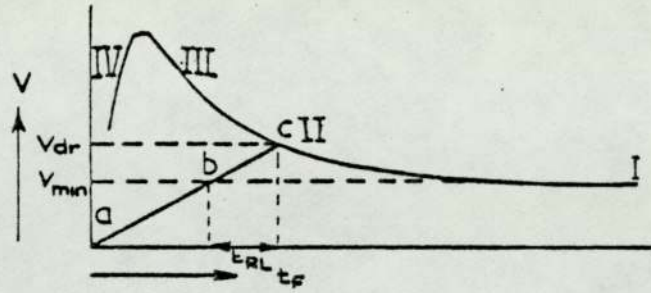


Fig. 4.2 The relation between drop volume and time of formation

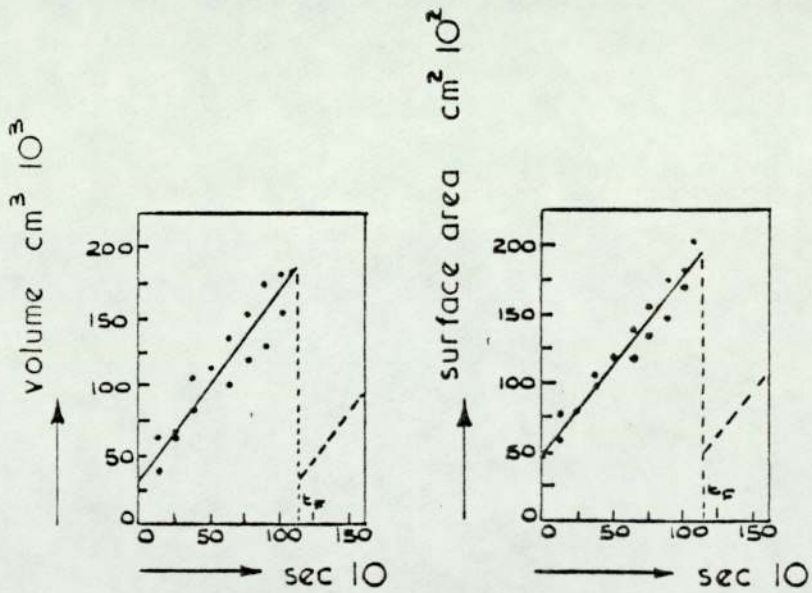


Fig. 4.3 Volume - time relation and surface area - time relation for drop formation

However, whilst studying absorption measurements with drops formed over the outside of capillaries, Dixon and Russell(72) found that they were not spherical. They therefore proposed a linear relationship between mean surface area and mean volume during formation.

From experiments with isobutanol-water Heertjes and de Nie (71) proposed the following relationship.

$$A = A_{\theta} + A_R = BV + A_R \quad (4.14)$$

where A is the total surface in cm^2 at any time between $\theta = 0$ and $\theta = \theta_F$.

B is a proportionality factor, in cm^{-1} , and independent of the flowrate and time, except at high flow rates, but dependent on the diameter of the capillary.

V is the volume of the growing drop between $\theta = 0$ and $\theta = \theta_F$;

A_R is the surface of the rest drop, i.e. the drop remaining at the capillary after the release of the drop;

A_{θ} is the surface area of the growing drop, at any time between $\theta = 0$ and $\theta = \theta_F$.

Nodberg (73) determined a relation between surface area and volume of a drop which is independent of time. The system used was methyl isobutyl ketone-water and the relation is presumably restricted to this.

Angelo, Lightfoot and Howard (74), measured the

change of surface area with time and the change of volume with time for the system isopar-Hx-water. The results presented in Fig. 4.3 point to a linear relationship between surface area and volume.

4.2 Droplet Break-Up

The break up of droplets in an R.D.C. occurs

- (a) when the magnitude of the dynamic pressure acting upon a drop, surpasses the magnitude of the cohesive surface forces, and
- (b) the droplet stays in the high shear zone for a sufficient period of time.

Kolmogoroff (75) first studied turbulent flow in a stirred tank and developed a theory of local isotropy. This postulated that 'in turbulent flow, instability of the main flow amplifies existing disturbances and produces primary eddies which have a wavelength, or scale, similar to that of the main flow. The large primary eddies are also unstable and disintegrate into smaller and smaller eddies until all their energy is dissipated by viscous flow'. When the Reynolds number of the main flow is high, most of the kinetic energy is contained in the large eddies, but nearly all dissipation occurs in the smallest eddies. If the scale of the main flow is large compared to that of the energy dissipating eddies, a wide spectrum of the intermediate oscillations or eddies exist, which

contain and therefore dissipate little of the total energy. These eddies transfer kinetic energy from the large to small eddies and, because this transfer occurs in different directions, directional information of the large eddies is gradually lost.

Kolmogoroff (75) concluded therefore that all eddies which are much smaller than the primary eddies are completely independent from them statistically. The only remaining information which these small eddies receive from the primary eddies is the amount of kinetic energy transferred by them to smaller eddies. If the main flow is time independent, the statistical properties of any oscillation of a scale much smaller than the main flow should therefore be determined by the local energy dissipation rate per unit mass.

Many authors have used the theory of local isotropy to derive expressions for the stable drop size in a turbulent field and supported it with experimental results.

Hinze (76) considered the fundamentals of the break-up process and characterised them by two dimensionless groups. A Weber group N_{We} and a viscosity group N_{Vi} . The analysis covered the mechanism of disintegration and all the constituent stages, from bulk liquid into globules of fluid and finally break up into small size droplets. The forces controlling the splitting up of a globule were postulated as a deformation force τ , a surface force (σ/d)

and a viscous stress $\frac{\mu_d}{D} \left(\frac{\tau}{\rho_d}\right)^{1/2}$. These three forces per unit area control the deformation and break up of a globule. The ratio between each two of the forces is a dimensionless magnitude; three dimensionless groups may therefore be formed in this way, only two of which are independent.

For one of the dimensionless groups the combination $N_{We} = \tau D / \sigma$ is a generalised Weber group. The other dimensionless group selected was $N_{Vi} = \frac{\mu_d}{\sqrt{\rho_d \sigma D}}$. The greater the value of N_{We} the greater the external force τ compared with the counteracting interfacial tension force σ/D , the greater the deformation. At a critical value $(N_{We})_{crit}$, break up occurs.

Hinze extended Kolmogoroff's (75) energy distribution law to predict the size of the maximum stable drop in a turbulent field as,

$$D_{max} \left(\frac{\rho_c}{\sigma}\right)^{3/5} E^{2/5} = C \quad (4.15)$$

where C is a constant. The value of C was calculated as .725 from experimental data of Clay. The difference in density between the dispersed and continuous phase was concluded to have an important effect on the way in which break up occurs.

Rushton (77) derived the following correlation for a fully baffled vessel,

$$We = \frac{K_1 N^2 R^{4/3} d^{5/3} \rho}{\sigma} \text{ for } d \gg y \quad (4.16)$$

Vermeulen (78) derived a similar type of expression which gave results in good agreement with Equation 4.16. A wide range of liquid systems were considered and coalescence of the droplets was also taken into account. This was omitted in all previous studies either by presenting results as discrete drop data, or by reducing the hold up to a minimum and then extrapolating to zero hold up.

Thus the minimum values of the mean drop diameter were expressed by the relation

$$\frac{N^2 d^{5/3} L^{4/3} \rho'}{\sigma f \phi^{5/3}} = 0.016 \quad (4.17)$$

where $f\phi$ is the function of hold up and coalescence.

Later Shinnar and Church (79) using an analysis based on consideration of local pressure fluctuation in the turbulence and the kinetic energy of the drop, gave the droplet break up mechanism for liquid systems of nearly equal densities and viscosities. The argument they put forward was that a droplet suspended in turbulent flow is exposed to local fluctuations. For nearly equal densities and viscosities of the two phases, the droplet could be assumed to oscillate with the surrounding fluid. An oscillating drop becomes unstable if the kinetic energy E_k is sufficient to make up for the difference in the surface energy between the single drop and two smaller

drops formed by break up. This leads to,

$$E_k/\sigma d^2 = \text{constant} \doteq .26 \quad (4.18)$$

Under conditions of local isotropy Shinnar and Church proposed that the E_k of the single oscillating drop was proportional to $\rho u^2 (d)d^3$, which on substitution into Equation 4.19, leads to the final result,

$$\rho u^2 (d)d/\sigma = We = \text{constant} \doteq .26 \quad (4.19)$$

Results of experiments using two baffled tanks with geometrically similar 4 blade paddle agitators and a variety of systems resulted in the following correlation from dimensional analysis,

$$\frac{\rho N^2 D^{4/3} d^{5/3}}{\sigma} = 0.016 \quad (4.20)$$

Levich (80) derived an expression for the size of the maximum stable drop in a turbulent field. Droplet rupture was assumed to occur when the difference in dynamic pressures at different points on the surface of a drop, which arise due to velocity variations within the continuous phase, exceeds the smallest value of surface force at any point. From the work of Kolmogoroff (75), the difference in dynamic pressure exerted on opposite sides of a drop of radius r is,

$$\Delta P_1 = \frac{K_f \cdot \rho_c (V_1^2 - V_2^2)}{2} \quad (4.21)$$

where K_f is the coefficient and V_1 and V_2 are the

velocities of the continuous phase at a distance $2r$ apart. Large scale eddies that do not vary over the drops diameter will not produce drop deformation and breakup. Therefore only relatively small eddies need be considered. The change in the eddy velocity over a length $d = 2r$ is,

$$\Delta V_{2r} = (2r \cdot E)^{1/3} \quad (4.22)$$

where $E = \epsilon/\rho$, is the energy dissipated per unit mass of liquid. Combining Equation 4.21 and 4.22,

$$\Delta P_1 = K_f \rho_c \left(\frac{2r\epsilon}{\rho} \right)^{2/3} \quad (4.23)$$

This is balanced by the force due to surface tension,

$$\Delta P_2 = \frac{\sigma}{d} = \frac{2\sigma}{r}$$

Equating ΔP_1 and ΔP_2

$$K_f \rho_c \left| \frac{2r\epsilon}{\rho} \right|^{2/3} = \frac{2\sigma}{r} \quad (4.24)$$

Since, however, $\epsilon = \rho (\Delta V)^{3/2}$ where L is a characteristic dimension of turbulence the radius of the stable size is,

$$r_{s.d} = \sqrt{2} \left| \frac{\sigma}{K_f \rho} \right|^{3/5} \frac{L}{V^{6/5}} \quad (4.25)$$

Coefficient K_f has a value of the order of 0.5 for the fragmentation of liquid drops falling in a gaseous medium and this value can be used in the calculations since the stable drop size is not a strong function of K_f .

Misek (50) considered droplet break up in an R.D.C. and postulated that as the rate of flow of both liquid phases is negligible compared with the peripheral velocity

of agitation, break up of drops in an agitated contactor can be considered as identical with the break up of drops in a closed system. It was further argued that there was similarity between the mixing and break up processes associated with a turbine mixer and the rotating disc. It was emphasised that theoretical derivations deal basically only with the break up of a single drop and no attention is given to the correct choice of the mean drop size for the practical solution involving a large number of drops.

The final correlation presented for the turbulent region, i.e. $Re > 5.74 \times 10^4$, with the exponents evaluated experimentally, was,

$$d_{1.2} \frac{N^2 R^2 \rho_c}{\sigma_{\exp}(0.0887\Delta R)} = 16.3 \left(\frac{H}{D}\right)^{0.46} \quad (4.26)$$

On diminishing the mixing intensity below a critical value of Reynolds number $(Re)_{\text{crit}} = 5.74 \times 10^4$. splitting of drops occurs in a transitive region in which viscous shear forces have some effect. The expression then valid is,

$$\frac{d_{1.2} N^2 R^2 \rho_c}{\sigma_{\exp}(0.0887\Delta R)} = 1.345 \times 10^{-6} \left(\frac{R^2 N \rho_c}{\mu_c}\right)^{1.42} \quad (4.27)$$

Further decrease in the mixing intensity into the laminar region results in the vertical droplet velocity becoming significant in that break up occurs mainly by successive impacts on the stators and discs. By analogy with break up in packings, therefore, for Reynolds numbers

below 10^4 (50),

$$d = .38 \left(\frac{\sigma}{\Delta \rho g} \right)^{0.5} \quad (4.28)$$

These equations are claimed to enable prediction of drop sizes with a fair degree of success, albeit under acollusive conditions. Under actual column operating conditions, however, droplets which travel in all directions may collide and coalesce.

In addition in an agitated column a distribution of drop sizes exists along the column length. Thus the assumption of a single mean drop size may lead to serious error in interpretation of mass transfer data in a column. Also the drop size is a function of hold up, which is itself a function of column height. This effect of hold up variation on drop size distribution is not accounted for in analyses based on single compartments, i.e. stirred tank data. Al-Hemiri (37), took all these factors into account in interpreting data from a 4 inch diameter R.D.C., using various systems. The correlation for Sauter mean drop size was,

$$\frac{d_{32}}{R} = 4.7 \times 10^{17} \left(\frac{NR^2 \rho_c}{\mu_c} \right)^{-3.33} \left(\frac{\mu_d}{\mu_c} \right)^{0.23} \left(\frac{NR \mu_c}{\sigma_c} \right)^{2.0} (X)^{0.225} \text{Exp} | 0.40 \left(\frac{n}{Z} \right) | \quad (4.29)$$

The data were correlated to within 20% by Equation 4.29.

The limitations of using stirred tank data is

discussed further in the following paragraphs.

The break up of drops entrained in a turbulent stream has been studied extensively. As mentioned earlier the theory was first established by Kolmogoroff and later treated on the basis of his theory of turbulence by Hinge (70) and by Shinnar and Church (79). Endoh and Oyama (81) elaborated this theory and verified it experimentally. The resultant relations depend on the energy dissipated by the agitator and according to their work, drop sizes can be estimated from the following relations.

$$d_{10/D} \sim We_N^{-1/3} Re_N^{-1/3} ; \lambda \gg d.$$

$$d_{10/D} \sim We_N^{-3/5} \quad \lambda \ll d.$$

$$We_N = D^3 N^2 \rho_c / \sigma ; \quad Re_N = \frac{D^2 N}{\nu_c} \quad (4.30)$$

Transition between the regimes is gradual. Vermeulen and Williams (78) arrived at similar results from their experimental work. This can be taken as confirmation of Equation 4.30. In their investigation the size of drops was measured in a system agitated by a six-bladed turbine by means of light diffraction and the Sauter mean diameter correlated by the relation,

$$d_{32/D} \sim f_1(x) We_N^{-0.6} \quad (4.31)$$

$f_1(x)$ denotes the empirically determined function of hold-up

of the dispersed phase, which corrects the results for the effect of the coalescence of drops. Similar results were reported by Kafarov and Babanov (82), who determined the mean diameter of drops by means of sedimentation analysis. They assumed that the drop size is related to the physical state of the system and correlated their results on the basis of dimensional analysis by the relation,

$$d_{32}/D \sim f_2(x) We_N^{-0.5} Re_N^{-0.1} \quad (4.32)$$

in which $f_2(x)$ serves a similar purpose to the $f_1(x)$ function of Vermeulen, but is of different form.

The relation derived by Levich (80) for the break up of drops in the turbulent region is of a somewhat different form. In the proximity of the agitator and vessel walls this is,

$$d/D \sim We_N^{-1/2} Re_N^{-1/2} \quad (4.33)$$

which suggests a more pronounced effect of viscosity on drop size. For drops falling in a motionless medium the relation,

$$dN^2\rho/\sigma = \text{const.} \quad (4.34)$$

was derived and verified. This expression also holds, with different values of the constants, for the break up of a jet of liquid in a stream of fluid.

The fact that the results of Misek (50) do not agree with Equations 4.30 and 4.33 but show agreement with Equation 4.34 may be explained by:

- (1) Possibly different mechanisms of drop break up with a rotating disc and turbine mixer.
- (2) The theoretical derivations deal only with the break up of a single drop and no attention is given to the correct choice of the mean drop size for a process involving a large number of drops. The distribution of drop sizes would be expected to vary with the intensity of mixing and different relations will be found for different mean values of drop sizes. Hence it can be shown from Equation 4.27 and 4.31 that, as would be expected, with higher values of the Weber number, the fraction of small drops increases.
- (3) In the published experimental work the effect of coalescence of drops has not always been eliminated in a suitable manner.

Finally, from work on droplet break up in an R.D.C., Mumford and Jeffreys (54) concluded that drops below the minimum stable size do not break up and, for any application, there is a minimum speed below which the rotating disc does not affect the drop size distribution. The upper limit may be determined by the inlet distributor and the lower limit by the impact mechanism.

They also concluded that the mean drop size cannot be predicted from fundamentals for several reasons, viz:

- (a) Whilst for a given velocity (V) of a homogeneous isotropic flow drops formed in it should be of single size (81), droplets were observed to produce four or more unequal sized daughter drops on rupture.
- (b) In small columns with large drops, the proportion of drops which impinge vertically within one drop diameter of the disc or stator peripheries, or horizontally on the edge of a stator ring, and which would be expected to suffer break up is no longer insignificant.
- (c) In columns with large discs, there is a wide variation of V in the unstable region and hence a spectrum of stable drop sizes.

4.3 Drop Size Distribution

To achieve a useful analysis of extraction data for agitated columns the assumption is commonly made that the drops are spherical and of uniform size. An interfacial area \bar{a} , contact time \bar{t} , and transfer coefficient \bar{k} can then be defined, based on the average drop. From this the characteristic number of transfer units $\bar{T} = \bar{k} \bar{a} \bar{t}$ can be obtained at a certain plane in contactor space and for the drop population as a whole.

However, a rather wide distribution of drop sizes

is frequently encountered. Moreover, beyond the inlet there are the competing effects of generation of new drops due to shear or local turbulence in the bulk flow, and of droplet coalescence due to drop interaction effects. Depending upon the characteristics of the flow there will be a balance between these processes such that, at a distance considerably removed from the inlet, two limiting situations may be visualised. These are, either a distribution of drop sizes and drop residence times, i.e. little drop interaction, or a size distribution of drops all essentially of the same age, i.e. equal probability of repeated coalescence and redispersion among drops of all sizes. This size distribution is bounded by an upper limit or maximum stable size and a lower limit or minimum size, depending upon the break up process prevailing. The minimum size, as viewed at a fixed station by an observer, may be dictated by the size that is just entrained by the counter flowing continuous phase. In the simplest analysis, the age distribution mentioned, is given directly, in the absence of coalescence effects, by the hindered settling rates of the size fractions present.

Extending the non-coalescing drop picture one step further to include axial mixing effects in the contactor, the large drops which are present escape, or bypass through, the contact zone much more readily than the average drop. Whereas the smallest drops persist for long times, owing to their small inertia, and may be highly back-mixed by any gross eddy motions in the continuous phase. When mass

transfer is occurring between the phases, then these effects lead to a transfer process that is not described, except fortuitously by the usual simplified transfer mechanism based on the volume surface mean diameter drop. The difference between the real and idealised situations will depend upon the particular transfer mechanism between drops and continuous phase and may be particularly acute for high-purity extractions or when back-mixing is severe.

Therefore the assumption of uniform drop size may lead to serious error, when interpreting mass transfer and related processes in a rotary agitated contactor.

Olney (52) studied the variation of drop size distribution with rotor speed, drop hold up and system properties, ρ_c , ρ_d , μ_c , μ_d and σ . It was found that these variables, and in particular rotor speed, had a marked effect on the average or characteristic drop size but not much effect on the parameters of size distribution. As one example, the data for white oil dispersed in water reproduced in Fig. 4.5 shows that the volume median drop size d_{50} decreased from 3.1 to 0.8 m.m. as rotor speed was increased from 650 to 1100 rev/min but the width of the size distribution, described by d_{95}/d_5 , changed only from 4.5 to 4.2. The increase in drop size over the whole spectrum, with increase in drop hold-up may have been caused solely

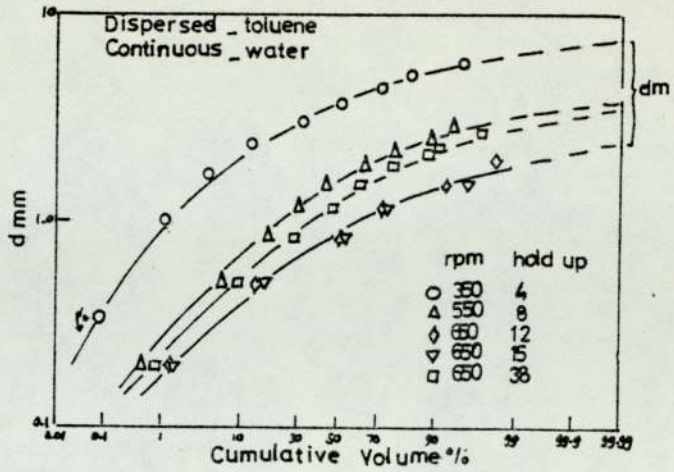


Fig 4.4 DROP SIZE DISTRIBUTIONS, 6 in.R.D.C.

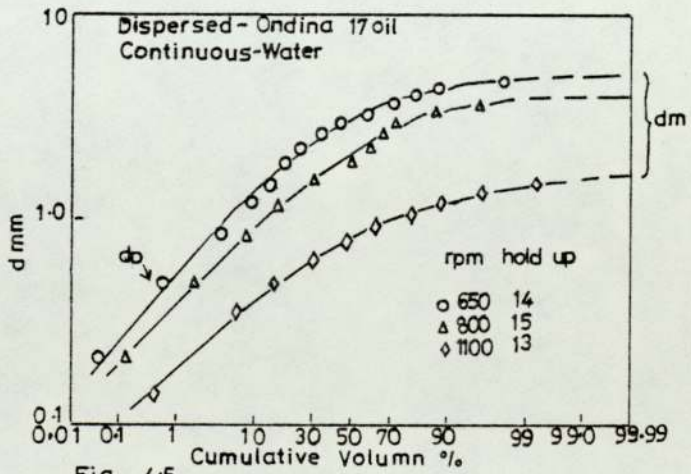


Fig 4.5
DROP SIZE DISTRIBUTIONS, 6 in. R.D.C.

by the higher drop interaction rates due to smaller interparticle distance. Olney (52) recognised several parameters of the size distribution. In addition to d_{32} defined as,

$$d_{32} = \frac{\sum n_i d_i^3}{\sum n_i d_i^2} \quad (4.35)$$

these are d_{50} and the ratios d_{32}/d_{50} , d_{95}/d_{50} and d_5/d_{50} .

To sum up, the fact that the characteristic settling diameter for a drop population can be predicted from single drop dynamics does not mean that this diameter is suitable to characterise all events of interest in a countercurrent flow device. The appropriate drop diameter that represents the average transfer rate for a mass transfer process depends upon the transfer mechanism and the parameter of the size distribution, and this diameter will not necessarily be d_{32} . Addition of axial diffusion effects for the drop and continuous phases further complicates the computation of an 'average' diameter which may be used to represent the average transfer unit.

The droplet distribution in a conventional R.D.C. differs from that in other counter current extractors, because of different breakup and drop interaction mechanisms.

Hence Jeffreys and Mumford (54) found that in the R.D.C. droplet break up was limited to the transitive and laminar regions by virtue of equipment size. Over

the range of interfacial tension studied a critical minimum speed was established, below which a layer of dispersed phase droplets built up beneath the rotor disc and the mean droplet size was independent of the hold up. At higher speeds, the overall tendency was for drop sizes to increase over the whole spectrum with hold up as described by Olney (52).

Vermeulen (78) studied the effect of volume fraction on the mean diameter in a stirred tank and correlated it by,

$$\frac{d}{D\phi} = G N_{We}^{-0.6} \quad (4.36)$$

This was confirmed by Calderbank (83) who varied the hold up from 0 to almost 20% and proposed a similar correlation,

$$\frac{d}{D} = \epsilon (1 + 9\phi) N_{We}^{-0.6} \quad (4.37)$$

Skinner and Church (79) confirmed the above findings and proposed the following correlation for acollusive conditions,

$$\frac{d}{D} = C_3 N_{We}^{-0.6} \quad (4.38)$$

They added an extra term, energy of adhesion between two drops, for high hold-up and gave the expression,

$$\frac{d}{D} = C_4 N_{We}^{0.375} \left| \frac{A(h)}{YL} \right|^{0.375} \quad (4.39)$$

Skinner and Church (79) also showed that for very small drops, where drop diameter was small compared with the

Kolmogroff length, the drop broke up through viscous shear. Local velocity gradients would be expected to be a function of the kinematic viscosity and the energy dissipated per unit mass. The Kolmogroff length η is defined

$$\eta = \left(\frac{\nu_c^3}{\epsilon}\right)^{\frac{1}{4}} \quad (4.40)$$

The velocity gradient would be

$$\bar{V} = f(\epsilon, \nu) \quad (4.41)$$

which by dimensionless analysis becomes

$$\bar{V} = c_s \left(\frac{\epsilon}{\nu_c}\right)^{\frac{1}{2}} \quad (4.42)$$

Equation 4.42 was used by Sprow (84) to develop a correlation for the maximum drop size existing in an emulsion. He used the criterion proposed by Taylor that break up by viscous shear was a primary function of the Weber number and that for every system there would be a critical Weber number at which the break up of the drops would occur. That is

$$We_{crit.} = f\left(\frac{\mu_d}{\mu_c}\right) = \frac{c_s \mu_c \epsilon^{0.5} d_m}{\mu \nu_c^{0.5}} \quad (4.43)$$

For drops smaller than the Kolmogroff length the maximum drop size in a dispersion could be correlated by

$$d_m = c_5 \cdot \mu \cdot \nu_c^{0.5} \cdot \mu_c \cdot N^{-1.5} D^{-1} f\left(\frac{\mu_c}{\mu_d}\right) \quad (4.44)$$

where N was the speed of the agitator and D was the diameter of the agitator.

Bouyatiotis and Thornton (63) found that for both batch and continuous operation in an agitated tank the measured distribution approximated to a normal one. Similar results for different systems have been reported by Chen and Middleman (85) and Brown and Pitt (86). However, Pebalk and Misher (87), reported that for a variety of liquid-liquid systems, including Kerosene-water as used by Brown and Pitt (86), the drop size distribution in the stirred tank was lognormal. Similarly, Giles et al (88) reported a lognormal distribution during nitration of toluene in a stirred tank.

Whether the drop size distribution is normal or lognormal is of practical importance in an extraction column. For a fixed volumetric throughput, a comparison of the two types of dispersions is illustrated in Table 4.3.

For the prediction of hydrodynamics and mass transfer performance the preferred distribution is a mono-dispersion with a consequent standard deviation of zero. Although this is impracticable in an extractor, a distribution where the mode is equal to the mean results in more drops being nearer the mean size than with a lognormal distribution. Droplet characteristics are thus more predictable with a normal distribution. Therefore it is desirable to obtain a normal distribution around a certain mean drop diameter rather than a lognormal one.

TABLE 4.3

PROPERTY OF DISPERSION	NORMAL	LOGNORMAL
Proportion of smaller droplets	lower	higher
Mean mass transfer coefficients	Higher because more drops are circulating	Lower. More stagnant drops
Interfacial area	lower	high
Settling rate	higher	lower
Tendency to flood the column	higher	lower

Mugele and Evans (89) have proposed an upper limit distribution (ULD) defined in terms of maximum particle size. This is in line with the concept of a maximum stable drop size in a turbulence or in shear flow, as discussed by Hinze (75), Sleicher (90) and others. Its application to experimental data for an R.D.C. has been demonstrated by Olney (8) and co-workers. The spacial upper limit function as applied to log probability distribution, was given by,

$$\frac{dv}{dy} = \frac{\delta}{\sqrt{\pi}} e^{-\delta^2 y^2} \quad (4.45)$$

where $y = \ln\left(\frac{ad}{dm-d}\right)$

A straight line plot of $d/(dm-d)$ vs. v on log probability paper gives

$$a = \text{skewness parameter} = \frac{dm-d_{50}}{d_{50}} \quad (4.46)$$

$$\delta = \text{uniformity parameter} = \frac{.907}{\ln_e \left(\frac{d_{90}}{dm-d_{90}} \times \frac{dm-d_{50}}{d_{50}} \right)} \quad (4.47)$$

The value dm used in each experiment was the maximum stable drop size observed on that particular photograph; the number of drops of size dm used in the calculation was,

$$nm \frac{A_c}{A_t} \quad (4.48)$$

where nm = number of drops of size dm on entire photograph generally one.

A_t = Area of entire photograph, and

A_c = Area of portion of photograph on which the drop size count was made.

The index δ determines the spread of the distribution, a smaller value indicating a wider range of drop sizes; a value greater than unity indicates a wider range of drop sizes larger than d_{50} .

The minimum drop size d_o is also of practical importance for countercurrent flow conditions, since drops of sufficiently small size will be entrained by the continuous phase. Eddy diffusion and drop redispersion will tend to cause some very fine drops to be present at a photographic station in any event. Nevertheless, the d_o corresponding to $U_d = 0$ should be in rough agreement with smallest drops observed in the photographs. Agreement with the smallest observed drops was in fact fair, most deviation occurring when the continuous phase was viscous.

4.4 Coalescence Processes

Coalescence processes are of importance in agitated columns since interdrop coalescence in the agitated zone is one factor determining the equilibrium drop size generated and coalescence is required at the interface near the dispersed phase outlet to achieve phase separation.

Within the agitated zone the drop size is determined by the balance between break-up and coalescence. This size determines the interfacial area and drop rise velocity.

The height of the dispersed phase separation zone at the top or bottom of the column depends on the ease with which phase coalescence occurs at the interface after mass transfer has taken place in the effective length of the column. This is also a function of the drop size generated.

The coalescence rate depends on the system properties, drop size and coalescence mechanism. There are three separate mechanisms of coalescence in any column.

- (a) Drop interface coalescence
- (b) Drop-drop coalescence
- (c) Drop-solid surface coalescence.

Since (c) is a special case of drop coalescence on the internals or the column wall, if wetted, in the mixing section it is discussed in detail in Chapter 7. Case (a) drop interface coalescence, must always occur in the settling section and is preceded by flocculation and

inter-drop coalescence.

4.4.1 Coalescence Fundamentals

Liquid-liquid dispersions are usually thermodynamically unstable systems. Since the free energy associated with the large interfacial area between the phases can decrease by aggregation or coalescence of the dispersed phase, from energy balance considerations coalescence of a liquid dispersion would be expected, until ultimately two liquid layers are formed. Coalescence generally occurs in three steps.

- (i) Flocculation of drops
- (ii) Collision and drainage of the continuous phase film until it reaches a critical thickness
- (iii) Rupture of this film.

The ease with which coalescence occurs depends on these steps, which are dependent on many variables. These are summarised in Table 4.4.

4.4.2 Interdrop Coalescence in the Agitated Zone

The extent to which interdroplet coalescence occurs in a column is of fundamental importance since, in conjunction with subsequent break-up by turbulence it results in the drop size distribution. Hence it determines the interfacial area and mean droplet velocity. It may also lead to an enhancement of mass transfer rate.

By analogy with droplet coalescence at a plane

interface, drop-drop coalescence can be deduced to occur in two stages, viz:

- (a) drainage of continuous phase from between elements until a critical film thickness is achieved, and
- (b) rupture of the critical film.

Therefore the speed of coalescence is dependent on the forces impelling droplets towards each other, the resistance to liquid film drainage and the thickness and ultimate strength of the critical film. Common experience is that the presence of grease or dirt aid droplet interaction, whereas surfactants profoundly decrease the tendency for coalescence. In systems in which mass transfer is taking place, coalescence is favoured when the direction of transfer is from the dispersed to the continuous phase and hindered when it is in the opposite direction (8, 9, 41). Therefore hydrodynamic correlations which are determined in the absence of mass transfer may require considerable modification in practice. Furthermore, since the effect is usually a function of solute concentration, Sauter mean drop size d_{32} would be expected to vary with the contactor height.

The analysis of drop-drop coalescence, which represents a dynamic situation in agitated systems is rather difficult because,

1. It is difficult to reproduce a controlled collision between two drops which have not been restrained in some way.
2. There is an inherent randomness in the manner in which the drops rebound or coalesce. Thus drop-drop coalescence studies necessitate consideration of both collision theory and the coalescence process. It follows that the prediction of coalescence frequency requires a knowledge of both collision frequency and coalescence probability.

From the above consideration and using a purely theoretical approach, Howarth (91) developed an equation to relate the frequency of coalescence with hold-up in a homogeneous isotropic turbulent flow,

$$V = \left| \frac{24x_d x \bar{V}^2}{d^3} \right|^{\frac{1}{2}} \exp(-3W_*^2/4\bar{V}^2) \quad (4.49)$$

Although this equation showed good agreement with Madden and Damerell's (92) observation for water drops dispersed in toluene in an agitated tank, the assumptions made in the derivation seriously limit the application to real systems (40).

There is little data on coalescence in agitated columns. In a pilot scale R.D.C. with the system kerosene-water, Davies et al (41) found that drop-drop coalescence was not significant. However, this was with phase ratios of 12 to 16 : 1, continuous:dispersed phase basis, compared with the 0.5 to 4:1 used in practice.

Misek (53) demonstrated the presence of coalescence in an R.D.C. at a high hold-up (18%). Later Mumford (54) found that interdroplet coalescence was significant only at very high hold-ups at a peripheral speed of the order of 460 ft/min. i.e. conditions approaching flooding.

In a later study Misek (53) characterised the dispersion by a hydraulic mean drop diameter and assumed that these drops exactly followed the turbulent fluctuations in the continuous phase. Every collision of droplets was assumed to result in coalescence. Since drop-drop coalescence can take place, either in the bulk of liquid or at the column wall. Misek proposed a different correlation for each case. For coalescence in the bulk of the fluid,

$$\ln \frac{d}{d_0} = k_7 (n' d^3) V_0^{\frac{1}{2}} \left(\frac{D}{\gamma}\right)^{\frac{1}{2}} = k_8 x \left(\frac{\sigma}{d_0 \rho}\right)^{0.5} \left(\frac{D}{\gamma}\right) = Z_2 x \quad (4.50)$$

For drop coalescence at the wall,

$$\ln \frac{d}{d_0} = k_5 (n' d^3) V_0 \left(\frac{D}{\gamma}\right) = k_6 x \left(\frac{\sigma}{d_0 \rho}\right)^{0.5} \left(\frac{D}{\gamma}\right) = Z_2 x \quad (4.51)$$

Coefficients Z_1 and Z_2 were determined indirectly based on phase flowrate measurements using equation,

$$\frac{V_d}{x} + \frac{V_c}{1-x} = \bar{V}_N (1-x) \exp \left| x \left(\frac{Z}{M} - 4.1\right) \right| \quad (4.52)$$

Drop size d_0 was calculated from the terminal falling velocities of solid spheres.

Fair agreement was obtained with this equation for a number of binary systems in various column designs; it was found to have a value of 1.59×10^{-2} independent of the type of agitator. The equation was applied but it is questionable, whether coalescence characteristics in different columns can, in fact be described by a single equation. For example equation 4.50 makes no allowance for the known variation in ease of coalescence with drop size.

The ease with which the coalescence takes place depends on a number of parameters. A summary of these along with the explanation is outlined in Table 4.4.

4.4.3 Flocculation and Coalescence in the Phase Separation Zone

After the mass transfer in the mixing section drops of the dispersed phase flocculate collide and finally coalesce into the interface. The ease with which the flocculated drops coalesce into the interface determines the height of the coalescing zone.

Studies of the coalescence of drops on the interface have revealed that the process takes place in the following stages:

1. Flocculation
2. Packing
3. Homonisation with the interface.

TABLE 4.4

VARIABLE	EFFECT ON COALESCENCE TIME	EXPLANATION IN TERMS OF EFFECT ON PHASE-2 FILM DRAINAGE RATE	
1. Drop size	Longer	More phase 2 in film	
2. Length of fall	Longer	Drop 'bounces' and film is replaced.	
3. Curvature of interface towards drop	(a) Concave	Longer	More phase 2 in film
	(b) Convex	Shorter	Less phase 2 in film
4. Interfacial tension	Shorter	Less phase 2 in film (more rigid drop)	
5. Phase ratio $\left(\frac{\mu_{\text{drop}}}{\mu_{\text{continuous}}}\right)$	Shorter	Either less phase 2 film or increase in drainage rate	
6. Phase $\Delta\rho$	Longer	More deformation of drop more phase 2 film	
7. Temperature	Shorter	Increases phase ratio	
8. Temperature gradients	Shorter	Thermal gradients 'weaken' film	
9. Presence of a third component			
(a) stabiliser	Longer	(a) Forms 'skin' around drop	
(b) mass transfer into drop	Longer	(b) Sets up interfacial tension gradients which oppose flow of film	
(c) mass transfer out of drop	Shorter	(c) Sets up interfacial tension gradients which assist flow of film	

(Effects of other parameters have been reviewed by Lawson (97))

The majority of time during the process of drop-interface coalescence is taken by the formation and drainage of the continuous phase film between the homo-phase. This is termed the 'rest time'. Workers have found that drops of the same size and properties coalescing under identical conditions exhibit a variation of coalescence times (93, 94, 95). Hence the coalescence times are reported as the mean times of numerous determinations; these are expressed as mean rest times, t_m or half rest time, $t_{\frac{1}{2}}$. The half rest time is the time taken for half the drops in the sample studied to coalesce. Generally $t_{\frac{1}{2}}$ has been found to be more reproducible than t_m , and the ratio ($t_m/t_{\frac{1}{2}}$) is always in the range of 1.01 to 1.27.

Several attempts have been made to correlate the coalescence time with the physical properties of the system. Jeffreys and Hawksley (94) proposed a correlation of the form

$$t_{\frac{1}{2}} = 4.5 \times 10^5 \left| \left(\frac{\mu^{\frac{1}{2}} \Delta \rho}{\gamma^2} \right)^{1.2} \left(\frac{T}{25} \right)^{-0.7} \mu^{\frac{1}{2}} \right. \\ \left. d^{0.02} \left(\frac{\gamma^2}{\mu^{\frac{1}{2}}} \right)^{0.55} L^{0.001} \left(\frac{\gamma^2}{\mu^{\frac{1}{2}}} \right)^{0.91} \right| \quad (4.53)$$

Jeffreys and Lawson (97) simplified the analysis on the basis that temperature affected only the physical properties so that it need not be considered as a variable as such. The resulting correlation was,

$$\frac{\gamma t}{\mu d} = 1.32 \times 10^5 \left(\frac{L}{D}\right)^{0.18} \left(\frac{d^2 \Delta \rho g}{\gamma}\right)^{0.32} \quad (4.54)$$

This correlation was supported by Smith and Davies (98) for drop interface and drop-drop coalescence. They showed that,

$$\left(\frac{\gamma t}{\mu d}\right) \propto \left(\frac{d^2 \Delta \rho g}{\gamma}\right)^{0.25} \quad (4.55)$$

The most recent study of residence times for single drop at an interface was by Hitit (96). Using pilot plant size 6 inches and 9 inches diameter spray columns, it was observed that there was no significant difference in the mean and half life coalescence times. Moreover, changing the distance of fall and the bulk dispersed-phase static head above the interface had no significant effect on the rest times. It was concluded that it was difficult to obtain reproducible results in large equipment. The applicability of laboratory single drop measurements in specially constructed cells to the behaviour of drops in swarms in pilot plant or industrial settlers, was considered questionable.

Hitit produced a number of correlations for height of coalescence zone for columns of different sizes, using the system toluene-water. The correlations are expressed as,

$$H = a_1 d_{12}^c V_d^b \quad (4.56)$$

The a_1 , c and b for different size columns are tabulated in his work.

This brief review of coalescence, of which many

conflicting studies have been reported, demonstrates the need for experimentation when scaling-up both the agitated region and the flocculation coalescence zone of R.D.C.'s. The coalescence rate is sensitive to impurities, for example interfacial scum, and surfactants, so that practical studies involve actual systems with recycle.

5. MASS TRANSFER FUNDAMENTALS

5.1 Mass Transfer During Drop Formation

The rate of mass transfer in an R.D.C. depends on the overall mass transfer coefficient, the interfacial area, and the driving force, as given by Equation 1.1. The overall coefficient of mass transfer depends on the rate of diffusion inside, across the interface, and outside the droplet. Although recent studies have shown that interfacial resistance may be important, for example when chemical reaction occurs, (56, 99) for all practical purposes it can be neglected in the design of industrial extractors (57). Equations 1.1 and 1.2 are then applicable.

To calculate the drop side coefficient it is necessary to analyse the different phases of a droplet's life inside a contactor. These comprise,

- (a) Formation at the distributor,
- (b) Travel through the continuous phase,
- (c) Coalescence at the bulk interface at the top or bottom of the column.

Various workers have determined the extent of mass transfer during initial drop formation in spray columns. Sherwood (100) found 40% of the transfer occurring during this period, West (101) only 15% and Licht and Pensing (102) found no special effect. However, recent studies (103, 104, 105) have shown that about 10% of the extraction

occurs during this period. Sawistowski (105) has outlined the difficulties involved in obtaining meaningful results due to the very rapid change in the interfacial tension associated with drop formation. Despite these difficulties numerous mathematical models have been presented to predict the transfer rate during drop formation.

For a stable interface, four models have been visualised for the behaviour of the growing boundary layer which increases in surface area. The bases are

- (1) In the first model an ageing rigid boundary layer which increases in surface area.
- (2) In the ageing boundary layer, the concentration gradient increases because of the increase of surface area by stretching: the balloon model.
- (3) The boundary layer ages as with a rigid layer. Surface is increased by addition of fresh surface elements: the fresh surface model.
- (4) For the boundary layer a flow pattern has been developed in which a varying rate of stretching occurs.

Various modifications of the models are possible and have been suggested. However, all models lead to a similar type of expression, describing the efficiency as proportional to the square root of the time of formation;

$$E_F = F \left(\frac{Dt_F}{\pi} \right)^{\frac{1}{2}} \quad (5.1)$$

in which F = proportionality constant which depends on the model used and on the surface area/volume relation of the growing drop.

The difference between the factors F for each of the four models has been compared for the simplified case of a spherical drop. For the drop of diameter d, the different models are presented in Table 5.1 and the F values collated in Table 5.2.

TABLE 5.1

EQUATION NUMBER	MODEL	AUTHORS AND REFERENCE NO.
5.2	$K_{df} = \frac{6}{7} (D_d / \pi t_f)^{\frac{1}{2}}$	Licht and Pensing (102)
5.3	$K_{df} = \frac{24}{7} (D_d / \pi t_f)^{\frac{1}{2}}$	Heertjes et al (104)
5.4	$K_{df} = \frac{4}{3} (D_d / \pi t_f)^{\frac{1}{2}}$	Groothuis and Kramer (106)
5.5	$K_{df} = 2\sqrt{3/5} (D_d / \pi t_f)^{\frac{1}{2}}$	Coulson and Skinner (107)
5.6	$K_{df} = 2(7/3) (a_o/a_r + \frac{1}{3}) (D_d / \pi t_f)^{\frac{1}{2}}$	Heertjes and De Nie (108)
5.7	$K_{df} = 1.31 (D_d / \pi t_f)^{\frac{1}{2}}$	Ilkovic (126)
5.8	$K_{df} = \frac{2}{\tau} \sqrt{\tau} (D_d / \pi t_f)^{\frac{1}{2}}$	Angelo et al (109)

TABLE 5.2

MODEL	$\frac{Fd}{6}$
1	.86
2	1.31
3	1.48
4	1.78 front
	1.31 equator
	0.50 rear

The selection of the appropriate model for a specific application is difficult because of the inaccuracies inherent in most of the experiments. However, model 1 seems unlikely, and there is little difference between models 2, 3 and 4.

Model 1 (102) has been recommended by some authors but has not been verified experimentally. At best it is a limiting case giving the lowest possible value of F . Model 2 (109, 110) has been applied to the case of uniform drop stretching. It was used by Baird (111) to test experimental results, and deviations from theory were less than 20%. These deviations may be explained by the existence of extra contributions to solute transfer because of turbulence.

Following experiments in which drops were formed at a capillary and sucked back again, Popovich et al (112) also concluded that model 2 could be used. This model can be applied for cases in which the major resistance to mass transfer is in the continuous phase but Baird (111) used it for a case where the resistance should be in the drop phase.

In model 3, the surface elements may have a time of contact with the continuous phase ranging from $t = 0$ to $t = t_F$. This model has been tested by Groothuis and Kramers (106) for mass transfer from a gas to a growing

droplet. Heertjes and de Nie (108), from a single drop study using the system isobutanol-water, concluded that model 3 could best explain their experimental results. However, this remains to be verified for other systems.

Model 4 has not yet been investigated for a liquid-liquid system but Nichols (113) tested it for gas bubbles growing in a liquid. The relations given, therefore, hold for the continuous phase during the formation of gas bubbles. The basic concept seems sound providing stretching occurs.

Skelland and Minhas (114) concluded that the above models are unrealistic because they fail to allow for the effects of internal circulation, interfacial turbulence and the disturbances caused by drop detachment. A modified expression was proposed for mass transfer coefficient,

$$K_{df} = 0.0432 \left(\frac{d}{t_f} \right) \left(\frac{v_n}{dg} \right)^{0.089} \left(\frac{d^2}{t_f D_d} \right)^{-0.334} \left(\frac{\mu_d}{\sqrt{\rho_d d \sigma}} \right)^{-0.601} \quad (5.9)$$

Approximately 25% deviation was obtained from this correlation with the system acetic acid-chloro-benzene-water and acetic acid-nujol- CCl_4 -water. The correlation represents the overall mass transfer occurring during drop formation, which includes mass transfer during drop growth,

during the detachment of the drop and the influence of the rest drop. A theoretical expression for K_{df} was also given,

$$K_{df} = \frac{V_d}{a_f t_f} \left(\frac{2I_f}{4V_d - I_f} \right) \quad (5.10)$$

The symbols are defined in the Nomenclature.

5.1.1 Mass Transfer at Different Rates of Formation

The models presented above are only valid in cases where no extra mass transfer occurs by liquid flow, or by eruptions at the interface, i.e. for stable interfaces. Furthermore, when considering the different models little attention has been given to the different regions of drop formation. Three regions, shown earlier in Fig. 4.2, are important in this respect.

Region I - Formation at Low Speed

Mass transfer is always accompanied by local changes in density. If the speed of formation is low, this results in free convection effects.

In this case, mass transfer is therefore comparable to that with drops formed at moderate speed but with a superimposed contribution due to free convection. Quantitative data are lacking on this phenomenon.

Region II - Formation at Moderate Speed

In this case mass transfer can be described by means of a diffusion mechanism. Both the surface stretch or fresh surface models may be used, but the fresh surface

model relates more closely to the actual process. Thus for the prediction of mass transfer the following general equation may be used (112),

$$E_F \cdot V_{dr} = \frac{4n}{2n+1} \int_0^1 \{ (1-y^2) dy \cdot (C^* - C_0) \left(\frac{D}{\pi} \right)^{\frac{1}{2}} B_P t^{(2n+1)/2} \} \quad (5.11)$$

where n and B_P are defined by the surface area $A = B_P t^n$ and $y = (1-t/t_1)^{\frac{1}{2}}$; t is the time at which a fresh surface element is formed and t_1 that when mass transfer is considered. For the special case of a spherical drop the equation reduces to,

$$E_F = \left(\frac{A_R}{2V_{dr}} + \frac{4}{3} B \right) \left(\frac{Dt_B}{\pi} \right)^{\frac{1}{2}} \quad (5.12)$$

Region IV - Formation at High Speed

In this region, large contributions to mass transfer are caused by strong circulation in the drop. Thus Groothuis and Kramer (106) observed a jet action in the drop at $Re > 40$ to 50; the characteristic diameter here was based on the inside diameter of the capillary. This is in agreement with the results of Dixon and Russell (115). Ueyama and Kida (116) also found a marked increase in mass transfer at high speed of formation. Heertjes and de Nie (108) reported that deviations from the diffusion model occur at $Re > 15$.

The present information leads to the conclusion

that circulation will occur in drops formed at high speeds. However, no theory or experimental data has been presented for this region.

5.2 Mass Transfer During Droplet Release

During the release of a drop, changes occur at the interface as a result of deformation; release causes oscillation of the drop. Little is known about the effect of this phenomena on mass transfer but Licht and Conway (117) concluded that it is approximately equal in magnitude to the effect of drop formation. Conversely, Popovich et al (112) stated that release has no effect at all. These differing conclusions may result from the fact that, in the latter investigation, the main resistance to mass transfer was in the continuous phase. Marsh and Heideger (118) deduced that a high contribution to mass transfer occurred during release and the first second of rise. Recently Heertjes and de Nie (108), showed that, for isobutanol drops in water, the mass transfer coefficient during release was six times greater than the value for the preceding section. However, further work is needed before this is completely established.

5.3 Mass Transfer Within Droplets

In agitated columns the proportion of mass transfer which occurs during droplet travel would be expected to be very much greater than during release or detachment from the inlet distributor. Therefore mass transfer mechanisms

within droplets, which will now be discussed, and in the continuous phase are of more relevance than sections 5.1 and 5.2.

The coefficient of mass transfer inside the droplet depends on the velocity of internal circulation. Circulation rate is known to increase with the droplet diameter and with the ratio of the viscosity of the continuous phase to that of the dispersed phase. Thus Hadamard (119) showed that the liquid inside the droplet would circulate at Reynolds numbers ($d\rho_c V/\mu_c$) greater than 1.0, and Levich (120) has postulated that circulation would occur between Reynolds numbers of 1 and 1500. Levich considered that the surface tension of the dispersed phase would affect the circulation rate. Garner and Skelland (121) showed that the interfacial tension between the dispersed phase and the continuous phase was also an important factor, and presented a correlation for the critical Reynolds number required for internal circulation. When the interfacial tension was of the order of 1 dyne/cm, toroidal circulation was initiated when the critical Reynolds number was exceeded. As the interfacial tension increased from 1.0 to 15.0 dynes/cm the critical Reynolds number increased from 70 to 120.

Finally Linton and Sutherland (122) have shown that the nature of the original interface affects circulation. Thus droplets of polar solvents in water, initially

having a low interfacial tension, readily circulated; whereas droplets of non-polar solvents in water having a high initial interfacial tension did not circulate.

Clearly liquid systems with different properties produce drops with widely different mass transfer characteristics. The range of behaviour from rigid drop to oscillating drops are therefore considered below.

5.3.1 The Rigid Drop

Drops of very small diameter, usually below 1mm, or larger drops in the presence of surface active agents or impurities behave as 'rigid' drops. For the case of no resistance to mass transfer in the continuous phase, the unsteady state variation of average solute concentration C_D with time θ is adequately represented by Newman's (123) relation,

$$\frac{C_D^0 - C_D}{C_D^0 - C_{Di}} = 1 - \frac{6}{\pi^2} \sum_{n=1}^{\infty} \frac{1}{n^2} \exp\left(\frac{-4D_D \pi^2 n^2 \theta}{d^2}\right)$$

$$\cong \left| 1 - \exp\left(\frac{-4D_D \pi^2 \theta}{d^2}\right) \right|^{0.5} \quad (5.13)$$

where C_D^0 is the initial uniform concentration of solute, and C_{Di} the constant interfacial value. The left hand side of equation 5.13, then represents the fractional approach of the solute concentration to equilibrium with the continuous phase. The first expression on the right

is exact (123), and the second is an empirical approximation (124). A mass transfer coefficient, for use with a linear concentration-difference driving force is

$$k_d = \frac{2\pi^2 D_D}{3dp} \quad (5.14)$$

Recently, Skelland and Minhas (114) proposed an expression for mass transfer coefficient of a drop during free fall,

$$k_{dr} = \frac{S_{drc}}{t_{cr} a_r | \frac{1}{2}(C_{di} + C_{df}) - C_d^* |} \quad (5.15)$$

where S_{drc} is the solute transferred per drop, t_{cr} is the contact time, C_{di} , C_{df} and C_d^* are the initial, final and equilibrium concentrations, and a_r is the surface area, taken as that of an oblate spheroid having the same volume as that of the falling drop. The validity of this expression remains to be proven.

5.3.2 The Non-rigid Drop

There are two kinds of non-rigid drops; circulating and oscillating. The circulating drops are those in which the fluid inside the drop is in a state of rapid circulation. This circulation is laminar at drop Reynolds numbers less than 1 and turbulent at Reynolds numbers greater than 1. As a result of circulation the fluid inside the drop is completely mixed and this results in higher mass transfer coefficients. At even higher drop Reynolds number, $Re > 200$,

as the drop size in any given system increases above the laminar flow region; a size is reached at which the drop flattens and assumes a generally oblate ellipsoidal shape. This shape is unstable in fields of low viscosity, and the drop begins to oscillate (125). The term 'oscillation' denotes the axially symmetric periodic change from an oblate ellipsoid to a prolate form and back to oblate again.

The shape of a liquid drop moving in a liquid field is dependent on a balance between the hydrodynamic pressure exerted because of the velocity of the drop relative to the field liquid and the surface forces which tend to hold the drop spherical.

A theoretical analysis of mass transfer inside a circulating droplet has been made by Kronig and Brink (5). The motion was assumed to take place in Stokes regime, and with the circulation rate being sufficiently rapid to maintain the streamlines at constant, but different concentrations. Hence mass transfer occurred by molecular diffusion in a direction perpendicular to the streamlines. The rate of mass transfer inside circulating drops was shown to be far greater than in stagnant drops. The results were correlated by

$$\frac{C_D^o - C_D}{C_D^o - C_{Di}} = 1 - \frac{3}{8} \sum_{n=1}^{\infty} A_n^2 \exp\left(1 - \frac{\psi_n 64 D_D \theta}{dp^2}\right)$$

$$\approx \left\{ 1 - \exp\left[-\frac{2.25(4) D_D \pi^2 \theta}{dp^2}\right] \right\} \quad (5.16)$$

$$\text{or } k_D \doteq \frac{17.9D_D}{dp} \quad (5.17)$$

The second half of Equation 5.16 is an empirical approximation (126). Comparison with the case for rigid spheres shows that an oscillating drop is equivalent to a rigid sphere for which the effective diffusivity D_D equals 2.25 to 2.7 times the true molecular diffusivity D .

Alternatively, Handlos and Baron (127) considered the case of a fully turbulent drop, with the circulation pattern simplified to concentric circles. It was assumed that the liquid between two streamlines became readily mixed after one circuit. Since the average circulation rate is related to the drop velocity, an eddy diffusivity was obtained,

$$\epsilon = dpV_t \left(\frac{fr^2 - 8r + 3}{1 + \frac{\mu_d}{\mu_c}} \right) \quad (5.18)$$

where $r = dp/4$ times the radius of the circulating streamline. This expression when solved with the continuity equation for the case of no continuous phase resistance, gave,

$$k_D = \frac{0.00375V_t}{1 + \mu_d/\mu_c} \quad (5.19)$$

$$\frac{k_D d}{D_D} = N_{sh,D} = \frac{0.00375d_p V_t D_D}{1 + \frac{\mu_d}{\mu_c}} = 0.00375N'_{pe,D} \quad (5.20)$$

$N'_{pe,D}$ is a modified Peclet number. Comparison of this with Equation 5.14 indicates that a turbulent sphere

behaves like a rigid sphere with an effective diffusivity D_D larger than the molecular D_D by a factor of $0.0057N'_{Pe,D}$.

Equation 5.19 has been verified experimentally by Skelland and Wellek (128) and Johnson and Hamilec (129). However Olander (130) observed some discrepancy when applying the Handlos and Baron model to cases involving short time of contact. This is due to the fact that, in the derivation of Equation 5.19, only the first term of the series has been used. This is permissible only when the contact times are large. Thus Olander proposed a correlation for the calculated mass transfer coefficient,

$$k_d = .972 k_{HB} + 0.075 d_t \quad (5.21)$$

where k_d is the actual transfer coefficient and k_{HB} is that calculated by means of Handlos and Baron's model. Equation 5.21 is for cases where there is no resistance in the continuous phase.

5.3.2.1 Oscillating Drops

In general drops which exceed a critical size for a given system exhibit oscillations. This is particularly true when the drop Reynolds number exceeds 200 in a continuous phase of low viscosity. Under these circumstances the models described for the circulating drops are inapplicable (6).

Droplet oscillation is a major factor affecting

mass transfer. It may be initiated by the tearing away of the droplet from the forming device or by intermittent shedding of vortices from the droplet wake (125, 131). Droplet oscillations are not necessarily restricted to oblate-prolate, or spherical-oblate oscillations. As droplet size increases beyond the point where oscillations begin, the droplet oscillation tends towards a more random fluctuation in shape (6).

Garner and Tayeban (132) found that for a given droplet size oscillation was greater for a system with a low continuous phase viscosity, a low interfacial tension and a low dispersed phase viscosity. Garner and Haycock (133) found that the period of oscillation was dependent on the physical properties of the liquid-liquid system, particularly the densities. Once oscillations were set up in drops, Johnson and Hamielec (129) reported effective diffusivities as high as 52 times the molecular value. Garner and Skelland (134) reported that the rate of transfer of an oscillating nitrobenzene drop in water was 100% greater than that for an equivalent stagnant drop. Heat transfer rates are also greatly increased for oscillating droplets (131).

Rose and Kintner (6) have proposed a model for mass transfer from vigorously oscillating, single liquid drops moving in a liquid field based upon the concept of interfacial stretch and internal droplet mixing. Their

model takes into account both an amplitude factor and the frequency of drop oscillations. They also stated that oscillations break-up internal circulation streamlines and turbulent internal mixing is achieved. The proposed model gives,

$$E = 1 - \exp \left[- \frac{2\pi D_E}{V} \int_{t_0}^{t_6} \frac{1}{f_1(t)} \left\{ \left(\frac{3V}{4\pi (a_o + a_p |\sin \omega t|)^2} \right)^2 \right. \right. \\ \left. \left. + \frac{1}{2\alpha} \ln \frac{1+\alpha}{1-\alpha} + (a_o + a_p |\sin \omega t|)^2 \right\} dt \right] \quad (5.22)$$

where the symbols are given in the nomenclature.

Experimental results for different systems deviated from the model by approximately 15%. The reasons for this may be

- (i) wall effects
- (ii) the degree of oscillation and
- (iii) the possible presence of impurities and surfactants.

Angelo et al (103) also based their model on surface stretch and internal mixing of the drop. However in this model, no account is taken of differences in the rate of stretching. An empirical relation is given for k_d ,

$$k_d = \left(\frac{4D_d \omega (1 + \epsilon_o)}{\pi} \right)^{\frac{1}{2}} \quad (5.23)$$

in which ω is the frequency of oscillation and ϵ_o a dimensionless factor for the amplitude which can be found

from,

$$\epsilon_0 = \epsilon + \frac{3}{8} \epsilon^2 \quad (5.24)$$

The surface time relation is,

$$A = A_0 (C_1 + \epsilon \sin^2 \tau) \quad (5.25)$$

in which τ is a dimensionless time. The model is only strictly valid for a whole number of oscillations, i.e. for a fractional number it will give too low a result. Furthermore, the values predicted by this model do not differ significantly from those obtained using Rose and Kintner's model or even from those predicted by the Handlos and Baron model, for drops with very rapid circulation.

5.4 Mass Transfer in the Continuous Phase

Little attention has been given to the relative importance of the effects of internal droplet circulation on the outside mass transfer coefficient, or of the continuous phase resistance in relation to the dispersed phase resistance. However, Conkie and Savik (135) have shown that the velocity boundary layer thickness around a circulating droplet is reduced by a factor $(1-\phi)$, where ϕ is the ratio of the surface velocity to the velocity of the potential flow, and this boundary layer disappears. Using this basis Ruckenstein (136) showed that the outside mass transfer coefficient could be correlated by the equation,

$$Sh = 1.13\sqrt{Pe} \quad (5.26)$$

where $Sh = \text{Sherwood Number } kd/D$,
 $Pe = \text{Peclet Number } d U/D$, and $U = \text{mean droplet velocity}$.
The results from equation 5.26 were compared satisfactorily with the experimental results of Garner and Hale (137). Griffiths has shown that, even when the dispersed phase viscosity is high, mass transfer coefficients predicted by Equation 5.26 should agree with experimental results within 20% provided $(\mu_c/\mu_D) Re^{\frac{1}{2}} > 10$. This agreement is probably due to boundary layer separation occurring near the rear of the droplet.

In general mass transfer coefficients in the continuous phase can be classified under two headings, namely for 'rigid' drops and for 'non-rigid' drops.

5.4.1 From and to 'Rigid' Drops

For the case of a rigid drop, Garner and Suckling (138) and Garner et al (139) have shown that the rate of mass transfer from or to a solid sphere can be correlated by a general equation of the form

$$Sh = A + C Re^m Sc^n \quad (5.27)$$

Examples from the literature are reproduced in Table 5.3.

5.4.2 From and to Non-Rigid Drops

The mass transfer is described by k_c and many correlations have been made with Sherwood number. Because the velocity at the interface is not zero, the power of the Schmidt number should be larger than $\frac{1}{3}$ and is generally taken as $\frac{1}{2}$, as would be the case for potential flow. For

this limiting case, Boussinesqu (140) has derived

$$Sh = 1.13(Re)^{\frac{1}{2}} (Sc)^{\frac{1}{2}} \quad (5.28)$$

Because of the existence of a wake, the proportionality constant should in practice be lower than 1.13. Garner and Tayeban (148) therefore suggested,

$$Sh = 0.6(Re)^{\frac{1}{2}} (Se)^{\frac{1}{2}} \quad (5.29)$$

Harriot (141) claims however that Equation 5.28 is valid for many cases.

One of the main difficulties encountered is to estimate the contribution to mass transfer by the wake of the drop. Thus Kinard et al (142), using the work of White and Churchill (143), attempted to include the wake effect together with other effects. Their correlation is reproduced in Table 5.3. Although significant for quiescent flow the wake may become less important in turbulent flow, i.e. in agitated systems, because the continuous phase is continually renewed and the wake is not allowed to develop. Therefore although the contribution of the wake is difficult to quantify, it has been shown to be significant only in simple discrete drop contactors, e.g. the spray tower (144).

For non-rigid drops the value of e in Equation 5.2 varies from 1.13 (145) to 0.6 (132). Thorsen (146) proposed a correlation for the coefficient,

$$C = 1.13 \left| 1 - \frac{4(3\sqrt{3}-2)}{5\sqrt{\pi}} \cdot \frac{1}{\text{Re}^{\frac{1}{2}}} \cdot \frac{1+4\mu_d/\mu_c}{1+(\rho_d/\rho_c \cdot \mu_d/\mu_c)^{\frac{1}{2}}} \right|^{\frac{1}{2}} \quad (5.30)$$

TABLE 5.3

EMPIRICAL CORRELATION FOR MASS TRANSFER IN THE CONTINUOUS

PHASE

Reference	Equation	Hydro dynamic regime of drop	Equation number
152	$\text{Sh}=0.582 (\text{Re})^{\frac{1}{2}} (\text{Sc})^{1/3}$	Solid sphere	5.34
153	$\text{Sh}=2+0.76 (\text{Re})^{\frac{1}{2}} (\text{Sc})^{1/3}$	Solid sphere	5.35
142	$\text{Sh}=2+(\text{Sh})_n + 0.45 (\text{Re})^{\frac{1}{2}} (\text{Sc})^{1/3} + 0.048 (\text{Re}) (\text{Sc})^{1/3}$	Solid sphere	5.36
145	$\text{Sh}=1.13 (\text{Re})^{\frac{1}{2}} (\text{Sc})^{\frac{1}{2}}$	non-rigid drop	5.37
132	$\text{Sh}=0.6 (\text{Re})^{\frac{1}{2}} (\text{Sc})^{\frac{1}{2}}$	non-rigid drop	5.38
132	$\text{Sh}=50+0.0085 (\text{Re}) (\text{Sc})^{0.7}$	oscillating drop	5.39
151	$\text{Sh}=2+0.084 (\text{Re})^{0.484} (\text{Sc})^{0.0339} (d_g^{1/3}/D^{2/3})^{0.072}$	Oscillating drop	5.40

For oscillating drops, Garner et al (147) proposed a correlation of the form,

$$\frac{kd}{D} = -126 + 1.8 \text{Re}^{\frac{1}{2}} \text{Se}^{0.42} \quad (5.31)$$

This correlation fits a selection of experimental data, but Hughmark (167) has suggested the use of equation 5.40

Recently Treybal (20) has recommended use of the relation of Ruby and Elgin (148) for swarms of drops. This relation is a modified Boussinesqu equation,

$$Sh = .725 (Pe)^{0.57} (Sc)^{-0.15} (1-\phi_d) \quad (5.32)$$

where ϕ_d is the dispersed phase hold up. Experimental results fall between this new correlation and a correlation suggested by Treybal, based on an oversimplification of the results given by Heertjes et al (149) using Boussinesq's equation with a constant of 0.8 instead of 1.13.

More recently, Galor and Hoelscher (150) derived a mathematical model for unsteady state mass transfer with and without chemical reaction. Interaction between drops in swarms, and the effect of particle size distribution, have been taken into account. In their equation K_c should be linearly proportional to a mean diameter $d_{32}^{\frac{1}{2}}$:

$$K_c = 0.371 \left\{ \frac{D(\rho_c - \rho_d)g}{2\mu_c + 3\mu_d} \left(\frac{1}{2} d_{32} \right) \right\}^{\frac{1}{2}} \quad (5.33)$$

Finally, Hughmark (151) has concluded that for a swarm of drops in a system for which the ratio of viscosities of the continuous to the dispersed phase is less than one, the mass transfer coefficient for the continuous phase is the same as for single drops. For a ratio larger than one, an interaction effect in the continuous phase has to be recognised.

5.5 Mass Transfer During Coalescence

Eventually each drop leaving the last compartment of an R.D.C. is required to flocculate and then coalesce, either via interdrop or drop interface coalescence. Some mass transfer occurs during this process.

The effect which mass transfer has upon coalescence has been investigated in some detail. However, very few attempts have been made to quantify the extent of mass transfer during coalescence. Johnson and Hamielec (129) derived an expression for the mass transfer during coalescence, (k_{d_c}) , for the simple case of a drop coalescing into an interface immediately upon its arrival. The drop contents were also assumed to spread over the entire interface in the form of a uniform layer. Mass transfer was correlated according to penetration theory with the time for the exposure of the layer taken as identical to that for formation of the drop. Thus,

$$k_{d_c} = (D_d / \pi t_f)^{\frac{1}{2}} \quad (5.41)$$

Licht and Conway (117) and Coulson and Skinner (107) reported similar results. However, these were later criticised by Licht and Pensing (102) and Skelland and Minhas (114) due to the fundamental difference between the mechanism of drop formation and coalescence. In fact very little mass transfer takes place during coalescence

compared to formation since the concentration driving force is generally low. However, Skelland and Minhas (114) derived an expression for the mass transfer coefficient at coalescence k_{dc} . This is given by,

$$k_{dc} = \frac{2V_d}{a_{c f} t_f} \left| \frac{2I_{f,c} + (k_{df}/V_d) a_f t_f (I_{f,c} - 4V_d)}{8V_d - 2I_{f,c} - (k_{df}/V_d) a_f t_f I_{f,c}} \right| \quad (5.42)$$

where the symbols are defined in the nomenclature. They also correlated their experimental results by an expression similar to that proposed in the same study for drop formation. The correlation for drop coalescence is:

$$\frac{k_{dc} t_f}{d} = 0.1727 \left(\frac{\mu_d}{\rho_d D_d} \right)^{-1.115} \left(\frac{\Delta \rho g d^2}{\sigma} \right)^{1.302} \left(\frac{v_t^2 f_t}{D_d} \right)^{0.146} \quad (5.43)$$

The average absolute deviation from the data was approximately 25%.

Recently Heertjes and de Nie (145, 154) concluded that mass transfer during the actual process of coalescence can be neglected for two reasons. Firstly, the mechanism of coalescence shows that drainage of a drop into the homophase does not permit entrainment of continuous phase in the homophase and secondly coalescence is so rapid, occurring in approximately 3×10^{-2} sec. in pure systems, that there is insufficient time for a significant transfer of solute. Reference here is only made to the coalescence of drops on the interface. No research work has been presented as yet on the influence of drop-drop coalescence

on mass transfer. However generally the coalescence of drops in swarms causes an increase in drop size, and thus oscillation, and a decrease in surface area. These factors counteract each other with respect to mass transfer rate. In any event when a drop approaches an interface, oscillations will occur which will temporarily increase mass transfer rate considerably. The thin liquid film between the drop and the interface, when the drop is at rest, will be rapidly exhausted or saturated as regards solute. Since the surface areas covered by drops in this way can be relatively large the effect may therefore be pronounced.

5.6. Overall Coefficient of Mass Transfer

The overall resistance to mass transfer is the sum of the resistances of the individual phases and is given by Equation 1.2. The resistance to transfer in one of the phases is often predominant. The design equations can then be based on the coefficient in that phase only. There is no established method to predict which coefficient will control the mass transfer process, but a fairly reliable indication can be obtained by the following observations. (57). If the physical properties of the system predict a droplet size greater than 2mm the liquid inside the droplet will most probably circulate, and the mass transfer coefficient of the continuous phase will control the extraction rate. This indication may be confirmed by estimating the time taken for the concentration of the

droplet to change by 95%, using the equation derived by Crank (155) that

$$\frac{Q_t}{Q_0} = \eta = 1 - \frac{6}{\pi^2} \sum \frac{1}{n^2} e^{-\frac{(Dn^2\pi^2 t)}{r^2}} \quad (5.44)$$

or the experimentally modified version proposed by Calderbank and Karchinski (126),

$$\frac{Q_t}{Q_0} = \eta = 1 - e^{-2.25 \frac{(4D\pi^2 t)}{d^2}} \quad (5.45)$$

If the time required is short, that is, of the order of 30 sec., then the rate of extraction will be controlled by the continuous phase coefficient and the design calculations will be based on this coefficient.

In the majority of industrial extractors the continuous phase coefficient would be expected to control the rate of extraction.

5.7 Miscellaneous Phenomena

5.7.1 Mass Transfer and Interfacial Instability

Various types of small flows generated at the interface and in the layers immediately adjacent to it are usually classified as interfacial turbulence. Such disturbances and their effects have been summarised in several publications (55, 56, 156, 157). Spontaneous emulsification, localised stirring with rippling and twitching of the interface, slowly moving streamers of one phase moving into

another, drop formation from the tips of such slowly moving streams, local eruptions at the interface, violent and erratic pulsation in drops and unsteady flow along the interface have all been recorded. The action is three-dimensional and the interface is regarded as including the immediately adjacent sub-layers on either side of the bulk phase separation plane.

All these disturbances have been found to cause a many-fold increase in the rate of transfer of solute across the interface. If a chemical or thermal difference along an interface causes an interfacial tension gradient, a violent flow in the direction of low σ results. This phenomena is termed the Marangoni effect.

Sternling and Scriven (56) analysed the hydrodynamic aspects of interfacial turbulence by means of a greatly simplified two-dimensional roll cell model. Their analysis suggests that interfacial turbulence is usually promoted by solute transfer into the phase of lower viscosity, solute transfer towards the phase of higher diffusivity, large viscosity and diffusivities differences between the phases, large concentration gradients near the interface, or a low order of viscosities and diffusivities. It is inhibited and damped by the presence of surfactants and by nearly rigid boundaries.

Whilst the model of Sternling and Scriven is oversimplified, it serves remarkably well to predict the

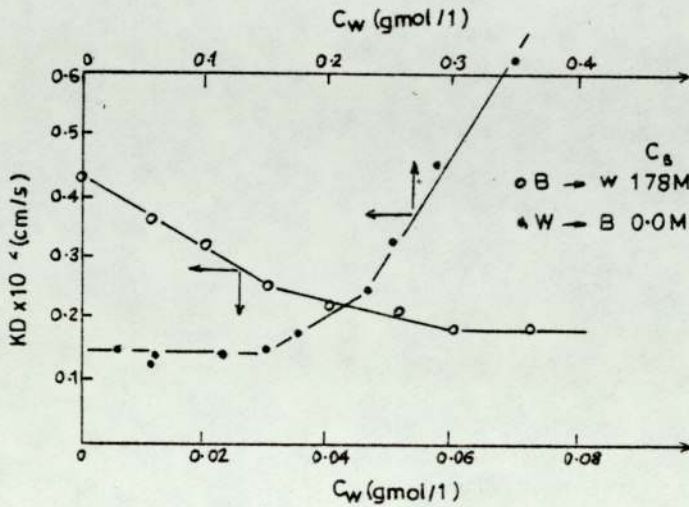


FIG. 5.1 MASS TRANSFER COEFFICIENTS FOR THE TRANSFER OF PHENOL BETWEEN BENZENE DROPS (B) AND WATER (W) AS A FUNCTION OF PHENOL CONCENTRATION (C_w) IN WATER AT A CONSTANT CONCENTRATION (C_B) IN THE DROPS.

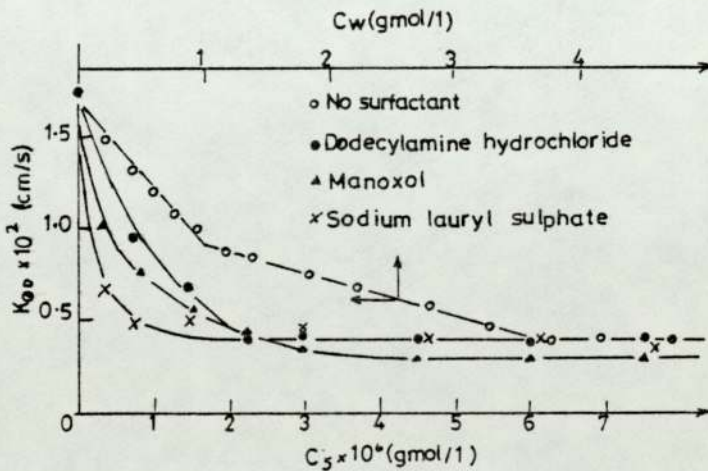


FIG. 5.2 EFFECT OF PRESENCE OF SURFACTANTS ON MASS TRANSFER COEFFICIENTS FOR THE TRANSFER OF ACETIC ACID FROM 0.98M SOLUTION IN BENZENE DROPS INTO SOLUTE-FREE WATER. C_s - concentration of surfactant. C_w concentration of acetic acid in water.

creation, propagation, and damping of turbulence. Orell and Westwater (157) used Schlieren photography to record effects in two three-dimensional convection cells, including polygonal cell clusters, stripes and ripples. Their polygonal cell clusters, exhibited a size an order of magnitude larger than the dominant wavelength for roll cells as predicted by the Sternling and Scriven development.

Sawistowski and co-workers studied the effect of interfacial convection on mass transfer during drop formation, in horizontal contactors, wetted wall columns and a stirred cell. In the investigation of mass transfer from drops (158, 159, 160, 161) the results for the transfer of phenol are shown in Fig. 5.1. Three regimes were distinguished for both directions of transfer. The diffusional value of mass transfer coefficient for the transfer of phenol in the stable direction was found to be greater than the unstable direction. This was also observed by Austin (162) and Marindas and Sawistowski (163). In Austin's work for the transfer of propionic acid from water to benzene in a stirred cell, the diffusional value of the overall mass transfer coefficient was 3.9×10^{-4} cm/sec., whereas in the reverse direction it was 6.4×10^{-4} cm/sec. Similarly, Maroudas and Sawistowski (163) found that, during the transfer of propionic acid in a wetted wall column under a variety of conditions, the resistance to transfer was always larger

from water to carbon tetrachloride than in the opposite, convectionally stable, direction. They attributed this to an interfacial resistance caused by breaking of hydrogen bonds when the transfer took place from water into the organic phase.

Marsh et al (164) also proposed a transient model identical to that of Sternling and Scriven, except that the concentration profile was assumed to be time dependent. From the analysis of the characteristic equations it follows that instability is promoted by,

- (i) Solute transfer out of the phase of higher viscosity;
- (ii) a large difference in kinematic viscosity between the phases;
- (iii) large differences in diffusivity between the phases, up to a factor of 10;
- (iv) a large initial concentration;
- (v) a large value of $d\sigma_0/dc$; and
- (vi) low viscosities and diffusivities in both phases.

Marsh et al have outlined the differences between their transient model and Sternling and Scriven's steady state model.

In conclusion quantitative analysis of interfacial turbulence is far from complete and the results are unlikely to be applicable to the design of extraction equipment in the near future.

5.7.2 Effect of Surface Active Agent

The introduction of surfactants into a two-phase system affects the properties of the interface in several ways. Interfacial tension is reduced, thus becoming less dependent on solute concentration. Interfacial compressibility also decreases, thus adversely affecting surface renewal. In addition, surface viscosity increases and tends to slow down any movement of the interface. Hence only a small amount of surfactant should suffice to eliminate, or markedly reduce, interfacial convection. This is important since traces of surfactants are common in commercial liquid-liquid extraction operations.

The effect of surfactants on mass transfer coefficients is shown in Fig. 5.2 for the transfer of acetic acid into water from a .98M solution in benzene (160, 161). The overall mass transfer coefficient is plotted against the concentration of surfactants. In the case of Teepol (160), Lissapol, dodecylamine hydrochloride and sodium lauryl sulphate, the addition of a small quantity of surfactant reduced the mass transfer coefficient to a value equal to that obtained in the diffusional regime in the absence of surfactants. This indicates that the action of these surfactants was entirely hydrodynamic in nature, i.e. they suppressed interfacial convection. In the case of Manoxol (sodium dioctyl sulphosuccinate), there was also some evidence of a barrier effect. This corresponds

to an interfacial resistance of around 50 cm/cm. In general, as was shown by Plevan and Quinn(165) for gas absorption, \times the action on rates of mass transfer of surfactants producing gaseous and expanded films is hydrodynamic in nature but an interfacial resistance is also introduced when surfactants forming condensed films are added to the system.

5.7.3 Wall Effects

Most data on the gross terminal velocities of drops have been determined in vertical cylindrical glass tubes of limited size. A wall correction factor is necessary to interpret such data in terms of a drop moving in an infinite medium.

A number of workers (166, 167) have derived such correction factors for the movement of a fluid past a rigid sphere held on the axis of symmetry of the cylindrical container. Brenner has generalised the usual method of reflections. He solved the Navier Stokes equations of motion around a rigid sphere, with use of an added reflection flow, to give an approximate solution for the ratio of sphere velocity in an infinite space to that in a tower of diameter D_T .

$$K_w = \frac{U_\infty}{U} = \frac{1 - 0.759 (D_D/D_T)^5}{1 - 2.105 (D_D/D_T) + 2.087 (D_D/D_T)^3} \quad (5.46)$$

Haberman and Sayre (168) used the same method to

provide an expression for circulating fluid spheres in a stationary field,

$$K_{w1} = \frac{1 - 0.759 \left(\frac{1-r}{2} \right) \lambda^5}{1 + \frac{2}{3}r} \psi \quad (5.47)$$

in which

$$\begin{aligned} \psi = & 1 - 2.105 \left(\frac{1 - \frac{2}{3}r}{1+r} \right) \lambda + 2.807 \left(\frac{1}{1+r} \right) \lambda^3 \\ & - 1.707 \left(\frac{1 - \frac{2}{3}r}{1+r} \right) \lambda^5 + 0.726 \left(\frac{1-r}{1+r} \right) \lambda^6 \end{aligned} \quad (5.48)$$

$$r = \mu_c / \mu_D$$

$$\lambda = D_D / D_T$$

They also derived correction factors for a fluid sphere moving along the axis of a cylinder in which the field fluid was also in axial motion;

$$K_{w2} = \frac{1 - \frac{2}{3} \left(\frac{1}{1 + \frac{2}{3}r} \right) \lambda^2 - 0.202 \left(\frac{1-r}{1 + \frac{2}{3}r} \right) \lambda^5}{\psi} \quad (5.49)$$

These factors were to be used in the equation,

$$F = 6\pi\mu k \left(\frac{1 + \frac{2}{3}r}{1+r} \right) (U K_{w1} - v_m K_{w2}) \quad (5.50)$$

in which v_m is the maximum velocity in the parabolic velocity distribution of the moving field phase. The correction was found applicable for λ values of 0.5 or less.

The above equations are limited to the creeping-flow range. For large drops moving under conditions such that inertial terms are not negligible, an empirical equation based on experimental data (169) is,

$$\frac{U}{U_{\infty}} = \frac{1}{K_w} = \left| 1 - \left(\frac{De}{D_T} \right)^2 \right|^{1.43} \quad (5.51)$$

This relation has proved useful for systems in which the field fluid was stationary.

5.8 Applicability of Single Drop Mass Transfer Models for the Design of Agitated Columns

The application of single drop correlations to agitated extraction columns requires caution for the following reasons:

- (1) The evaluation of the driving force is subject to the difficulties discussed, coupled with additional disturbances due to the mixing action of impellers, and the back mixing of the two phases. This is discussed in detail in Chapter 6.
- (2) When a swarm of drops rise up to column in a helical flow pattern, drop-drop coalescence can occur. This reduces the surface area but increases the internal mixing inside the drop. Coalescence may also take place into films retained on the column wall and internals resulting in unpredictable effects.

- (3) Drop break up may lead to a higher surface area but a lower mean mass transfer coefficient due to the change in mode of mass transfer.
- (4) When turbulence present in the agitated contactors is passed on from the continuous to the dispersed phase it increases the internal mixing and results in higher mass transfer coefficients than predicted by the correlations.
- (5) A wide range of drop sizes exists in the column giving rise to different modes of mass transfer and also a residence time distribution.

Important effects also arise from dirt, impurities and surface active agents in industrial contactors. Most mass transfer correlations presented in sections 5.3 and 5.4 apply to pure systems, with a minimum of impurities under ideal conditions, and these seldom exist in practice. Recently some attention has been given to the effect of surface active agents on mass transfer coefficients (170, 171), but these correlations cannot yet be applied to the column design, unless, as a conservative approach, drops are all considered as rigid bodies. However, these correlations do provide an insight into the mechanism of mass transfer and indicate the important parameters to be controlled on scale up. Critical analysis reveals that,

- (1) Drop size and characteristic velocity are the most important parameters determining the overall mass transfer coefficient.

- (2) Individual mass transfer coefficients are not affected by the scale of the apparatus and thus provide a good scale up criteria.

The theory of scale up based on these observations is discussed in detail in Chapter 10.

6. Axial Mixing

In the past the calculation of separation efficiency in continuous countercurrent columns assumed piston flow of both phases. This assumption is only valid if the velocities of all the particles of each phase are equal throughout any cross-section of the column. Such an assumption is unrealistic in the case of an industrial contactor. Extensive back mixing occurs in both phases in the R.D.C. (8, 58), together with other effects, viz, Taylor type diffusion, and longitudinal mixing. The longitudinal mixing comprises eddy and diffusional mixing. The combined effect of all these phenomena is generally termed axial mixing.

The effect of axial mixing is to lower the separation efficiency of a contactor compared with the value predicted assuming piston flow. To disregard axial mixing may therefore result in considerable errors in the estimation of column height from correlations obtained on model equipment.

In this chapter analysis of mass transfer in countercurrent differential contact equipment is first considered, based on the simplest mass transfer model, which neglects axial mixing. This is followed by a discussion of the various factors which contribute to the axial mixing and models which take it into account. Finally the application of these models to an R.D.C., and the technique used to determine the axial diffusivity coefficient, are described.

6.1 Models Describing the Performance of an Extraction Column

6.1.1 Plug Flow Model

The plug flow model is derived from the fundamental analysis of an extraction process. In its simplest form the extraction rate is expressed as,

$$N = k_x (x - x_i) \quad (6.1)$$

$$= k_y (y - y_i) \quad (6.2)$$

where N is the number of moles transferred across the interface per unit area, per unit time and x_i ; y_i are the concentration of solute in the raffinate and extract phases at the interface respectively. If the concentrations x_i , y_i are at equilibrium, and the distribution coefficient is defined as,

$$m = \left(\frac{y_i}{x_i}\right)^* = \text{constant} \quad (6.3)$$

then based on two film resistance theory (20), the rate of mass transfer can be expressed as,

$$N = K_x (x - x^*) \quad (6.4)$$

where K_x is the overall mass transfer coefficient and is expressed in terms of the individual resistances in the two phases, thus,

$$\frac{1}{K_x} = \frac{1}{k_x} + \frac{1}{mk_y} \quad (6.5)$$

and $x^* = y/m$ (6.6)

A similar expression can be written for overall mass transfer coefficient expressed for the extract phase. Equation 6.5 is widely applied even under conditions when m is not constant and relation 6.6 is not entirely valid.

To calculate the column height for a particular duty, mass transfer is assumed to occur by diffusion with the two phases in plug flow. This condition is shown diagrammatically in Fig. 6.1. If R and E are the flow rates of the raffinate and extract phases, a is the interfacial area per unit volume and H is the height of the column (20),

$$N_{toR} = \int_{x_{R2}}^{x_{R1}} \frac{dx_R}{(1-x_R) \ln \frac{1-x_R^*}{1-x_R}} = \frac{H}{H_{toR}} \tag{6.7}$$

where

$$H_{toR} = \frac{R}{K_R a (1-x_R)_{om} C_{Rav}} \tag{6.8}$$

The terms N_{toR} and H_{toR} are defined as the number of overall transfer units, and the height of a transfer unit respectively, based upon the raffinate phase. Similar expressions may be derived based on the extract phase. However, this model does not accurately represent the situation inside the column. Therefore it is not applicable

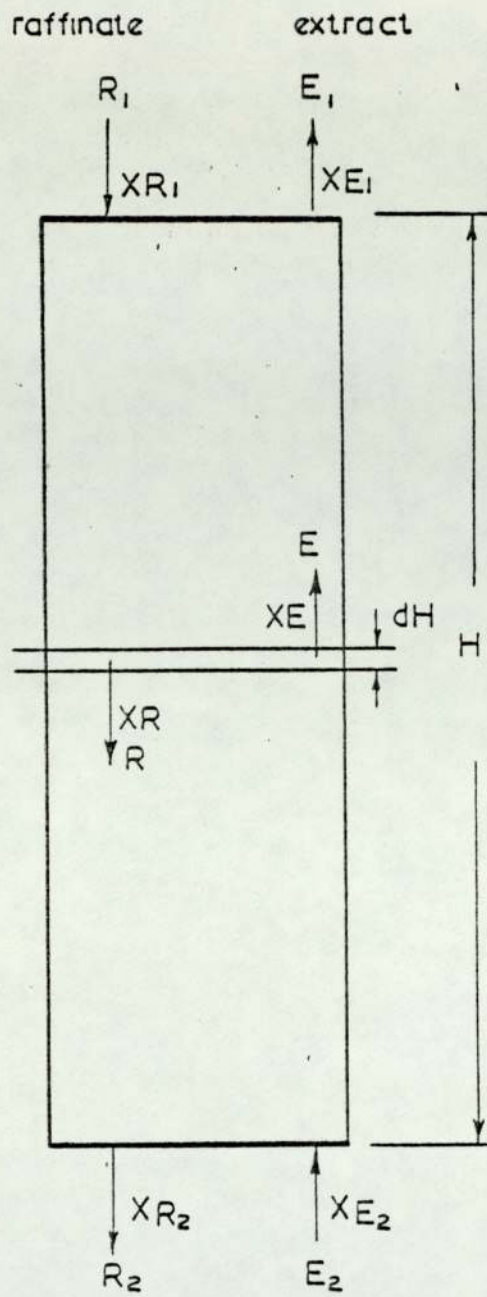


Fig. 6.1 . Piston flow condition in a countercurrent extractor

for the prediction of column height of an industrial extractor using data obtained on a small column, in which the longitudinal mixing effects are small and may be neglected. A more fundamental approach is therefore necessary because existing correlations of mass transfer performance are extremely unreliable for scale up, or for application to a new set of circumstances, unless the effect of longitudinal mixing is accounted for, or shown to be negligible (172).

The overall effect of longitudinal mixing in a liquid-liquid extraction column arises from a combination of several factors which vary according to the type of contactor and the liquid flow conditions. According to Sleicher (58), axial dispersion in the continuous phase may be considered to be the sum of two effects. Firstly, the true turbulent and molecular diffusion in the axial direction, may be manifested by vertical circulation currents, or mixing in the eddies from the wake of the dispersed droplets, entrainment of the continuous phase by the droplets, or a forced backmixing action due to turbulence in the contactor. Secondly, longitudinal mixing may also be caused by non-uniform velocity and subsequent radial mixing, or Taylor diffusion (173). At low agitation this may predominate over eddy diffusion.

In these circumstances, there may be little

justification for representing the velocity profile effects by means of an eddy diffusivity, or back mixing, coefficient. Although turbulent effects may also be important for the dispersed phase, an added contribution to the overall longitudinal mixing can be caused by the distribution of residence times in the droplet swarms. This distribution results from the distribution of droplet sizes and therefore in their rise velocities; this is termed forward mixing. Channelling effects may also be important for both phases but such effects are assumed to be absent from a well-designed column.

Misek and Rod (174) have shown that the mass transfer process can be better represented by models which take longitudinal mixing into account. Four such models will be discussed here and they are shown diagrammatically in Figs. 6.2, 6.3, 6.4, and 6.5.

6.1.2 Stage Model

The stage model is the simplest model to describe mass transfer with longitudinal mixing in countercurrent extraction columns (175). The model is described in Fig. 6.2. It is assumed that each stage is perfectly mixed and that the distribution coefficient m is constant. The concentration profile is described approximately and the use of this model is only recommended for cases where the extent of longitudinal mixing in both phases is similar and where its influence on mass transfer is not high.

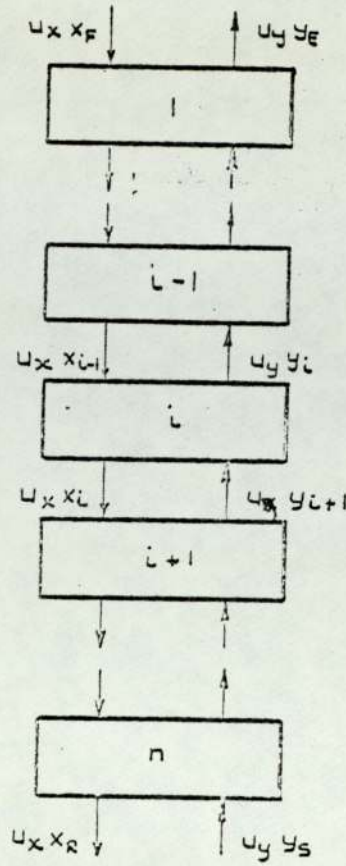


Fig. 6.2. Stage model

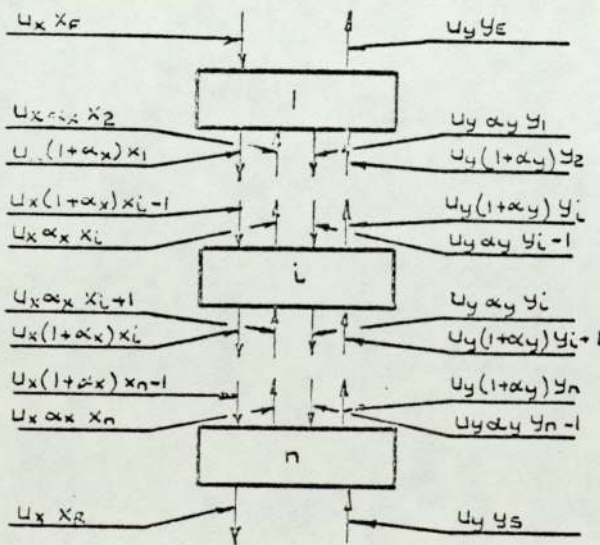


Fig. 6.3 Backflow model

Miyachi and Vermeulen (1966) considered the model could only be used when,

- (1) Interdroplet coalescence is frequent, or,
- (2) If interdroplet coalescence is infrequent, the drop size distribution should be narrow and m , x_d and K should be constant.

A material balance on the i th stage is described by:

$$U_x(x_i - x_{i-1}) = U_y(y_{i+1} - y_i) \quad (6.9)$$

and the mass transfer in the i th stage by

$$x_i - x_{i-1} = - \frac{K_x a h_m}{U_x} (x_i - x_i^*) \quad (6.10)$$

the boundary conditions being,

$$\begin{aligned} x_0 &= x_F & y_1 &= y_E \\ x_n &= x_R & y_{n+1} &= y_S \end{aligned} \quad (6.11)$$

The analytical solution of the finite difference Equations 6.9 and 6.10 for the linear case has been given by Sleicher (58) in the form,

$$\xi = \frac{A-1}{A - \lambda h_c / h_m} \quad (6.12)$$

$$\text{where } \lambda = \frac{H_x + A h_m}{H_x + h_m} \quad (6.13)$$

For the non-linear case a graphical solution is necessary. The main advantages of this model lie in its simplicity

and the ease of evaluation of design data. However, it is of limited applicability due to the assumption of equal mixing in both phases.

6.1.3 Back Flow Model

When one phase is entrained in the main flow of the other in a stagewise system, the flow conditions may be described by a backflow model as shown in Fig.6.3.

A material balance on the i th stage is represented by,

$$U_x \left[(1+\alpha_x) x_{i-1} - (1+2\alpha_x) x_i + \alpha_x x_{i+1} \right] = -U_y \left[-\alpha_y y_{i-1} + (1+2\alpha_y) y_i - (H\alpha_y) y_{i+1} \right] = N \cdot h_m \cdot a \quad (6.14)$$

and the mass transfer described by the relation,

$$N = K_x (x_i - x_i^*) \quad (6.15)$$

The governing finite difference equation is obtained by a combination of Equations 6.14 and 6.15. The boundary conditions result from balances around the end stages.

$$U_x (x_F - x_1) + U_x \alpha_x \sum_{i=1}^{i=1} (x_2 - x_1) = K_x a (x_1 - x_1^*) h_m \quad (6.16)$$

$$y_1 = y_E$$

$$i = n:$$

$$U_x (x_{n-1} - x_n) + U_x \alpha_x (x_{n-1} - x_n) = K_x a (x_n - x_n^*) h_m \quad (6.17)$$

$$x_n = x_R$$

Hartland and Mecklenburg (177) have given the solution for the simple linear case. The general solution can be obtained by using a graphico-numerical procedure (178).

The model represents a very good description of a number of real extraction units, especially those operating under conditions where intensive coalescence and re-dispersion takes place.

6.1.4 Diffusion Model

For a continuous countercurrent differential extraction column in which the change in concentration takes place along the column axis, an analogy to Fick's law of diffusion can be used to describe back mixing. Solute transfer in a single phase is assumed to take place from high to lower concentration and mass flux is assumed proportional to the concentration gradient. Theoretical development of a model on this basis was due to several authors (58, 176, 179, 180, 181, 182, 183).

Misek (174) has pointed out that the formulation of boundary conditions is usually based on a physical situation in which the solvent and feed inlets are placed at the end of the column, thus neglecting the influence of the end section in a real column.

From Fig. 6.4. a material balance over height element dh is:

$$-U_x \frac{dx}{dh} + e_x \frac{d^2x}{dh^2} = U_y \frac{dy}{dh} - e_y \frac{d^2y}{dh^2} = N.a. \quad (6.18)$$

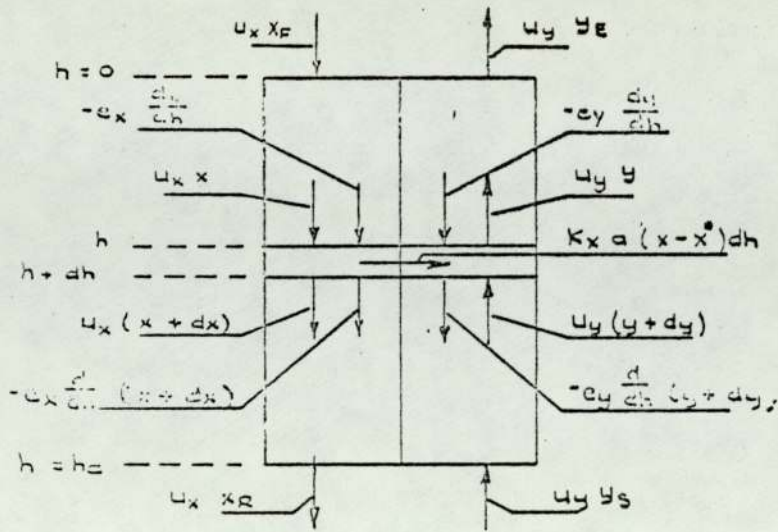


Fig. 6.4 Diffusion model

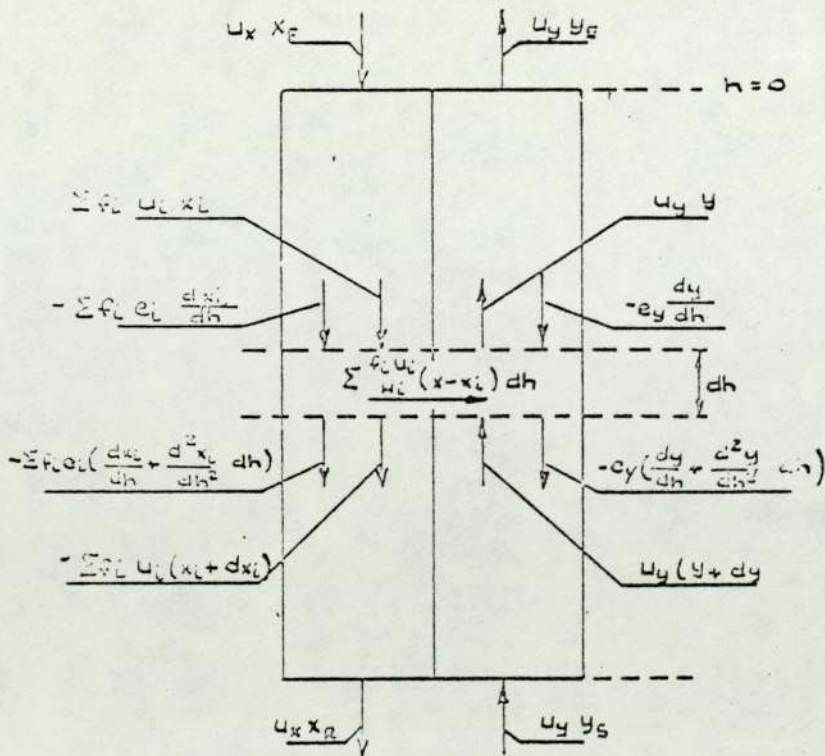


Fig. 6.5 Combined model

The mass transfer between the phases is given by.

$$N = K_x (x - x^*) \quad (6.19)$$

The boundary conditions are obtained by performing material balances for both ends of the column thus, (179)

$$U_x x_F = U_x x - e_x \frac{dx}{dh}; \quad \frac{dy}{dh} = 0 \text{ at } h = 0 \quad (6.20)$$
$$U_y y_s = U_y y + e_y \frac{dy}{dh}; \quad \frac{dx}{dh} = 0 \text{ at } h = h_c$$

The dispersion coefficients e_x and e_y outside the mass transfer sections are considered zero.

A graphico-numerical procedure is again required for solution of the general case (174). Several solutions have been obtained for the linear case (58, 177); one solution for an R.D.C. is given in para. 3.4.3 (58) as Equation 3.39.

6.1.5 Combined Model with Forward Mixing

Recent work on longitudinal mixing in the dispersed phase (52, 184) has indicated that neither the diffusion nor the backflow model describes the mixing of the dispersed phase adequately when this phase has a significant polydisperse character and coalescence-redispersion occurs. This is especially true when a solvent is dispersed in mechanically agitated column extractors operating with high hold ups. Another mechanism of longitudinal mixing then arises due to different rise velocities of drops of differing sizes. This phenomenon influences the residence

time distribution of the dispersed phase. It is termed (184) 'forward mixing' to distinguish it from back mixing, where displacement of fluid elements occurs in a backward direction with respect to normal flow in the equipment.

The combined effect of polydispersity and the velocity distribution which it causes in the dispersed phase result in a concentration distribution of solute at any column cross-section. This causes a decrease in the effective driving force for mass transfer in comparison with that for true piston flow, which would produce a uniform cross-sectional concentration (185). Olney considered the effect of polydispersity and derived a mathematical model for R.D.C. (52). Analytical solutions were not provided for the complex differential equations but Misek used the same method as for the diffusion model and provided a numerical solution (174).

6.2 Application to the R.D.C.

The suitability of any particular model to describe the extraction process in an extractor will depend on the difference between the real situation and the assumptions on which the model is based. Thus a diffusion model is more applicable to a spray column and a back flow model to a discrete stage mixer-settler.

A diffusion model has generally been used to describe the operation of an R.D.C. However, conditions

in an R.D.C. would be expected to fall between the two limits, i.e. discrete stage and plug flow, spray column operation. Therefore to utilise the models described earlier a knowledge is required of the extent of longitudinal dispersion in an R.D.C. in association with mass transfer data.

To apply the methods of calculation outlined in Section 6.1, experimental values of the longitudinal dispersion and back mixing coefficients are required for the appropriate conditions, together with the knowledge of the true values of the coefficients of mass transfer.

The extent of longitudinal mixing in an extractor can be evaluated by several methods. The most straightforward method is to measure the concentration of a solute along the extraction column length during steady state operation. The longitudinal mixing can then be evaluated by comparing the experimental concentration profile with the theoretical values computed by Miyauchi and Vermeulen using the one-dimensional longitudinal dispersion model (176), or the mass balance relationship using the method of Prochazka and Landau (186). Owing to experimental difficulties in the measurement of solute concentrations, alternative methods, which involve injection of tracers into the system during steady state operation, are usually preferred. Two types of experiment can be performed depending on whether a steady state or

transient injection of tracer is used. In the steady state method a stream of tracer is injected continuously into the column and the steady state concentration profile of the tracer is measured along the column upstream from the point of injection. In the dynamic method, a tracer is injected into the system and the time dependence of the tracer concentration is measured at a fixed point downstream from the point of injection. This results in a break through or response curve, as in the normal determination of the residence time distributions in flow systems.

The use of the forms of response calculated according to the appropriate mathematical model requires perfect step and perfect pulse inputs of tracer. These conditions are difficult to attain in practice. Aris (187), Bischoff (188), and Bischoff and Levenspiel (189) have developed a method which avoids the mathematical requirement for perfect pulse injection. In this method concentration measurements of the tracer are taken at two points within the test section; the variances are calculated for the two experimental break-through curves and the difference in the variances determined.

Recently a method has been developed by Miyauchi and co-workers (190) which avoids the use of a complete column and assembly. This uses a simple two stage column under non-flow and single liquid phase conditions, and

is particularly useful for testing the effects of change in the geometrical design, of the compartments in multi-stage extraction columns, on the rate of inter-stage mixing.

As discussed in Chapter 3, the geometry of an R.D.C. is variable within certain limits of $\frac{H}{D}$, $\frac{R}{D}$ and $\frac{S}{D}$, and this could provide a means of a first prediction of the optimum for a given duty.

Numerous tracers have been used in longitudinal mixing experiments. Clearly the tracer should be soluble in only one of the liquid phases. Types of tracer experiments include the use of ionisation current, counting of radio-active tracers, measurement of electrical conductivity or electrode potential or measurement of the absorption of ultra-violet light. A proper choice of tracer is extremely important.

Souhrada et al (191) has discussed the various tracers and their use in the determination of longitudinal dispersion coefficients. These tracer methods provide a good guide line for design of extractors. However, in view of the possible complexity of the actual flow patterns in an extractor, their use in conjunction with the theoretical flow models may have severe limitations (192). It is very important, therefore, that the results of these experiments should be checked with basic determination of actual mass transfer performance.

Several attempts have been made to correlate the axial diffusion coefficients E_c , and E_d in the two phases, with the column geometry and operating parameters (V_C , V_D , N). The diffusion model has mainly been used to describe the mass transfer behaviour in the R.D.C. The axial diffusivity coefficients were generally determined and correlated using a tracer injection technique.

Westerterp and Landsman (209) studied axial mixing in two small Rotating Disc Columns, of 4.1 and 5.0 cm. diameter respectively, using water as the homogeneous liquid phase. The degree of axial mixing was determined using a step injection technique with a caustic soda tracer. Results were interpreted by means of the diffusion model. The axial diffusivity was represented as the sum of two effects; a flow contribution independent of rate of mixing and proportional to the liquid velocity, and a mixing contribution independent of the liquid velocity and approximately proportional to the rate of mixing.

Thus,

$$E_A = K_1 N + K_2 F_C \quad (6.21)$$

where K_1 and K_2 are constants.

The overall results were correlated by.

$$P_{CB} = \frac{E_C L}{E_A} = \frac{2n}{1 + 13 \times 10^{-3} \frac{NR}{F_C}} \quad (6.22)$$

Earlier results obtained by Nagata et al (194) using a 10 cm diameter column could also be correlated by Equation 6.22

Separate experiments were carried out by Westerterp and Meyberg (195) using the steady state injection technique in the 50 cm. diameter column, in order to determine back mixing eddy dispersion coefficients. The values obtained were independent of the flow rate but were in excellent agreement with the magnitude of the rotational component in the correlation obtained for the overall axial dispersion coefficient in Equation 6.21.

They concluded that for the R.D.C., there is a difference in the apparent axial mixing and the back mixing in the column, where the apparent axial mixing (E_A) is equal to the sum of a rotational term, identical to the back mixing contribution (E_B), plus an additional term which represents a forward flow contribution.

Strand et al (8) considered that the overall axial dispersion process for the continuous phase comprised two main components, i.e. an eddy diffusion, or back mixing contribution, and a Taylor type diffusion, or channelling phenomenon, which is specifically in the forward direction. Eddy diffusion or back mixing coefficients were determined in the steady state tracer injection experiments, whilst overall apparent axial dispersion coefficients were measured in the transient experiments using tracer. Values

of E_A and E_B were reported for single phase studies in 15.2 cm and 105 cm. diameter columns. A plot of E/FH against RN/F produced a unique correlation of the data for a given column. E_A was greater than E_B at equivalent rotor speeds. The curves for E_A and E_B tended to approach each other at high rotor speeds, demonstrating that eddy diffusivity is the dominating axial mixing process under these conditions. The two curves, however, diverge at low speed with the values of E_A passing through a minimum. This is thought to be due to the competing effects of eddy diffusivity with increasing rotor speed. The data for single-phase flow was correlated by;

$$\frac{E_A}{FH} = 0.5 + 0.09 \left(\frac{RN}{F} \right) \left(\frac{R}{D} \right)^2 \left| \left(\frac{S}{D} \right)^2 - \left(\frac{R}{D} \right)^2 \right| \text{ for } \frac{RN}{F} > 30 \quad (6.23)$$

For the case where dispersed phase flow was present, equation (6.23) was modified to

$$\frac{(1-h)}{F_c H} E_A = 0.5 + 0.09(1-h) \left(\frac{RN}{F_c} \right) \left(\frac{R}{D} \right)^2 \left| \left(\frac{S}{D} \right)^2 - \left(\frac{R}{D} \right)^2 \right| \quad (6.24)$$

and for dispersed phase axial mixing, assuming an analogous form:

$$\frac{hE_A}{F_D H} = 0.5 + 0.09h \left(\frac{RN}{F_D} \right) \left(\frac{R}{D} \right)^2 \left| \left(\frac{S}{D} \right)^2 - \left(\frac{R}{D} \right)^2 \right| \quad (6.25)$$

A fair agreement with equation (6.25) was found for dispersed phase axial mixing data obtained in a 15.2 cm. diameter column using two narrow-sized fractions of solid particles settling in a continuous kerosene phase, and

kerosene dispersed in water. The results are reproduced in Figs. 6.6 and 6.7.

A description of the axial spreading of a droplet population by means of a simple diffusivity E_A , however, is subject to many limitations. Many factors affect the distribution of residence times of the droplets, including

- (1) The effect of drop-drop coalescence and redispersion.
- (2) Distribution of droplet velocity owing to distribution in droplet sizes and therefore in settling velocities.
- (3) Radial variations in the droplet velocity distribution owing to the vessel geometry and rotor speed, and
- (4) The axial distribution of small liquid droplets, owing to turbulent velocity fluctuations in the continuous phase.

The correlation of E_A for the dispersed phase therefore represents only a first approximation. Equation 6.25 would be expected to represent the droplet behaviour best at high rotor speeds. Since droplet interaction should make the dispersed phase approximate more to the conditions of a second continuous phase, as assumed in the longitudinal dispersion model.

Measurement of single phase, and two phase counter-current flow, axial dispersion coefficients in an R.D.C. have been reported by Stemerding, Lumb and Lips (196). The column ranged from 6.4 to 218 cm. in diameter. Measurements were restricted to the aqueous phase and were

- solid particles 140-175 μ
- △ solid particles 420-590 μ
- ◻ kerosene dispersed in water

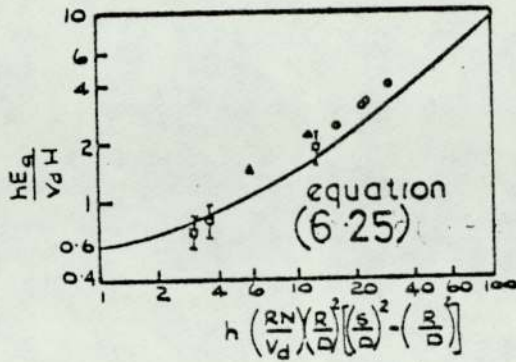


Fig. 6.6 Dispersed-phase axial diffusion 6-in diam. rotating disk contactor (8)

- 6" dia. R.D.C. (two units)
- △ 42" dia. R.D.C.

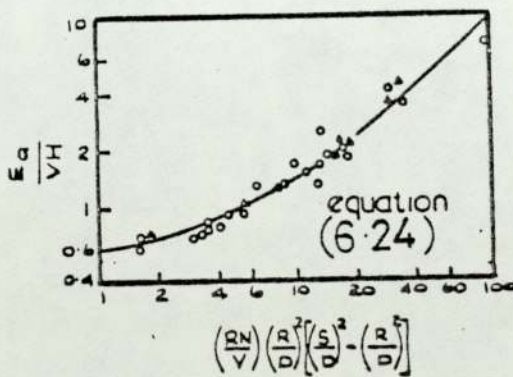


Fig. 6.7 Axial diffusion, single-phase flow $RN/V > 30$ (8)

interpreted using the dispersion model. Continuous phase axial dispersion coefficients were correlated by,

$$\frac{1}{P_i B} = \frac{E_C}{F_C H} = 0.5 + 0.012 \left(\frac{RN}{F_C} \right) \left(\frac{S}{D} \right)^2 \quad (6.26)$$

The numerical constant .012 was determined empirically for R.D.C. columns in the range studied. The degree of back mixing was found to decrease with an increase of viscosity of the continuous phase for $Re < 3000$. Values of the dispersed phase axial diffusivities obtained in 6.4 and 64 cm. diameter columns were much higher than those found for the continuous phase and did not obey the form of Equation (6.26). The ratio of dispersed to continuous phase axial dispersion coefficient varied from 100 to 1, (192), approaching unity at decreasing velocities of the dispersed phase. At flooding conditions the droplet velocity is low and dispersed phase axial diffusivities approximate to values obtained for the continuous phase. Under normal conditions of column operation, corresponding to about 80% flooding, the magnitude of the ratio E_D/E_C is about 10. Based on calculation of phase velocities under these conditions, Peclet numbers for the dispersed and continuous phases are about equal.

Stainthorp and Sudall (197, 198) determined back-mixing in both phases using a 3.5 cm. diameter R.D.C. under mass transfer conditions with the system water, -O-cresol-kerosene. Measurements were obtained by using a

pulse input of dye tracer and analysing the response using the mixing cell model. With back flow, values of continuous phase back mixing coefficients were about 15% higher than would be predicted using Strand's et al equation. Values for dispersed phase back mixing were inapplicable. It was proposed that conservative values of dispersed phase back mixing coefficient would be about twice those predicted by Strand.

Large differences between experimental values for the continuous phase axial mixing and those predicted by the equations of Strand et al were also found by Misek and Rozkos (30). The values of axial diffusivities were only 27 to 55% of the predicted values. Misek (199) analysed the available data for axial dispersion in the R.D.C. on the basis of the mixed cell model. With back flow, continuous phase back mixing was correlated by,

$$F_B = KNR \quad (6.27)$$

$$\text{where } K = -0.00212 + 0.00434 \left(\frac{S}{D}\right)^2 + 0.0264 \left(\frac{R}{D}\right)^2 \quad (6.28)$$

considerable scatter was found in the data especially with the results obtained in larger columns. A tendency was noted for longitudinal mixing to be reduced with the increased size of column. This was attributed to the prevalence of laminar conditions and reduced intensities of mixing in large diameter columns, which probably rendered inapplicable the assumption of perfect mixing for

the cell model. Attempts to correlate the back mixing of the dispersed phase in a similar manner were unsuccessful.

The effect of column geometry on the axial dispersion coefficients were studied by Miyauchi and co workers (190). The equipment used was a simple two stage column and a 15 cm. diameter multistage column. Water was the continuous phase and M.I.B.K. the dispersed phase in all studies. Results were obtained using a pulse injection of a salt tracer into the system. In the continuous column experiment the hold up of organic phase was varied between 0% and 18%. Data obtained for both flow and non-flow experiments were in good agreement and were correlated as,

$$\text{For } \frac{NR^2}{\nu} > 1.2 \times 10^5: \frac{f}{NR} = 4.3 \times 10^{-3} \left(\frac{D}{H}\right)^{\frac{1}{2}} \left(\frac{D}{S}\right)^{\frac{1}{4}} \quad (6.29)$$

$$\text{For } \frac{NR^2}{\nu} < 1.2 \times 10^5: \frac{f}{NR} = 4.5 \times 10^{-2} \left(\frac{D}{H}\right)^{\frac{1}{2}} \left(\frac{D}{S}\right)^{\frac{1}{4}} \left(\frac{NR^2}{\nu}\right)^{-1/5} \quad (6.30)$$

f is the mean actual rate of interstage mixing per unit area of stator opening, ν is the kinematic viscosity of the mixed phases, μ_m/ρ_m , with the mean density,

$$\rho_m = \rho_c h_c + \rho_d h_d \quad (6.31)$$

and the mean viscosity $\mu_m = \frac{\mu_c}{h} \left| 1 + \frac{\mu_d \mu_d}{(\mu_c \mu_d)} \right| \quad (6.32)$

In the same study, basing the results on the concept that the mean rate of energy dissipation in the column determines the turbulent dispersion in the fluid, a common correlation for both R.D.C. and Old-shue Rushton column, was tested against the data of various workers (8, 190, 193, 196, 200). It was found to provide an excellent basis for predicting the rates of interstage mixing in the continuous phase for various combinations of column geometry and mixer design. The correlation is reproduced in Fig. 6.8.

MIXCO - type columns

- △ two stages non-flow exp.
- ▲ continuous column exp.
rotating disc columns
- two - stages non - flow exp.
- continuous column exp.

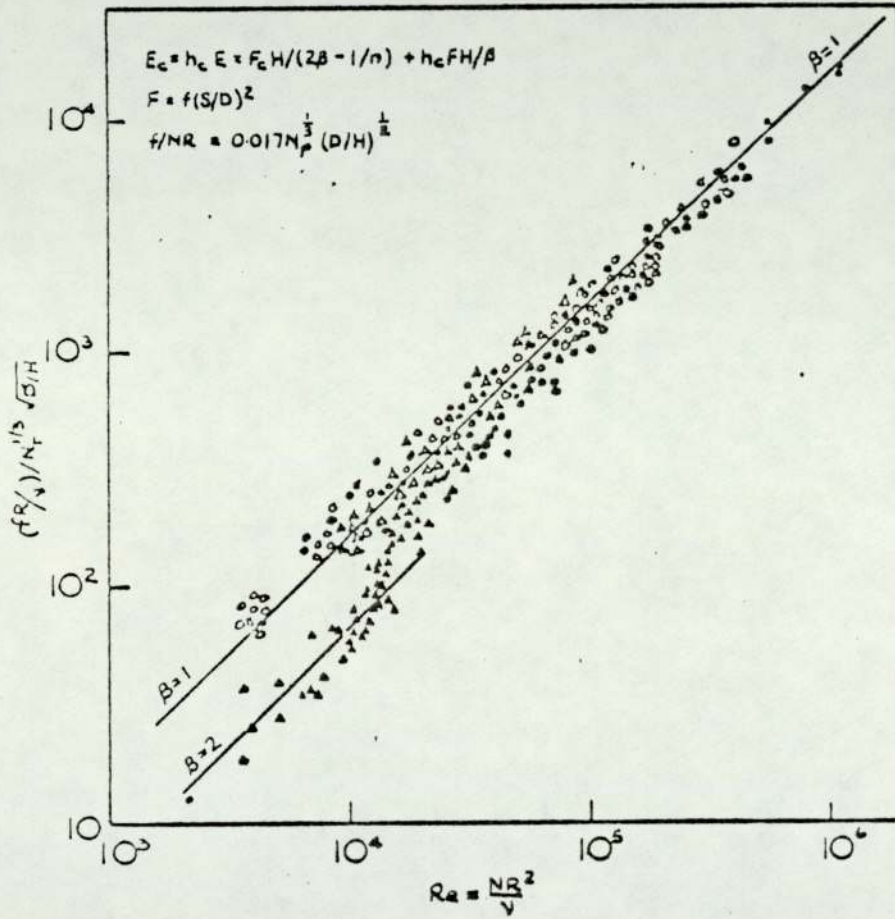


Fig. 6.8 Unified correlation of continuous phase backmixing for rotating disc and Oldshue-Rushton columns (190)

7. THE ROTATING DISC CONTACTOR - OPERATING EXPERIENCE

7.1 Wetting Effects

The effect of the wetting characteristics of column walls and internals upon column performance is of particular relevance to scale up studies. The performance of a large column may be significantly different from a laboratory column, due to differences in the materials of construction and the frequency, and thoroughness, of cleaning.

The terms wetting and non-wetting are generally used to describe whether or not a liquid spreads on a particular solid surface. For a solid adsorbed surface film the spreading coefficient is given by,

$$Sc(s) = \gamma_S - \gamma_{SL} - \gamma_{LV} \quad (7.1)$$

where γ_{SV} , γ_{SL} and γ_{LV} denote the solid-gas, solid-liquid and liquid-gas interfacial tensions respectively.

In many instances when a liquid is placed upon a surface it will not completely 'wet' it, but remain as a drop with a certain angle of contact exhibited between the liquid and the solid. The spreading coefficient is defined in terms of the contact angle and the surface tension of the liquid. (201, 202). Thus for a liquid to spread as a very thin film on a solid surface, i.e. conditions for a positive spreading coefficient, θ is finite. γ_{SL} and γ_{LV} should be as small as possible in

order to achieve good spreading. This may be promoted by the addition of a surfactant to the liquid. Alternatively, the liquid and solid may be chosen such that spreading will occur.

A difference has been observed between the advancing and receding contact angles. Generally, however, wetting corresponds with a contact angle of zero, and non-wetting represents an angle greater than 90° . In the absence of interfacial scum or dirt deposits, high surface energy materials, e.g. most metals and glass, are wetted by liquids with a high surface tension such as water, whilst low surface energy materials, e.g. plastics, are wetted by liquids with low surface tension, including most organic liquids.

Since the efficiency of mass transfer in an extraction column depends upon interfacial area and turbulence in either or both phases, the degree of wetting exhibited by the internals, i.e. walls, stators, rotors or packing, may have a significant effect. Conflicting results have been reported in the literature (203, 204, 205, 206, 207), but it is generally accepted that the best efficiency is obtained when the continuous phase wets the internals. For example in an R.D.C. with dispersed phase wetted internals, Davies et al (211) found that the transfer rate of phenol from a dispersed aqueous phase to a kerosene phase was less than that achieved using a conventional R.D.C. Under normal

conditions a dispersion of small droplets is obtained rather than the films or globules produced by coalescence of dispersed phase on wetted internals. However, it has been suggested that an R.D.C. with only the rotors wetted by the dispersed phase could be more efficient when the dispersed phase film resistance is controlling (40).

It has frequently been observed that preferential wetting of the column internals by the continuous phase deteriorated with time. This results in a change in the mode of operation of the equipment, possibly at the expense of extraction efficiency. The effects were noted in a laboratory scale pulsed plate column by Coggan (22), who observed different types of dispersion at different times.

In a later study, using an aqueous continuous phase and organic dispersions in R.D.C., Scheibel column and Old-shue Rushton column sections, a variation was observed in the wetting properties (in the form of increased coalescence of the dispersed phase) on the glass and stainless steel column internals. This was attributed to the deposition of dirt or impurities on the column internals (40).

To produce a dispersion with a narrow drop size range from the distributor, the distributor plate should be preferentially wetted by the continuous phase. In a

study of the formation of droplets from a circular orifice at varying contact angles Haynes et al (224) found that as the contact angle was increased, i.e. as the dispersed phase wetted the plate, relatively large droplets were formed before breaking away under the action of gravity. Conversely, liquids with small contact angles formed from the orifice without spreading. For organic droplets formed from an orifice a 10 fold increase in size, has been reported for p.t.f.e. compared with metal (208).

Wetting has a very pronounced effect on the column performance. The flow characteristics of an R.D.C. with organic phase wetted walls and internals are entirely different to one in which only rotors are of organic phase wetted material. The coalescence redispersion mechanism predominates in the latter, whereas the former operates as almost a wetted wall column with large globules of organic phase being released intermittently and travelling between compartments. Wetting also significantly affects performance of the Scheibel column. With dispersed phase wetted packing the column operates like a series of vertical mixer settlers with a very low throughputs, instead of the normal operation as a continuous counter current differential column.

Al Hemiri (37) studied the performance of a range of systems and various rotor designs, such as stainless steel or p.t.f.e. discs or polypropylene cones,

in a 4" diameter R.D.C. with stainless steel stators. Comparison of results for wetted and non-wetted rotors demonstrated that,

- (1) Average hold-up decreased with the wetted rotors.
- (2) Phase inversion, instead of flooding, defined the limiting flow rates with wetted rotors.
- (3) Under non-mass transfer conditions a different drop break-up mechanism involving sheet and ligament disruption, existed with wetted rotors.
- (4) Under mass transfer conditions the mechanism of drop break-up were almost independent of the rotor wetting properties but strongly dependent of the direction of mass transfer. The drop break-up mechanisms were dependent on the direction of transfer, i.e. break up was by sheet or drip point formation for the case of 'dispersed to continuous phase' solute transfer and by discrete drop break up in the region near the tip of the disc for 'continuous to dispersed phase' solute transfer.
- (5) Experimental d_{32} values did not correlate with values predicted from the Misek correlation (50). The Sauter mean drop diameter for the wetted disc column was correlated by:

$$\frac{d_{32}}{R} = 2.75 \times 10^{-6} \left(\frac{NR^2\rho_c}{\mu_c}\right)^{0.42} \left(\frac{\mu_d}{\mu_c}\right)^{-0.314} \left(\frac{NR\mu_c}{\sigma}\right)^{-1.73}$$

$$(X)^{0.293} \text{Exp} \left| -0.55 \frac{n}{z} \right| \quad (7.3)$$

and for the wetted column by:

$$\frac{d_{32}}{R} = 2.47 \times 10^{-3} \left(\frac{NR^2\rho_c}{\mu_c}\right)^{0.13} \left(\frac{\mu_d}{\mu_c}\right)^{0.2} \left(\frac{NR\mu_c}{\sigma}\right)^{-0.88}$$

$$(X)^{0.35} \text{Exp} \left| -0.5 \frac{n}{z} \right| \quad (7.4)$$

- (6) Two different operating mechanisms existed in the column depending on the direction of mass transfer. With transfer from the dispersed to the continuous phase, coalescence was promoted giving rise to vortex and sheet formation and hence condition of repeated coalescence and redispersion. For the opposite direction of transfer, i.e. from the continuous to the dispersed phase, coalescence was greatly reduced and the column operated as a discrete drop contactor.
- (7) With the system studied, i.e. Toluene-Acetone-water, rotor wettability had no significant effect on mass transfer efficiency.

Although it appears from this work that rotor wettability has no appreciable effect on mass transfer efficiency, the possibility remains of higher mass transfer

rates due to coalescence and redispersion phenomena in wetted disc columns. The systems used by Al-Hemiri had the controlling resistance to mass transfer in the continuous phase. Even if the mass transfer efficiency in a wetted disc column is only equivalent to that in a conventional column the higher volumetric capacity, due to the larger coalesced drops rising faster (37), would give a better overall column performance.

In conclusion it is essential in scale-up for the wetting characteristic of the materials of construction of the two columns to be compared before applying pilot scale data for the design of the industrial contactor. This is necessary because in an R.D.C. wetting affects the break up mechanism, thus affecting both volumetric capacity and efficiency.

7.2 Phase Inversion

The diameter of an industrial scale column for a specific duty may be predicted from the results of limiting capacity experiments in a small scale column with the same system. The limiting capacity has recently been defined either by flooding or phase inversion (11, 16, 18), depending on the system characteristics column geometry, material of construction and operating parameters.

A brief account of phase inversion is therefore included both to illustrate the mathematical relationship with flooding and to show its application to column design

in those cases where its onset precedes flooding.

Phase inversion in liquid-liquid system refers to a particular flow condition when the continuous phase becomes dispersed and vice versa. It was first observed in a batch system by Ostwald (209). It occurred at a phase ratio of 3 : 1, subsequently termed the 'Ostwald ratio'. The phenomenon has recently been studied by Luhnig and Sawistowski (210) using a single stirred tank operated batchwise and by Quinn and Sigloh (211). The existence of an ambivalent range has been established in which the existing dispersion maintains its configuration with remarkable stability, e.g. an aqueous phase could be dispersed in an organic one to a volume fraction of 75% before inversion occurred, and, if under similar conditions, the organic phase could be dispersed in the aqueous one up to 90% hold up, then the range of ambivalence is 25 to 90% organic phase, or 10 to 75% aqueous phase. Within this range the phase which would be continuous depended upon the starting procedure, i.e. which phase contained the stirrer initially.

Mass transfer has been found to affect the ambivalent region (210). The presence of solute under the conditions of phase equilibrium, increased the ambivalence, while mass transfer (continuous \rightarrow dispersed) considerably narrowed it. The solute used in the above study (210) was propionic acid and the binary systems were benzene-water

and p-xylene and water.

Phase inversion will occur in a batch system when the rate of coalescence of drops exceeds the rate of break-up. Additional factors have to be taken into account in a continuous flow system.

In an agitated column a complex situation exists between consecutive compartments, because of the distribution of droplet diameters. Thus a polydispersion of droplets flows by buoyancy through the stator opening against the flow of continuous phase. Turbulent flow, mainly across the opening, is generated by the impellers at the centre of each compartment and is superimposed on the varying terminal velocities of the droplets in the dispersion. When the hold-up in the column is large, i.e. about .6 - .8, and the outer conditions, e.g. system properties, rotor speed, and flow structure, are favourable, phase inversion occurs prior to flooding.

Under these conditions, the limiting flow rate in a countercurrent flow device is defined by phase inversion rather than flooding.

Phase inversion studies in continuous countercurrent devices have been limited. Al-Hemiri (37) first observed phase inversion in a 4" diameter R.D.C. using a toluene-water system. At a specific operating condition with toluene dispersed, the onset of phase inversion occurred in

the bottom compartment giving rise to a very large 'slug'; this possessed a high terminal velocity, and travelled up the column and eventually dispersed in upper compartments. With further increases in the dispersed phase flow the effect was repeated at an increased frequency until all compartments reached their critical phase inversion hold-ups. Complete inversion then obtained in the mixing section, with the column still operating countercurrently. Phase inversion was more easily attained using dispersed phase wetted rotors. From a mathematical analysis of the phenomenon the following models were proposed for hold-up at inversion,

$$\frac{V_c}{V_d} = 1 - 1.5\left(\frac{1}{x_i}\right) + 0.5\left(\frac{1}{x_i^2}\right) \quad (7.5)$$

$$\frac{V_c}{V_d} = \frac{1}{K_1} \left| 1 - 1.5\left(\frac{1}{x_i}\right) + 0.5\left(\frac{1}{x_i^2}\right) \right| \quad (7.6)$$

To account for the effect of coalescence on hold up, the modified equation for hold up proposed by Misek, i.e. Equation 3.9 was used in subsequent calculations to form a modified equation,

$$\frac{V_c}{V_d} = 1 - \frac{1}{x_i} - \frac{1}{ax_i^2} + \frac{2}{a^2x_i^3} + \frac{2b}{a^3x_i^4} + \dots \quad (7.7)$$

where $a = 4.1$ and $b = 2.1$.

Arnold (11) subsequently studied phase inversion with

the system water-toluene in a 6 inch diameter Old-shue-Rushton column. Contrary to Al-Hemiri's observations inversion occurred on a cyclical basis. When one particular compartment had inverted, the inversion passed on to the next compartment and proceeded up the column. After a finite time the phases in the original compartment inverted again and the whole sequence was repeated. The hold up values at inversion ranged from 0.55 to 0.80 and were very dependent on the rate of energy input. Furthermore phase inversion only occurred within a certain range of rotor speed; outside this range flooding occurred. Similar observations were recently made in a second study using the same column with a different system, Kerosene-water (212).

Recently Sarkar (38), using the systems butyl acetate-water and toluene-water, was able to generate phase inversion in both a 4" diameter R.D.C. and a 4" diameter Old-shue-Rushton column. Contrary to Al-Hemiri's findings the phase inversion was again found to be cyclical in both contactors. Reinversion occurred in each compartment after a finite time, the whole process being repeated indefinitely. A model for predicting hold-up values was proposed,

$$R_r = 1 - \frac{a}{x_i} + \sum_{\substack{K=2 \\ J=1}}^K b^K / x_i \quad (7.8)$$

where R_r = Phase flow ratio (continuous to disperse)

$$a = 1.5, \quad b = 0.5$$

x = hold-up, x_i = hold up at inversion.

The model was tested for $R_r < 1.0$ and was found to be in good agreement with the experimental results.

The time for re-appearance of the inversion slug in a compartment was correlated by,

$$t = 0.048 (z)^{0.66} (x)^{0.33} (D_{tr})^{-1.0} \quad (7.9)$$

where z = volume of the compartment

D_{tr} = drop diffusion coefficient.

The deviation of experimentally determined times from those predicted by this correlation was within 25%; at higher energy input rates the deviation was negligible.

These studies were the first to characterise inversion in agitated columns. However, for scale up, a complete analysis of the phenomena and its distinction from flooding is required. There is a need for a method of prediction from a knowledge of system properties and column geometry. This should predict whether phase inversion or flooding would occur first in order to define the limiting capacity in a particular contactor and its industrial scale model. However, the scale up equation 10.34 discussed later in chapter 10 for the column diameter can also be used where phase inversion

instead of flooding defines the limiting capacity. This is because Al-Hemiri (37) has proposed the same mathematical treatment for phase inversion as used for flooding. Hence Equation 10.34 should be valid even in cases where phase inversion defines the limiting capacities.

7.3 LIMITATIONS OF R.D.C. SCALE-UP METHOD

Despite numerous studies of hydrodynamics and mass transfer in laboratory size R.D.C. columns (37, 38, 40, 46, 50), scale-up still presents problems.

For scale-up three main factors require prediction,

- (1) Column diameter
- (2) Column geometry
- (3) Column height.

The determination of these factors involve fundamental differences and they are therefore dealt with separately.

(1) Column diameter

At present no correlations are available in the literature for the estimation of large scale column diameter from a theoretical consideration, or pilot plant data. The method generally used, involves the measurement of flooding velocity at a similar energy input level $(\frac{N^3 R^5}{HD^2})$ in a pilot scale column and calculation of the diameter of the industrial unit from the operating linear phase velocities. However, this method is open to criticism since equal energy input per unit volume does not

necessarily correspond to equal flooding velocities. Therefore it might lead to the full-scale column being of low capacity. If this is corrected by varying the design rotor speed, it may result in an inferior quality product.

(2) Column Geometry

At present all the published information for the determination of column geometry is based on the column diameter. Therefore, the geometry cannot be established unless the column diameter is known with reasonable accuracy.

(3) Column Height

In the past column height has invariably been calculated from, $L = N.T.U. \times H.T.U.$ However, this method suffers from the fundamental error of considering an R.D.C. as a plug flow device, with the phases moving countercurrently and mass transfer taking place only in one direction, i.e. from one phase into another. This model is far from the real situation in which axial mixing occurs (8, 46). Attempts have been made to account for axial mixing by assuming different mechanisms of mass transfer, as outlined in Chapter 6. However, all these deviations involve assumptions to simplify the solution of complex differential equations. Therefore the accuracy of each model tends to break down at some point in the analysis.

To overcome this problem, a novel method for determining the column height is proposed from the fundamentals of droplet analysis. The mathematical model, and the reasoning behind it, are outlined in Chapter 10.

8. DESIGN OF EXPERIMENTS

8.1 Objectives

The objectives of this investigation were to:

- (a) Study the variation of drop-hydrodynamics and interphase mass transfer with the scale of turbulence in large columns.
- (b) Extend studies of phase inversion phenomena and to assess the feasibility of stable operation in a continuous flow regime.
- (c) Develop procedures for the realistic scale-up of laboratory data to enable column diameter, column geometry and column height to be predicted for industrial R.D.C.'s or similar columns.

8.2 Design of Equipment

Two Rotating Disc Contactors were employed. The pilot scale contactor had a diameter of 450 mm. and height of 4.3 m and the laboratory scale was of diameter 101 mm and height 1.5 m. These columns were geometrically similar to limit the parameters under investigation. Subsequently it was recognised that strict geometrical similarity was unnecessary.

The flow diagram of each equipment is shown in Figure 8.1 and 8.2 respectively. The general arrangements are shown in Fig. 8.3 and 8.4. The process lines, feed

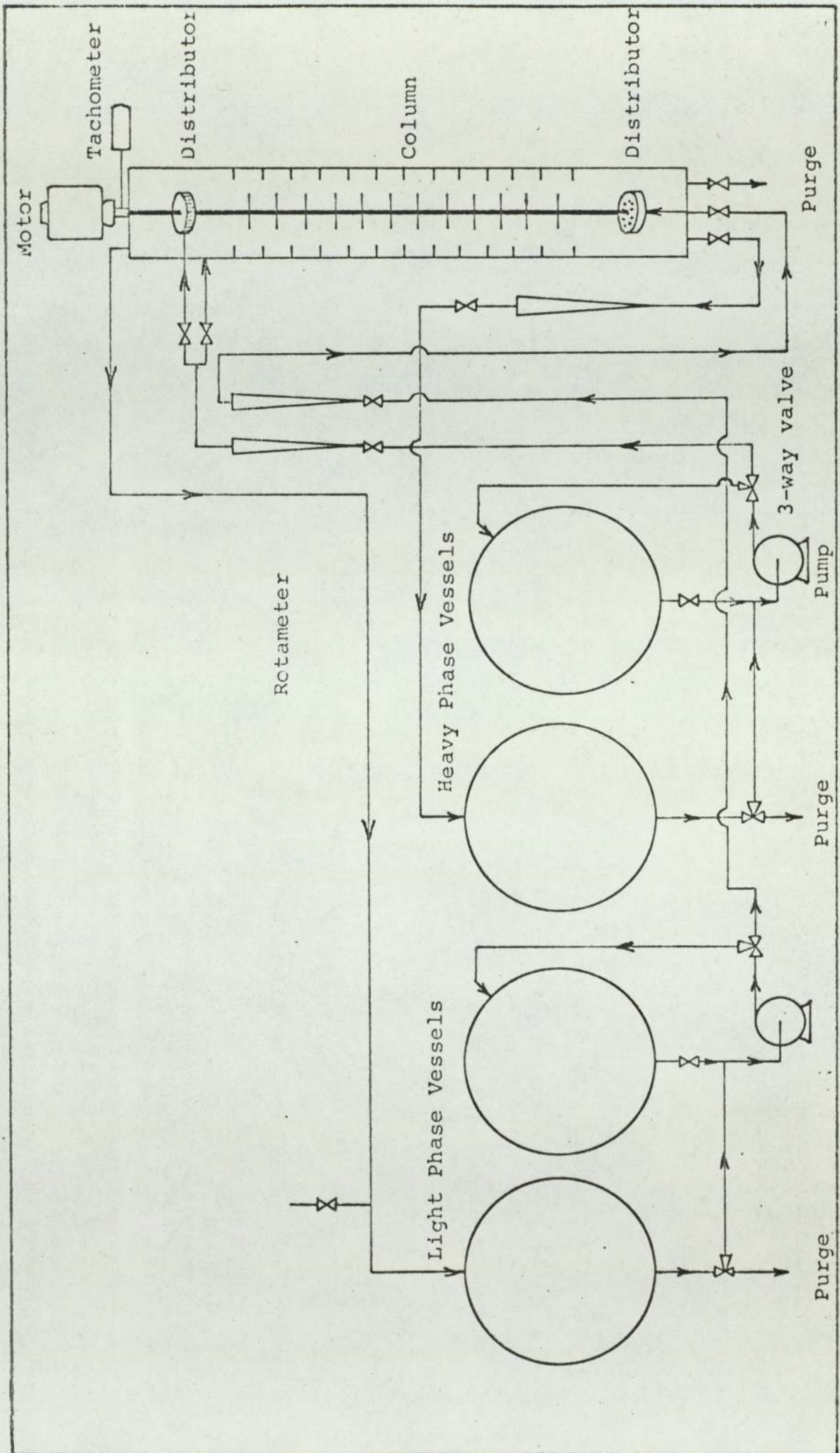


FIG. 8.1 Flow Diagram

FIG. 8.2 FLOW DIAGRAM OF 450 mm
DIAMETER R.D.C.

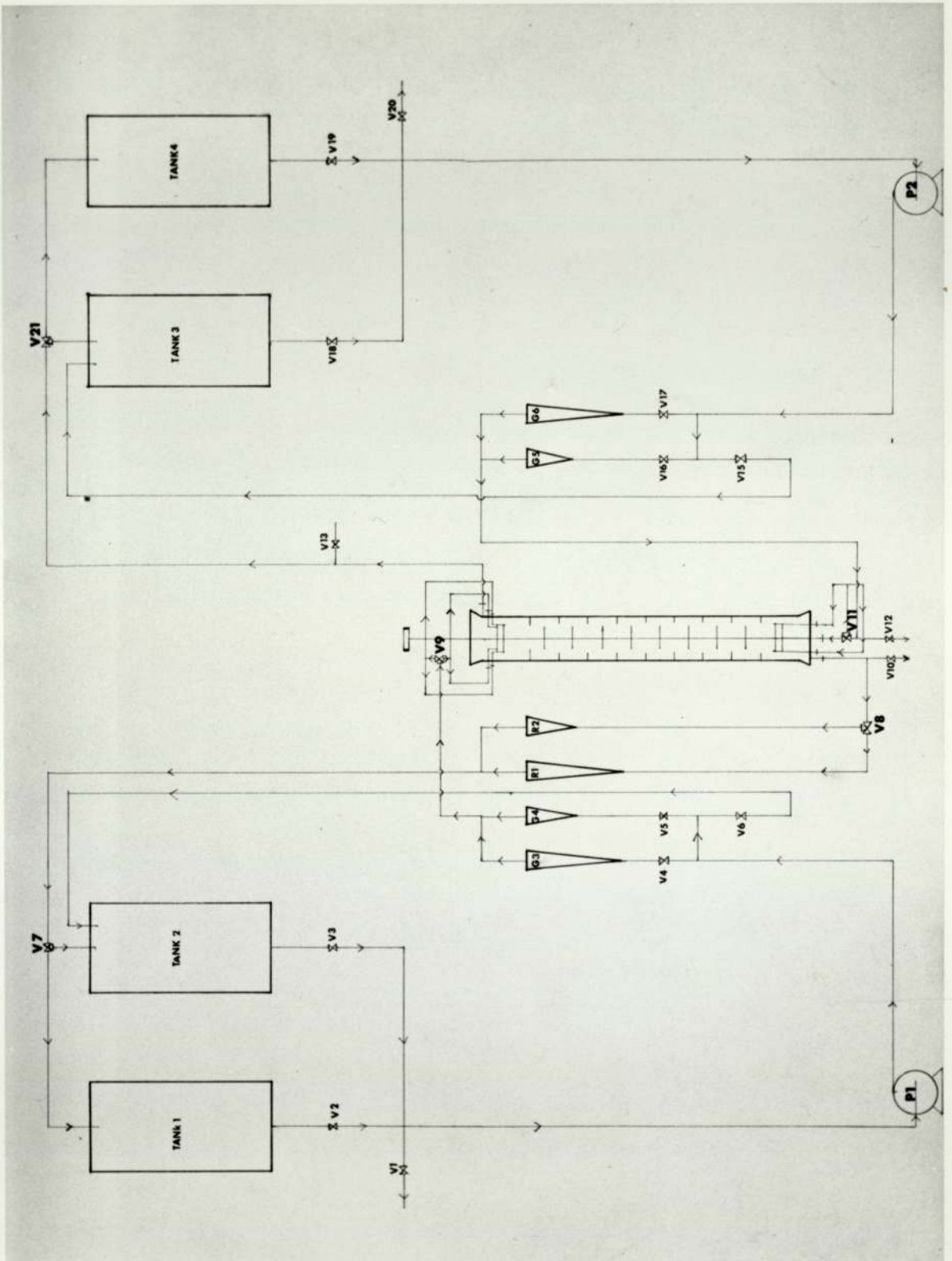


FIG. 8.3 GENERAL ARRANGEMENT OF
101 mm DIAMETER R.D.C.

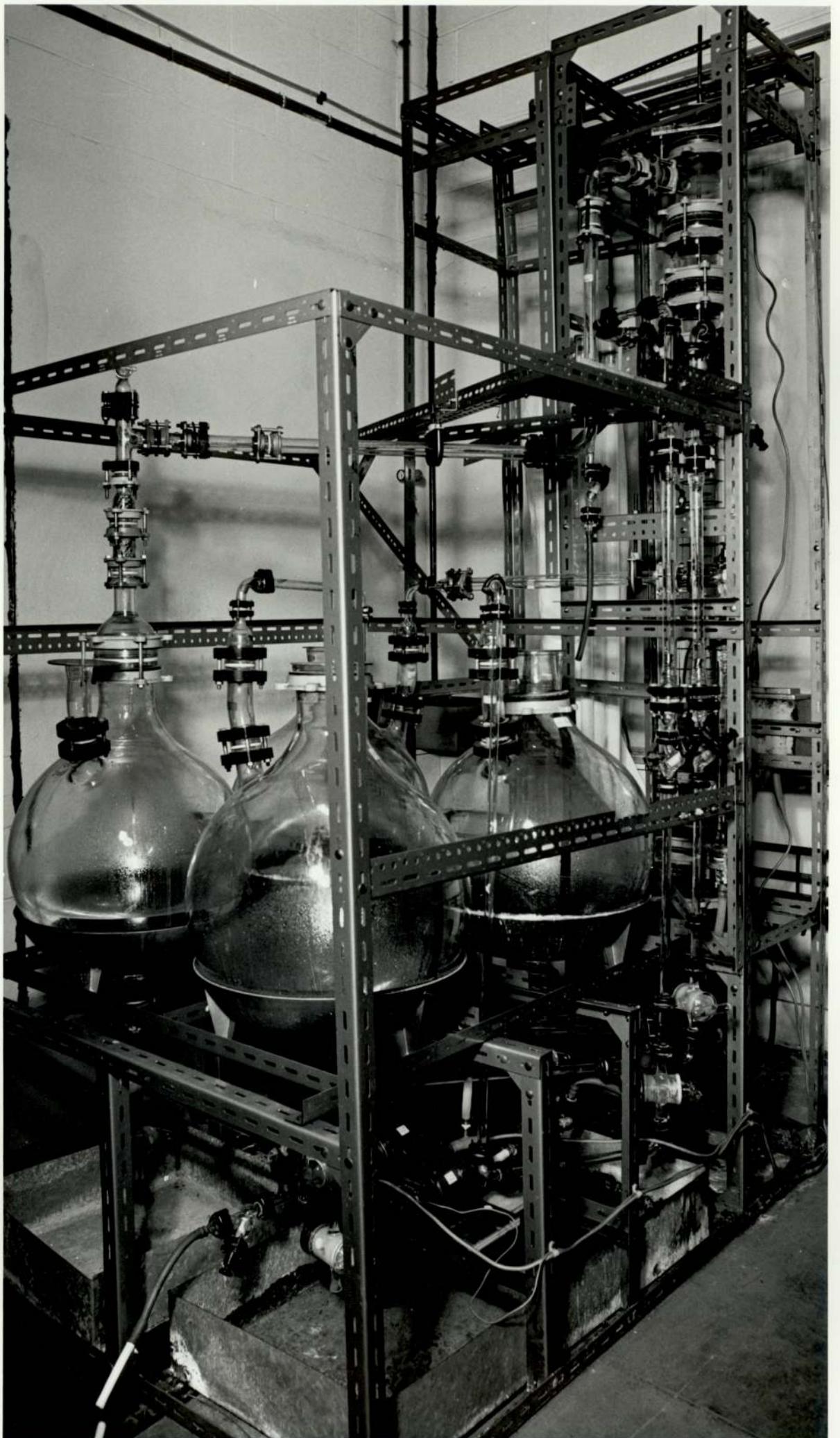
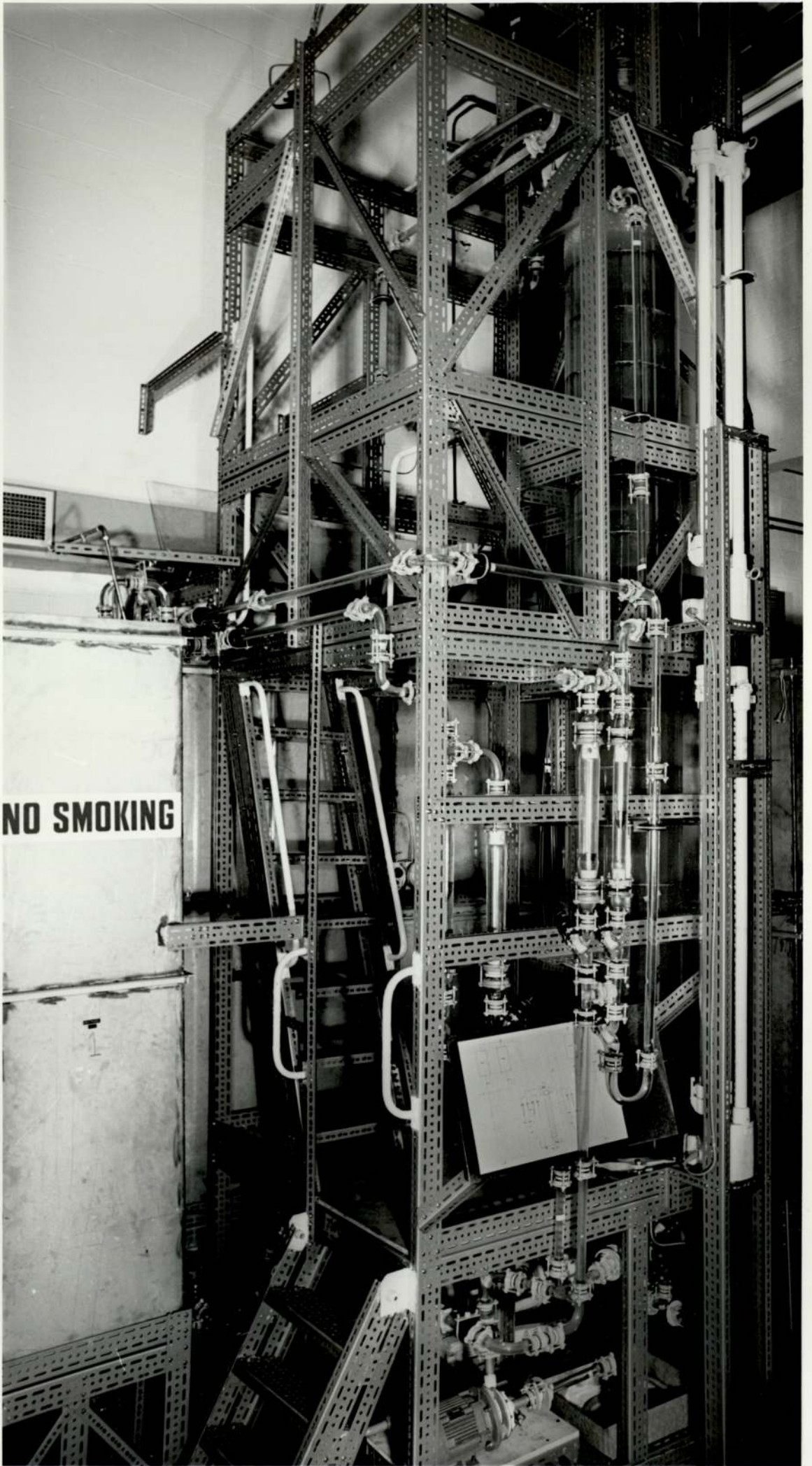


FIG. 8.4 GENERAL ARRANGEMENT OF
450 mm DIAMETER R.D.C.



NO SMOKING

and receiver tanks were arranged so that the columns were accessible from all sides. The sampling taps and control valves were arranged within easy reach. Drain points were located at the lowest points to allow for complete drainage and thus thorough cleaning.

No provision was made for temperature control of the environment but the temperature was always within 18.5 to 20°C. The equipment was in fact located in an isolated pilot plant provided with flame-proof switch-gear and lighting and an efficient low level air extraction system.

As illustrated in Fig. 8.4 a two-storied steel angle structure, with wooden working platforms was constructed for the 450 mm diameter R.D.C. All the control valves and instruments were located on the first floor of this structure so that column could be operated by one person.

8.2.1 450 mm Diameter R.D.C. Column

The dimensions of the large column, viz, 450 mm diameter by 4.3 m high, were chosen to eliminate the wall effects which are pronounced in small columns. It was constructed from two 2 metre high, 450 mm diameter borosilicate; QVF glass pipe sections. The stator rings were made of 12 gauge stainless steel sheet and were located and secured by means of 4 special $\frac{1}{4}$ " diameter stainless steel rods. The rods were designed so that the

sections holding the stator rings were threaded, the rings being held in place by two nuts. This allowed for flexibility, i.e. the possibility of changing the compartment heights.

The column contained 14 compartments, each 225 mm. high. The stainless steel discs were 225 mm. in diameter and were fabricated with straight edges. The stator openings were 337.5 mm. in diameter (1). These dimensions were in accordance with published design specifications (8, 9, 10, 43, 46, 213). Nine sample points were provided over the column height including one at the outlet and another at the inlet. These sample points were obtained by drilling $\frac{1}{4}$ " and $\frac{1}{2}$ " holes in the pipe sections at the centres of alternate compartments using an ultrasonic drill, and were fitted with stainless steel bulk head connections and toggle valves. The sample points were fabricated so that the tip could be moved across the column diameter to enable a radial hold-up profile to be determined.

Distributor plates were located at the top and the bottom of the column respectively. The top distributor made provision for the heavier phase to enter either via a side entry, or through the distributor plate. This was to facilitate operation with the heavy phase constituting either the continuous or dispersed phase. Similar provisions were made for the entrance of the light phase.

However, as described later the bottom distributor was 'water wetted' and the top distributor 'organic wetted'.

As shown in Figure 8.5, the bottom distributor plate was designed on the conventional basis, using the correlation by Treybal (20, 65). Since a punched plate distributor can only be designed for a narrow range of flow rates, i.e. for linear velocities below jetting, predicted flow rates of 60 - 80 lit/min. were used for the design. The distributor contained 700 holes each of 1.6 mm. diameter, arranged on a 10 mm. triangular pitch inside a 305 mm. diameter circle. The holes were drilled under size (1.2 mm.) and then counter punched to the correct size. This provided an upward projection around the periphery of each hole and hence more uniform droplets. The disperser was located 225 mm. above the bottom s.s. plate, to minimise the effects of heavier phase out flow on droplet formation. The distributor plate was located 200 mm. below the mixing section, so that initial droplet formation was substantially unaffected by agitation.

As shown in Figure 8.6, the top distributor was constructed of 10 gauge stainless steel, but the perforated plate was of 6.4 mm. thick polypropylene, with 1.6 mm. size holes drilled at a 10 mm. triangular pitch. Polypropylene was chosen because this material is hydrophobic and hence favoured drip point release of the heavy aqueous phase. As shown in Figure 8.6a 300 mm. long and 450 mm. diameter

FIG. 8.5 BOTTOM DISTRIBUTOR PLATE
450 mm DIAMETER R.D.C.

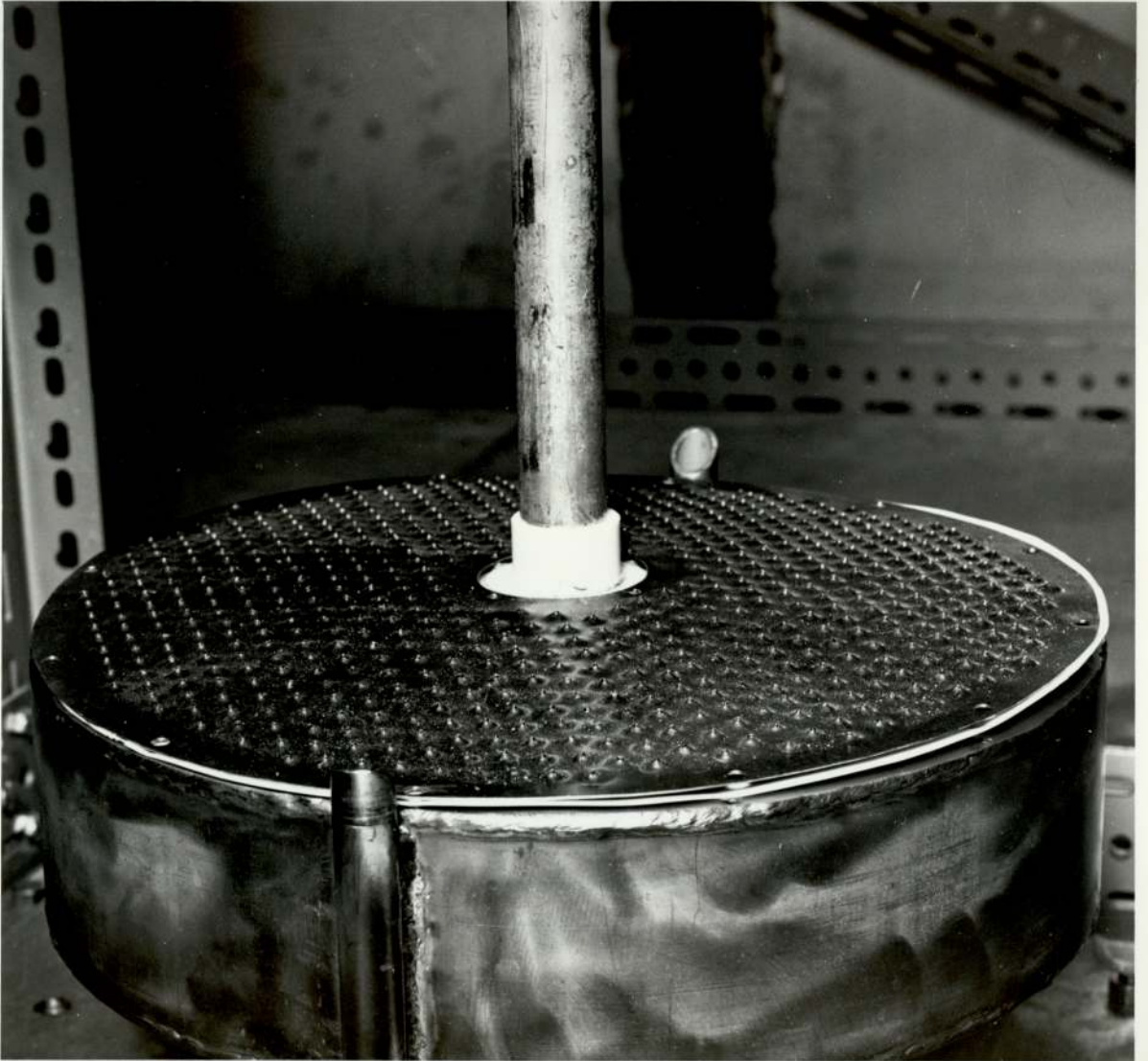


FIG. 8.6 TOP STAINLESS STEEL SECTION OF 450 mm
COLUMN IN INVERTED POSITION OUTSIDE THE
COLUMN; comprising top distributor,
inlets for heavy phase and outlet for
light phase.

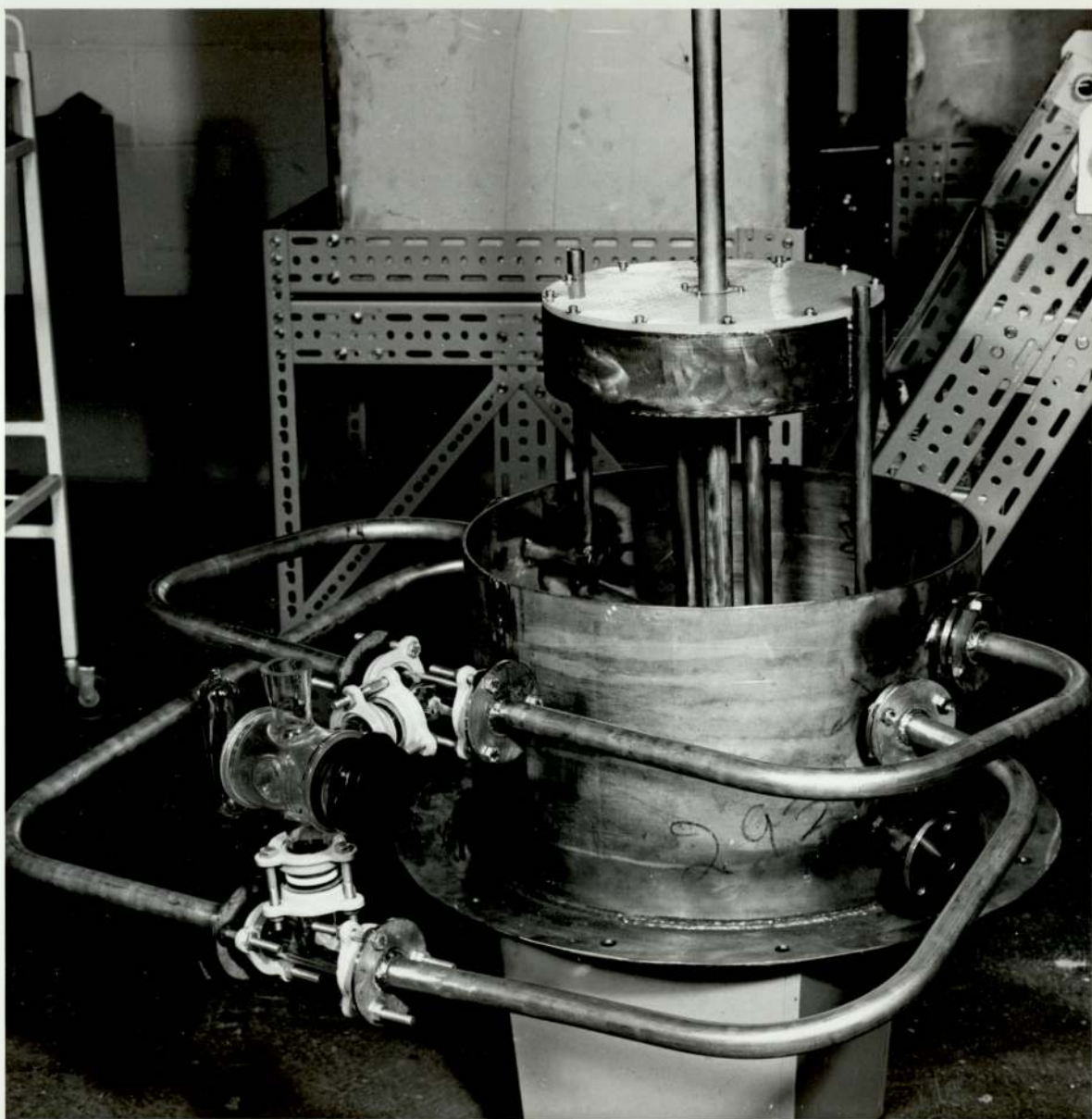
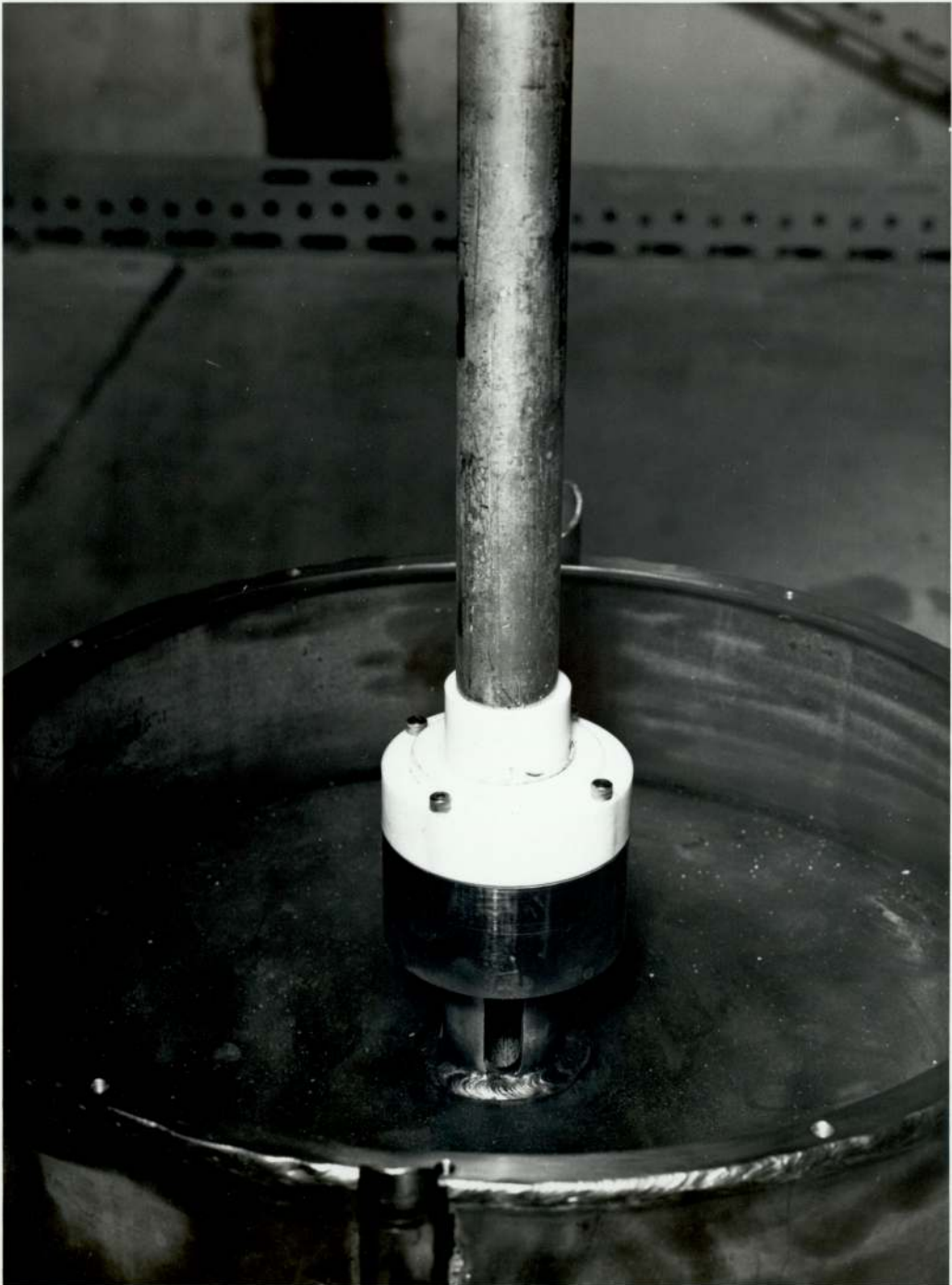


FIG. 8.7 THE BOTTOM DISTRIBUTOR;
450 mm diameter column with plate
removed. This shows the P.T.F.E.
bearing for the central shaft and
the type of slot (4 in all) for feed
to the distributor.



stainless steel section, fabricated from 10 gauge sheet, provided the light phase coalescence section and incorporated outlets, heavy phase inlets, support for the bearings and the top distributor. The light phase was withdrawn 75 mm. below the top bearing, thus leaving a dead space to avoid the need for a mechanical seal on the agitator shaft. A pair of self-lubricated and thrust bearings were provided at the top to retain and to support the weight of the shaft.

The shaft was fabricated from 25.4 mm. O.D. stainless steel pipe in two sections threaded at the centre. It was supported at three points, viz at the top and bottom distributors, and in the centre, by means of P.T.F.E. bearings.

The plates at the bottom and in the centre were fabricated from 6.35 mm. thick stainless steel. The bottom plate was drilled and incorporated pipes for the bottom distributor inlets and outlets, as shown in Fig. 8.5.

The column internals were fabricated from 12 gauge stainless steel. Each rotor disc was fixed to the shaft by means of a grub screw through its collar; this was counter sunk to eliminate any effect on the pattern of agitation.

8.2.1.1 Ancilliary Equipment

The shaft was driven by a 0.25 H.P., 240 volt., single phase, A.C. variable speed flame proof electric motor. The speed of the motor was controlled by means of

a gear box. The speed varied from 100 to 1500 r.p.m. This top speed was estimated from work of Al-Hemiri (37) and Sarkar (38) in the 101 mm. diameter column when 1500 r.p.m. was a maximum with the system toluene-acetone-water. The speed of rotation was measured by a Comark electronic tachometer 0-3000 r.p.m. used in association with a photo-electric probe located in level with a mark on the shaft at the top of the column.

As shown in Figure 8.4 stainless steel rectangular tanks, each with dimensions of 3.44 m x 1.22 m x .61m, and a capacity of 1815 litres, were used as feed tanks and receivers. The capacities were determined on the assumption that a total displacement of 2.5 times the column volume would be required to reach steady state. The effective column volume was approximately 600 litres, so that the total capacity of 3630 litres, for two tanks, provided sufficient time for each phase to reach steady state and about 20 minutes processing time for drop size measurement, photography and sample collection. A recycle line was provided for each phase for use during feed preparation and for mutual saturation of the phases by recirculation in a closed loop. Initially the liquids were transferred using two PVC flame proof pumps (PV71 supplied by Beresford Pumps, Birmingham), each capable of supplying 75-150 lit/mm against or head of 6 m - 3m. However, during the early limiting capacity experiments these were found to be undersized.

A third pump was found necessary to transfer the continuous phase from the column into the receiver tank, because due to head limitation and pressure losses in pipe work, the maximum flowrate under gravity was approximately 50 litres/min. whereas a maximum of around 100 litres/min was needed for flooding at low rotor speeds (450 r.p.m.). To obtain the desired flowrate the impellers of the two PV 71 pumps were therefore replaced by PV 101, the next size up in the range, thus increasing the maximum capacity from 150 lit/min. to 225 lit/min., against hydrostatic heads of 6 m. to 3 m. respectively.

A QVF glass pump, with a maximum capacity of 120 lit/min against the head, was used to replace the dispersed phase feed pump and the two PV 101 pumps were installed for continuous phase feed and discharge.

Dispersed phase flowrate was measured by 2 rotameters with stainless steel floats and a maximum capacity of 160 litres/min and 60 litres/min respectively, installed in parallel to provide fine control. Continuous phase flowrates at both the inlet and outlet were also measured using two rotameters, with stainless steel floats and a capacity of 100 litres/min. and 50 Litres/min. respectively, installed in parallel to obtain fine control.

1" QVF glass stop cocks were used as valves on all

applications except for fine control of flowrate. 1" QVF needle valves were used for fine control. Three-way QVF stop cocks were used for economy, where a division of streams was required, for example at the top and bottom feed distributor and on by-pass lines.

1 inch QVF glass pipe sections were used throughout the plant, except for the delivery line to the dispersed phase pump which was of 1.5 inch QVF glass pipe. An additional 2 inch QVF glass pipe line was subsequently installed for dispersed phase from the top settling section to the return tank, to eliminate leakage through the top bearing at very high flowrates of dispersed phase, 50-120 litres/min., during flooding determinations.

8.2.2 101 mm. Diameter (Small) R.D.C. Column

This equipment was essentially as described by Al-Hemiri (37) but modified by Sarkar (38). Further modifications were made by,

- (1) Extension of the height of the top coalescing compartment.
- (2) Installation of a new pair of thrust and self-lubricating self-centering bearings to minimise shaft whip and to take its weight and minimise wear on the bottom P.T.F.E. bush.
- (3) Inclusion of a glass section with an outlet 70 mm below the top of the column to remove the light phase and provide a dead zone. This avoided the need for a shaft seal.

- (4) Provision of a pulley drive instead of a direct drive to minimise fluctuation in the rotor speed. The driven pulley was set between a self lubricating self centering bearing and the bearing top of the column.

The column is shown in Figure 8.3. It consisted of 4 101 mm. diameter QVF glass sections with a total height of 1.5 m. It contained 16 compartments each 50 mm. high. The diameter of discs was 50 mm. and the stator openings were 76 mm. in diameter. These dimensions were originally determined from the design specification recommended by Reman (228), Strand et al (8), and Kung and Beckmann (43). Five sampling points were provided at 150 mm. intervals along the column length. Each point comprised a 10 mm. diameter hole fitted with a quick-acting stainless steel toggle valve. Additional sampling points were provided at the respective inlets and outlets. The column internals were fabricated entirely from 18/8 stainless steel, and were machined to obtain a close fit at the column walls, since the uncharacteristic performance of many laboratory columns may be attributable to phase flows between the column wall and the edge of the stator rings (40). The stators were supported by means of three equi-spaced lengths of 1 mm. S/S wire. This was found to be rigid enough to support the stators without introducing extraneous baffling effects. The

thickness of discs and stators was 2 mm. The discs were supported by means of a grub screw through the collar of the disc; this was counter sunk into the collar so as to eliminate any effect on the pattern of agitation. In any event, the neighbourhood of the collar has been found to be a relatively quiescent zone and any disturbances caused by protruding screws would be very small (40). The discs were fabricated with straight edges since sharp or tapered edges would tend to increase axial mixing effects (10). The agitator shaft was 9.6 mm. diameter stainless steel rod made in three sections. The shaft was supported at four points by means of a bottom P.T.F.E. bearing, a P.T.F.E. bearing in the top distributor, a bearing set at the top of the column and a self-lubricating, self-centering, bearing just above the pulley. The absence of a support bearing within the effective column length constituted a significant improvement over the early designs, since central bearing brackets have been found to cause extraneous effects in small diameter columns.

The phase entering the bottom of the column was dispersed as droplets of substantially equal size by a distributor designed according to the method of Treybal (20, 65). A mean value of expected flowrates between .7 and 1.5 lit/min. was used as a design basis. The distributor contained 46 2mm. diameter holes on a 6 mm. triangular pitch inside a 100 mm. diameter circle. The holes were

drilled under size (1.5 mm.) and then counter punched to the correct size. The inclusion of a distributor to disperse the lighter phase facilitated a rapid approach to equilibrium hydrodynamic conditions in the contactor by accounting for the initial droplet break-up stages which would otherwise have occupied useful column height. Provision was also made for dispersion of heavy phase via a distributor of similar design if required.

The heavy phase was introduced into the column just above the top compartment either through the distributor, if it was to constitute the dispersed phase, or a direct supply line.

The agitator shaft was driven by a 0.25 H.P., A.C. Voss motor, controlled by a Torovolt variable voltage mains transformer. The effective speed range was 100-3000 r.p.m. and this was recorded, using a high precision Comark type 2101 electronic tachometer.

Process fluids were stored in four 50 litre, Q.V.F. spherical glass vessels, mounted on special supports. Pipe work was mainly of 16 mm. i.d. borosilicate glass, but P.T.F.E. tubing was used in certain sections. Flow-rates were measured by independently calibrated rotameters with stainless steel floats. Provision was made for the circulation of the liquids within one vessel, or between two vessels, containing the same liquid, by means of by-passes on the pumps. Fluids were transferred by means of

two stainless steel, non-flameproof, Stuart Turner centrifugal pumps, type No.12, each capable of handling 1.25 to 0.45 m³S⁻¹ against a hydrostatic head of 2.0 to 10.0 m.

8.3 Selection of Liquid-liquid System

The storage and use of a relatively large quantity of solvent, i.e. about 1500 litres, required a low cost solvent to a fixed specification. Therefore the liquid-liquid system selected for study was kerosene-acetone-water. This was based mainly on the following considerations.

- (a) Low volatility of kerosene and relatively low toxicity, flash point > 23^o C and hence a reduced fire hazard compared with other commercially available solvents (e.g. toluol, dobane, butyl acetate). The low volatility resulted in both low vapour concentrations in the pilot plant during open handling operations and low solvent losses.
- (b) The availability of results from other studies for comparison.
- (c) The kinematic viscosity in the range 2-3 cs, interfacial tension with water in the range 20-40 dyne/cm. and density 0.7825 gm/cc of kerosene result in a system of the type ideal for operation with an agitated column as discussed earlier in Chapter 2.

The grades of kerosene and acetone were to the specifications given in Appendix 2.

A disadvantage with the use of kerosene, was that with ordinary filtered tap water an interfacial scum accumulated over a period.

The measured physical properties of the system are given in Appendix 2.

8.4 Experimental Techniques

8.4.1 Cleaning Procedure

All the column internals, the top stainless steel section, and the stainless steel tanks were initially cleaned with acetone to remove all residual grease or oil from the fabrication operations. During each series of runs the column, tanks, and pipe lines were cleaned by recirculation of an aqueous solution of a proprietary decontaminating cleaner, Decon 90. This solution was prepared by adding 1.0 to 1.5 parts of Decon 90 to 100 parts of water. The column was filled with this solution and left overnight; next morning it was pumped through all parts of the equipment for 1 - 2 hours with the agitator running and then drained. The equipment was then flushed with tap water 5 - 6 times and finally rinsed with the aqueous feed. Great care was taken to effectively drain all low points and pipe sections to avoid any retention of surfactant.

8.4.2 System Purity Check

The system purity was checked at regular intervals during the experimentation, by measuring relevant system

properties, i.e. density, viscosity and interfacial tension. Due to the scale of operation some change in the system properties was unavoidable; this was observed mostly during initial non-mass transfer runs when unfiltered tap water aggravated the formation of an interfacial scum with kerosene. This was made worse by some emulsification of kerosene in one pump during flooding runs, but entry ports for dust were eliminated from the equipment. This scum was removed by complete rejection of the water phase and rejection of the bottom settled layer of scum in the kerosene phase, followed by equipment washing using the method already described.

Typical results showing the variation of system properties over a period are given in Appendix. 2. This variation was restricted by adding fresh kerosene to the system in preference to relatively large scale redistillation.

8.4.3 Measurement and Calibration Technique

Solute concentrations were determined by measurement of relative absorbance. Calibration charts for relative absorbance Vs solute concentration were prepared by measuring the relative absorbance of solutions of known concentration. These data are given in Appendix 3. Only small quantities of the liquid under test, i.e. 10 mls., were required for this method.

Initially the solute concentration measurement was by the refractive index method used by other workers (37, (38)). However, the results using this methods were erratic in the concentration range .01 to 5%, in the case of Acetone/water samples, and 3 - 7% in the case of kerosene/Acetone samples. Differences in concentration were difficult to measure using the refractive index methods between 0.5% and 0.6% water-acetone solution, whereas distinct reproducible differences were demonstrated by the relative absorbance method.

A Pye unichem Ultra-violet spectrophotometer (SP1800) was used for the measurement of relative absorbance. The apparatus was first zeroed by inserting the blanks in both cells. The cell size was 2 mm. and the wavelength used was 238 mm. for kerosene/Acetone and 265 mm. for water/Acetone samples. The bandwidth in both cases was 3mm. The cell holder was maintained at a constant temperature of $22.5 \pm 0.2^{\circ}$ C, by means of a Townson and Merseer temperature control circulating unit.

For refractive index measurements, use was made of an Abbey A60 refractometer calibrated to five decimal points. This unit was maintained at a constant temperature of $22.5 \pm 0.2^{\circ}$ C by means of a Townson and Merseer temperature control circulating unit.

During early experiments to determine the time

required for steady state to be reached under mass transfer conditions an alternative chemical method was tested for the determination of solute concentration. This involved the addition of a measured volume of a known concentration of sodium bisulphite, usually 20 cc. of approximately N concentration, to 10 cc. of the sample, to form a complex with acetone. The excess sodium bisulphite was found by titration against a known concentration solution of potassium iodide and iodine, using starch as an indicator. The concentration was then determined by comparison with calibration charts prepared earlier. However, difficulty arose in the use of this method because the reaction between unused sodium bisulphite and $I_2 + KI$ was found to be very slow, so that a complete titration required about an hour. The problem was greater with two-phase titration, i.e. in the case of Kerosene/Acetone. Furthermore, it was not possible to differentiate between .5% Acetone and .6% acetone in a water sample. Therefore the method was discarded and results were checked using the refractive index method.

8.4.4 Determination of Equilibrium Distribution Diagrams

Equilibrium concentrations were determined by making up mixtures on a weight basis to represent points below the mutual solubility curve (214). Each mixture was contained in a stoppered flask and brought to equilibrium by repeated shaking and standing for several hours in a thermostat bath

at 22.5°C. The layers were then separated using a separating funnel and the sample analysed using the absorbance method. The equilibrium diagrams for the ternary system used, viz Kerosene-Acetone-water, are given in Appendix 3.

As expected the equilibrium data was found to differ slightly from that given in the literature, because of the different grade and origin of the kerosene and acetone and the difference in water supply.

8.4.5 Photography and Associated Techniques

Two cameras, a Nikkormat 35 mm. and Praktica 35 mm., were employed for still photography. The flameproof tube lights placed on the rig, although essential for visual observation, provided insufficient illumination for photography; therefore the lighting was provided by a 1000 watt Q.I lamp. The method of lighting was to put a 1000 watt photo flood lamp behind the column and take the photographs from the other side. In the case of the 101 mm. R.D.C. tracing paper was placed between the lamp and the object to diffuse and homogenise the light.

Kodak Tri.X400ASA films were used in most cases. Aperture opening, shutter speed and focal lengths were adjusted according to the lensometer reading. In general a shutter speed of $\frac{1}{1000}$ second was found to give best results. This speed was fast enough to 'freeze' the drop movement and hence excellent photographs were obtained, even at very high rotor speeds. Two photographs were

taken of each event. A photograph of a complete compartment was preferred to one of a very small, nearly square, section. A large number of drops, i.e. nearly 300, were required for Sauter mean drop size studies, and the distortion due to curvature was found to be negligible in previous studies (11, 37, 38), whereas the selection of representative square section could have produced inaccuracies.

For cine photography use was made of a Milliken (16 mm), DBM 45 model cine camera. Lighting was again provided by a 1000 watts Q.I lamp. The film used for this purpose was a Trix-Peresal film 7278.

8.4.6 Operating Procedure and Ranges

The procedure for column operation is outlined in Appendix 5.

The range of practical rotor speeds in the 450 mm. column was determined in commissioning runs. The minimum speed at which the drops became trapped beneath the rotating discs and stator rings, as described in para.3.1.1 was 100 r.p.m. The maximum speed without generation of a secondary dispersion of kerosene in water was 650 r.p.m. Therefore speeds of 150, 300, 450 and 600 were selected to characterise the complete operating range of the 450 mm. column with the Kerosene-Acetone-water system.

On this basis the corresponding rotor speeds in the

101 mm. diameter column, calculated at equal energy per unit mass ($\frac{N^3 R^5}{HD^2}$), were, 404, 808, 1213 and 1617. This calculation is summarised later in Table 11.1.

The operating flowrates for drop size, hold-up and mass transfer studies were taken below 60% of flooding flowrates determined as described in para. 9.1.1.

9. EXPERIMENTAL PROCEDURE AND RESULTS

9.1 Non-Mass Transfer Studies

9.1.1 Flooding Phenomena

Two types of flooding phenomena were observed; 'top flooding' and 'bottom flooding'. Top flooding was characterised by the rejection of heavy phase through the light phase outlet at the top of the column, so that normal counter-current flow was interrupted.

Bottom flooding was characterised by the rejection of a dense layer of droplets at the heavy phase outlet at the bottom of the column. This was the conventional flooding phenomenon described in the literature (8, 37, 38). The type of flooding encountered depended upon the flow rates of the two phases and the start-up procedure. However both types of flooding eventually led to 'complete flooding', i.e. the rejection of the two phases near their respective points of entry. The two types of flooding were more easily distinguished in the 450 mm. diameter column, than in 101 mm. diameter column. In the larger column the time between the onset of top or bottom flooding and complete flooding was of the order of 5 minutes, whereas in the small column it was only 1 minute, that is phase rejection at one end followed rapidly upon the onset of flooding at the other.

The flooding flowrates were determined in both columns

to find the range of operating variables (V_C, V_D, N) for subsequent experimentation. The results were then used to test the validity of the model, described in chapter 10, for the scale up of column diameter. The procedure used for determining flooding flowrates was as follows: The column was started up and run under steady state operating conditions at a fixed rotor speed. To achieve flooding, the volumetric flowrate of either of the two phases was then increased steadily, taking great care to maintain the interface level constant at the top of the column by adjustment of the outlet valves. This was continued until the onset of either top or bottom flooding. To check these results the column was then operated at the constant flooding flowrate of the phase for which flowrate had previously been varied, and the flowrate of the other phase increased until the column flooded. As before, great care was taken to maintain the interface level. Three to five readings were generally taken, depending upon the variation obtained, and a mean value noted. Intense mixing was observed prior to flooding, as reported by other workers (40, 43, 215). This resulted in the formation of a zone containing small droplets, i.e. < 0.5 mm., at the top of the column; this zone expanded until it caused flooding at the bottom in the form of a dense layer of droplets rejected through the continuous phase outlet.

Flooding was more easily recognised in either column

at higher rotor speeds; of the the order of 600 r.p.m. in the 450 mm. diameter, and 1618 r.p.m. in the small column.

Continuous operation of either column under flooding conditions was sometimes followed by phase inversion in the bottom compartments. This occurred particularly at low rotor speeds, of the order of 450 r.p.m. in the 450 mm. column and 1213 r.p.m. in the 101 mm. column. This confirmed the findings of other workers (11, 37), that flooding and phase inversion occur under very similar hydrodynamic conditions, and thus determine the maximum column capacity. However, continuous operation of either column under these conditions was not possible for an extended period, due to entrainment causing contamination of the phases.

The flooding data obtained in the two columns are given in Figs. 9.1 and 9.2. The four rotor speeds for the 101 mm. diameter column were chosen to provide data at values of energy per unit volume $\left(\frac{N^3 R^5}{HD^2}\right)$ equal to those in the large column to test the validity of the column diameter scale up model. The calculations relating to energy input are given in Table 11.1.

9.1.2 Drop Size Distributions

To study the variation of drop size with the operating parameters, that is V_C , V_D , N , and height from the bottom of the column, high speed still photographs were taken of compartments 2, 4, 6, 8, 10, 12, 14 and at

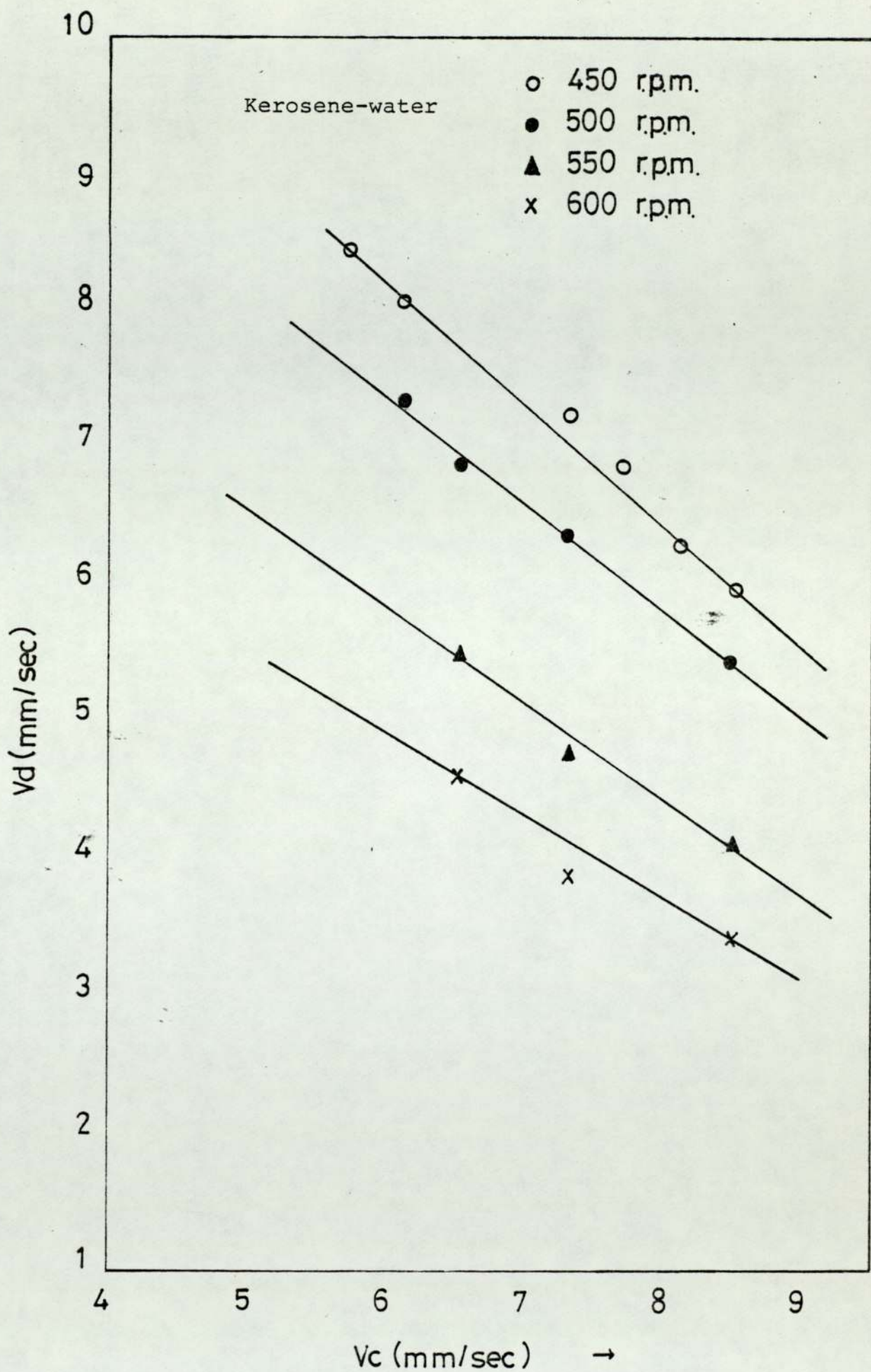


FIG. 9.1 FLOODING CURVES FOR 450 mm DIAMETER R.D.C.

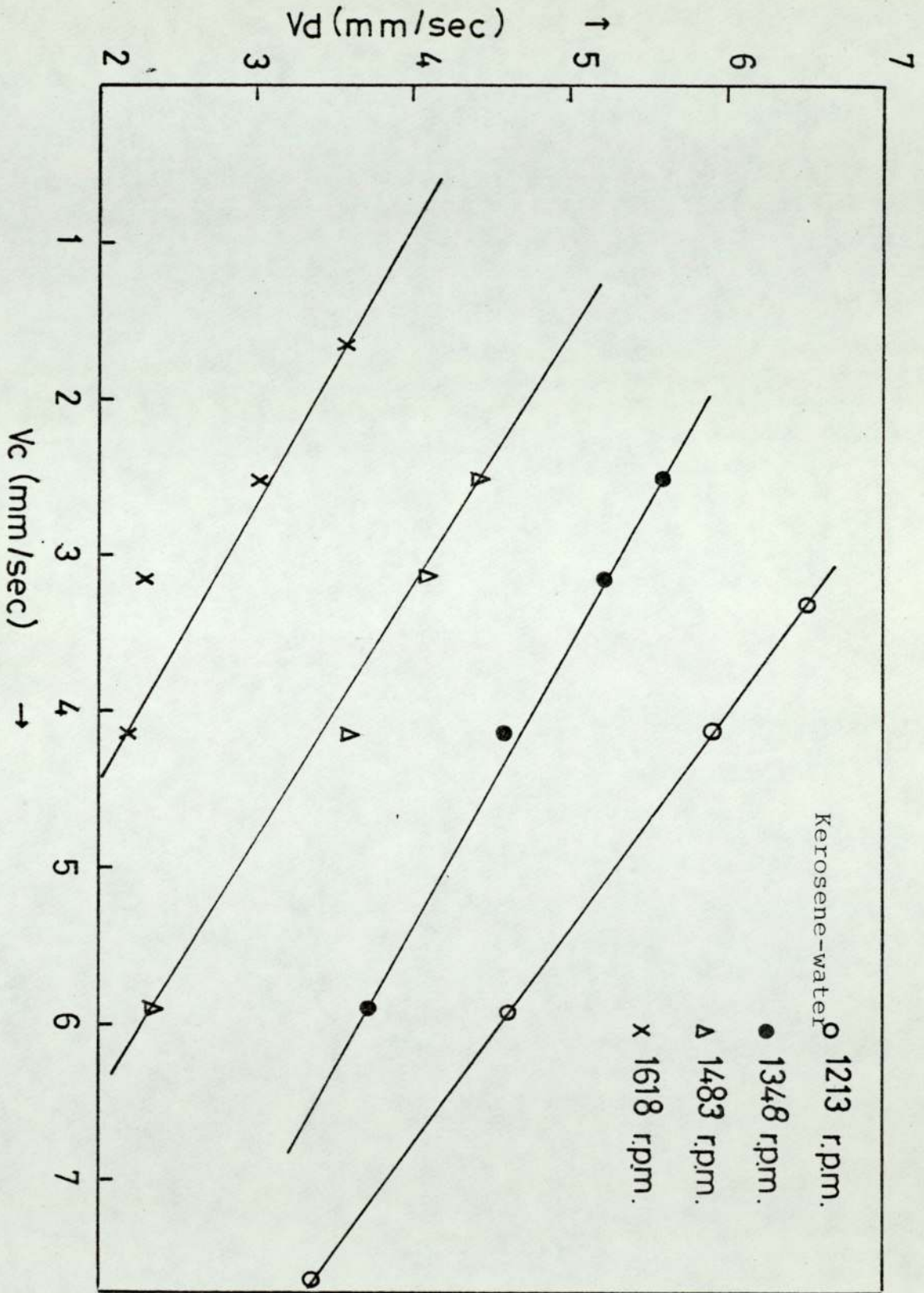


FIG. 9.2 FLOODING CURVES FOR 101 mm DIAMETER R.D.C.

the distributor. An attempt was made in preliminary experiments to determine a representative compartment in which the mean drop size approximated to the mean drop size throughout the column. This was intended to minimise the number of photographs to be analysed.

However, during early runs the drop size distribution was found to depend on the flowrate of both phases, rotor speed and the initial and final concentrations of solute. This dependence on continuous phase flowrate was not reported by other workers (37, 38), who therefore operated with it stationary.

The representative compartment was dependent upon these parameters and hence required careful selection after preliminary analysis of a set of photographs for each set of conditions. Hence in every case, to avoid loss of any results, photographs were taken of alternate compartments. The representative compartment was then chosen by analysing a complete set of photographs, that is by determining the Sauter mean drop size in each compartment and finding in which compartment this was equal to the arithmetic average Sauter mean drop size between compartments 1 to 14 (450 mm. diameter) or 1 to 16 (101 mm. diameter).

Some variation was found in the position of the representative compartments. This was contrary to the results of previous studies (37, 40) in which the middle compartment

was always taken as the representative compartment. However, the representative compartment was usually within ± 2 compartments of the middle one.

Two photographs were taken for each condition, after hydrodynamic equilibrium was attained. The criterion for equilibrium was taken as a steady interface. This was usually attained in 5 to 10 minutes after any change in any operating parameter. The photographs were taken using the technique described in para. 8.4.5.

Drop size measurements were taken from 250 mm. x 200 mm. prints with approximately 3 - 4 times magnification on the small column and 0.8 - 1.0 on the large column. Although an equivalent and larger magnification would have been preferable for both columns, for example a magnification of 5 - 6 has been reported (40) to give improved accuracy, this was impracticable because of the unusually large column diameter used. It was considered advisable throughout to photograph the complete width of the column. The reasons for this are outlined in para. 8.4.5.

The high magnification factor in the small column tended to produce a tail at the lower end of the drop size distribution range which was not measurable for the large column. This arose because upon magnification the small droplets, < 0.5 mm., in the small column came well within the counting range of the particle size analyser and thus were recorded. Conversely, in the large column, due to the smaller magnification factor, drops of this size either

remained indistinct or did not fall into the counting range. This would tend to give slightly larger Sauter mean diameter in the large column compared to that in the small column at 'equivalent' operating conditions. Equivalent conditions were considered to be characterised by equal velocities of the two phases and equal energy per unit mass $\left(\frac{N^3 R^5}{hD^2}\right)$ in the two columns.

The particle size counter used in the study was a Carl-Zeiss particle size analyser T4.Z.3. Because the standard scale would not cover the whole range of particle size, especially in the case of highly magnified photographs from the small column, the reduced scale was sometimes used. This may have created some discrepancy in the results since the analyser gives a mean value for a specific range.

When the scales were changed the results from one range may have fallen into the neighbouring range, thus giving a slightly different Sauter mean diameter in the final analysis. The other drawback with the particle size analyser was that it could not be used to estimate the axes of an ellipsoid or a near ellipsoidal drop. These were recorded as spheres of equivalent sizes. However, despite the potential inaccuracies introduced by reliance on the particle size analyser, a check involving duplicate determinations on the same photograph always gave results

within $\pm 5\%$ and in most cases ± 2 or 3% .

Sauter mean drop diameter was evaluated from,

$$d_{32} = \frac{\sum nd^3}{\sum nd^2} \quad (9.1)$$

A total of more than 300 drops were counted in a random manner from each photograph. A computer programme was written to evaluate the Sauter mean diameter from the drop size count. The computer programme and the count for a typical run are given in Appendix 4. The variation of drop size along the column height and the variation of drop size against the energy per unit mass group $\left(\frac{N^3 R^5}{HD^2}\right)$ under non-mass transfer conditions are plotted in Figures 9.3, 9.4 and 9.5a. Figures 9.5b and 9.5c illustrate the variation of drop size between the bottom and top compartments of the large and small columns respectively.

9.1.3 Hold-up

Three separate hold-up studies were performed, mainly,

- (1) A study of axial hold-up in both the 450 mm. diameter and 101 mm. diameter R.D.C.'s.
- (2) A study of radial hold-up in the 450 mm. diameter R.D.C. only.
- (3) A study of average hold-up in both the 450 mm. diameter and 101 mm. diameter R.D.C.'s.

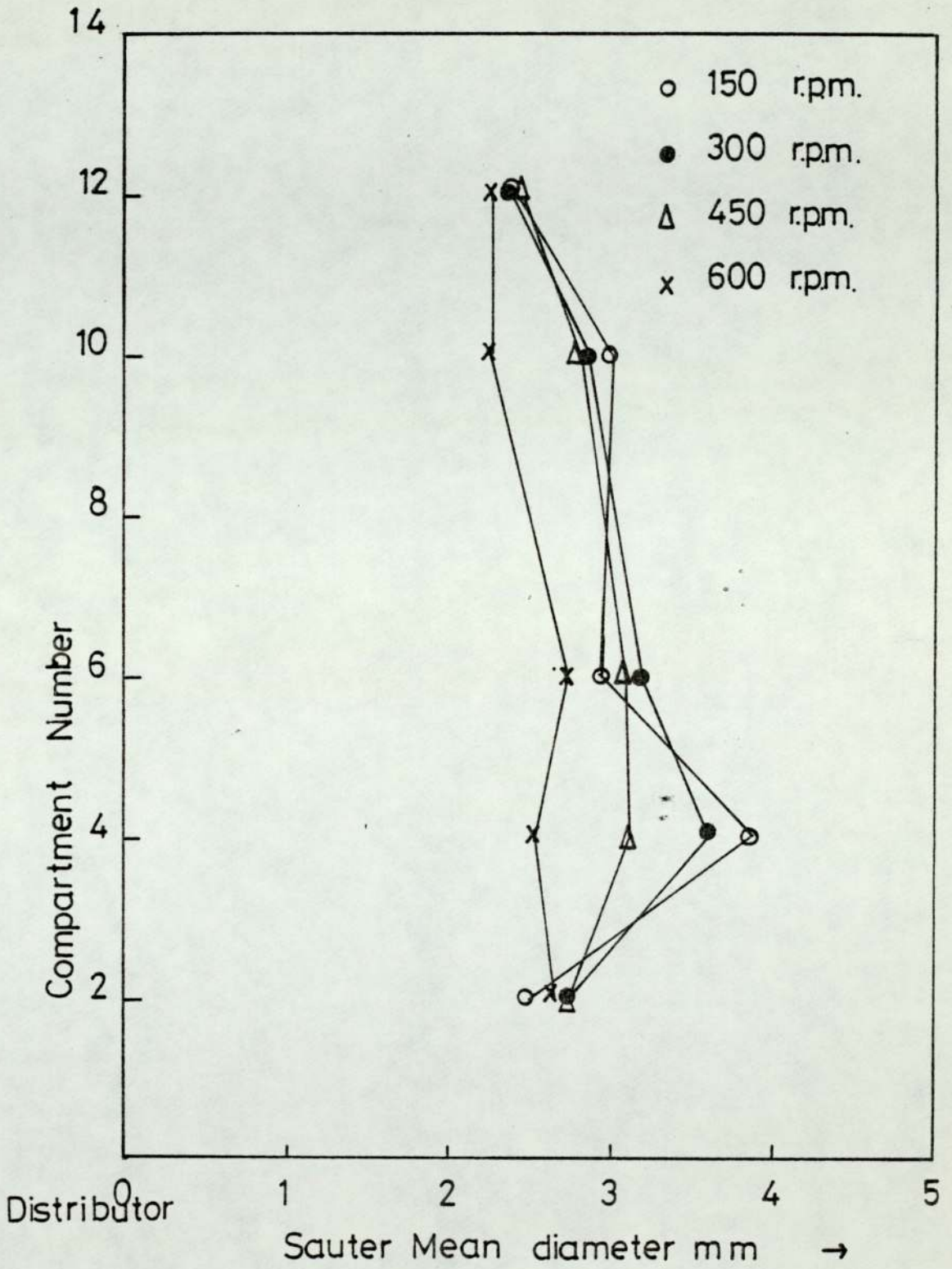


FIG. 9.3 VARIATION OF d_{32} WITH COLUMN HEIGHT
450 mm DIAMETER R.D.C.
Kerosene-water system

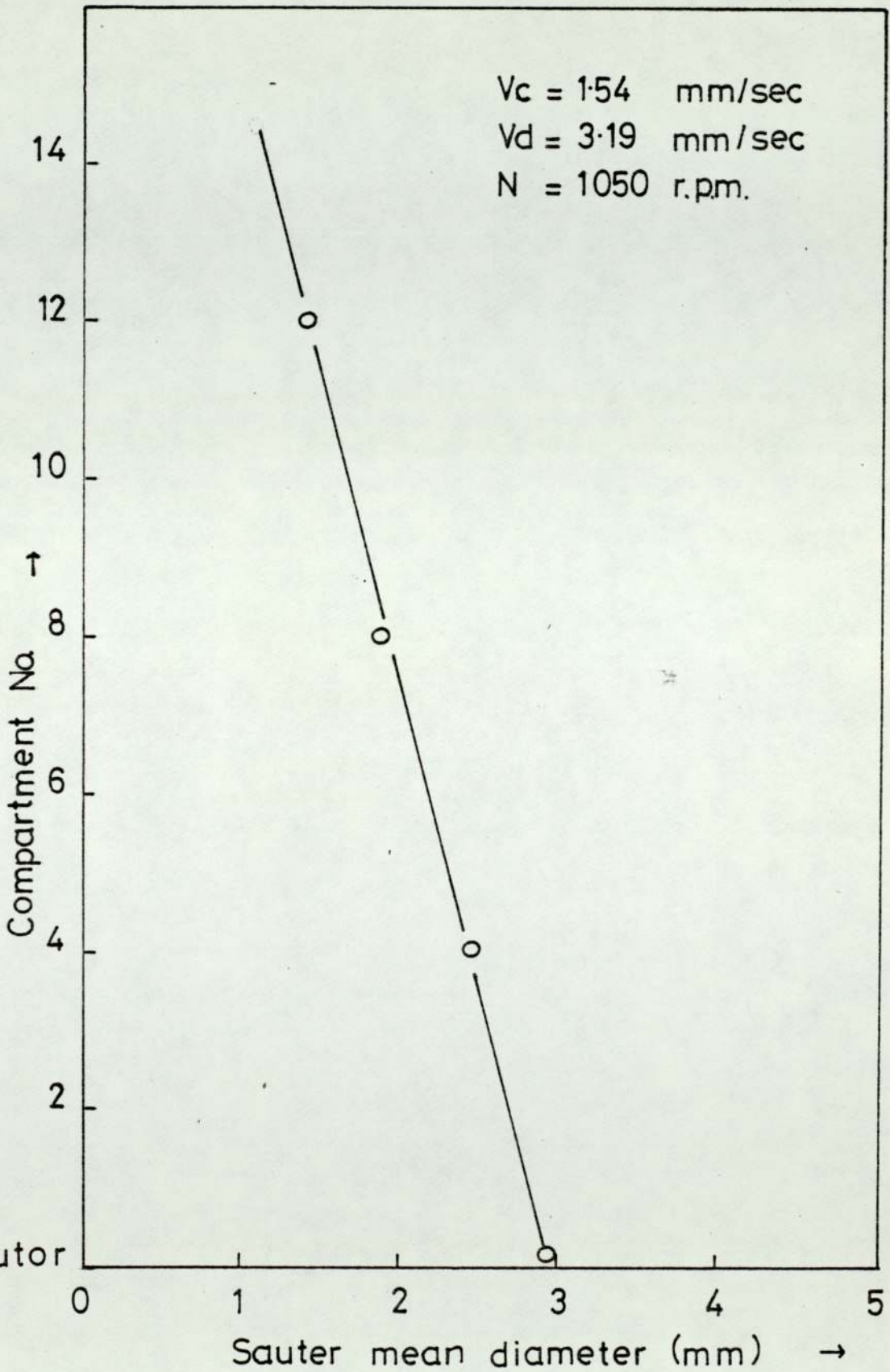


FIG. 9.4 VARIATION OF d_{32} WITH COLUMN HEIGHT.
101 mm. DIAMETER R.D.C.
Kerosene-water system

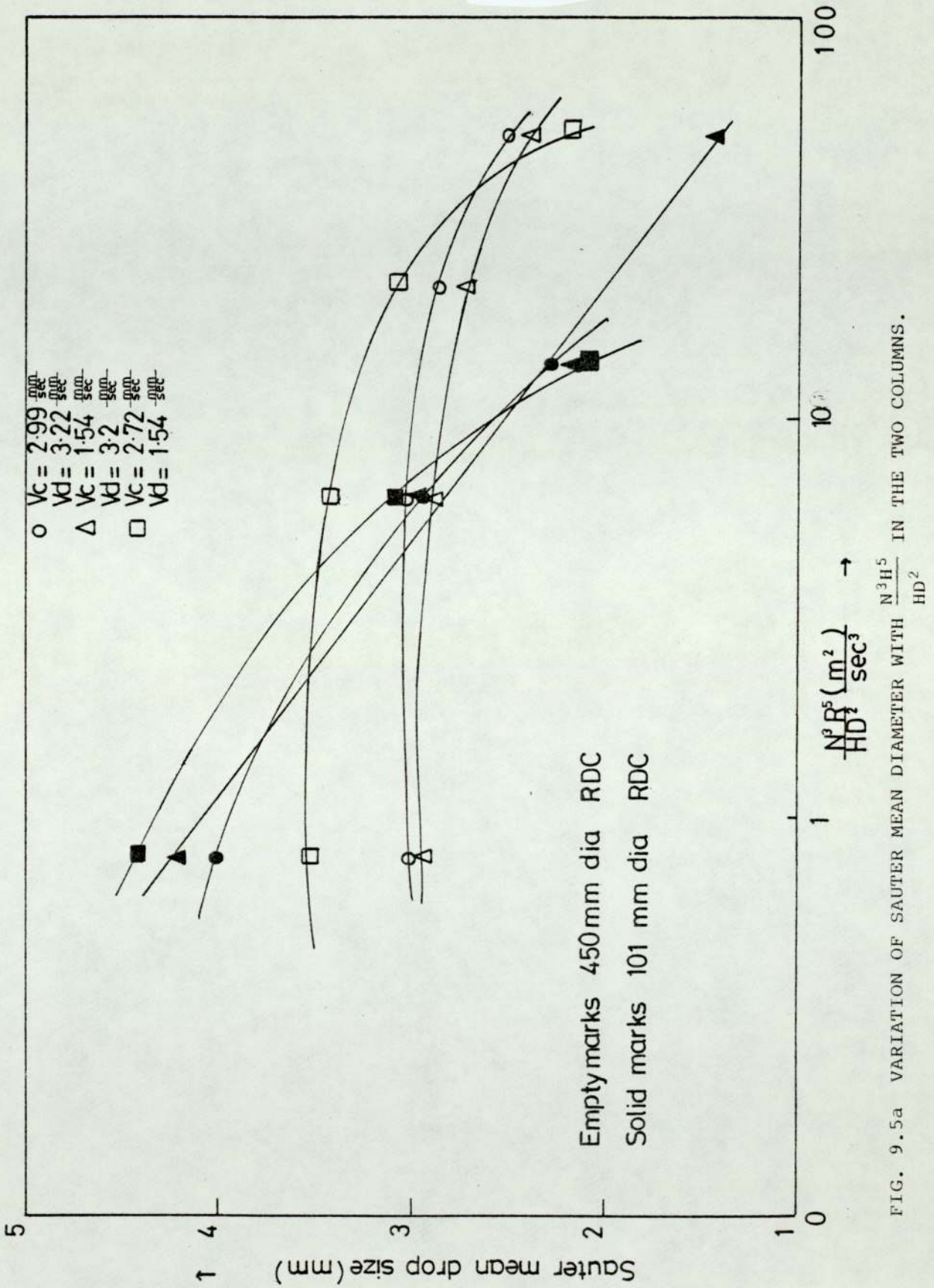


FIG. 9.5a VARIATION OF SAUTER MEAN DIAMETER WITH $\frac{N^3 H^5}{HD^2}$ IN THE TWO COLUMNS.

Compartment No. 2

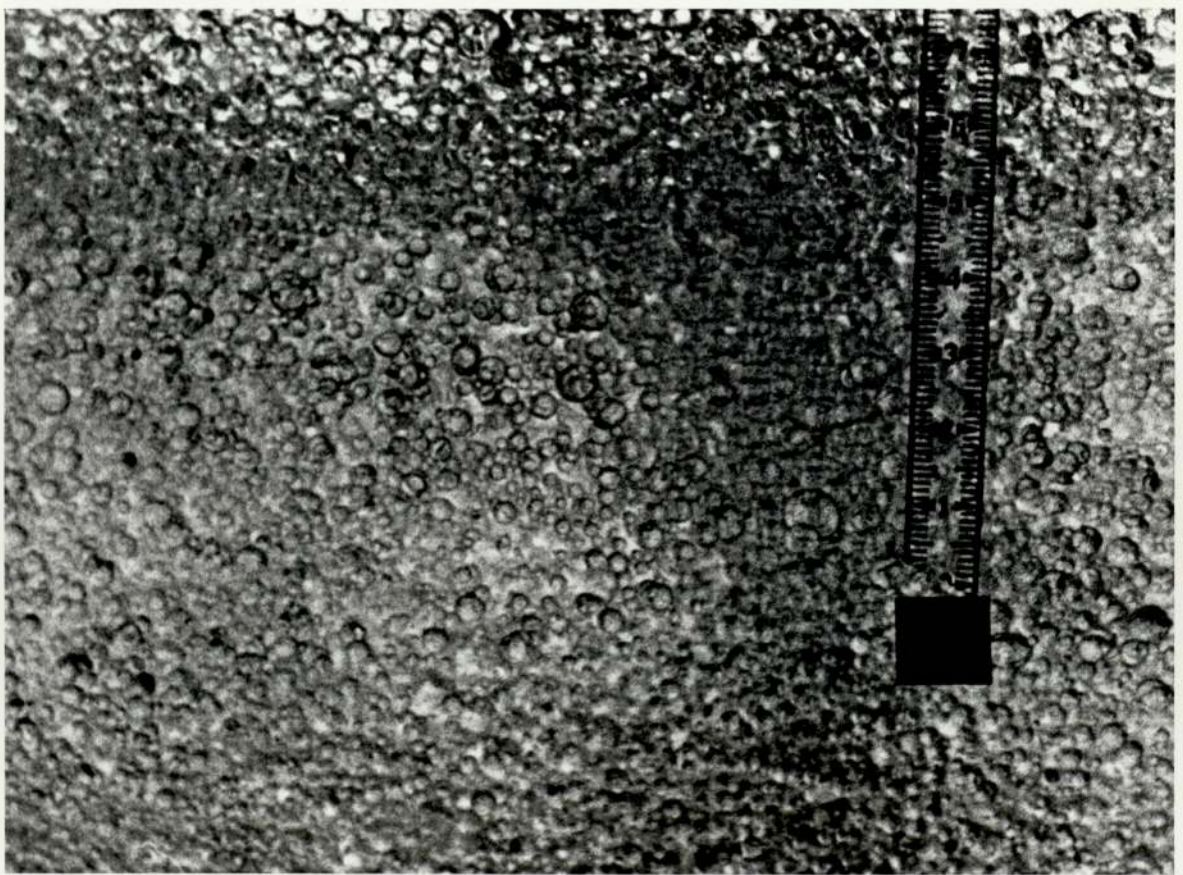
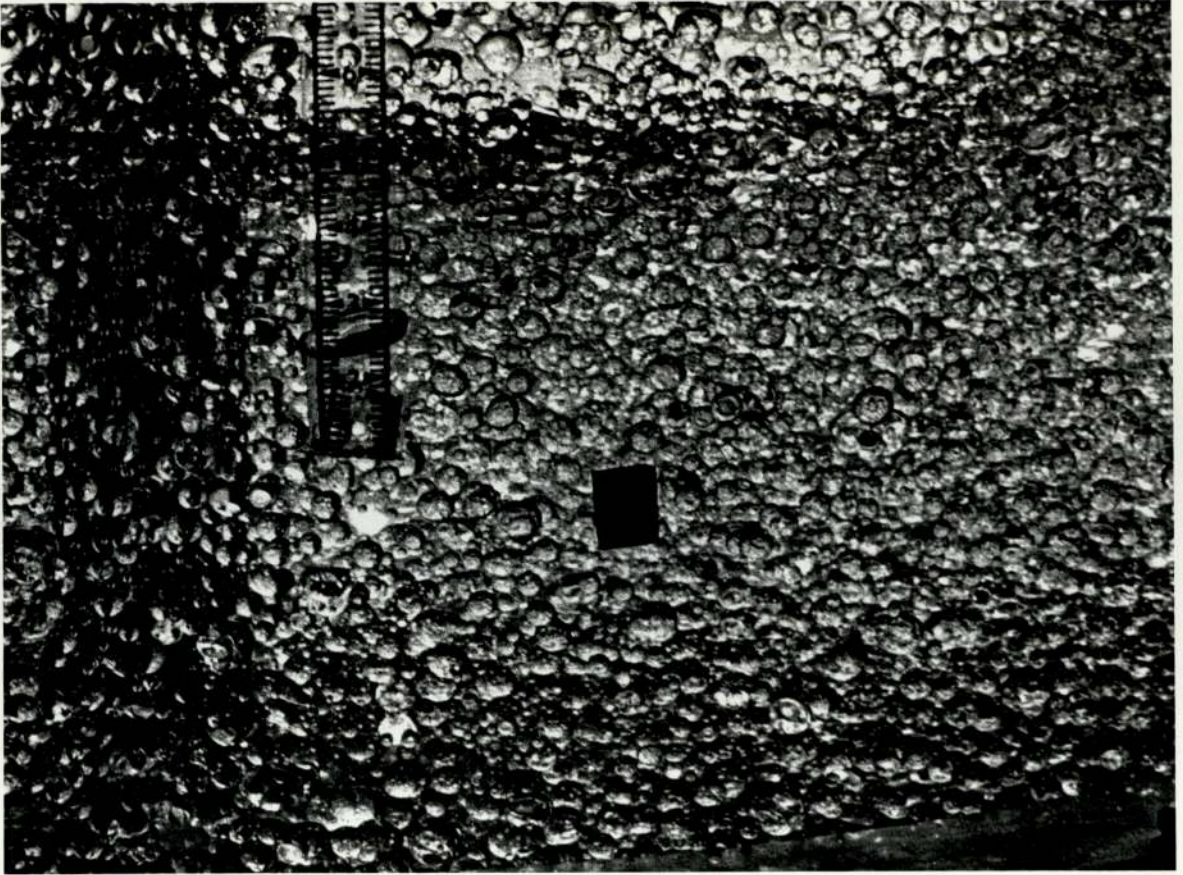
FIG. 9.5b VARIATION IN DROP SIZE BETWEEN COMPARTMENTS
2 and 12 UNDER NON-MASS TRANSFER CONDITIONS,
450 mm. R.D.C.

$V_c = 3.1$ mm/sec; $V_D = 3.22$ mm/sec;

$N = 450$ r.p.m.;

Magnification factor = 1.

Compartment No. 12



Compartment 12

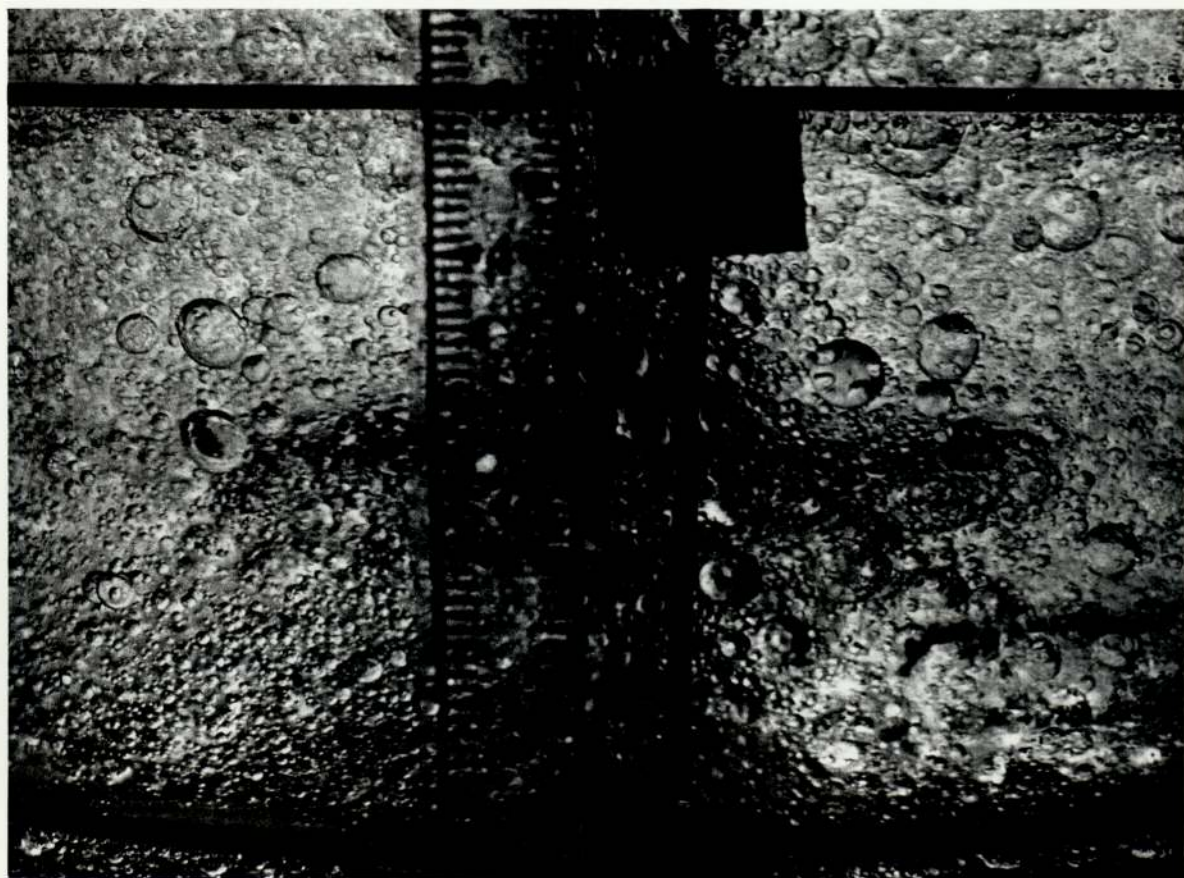
FIG. 9.5c VARIATION IN DROP SIZE BETWEEN COMPARTMENTS
2 and 12 UNDER NON-MASS TRANSFER CONDITIONS,
101 mm. diameter R.D.C.

$$V_C = 1.54 \text{ mm/sec}; \quad V_D = 3.19 \text{ mm/sec};$$

$$N = 808 \text{ r.p.m.};$$

$$\text{Magnification factor} = 2.$$

Compartment 2



9.1.3.1 Axial Hold-up in the Two Columns

Axial hold-up studies were performed in both columns

- (a) To study the reliability of sample collection via points located at equal intervals along the two columns, and
- (b) To find the appropriate sample point to obtain the mean hold-up.

The procedure used in the determination of axial hold-up profiles was to operate the columns at selected flowrates and rotor speeds, as described in para. 8.4.6, until steady state was reached. This usually took approximately 15 minutes, or a total displacement equal to 2.5 times the column volume, in either column. Samples were then withdrawn through the sample taps from alternate compartments into 100 c.c. measuring cylinders. Separation was complete in 3 to 5 minutes, and the phase ratio was then read off directly. Three 100 c.c. samples were taken for each reading.

The ratio of sample size to compartment volume was 1:358 in the case of the 450 mm. diameter R.D.C., and hence had no effect on the steady state conditions. Conversely, in the 101 mm. column the ratio was 1:4 but even then earlier workers (37, 38) reported no effect due to sample withdrawal. When there was any noticeable difference, a mean of the three readings was taken. The

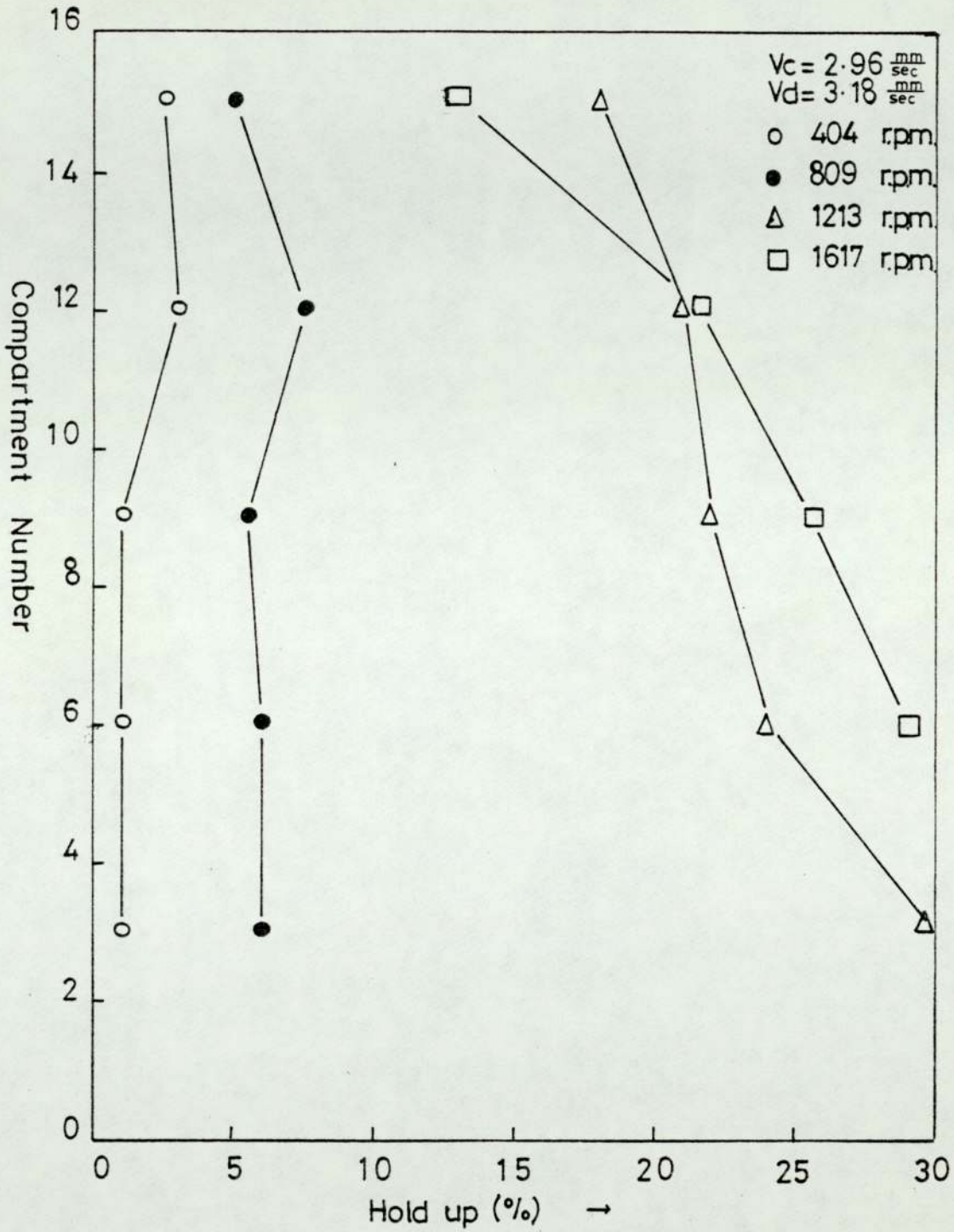


FIG. 9.6 AXIAL HOLD-UP PROFILE IN THE 101 mm DIAMETER R.D.C.
Sample point located at the column wall in line with the rotating discs.

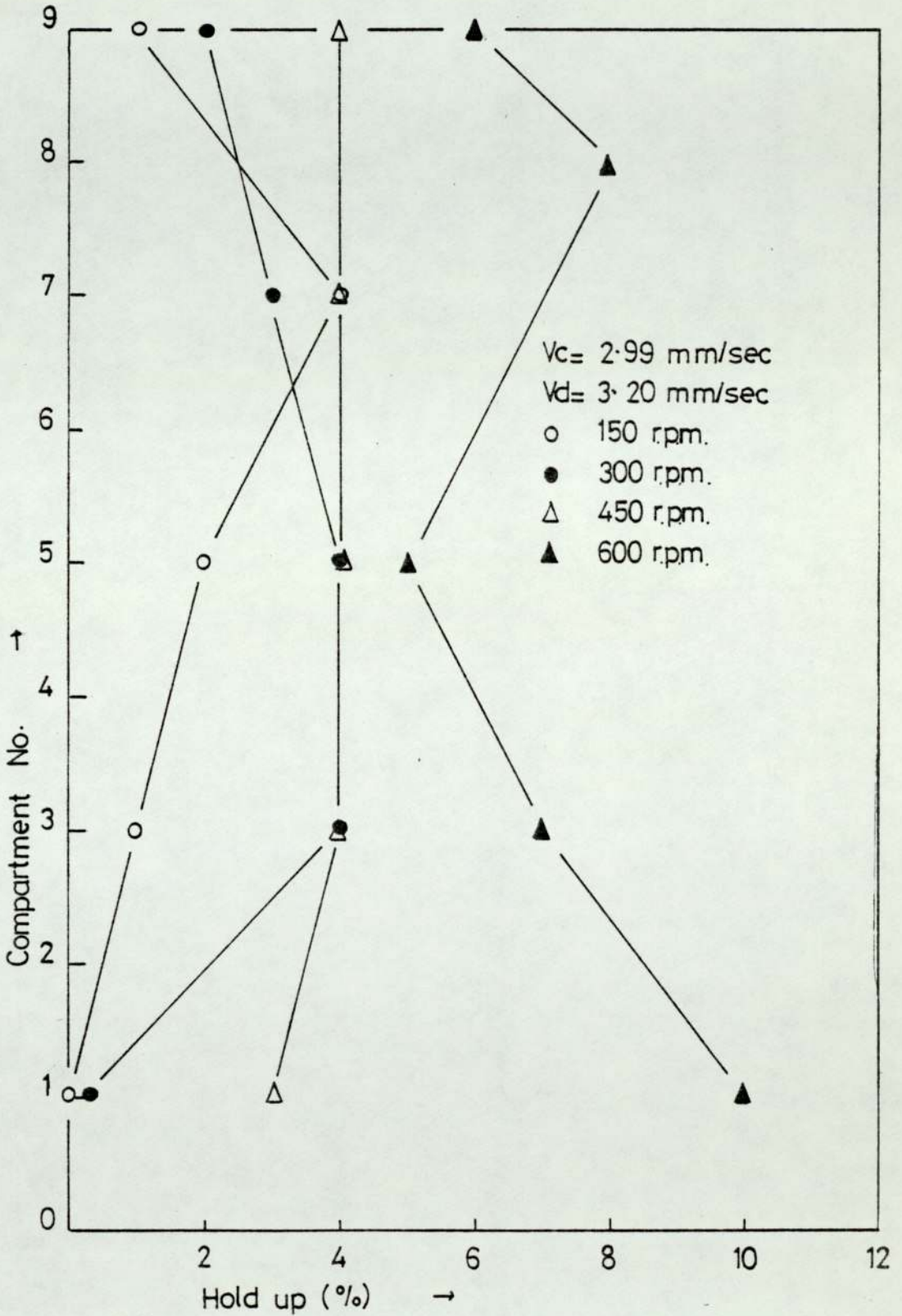


FIG. 9.7 AXIAL HOLD-UP PROFILE IN THE 450 mm DIAMETER R.D.C.
Sample point located at the column wall in line with the rotating discs.

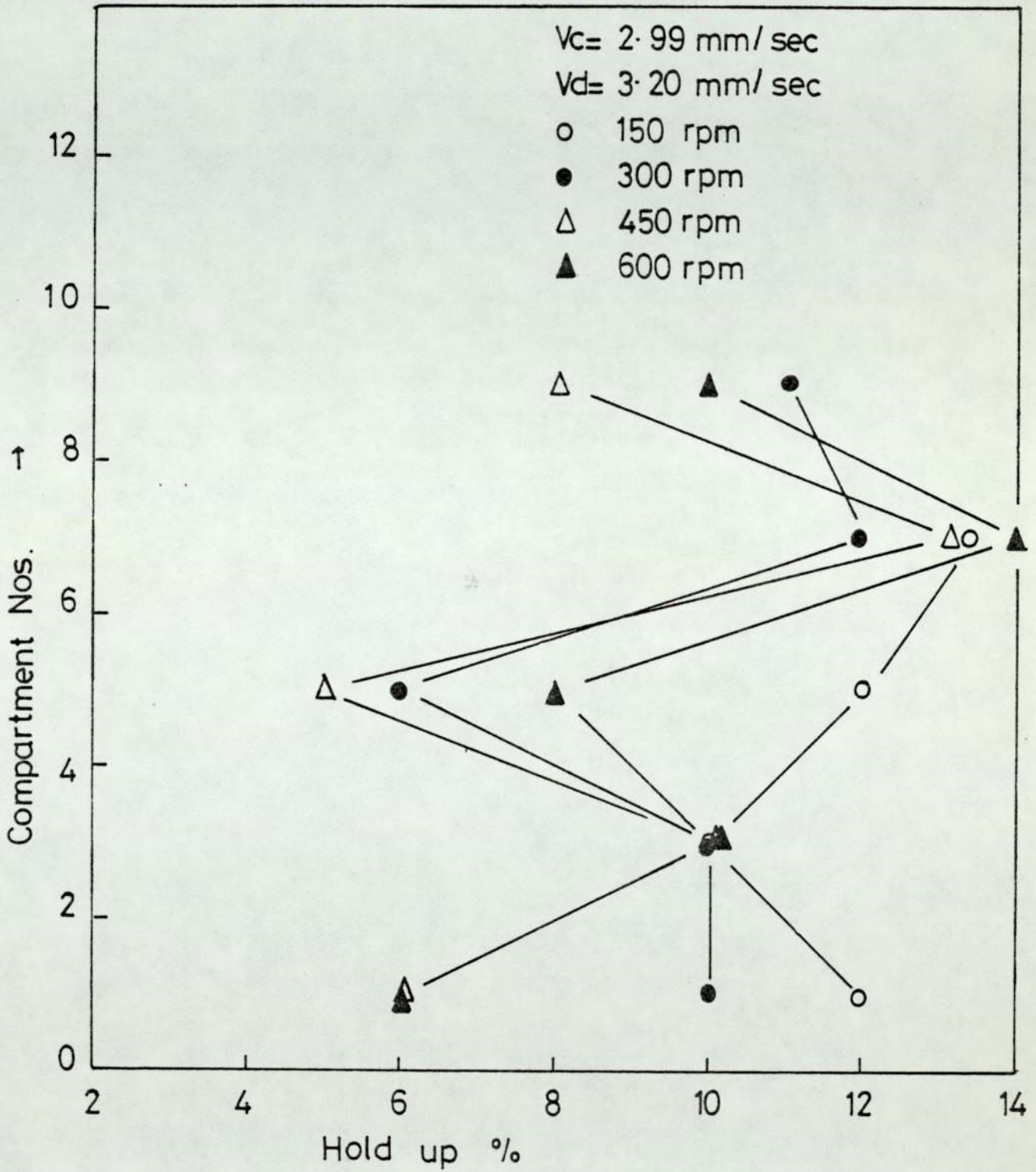


FIG. 9.8 AXIAL HOLD-UP PROFILE IN THE 450 mm. DIAMETER R.D.C.

Sample point located at $\frac{S-R}{2}$ in line with the rotating discs.

variation did not exceed $\pm 5\%$. Initial samples from the 450 mm. diameter R.D.C. were taken with the sample tube located either at the column wall, as in previous studies (11, 38), or midway between the edge of the rotor and stator, i.e. S-R, as recommended by Strand et al (8). In the 101 mm. diameter column axial hold-ups were in all cases determined with the sample tube located at the column wall, since variation in radial hold-up in small columns is indeterminable (8).

Typical results are reproduced in Figures 9.6, 9.7 and 9.8. As shown in Figure 9.8, results from the 450 mm. column were inconsistent, especially at higher rotor speeds (600 r.p.m), when they showed a decrease in hold-up compared with an expected increase. Since this cast doubts upon the positioning of the sample tube midway between S-R, it was necessary to study the radial profile to determine the correct position for the sample tube.

9.1.3.2 Radial Hold-up Study in the 450 mm. Diameter Column

Radial hold-up studies were performed to determine

- (a) the effect of locating the sample tube at different radial positions,
- (b) the variation in hold-up away from the plane of the disc, and
- (c) the effect of change in wettability, due to a change

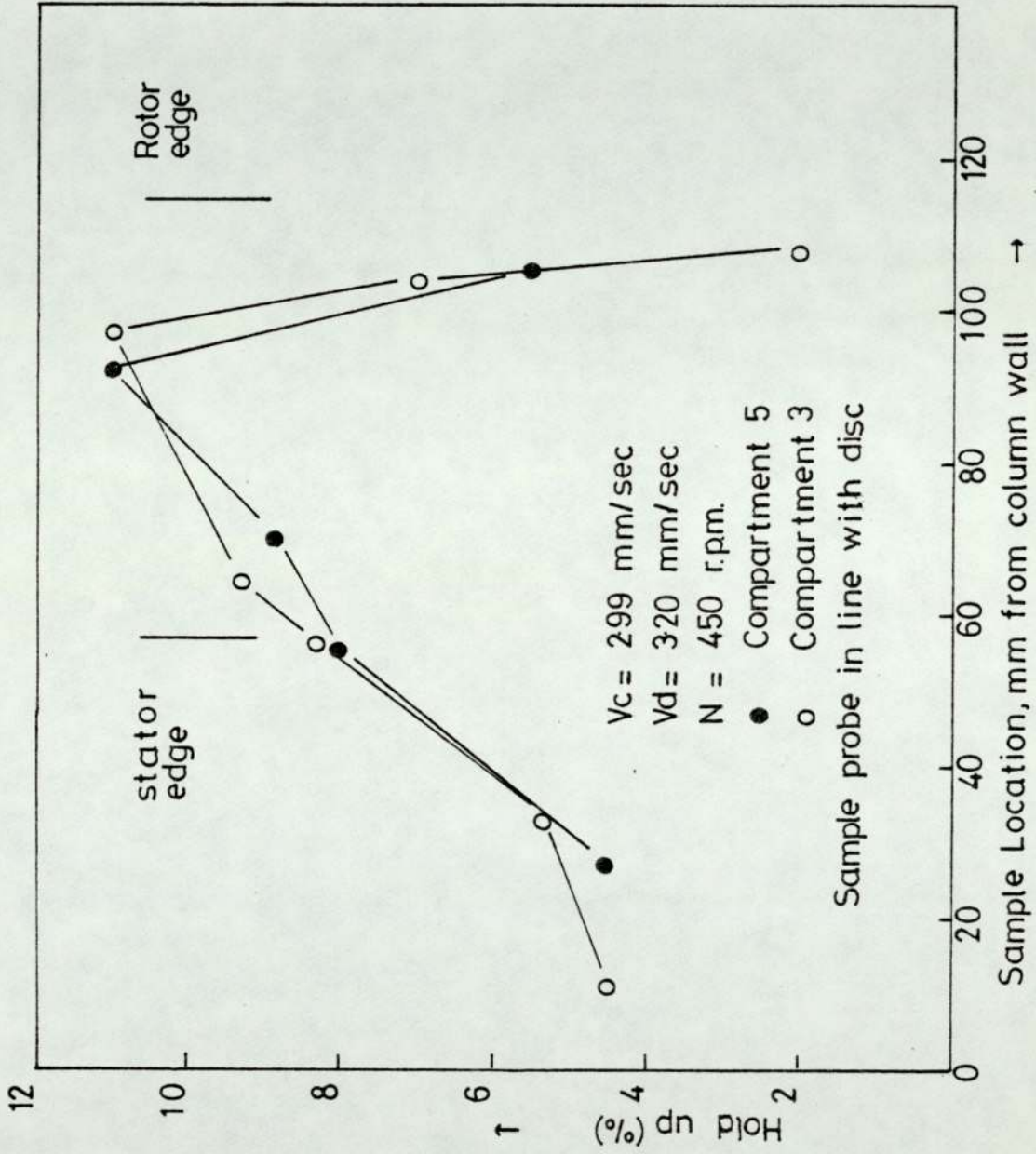


FIG. 9.9. RADIAL HOLD-UP PROFILE IN 450 mm. DIAMETER R.D.C.

in the material of construction of the sample tube, (37) on the hold-up of profile.

The method used was as described in section 9.1.3. Three or more samples were taken for each reading and a mean value calculated. The variation did not exceed $\pm 5\%$.

The results of the study are shown in Figure 9.9.

The radial profile of hold-up away from the plane of the disc was studied by means of the stainless steel tube construction shown in Figure 9.10a. An elevation of 59 mm. was given because that was the maximum possible elevation that could have been accommodated from outside without breaking the column into pieces. However, such an elevation is not unreasonable compared to the study of Strand, Olney and Ackerman (8), in which they studied the radial profile 57 mm. away from the stator ring in a 1067 mm. column, with compartment height of 254 mm. The variation of hold-up in the radial direction away from the line of the disc, is shown in Figure 9.11.

Al-Hemiri (37) and Arnold (11) reported that the samples withdrawn are likely to depend on the wettability of the material, diameter of tube, and the method of opening of taps. In order to study the affect of wettability on radial hold-up profile a sample tap was fabricated as shown in Figure 9.10b. The end was of 6.2 mm bore polypropylene tubing, into which was inserted 1.6 mm. stainless steel wire.

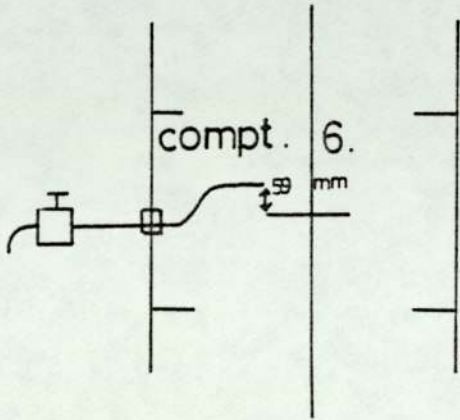


Fig 9-10 a

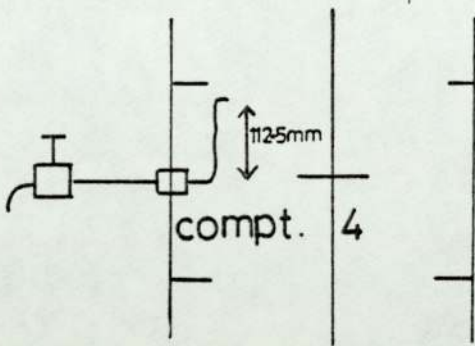


Fig 9-10 b

FIG. 9.10 DESIGN AND LOCATION OF SAMPLE TUBES

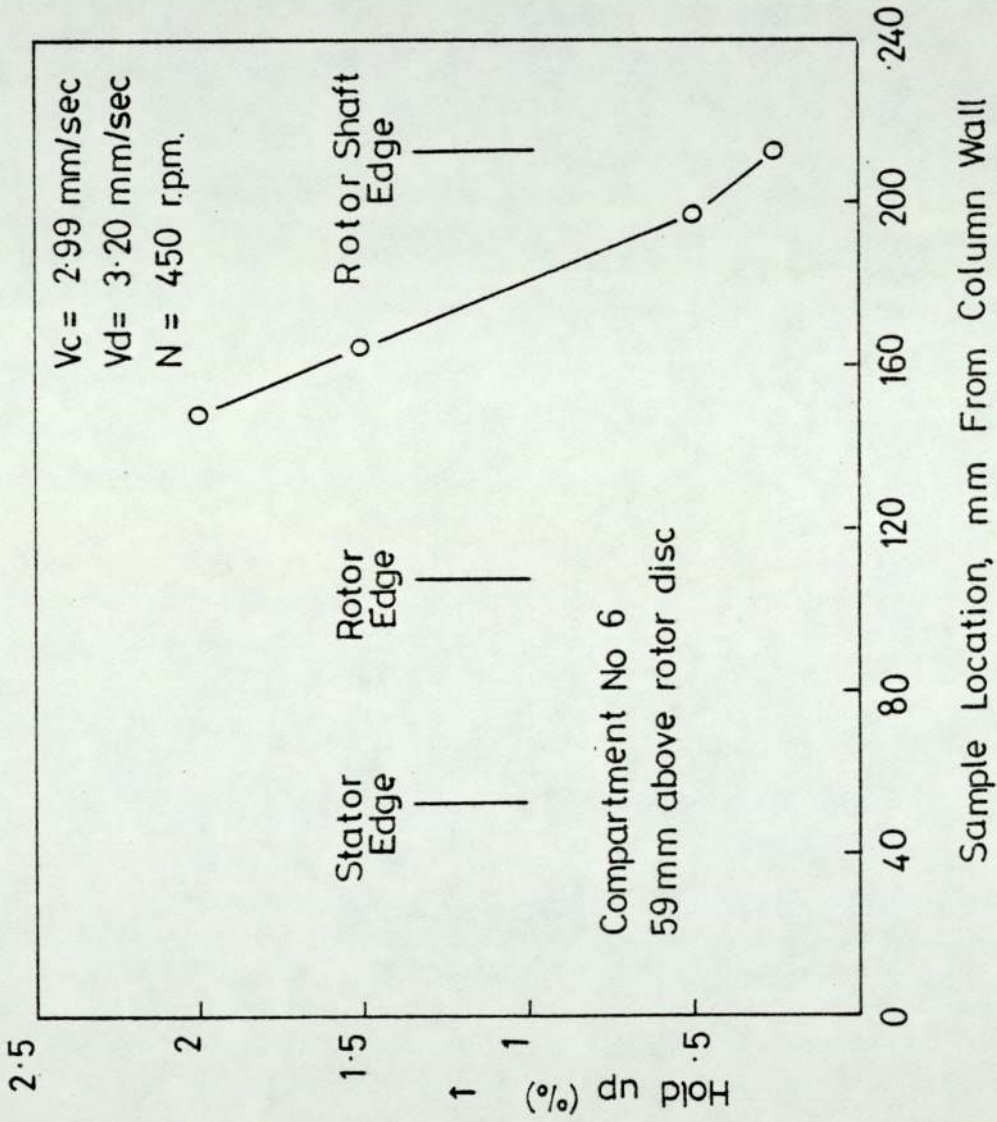


FIG. 9.11 RADIAL HOLD-UP PROFILE USING THE SAMPLE TAP SHOWN IN FIG. 9.10a.

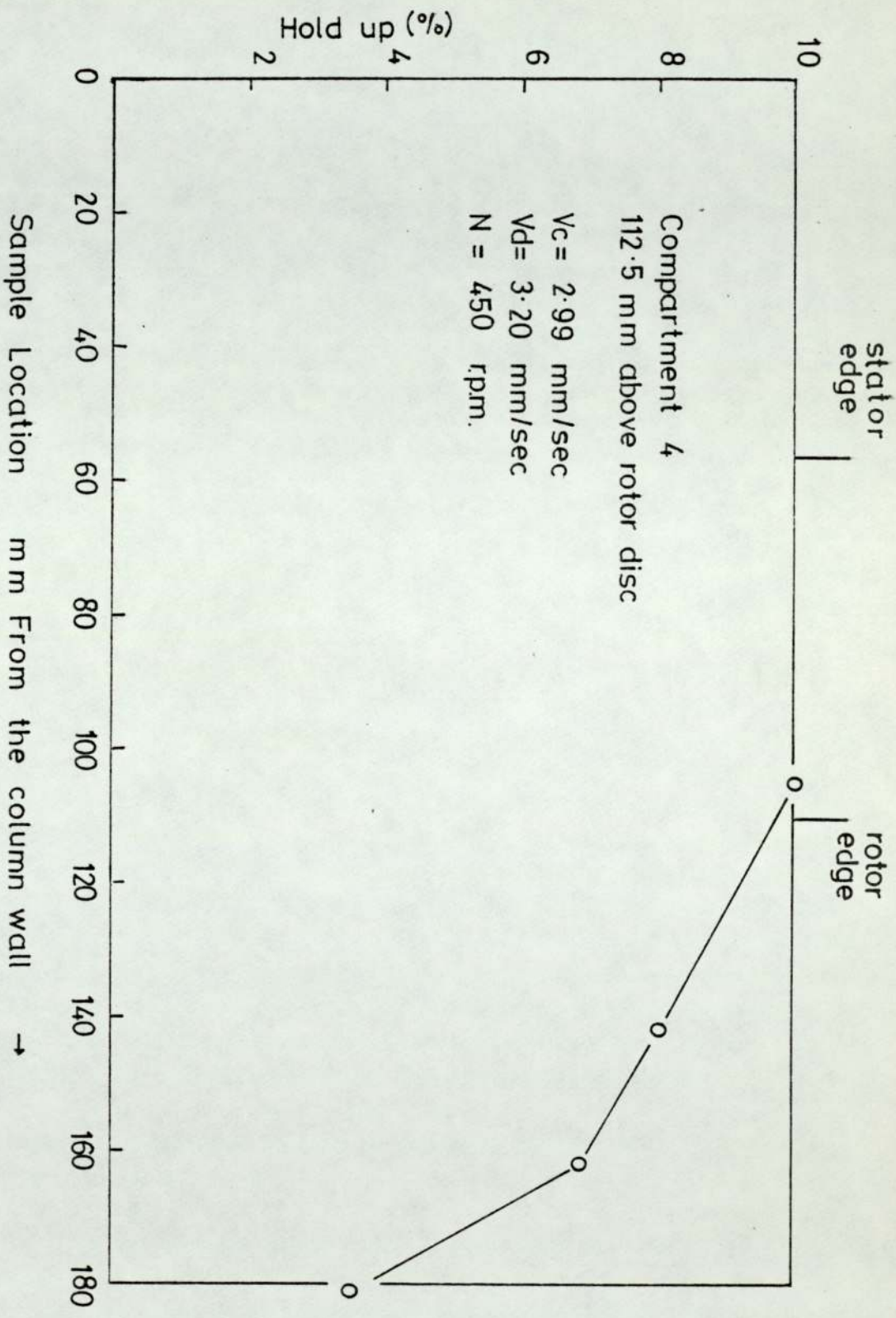


FIG. 9.12 RADIAL HOLD-UP PROFILE USING THE SAMPLE TAP SHOWN IN FIG. 9.10b.

The stainless steel wire was to maintain the shape and provide a tap with equal affinity for water and the organic phase.

Typical results are presented in Fig. 9.12.

9.1.3.3 Average Hold-up Studies in the Two Columns

Because of the inconsistency in results obtained during the point hold-up and radial hold-up profile studies, it was considered that for design purposes, average hold-ups would be more reliable. Therefore average hold-up was used to describe the volume fraction of dispersed phase in either column. The method used was similar to that used by other workers (11, 37, 38). For any set of operating parameters the column was operated for 15 minutes, in order to attain steady state. The inlet and outlet valves were then closed rapidly and the rotor stopped to allow the dispersion to settle under gravity and displace the interface. The average hold-up was then determined by dividing the shift in the position of the interface by the effective height, i.e. the height from the bottom distributor to the previous position of interface.

Although this method suffers from the fundamental disadvantage of including the unagitated top and bottom sections of the column in which hold-up is not representative (46), it proved to be very satisfactory compared with methods based upon point hold-ups. The alternative of suddenly withdrawing a large sample through a large

diameter tube (46) would not have been practicable and would have disrupted steady state operation.

Typical results of dispersed phase hold-up versus the superficial dispersed phase velocity at constant superficial continuous phase velocity at different rotor speeds, in the 450 mm. diameter R.D.C., are shown in Figure 9.13.

The effect of continuous phase flowrate on the average hold-up was found to be substantial, and increased with increase in the rotor speed, contrary to the findings of other workers (11, 37, 38). Hence all measurements were made with continuous phase flowing. The effect of change in continuous phase velocity on the hold-up is demonstrated in Figure 9.14. Finally, the effect of change of average hold-up with rotor speed in the 101 mm. R.D.C. is plotted in Fig. 9.15.

9.1.4 Drop Size Produced at the Distributor

The mean drop size produced at the distributor at fixed flowrates of the continuous and dispersed phases, varied with rotor speed. The results obtained with the two columns are reproduced in Figures 9.16 and 9.17. In both columns the drop size produced decreased with the increase in rotor speed due to turbulence extending to the plane of the distributor.

The experimental results were compared with values

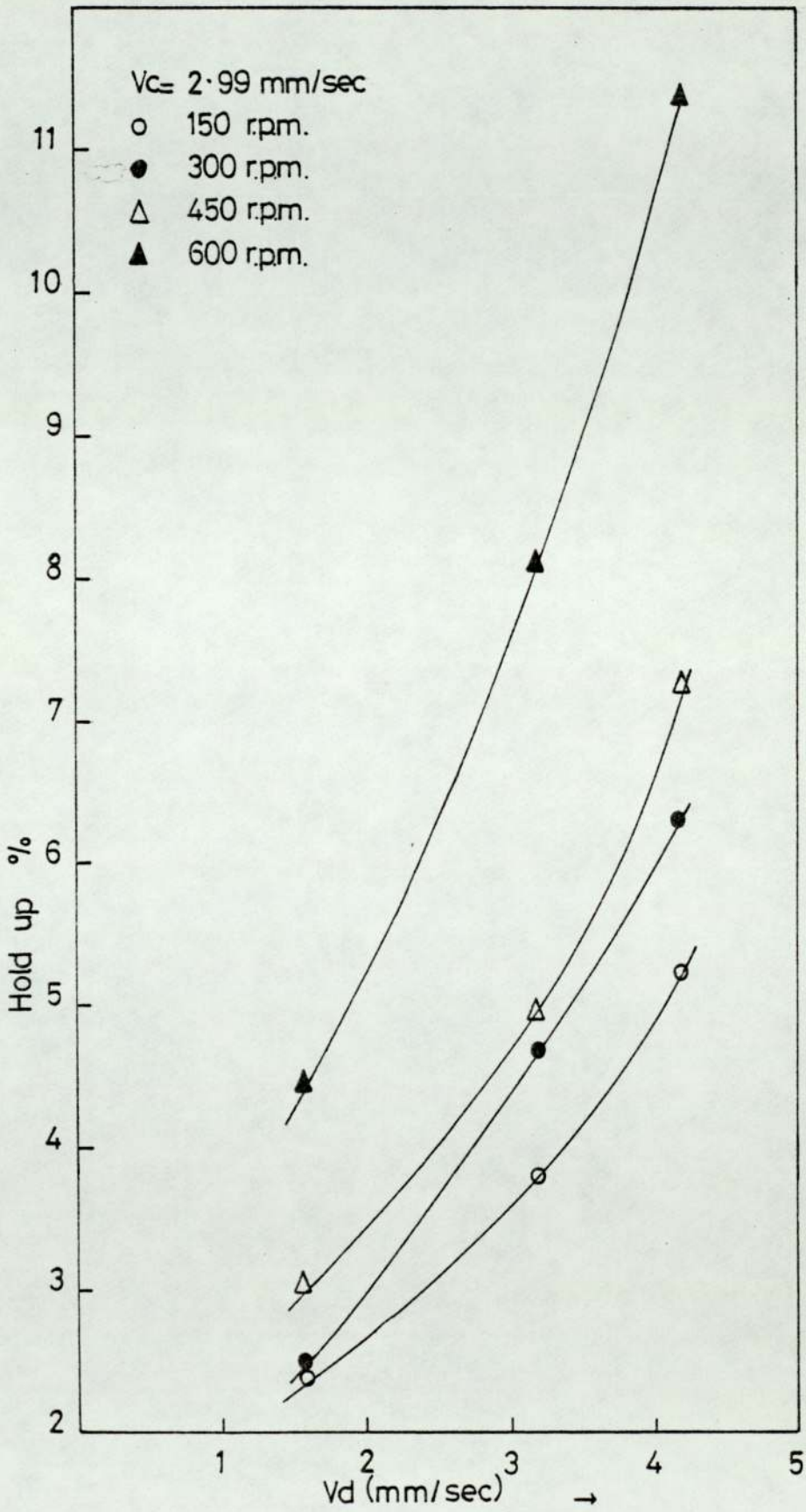
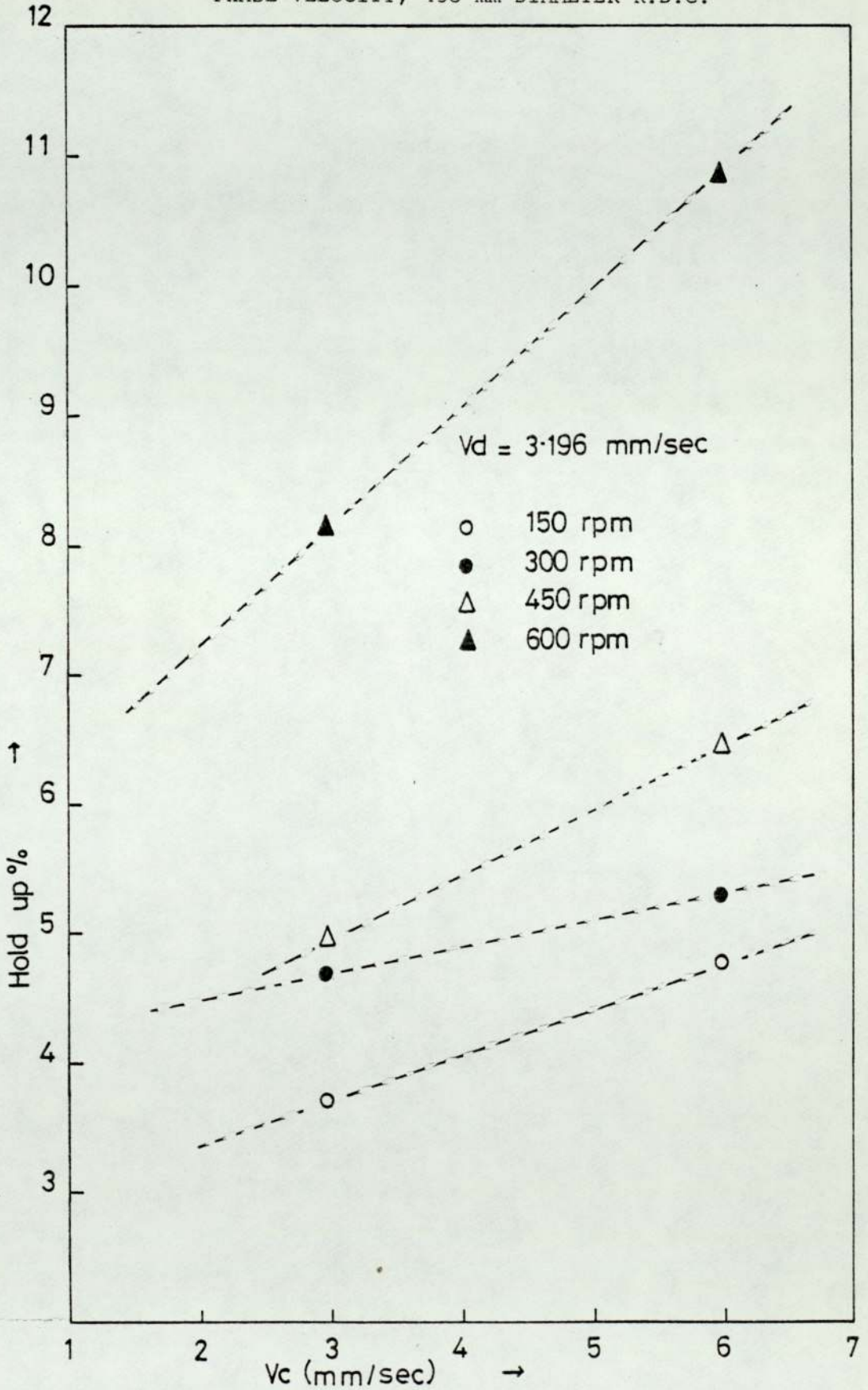


FIG. 9.13 AVERAGE HOLD-UP vs DISPERSED PHASE VELOCITY IN THE 450 mm DIAMETER R.D.C. Kerosene-water system.

FIG. 9.14 CHANGE IN AVERAGE HOLD-UP WITH CHANGE IN CONTINUOUS PHASE VELOCITY AT CONSTANT DISPERSED PHASE VELOCITY, 450 mm DIAMETER R.D.C.



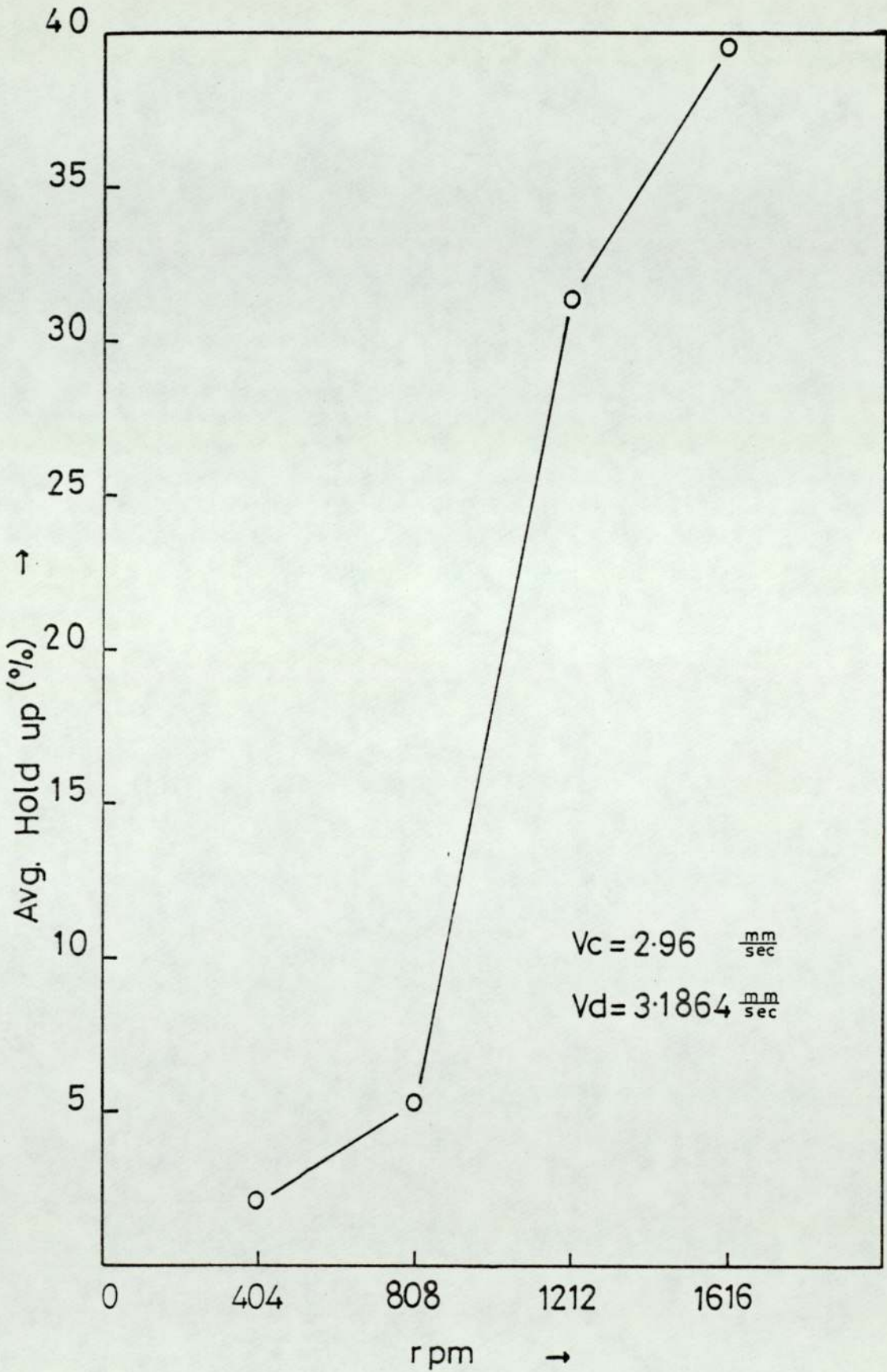


FIG. 9.15 VARIATION OF AVERAGE HOLD-UP WITH ROTOR SPEED 101 mm. DIAMETER R.D.C.

predicted from the correlations of Treybal (65) and Meister and Scheele (67). The values obtained using Treybal's correlation were found to be 10 - 25% lower than the experimental values, whereas the Meister and Scheele correlation gave values 50 - 100% higher than the experimental values. The discrepancies illustrate the limitation of these correlations for predicting drop size in a column where a large number of drops are produced under countercurrent flow conditions, together in this case, with the action of the rotors. The results can be summarised as,

- (1) Interference of rotors in an agitated column compared to no turbulence situation in the above authors' experiments.
- (2) Increased back-mixing at high speeds in agitated columns contaminating the samples taken for the comparison of drop sizes.
- (3) Mobile continuous phase compared to the stationary phase in the above studies. The mobile continuous phase entrained small drops also contaminating the sample.
- (4) Full feed of the nozzles in the above studies compared to the different feed rates of different nozzles in an agitated contactor.

The implication of this to the design and location of the distributor, is discussed in section 12.2.3.

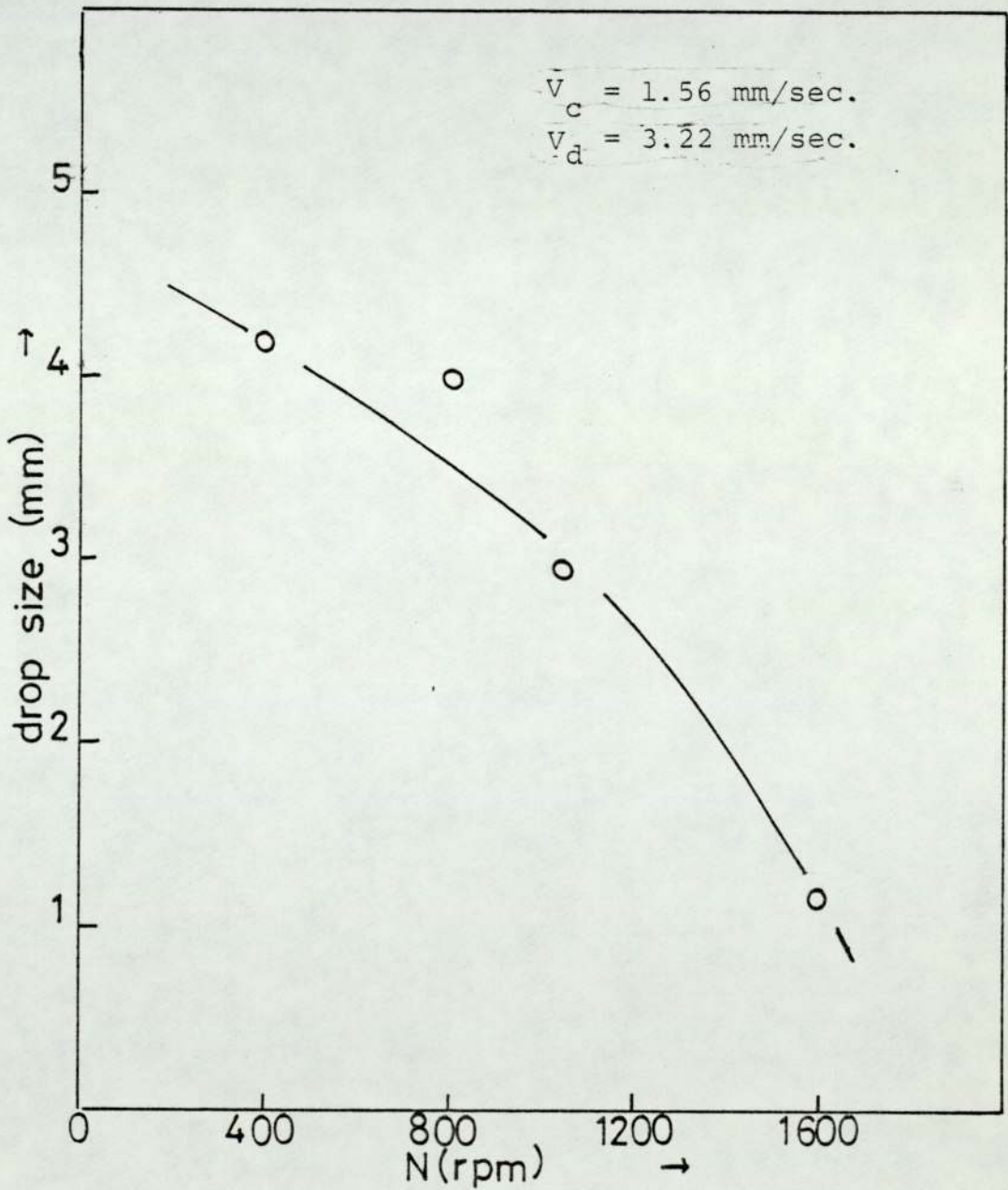


FIG. 9.17 VARIATION IN DROP SIZE PRODUCED AT THE DISTRIBUTOR WITH ROTOR SPEED, 101 mm. DIAMETER R.D.C.

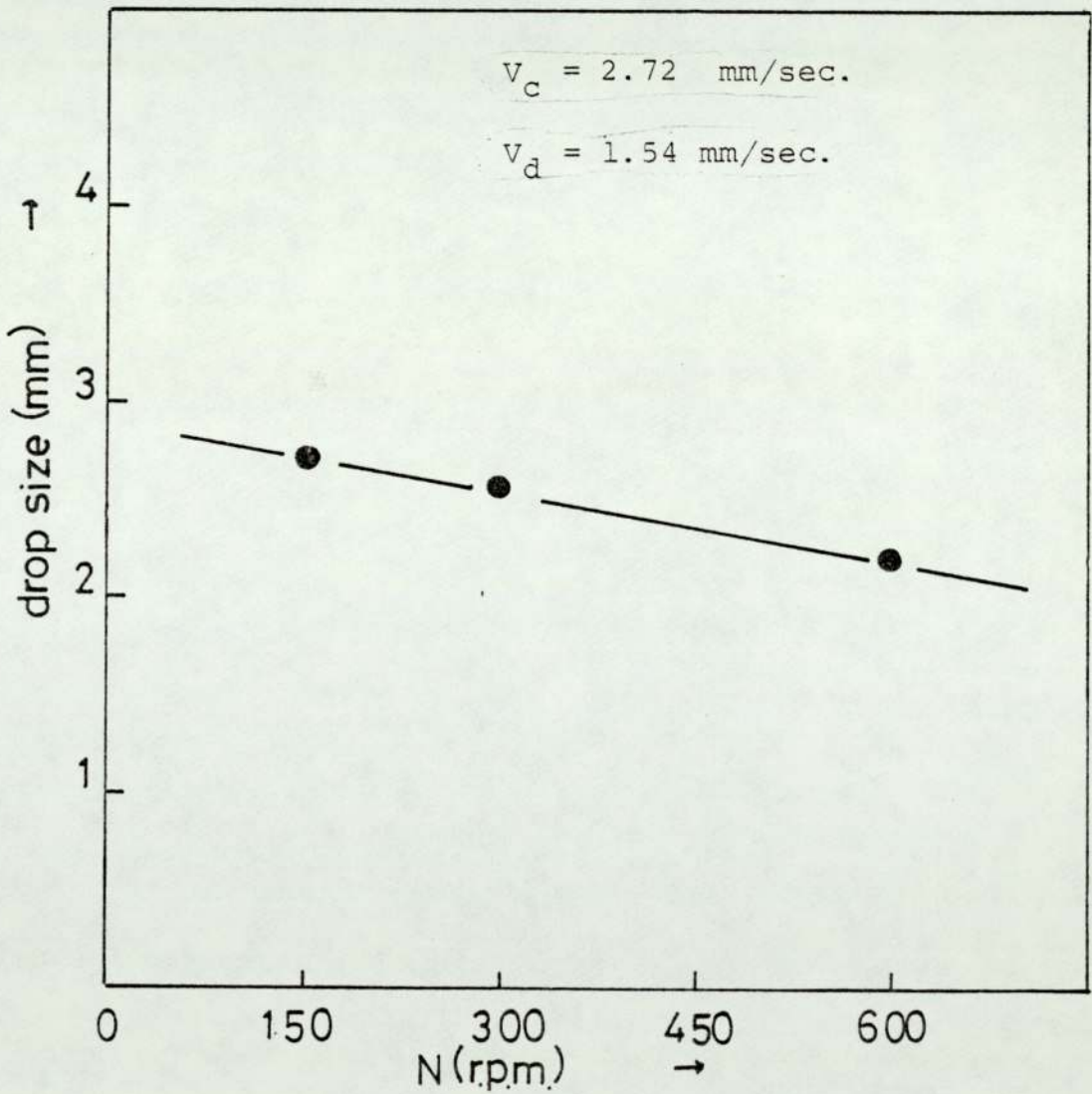
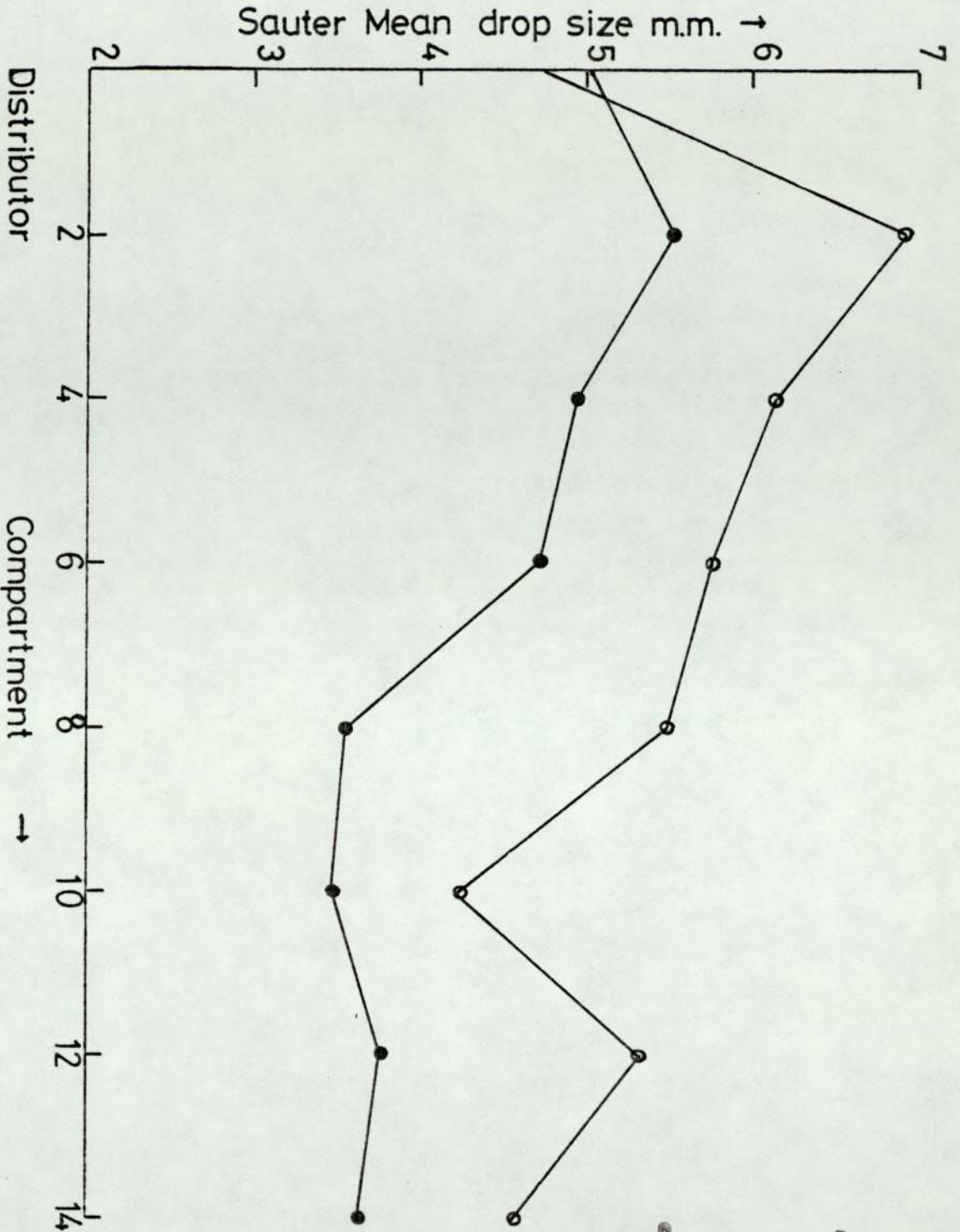


FIG. 9.16 VARIATION IN DROP SIZE PRODUCED AT THE DISTRIBUTOR WITH ROTOR SPEED 450 mm DIAMETER R.D.C.



○ $V_d = 2.82$ mm/sec.
 $V_c = 7.33$ mm/sec
 $N = 450$ r.p.m.
 Dispersed phase mean concentration = 6.05%

● $V_c = 7.33$ mm/sec.
 $V_d = 2.82$ mm/sec.
 $N = 500$ r.p.m.
 Dispersed phase mean concentration = 4.47%

FIG. 9.18 VARIATION OF SAUTER MEAN DIAMETER ALONG THE COLUMN HEIGHT. 450 mm. DIAMETER R.D.C. Kerosene-water-acetone system.

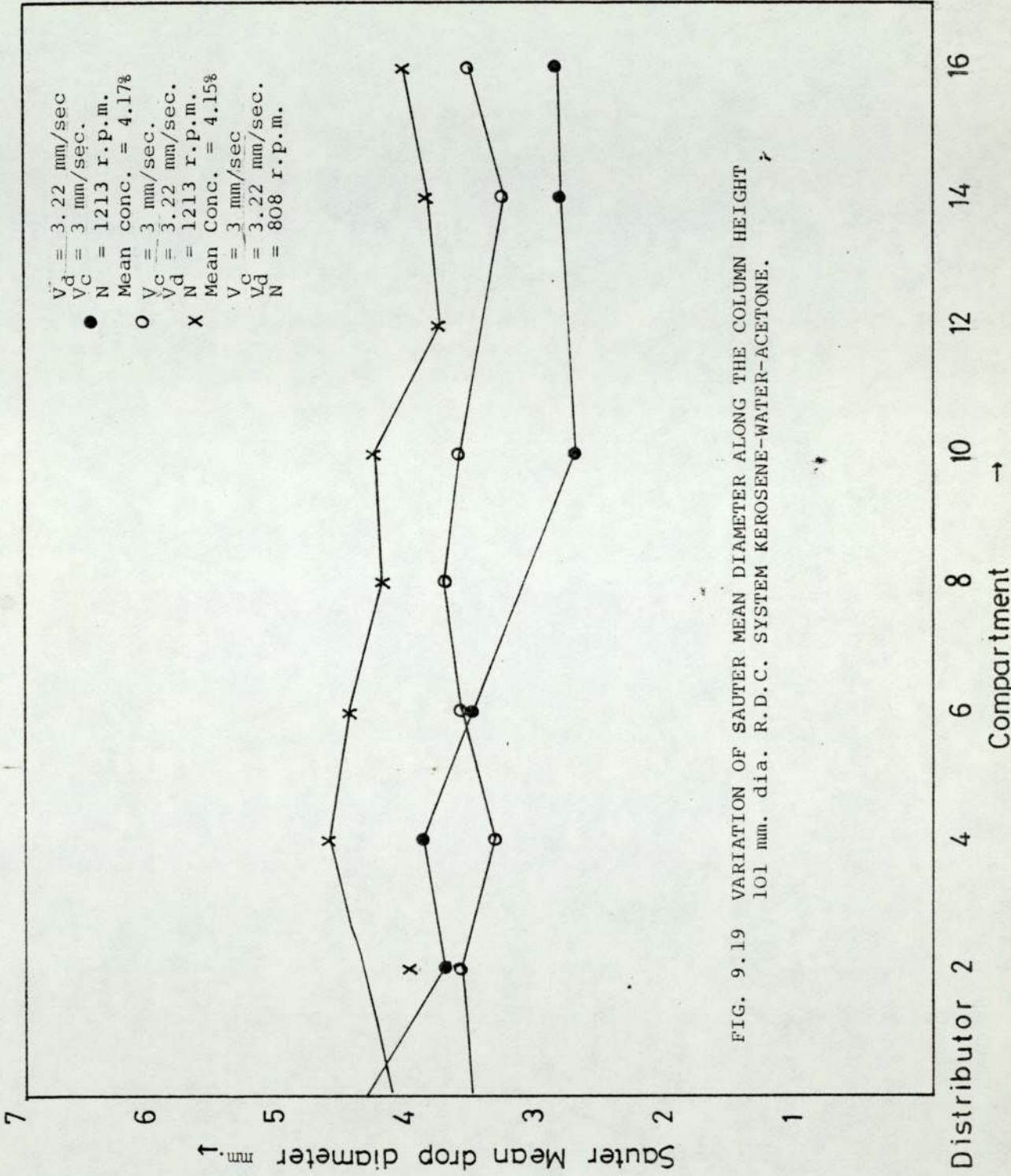


FIG. 9.19 VARIATION OF SAUTER MEAN DIAMETER ALONG THE COLUMN HEIGHT
 101 mm. dia. R.D.C. SYSTEM KEROSENE-WATER-ACETONE.

9.2 Mass Transfer Studies

It was not practicable to carry out separate experiments to measure flooding rate in the two columns under mass transfer conditions, because this would have consumed large quantities of solvents and no continuous distillation facilities were available. However, all the mass transfer runs were carried out below 70% of the flooding flowrates obtained during the non-mass transfer experiments as recommended by Treybal (20).

9.2.1 Hold-up

Only average hold-up measurements were made during the individual mass transfer runs, as described in para. 9.1.3.3, for the reasons given in section 9.1.3.

No attempt has been made to plot the hold-up against operating parameters because of change of more than one parameter during the mass transfer experiments. However, the hold-up was found to increase with increase in either phase flowrate or rotor speed. The results are presented in Tables 9.1 and 9.2.

9.2.2 Interfacial Area Estimation

Interfacial area was determined during each mass transfer run by taking two photographs of dispersion in alternate compartments, throughout the column length. A total of 300 photographs were taken. During the preliminary experiments an attempt was made to determine a 'representative' compartment in order to reduce the number of photographs requiring analysis.

During this initial analysis the drop size distribution was found to depend on the phase flowrates, the rotor speed, the height of the compartment from the bottom of the column and upon the concentration gradient. As discussed earlier this made it difficult to select a representative compartment for use throughout the mass transfer studies, as was done in previous studies (11, 37). However, rotor speed was found to be the most important factor influencing the drop sizes and visual observations indicated that little coalescence and redispersion occurred. Earlier work, albeit in the absence of mass transfer, suggested that coalescence and redispersion taking place in the R.D.C. was limited until conditions approached flooding (54). Therefore a representative compartment was selected for each rotor speed, and that this did not introduce any appreciable error was checked at intervals by analysing a complete set of photographs.

Typical results showing the variation of drop size with compartment number and rotor speed are reproduced and shown in Figures 9.18 and 9.19. A typical set of photographs showing the variation of drop size with compartment height in the two columns, are given in Figures 9.20 and 9.21.

9.2.3 Mass Transfer Experiments

Experiments involving the transfer of acetone from a dispersed kerosene phase to an aqueous continuous phase

Compartment No. 16

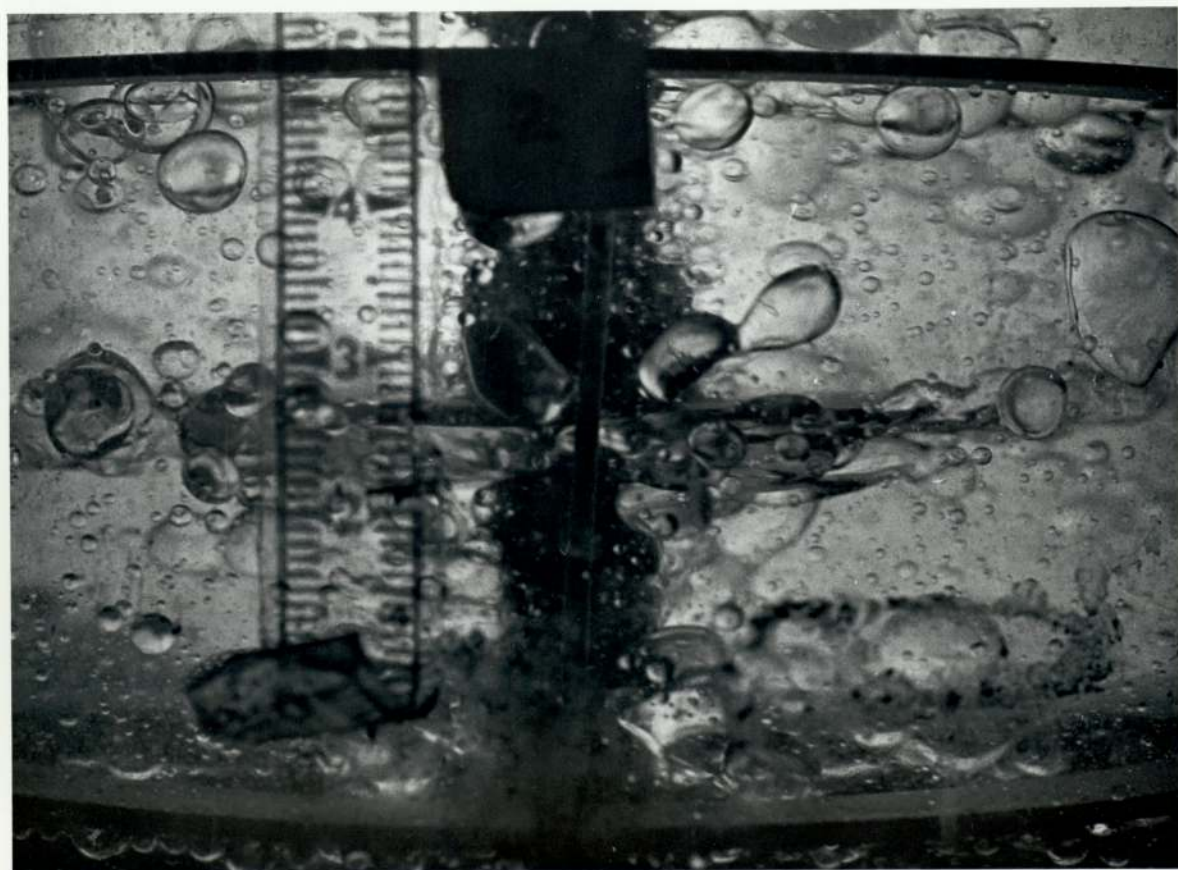
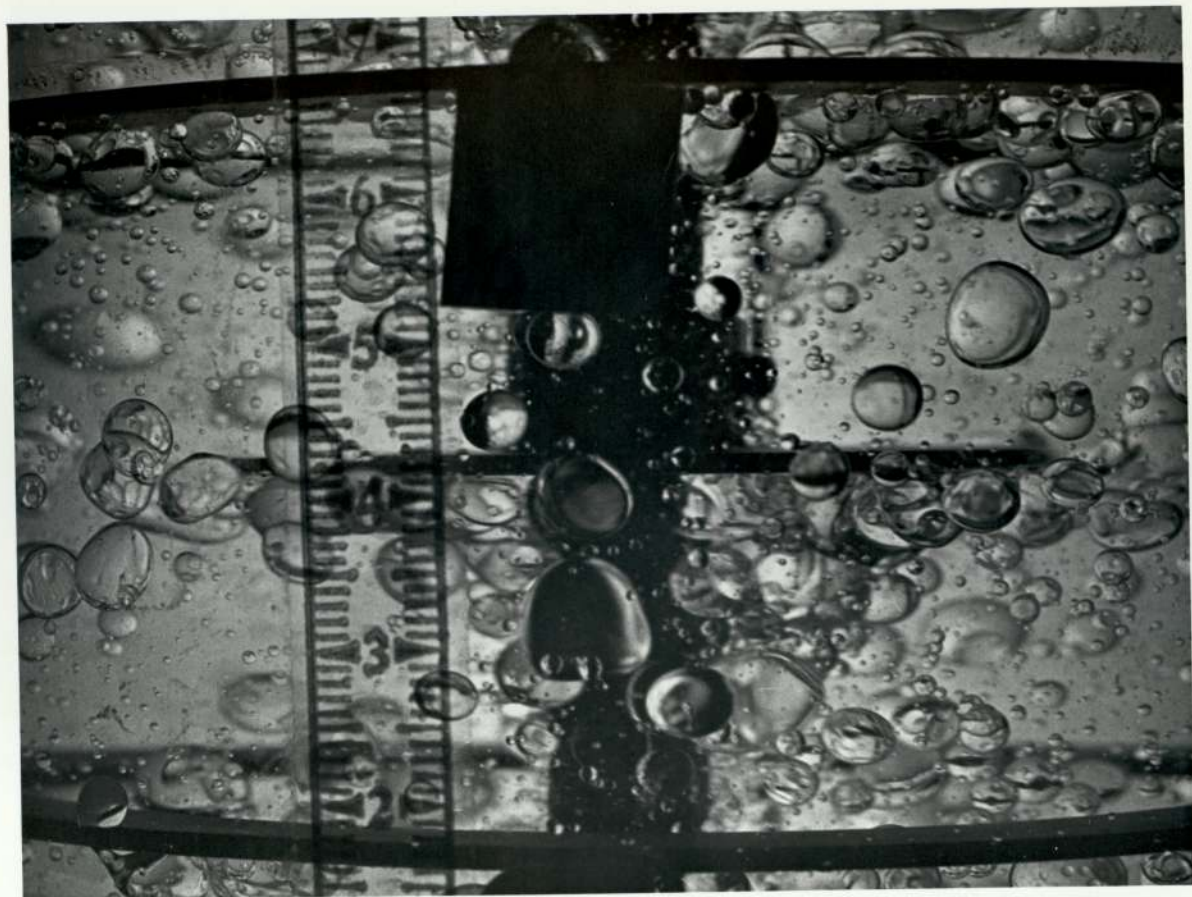
FIG. 9.20 VARIATION IN DROP SIZE BETWEEN COMPARTMENTS
2 and 16 UNDER MASS TRANSFER CONDITIONS;
101 mm. R.D.C.

$V_C = 11.92$ mm/sec; $V_D = 12.7$ mm/sec;

$N = 808$ r.p.m.;

Average conc. of the dispersed phase = 4%,
magnification factor = 2.

Compartment No. 2.



Compartment 14

FIG. 9.21 VARIATION IN DROP SIZE BETWEEN COMPARTMENTS
2 and 14 UNDER MASS TRANSFER CONDITIONS;
450 mm. diameter R.D.C.

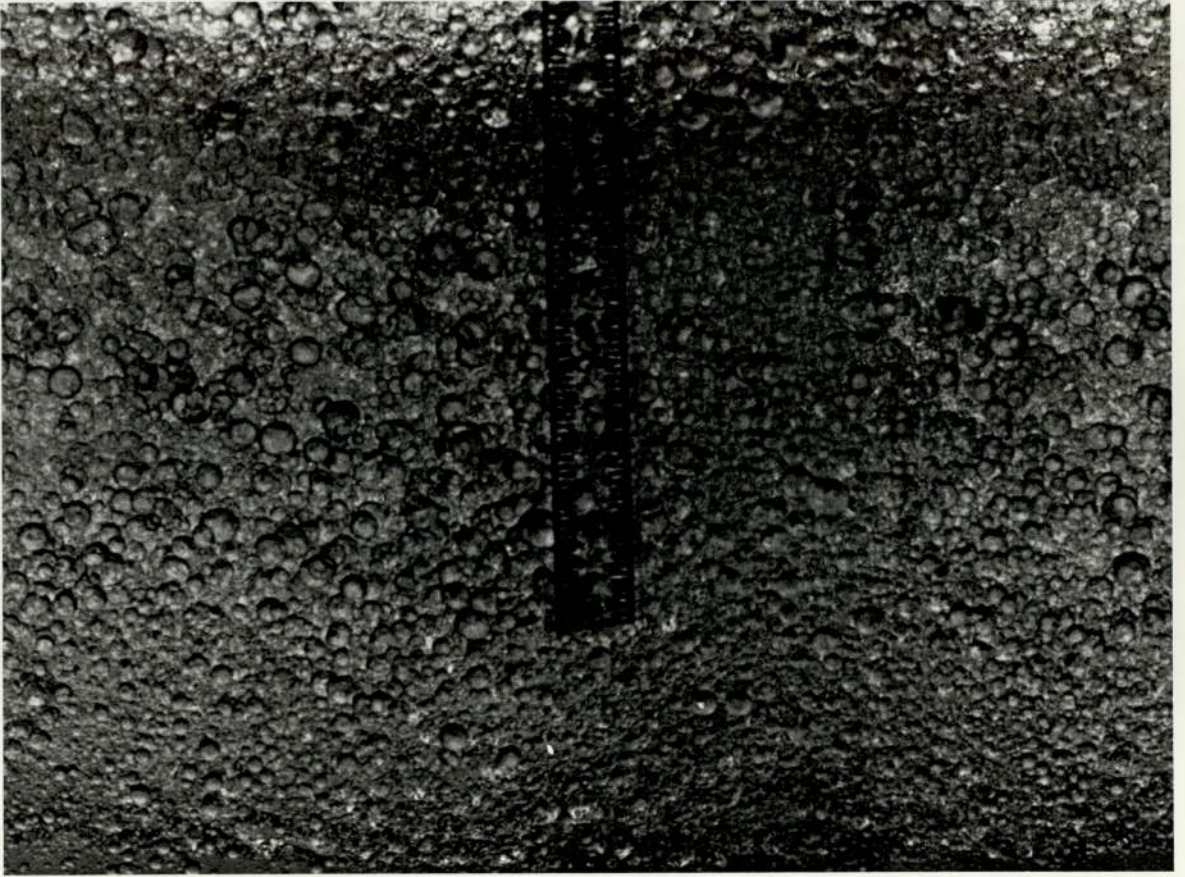
$$V_C = 7.33 \text{ mm/sec}; \quad V_D = 2.82 \text{ mm/sec};$$

$$N = 500 \text{ r.p.m.};$$

Average conc. of the dispersed phase = 4.5%

Magnification factor = 1.

Compartment 2.



52



TABLE 9.1
MASS TRANSFER RUNS - 450 mm Diameter

Run No.	Q_c lit/min	Q_d lit/min	V_c mm/sec	V_d mm/sec	N r.p.m.	Initial conc. dis. phase	Final conc. dis. phase	Final conc. cont. phase.	Average Hold-up	N rate of mass trans- fer.	Effective height of column.	Average d_{32} mm	Calculated K $\text{gm/cm}^2 \text{ min}$
MB1	29.55	30.75	3.09	3.22	450	5.25%	3.84%	.75%	.042	221.91 gm/min	367.5 cm	8.16	3.596×10^{-3}
MB2	50.0	30.75	5.23	3.22	450	4.87%	4.22%	.31%	.033	156 gm/min	354.5 cm	6.96	3.134×10^{-3}
MB3	50.0	30.75	5.23	3.22	450	6.0%	5.2%	.38%	.041	192 gm/min	359.5 cm	5.88	2.116×10^{-3}
MB4	70.0	27.0	7.33	2.82	450	6.53%	5.57%	.28%	.034	202 gm/min	357.8 cm	5.504	2.331×10^{-3}
MB5	70.0	27.0	7.33	2.82	500	6.1%	5.4%	.22%	.039	156 gm/min	354.5 cm	4.2335	1.288×10^{-3}
MB6	70.0	15.75	7.33	1.65	550	5.52%	5.06%	.08%	.031	57.44 gm/min	350.0 cm	3.43174	5.31×10^{-4}
MB7	70.0	15.75	7.33	1.65	500	5.5%	5.13%	.06%	.028	47.0 gm/min	354.5 cm	4.244	5.88×10^{-4}
MB8	62.5	19.5	6.54	2.04	450	5.55%	5.18%	.09%	.028	56.25 gm/min	357.3 cm	4.3881	6.99×10^{-4}
MB9	55.0	23.0	5.76	2.25	450	5.75%	5.2%	.18%	.043	99.0 gm/min	359.0 cm	3.855	7.057×10^{-4}
MB10	58.75	21.5	6.15	2.25	450	5.58%	5.2%	.10%	.046	63.0 gm/min.	368.9 cm	3.945	4.25×10^{-4}
MB11	58.75	21.5	6.15	2.25	500	5.6%	5.1%	.14%	.051	83.0 gm/min	366.5 cm	3.70109	4.814×10^{-4}

TABLE 9.1
 MASS TRANSFER RUNS - 450 mm Diameter
 (Contd....)

Run No.	Q _c lit/min	Q _d lit/min	V _c mm/sec	V _d mm/sec	N r.p.m.	Initial conc. dis. phase	Final conc. dis. phase	Final conc. cont. phase.	Average hold-up	N rate of mass trans- fer.	Effective height of column	Average d ₃₂ mm	Calculated K gm/cm ² min
MB12	62.5	19.5	6.54	2.04	500	5.6%	5.13%	.113%	.044	71 gm/min	369.0 cm	4.20	5.36x10 ⁻⁴
MB13	55.0	23.0	5.76	2.41	500	5.6%	5.0%	.193%	.046	107 gm/min	368.0 cm	3.50	6.465x10 ⁻⁴
MB14	55.0	23.0	5.76	2.41	550	5.6%	4.9%	.227%	.053	125 gm/min	367.5 cm	3.62	6.852x10 ⁻⁴
MB15	58.75	21.5	6.15	2.25	550	5.6%	5.0%	.192%	.049	113 gm/min	370.5 cm	3.98	7.29x10 ⁻⁴
MB16	62.5	19.5	6.54	2.04	550	5.63%	4.93%	.17%	.049	107 gm/min	367.3 cm	4.17	7.05x10 ⁻⁴
MB17	55.0	23.0	5.76	2.47	500	6.0%	5.36%	.212%	.049	115 gm/min	369.7 cm	4.02	7.008x10 ⁻⁴
MB18	70.0	15.75	7.33	1.65	450	5.6%	5.10%	.09%	.029	63 gm/min	357.5 cm	3.58	6.362x10 ⁻⁴
MB19	29.625	30.75	3.10	3.22	450	5.6%	4.9%	.566%	.046	168 gm/min	371.0 cm	5.55	1.61x10 ⁻³
MB20	50.0	30.75	5.23	3.22	450	5.6%	4.9%	.341%	.050	170 gm/min	365.7 cm	4.18	1.16x10 ⁻³
MB21	29.625	30.75	8.10	3.22	300	5.5%	5.1%	.35%	.040	104 gm/min	363.5 cm	4.11	8.64x10 ⁻⁴

TABLE 9.2
 MASS TRANSFER RUNS 101 mm DIAMETER COLUMN

Run No.	Q_c lit/min	Q_d lit/min	V_c mm/sec	V_d mm/sec.	N r.p.m	Initial Conc. Dis. Phase	Final Conc. Dis. Phase	Final Conc. Cont. Phase	Average Hold-up	N rate of Mass Trans. gm/min.	Effect- ive Height of the column cm.	Average d_{32} mm	Calculated K gm/cm ² min.
M1	1.44	1.55	2.96	3.18	809	5.9%	4.9%	.85%	.04	13.0	122	5.23	6.55×10^{-3}
M2	1.44	1.55	2.96	3.18	1050	4.53%	3.75%	.932%	.07	13.51	134	4.17	4.264×10^{-3}
M3	1.44	1.55	2.96	3.18	1213	4.53%	3.77%	.68%	.07	10.27	135	3.28	2.53×10^{-3}
M4	1.44	1.55	2.96	3.18	808	4.64%	3.7%	.84%	.06	12.28	133	4.17	4.14×10^{-3}
M5	2.52	1.55	5.19	3.18	1213	6.5%	5.3%	.62%	.10	15.75	127	3.70	2.31×10^{-3}
M6	1.44	3.13	2.96	6.43	1213	6.06%	4.95%	2.63%	.13	38.14	138	3.88	4.766×10^{-3}

were performed in both columns. Runs were performed at less than 70% of the flooding flowrates obtained during the non-mass transfer experiments.

9.2.3.1 Procedure

In all cases filtered tap water formed the extract phase and approximately 4 - 7 % by weight, acetone-kerosene solution, the raffinate phase. The initial concentration of acetone in the aqueous phase was always 0% and the acetone in kerosene concentration was returned to 4 - 7% after each run, by adding a precalculated amount of acetone. This procedure was adopted to avoid the need for batch redistillation of large quantities of kerosene.

Before starting experiments the two phases were mutually saturated using the procedure described in para.8.2.11. A feed of constant concentration was prepared by recirculating the acetone in kerosene mixture in a closed loop. Each time a fresh water phase was used, it was saturated with kerosene by pouring a layer of kerosene on to it, and recirculating the water in a closed loop such that it re-impinged on the top kerosene layer at a rate of 100 litres/min. for about half an hour. The kerosene phase was found in fact to remain saturated with water from the previous run.

For the purpose of a run the feed solution was first made up by the addition of a calculated amount of acetone

to the kerosene and recirculating it in the closed loop. Two samples were taken for the initial concentration measurement, one via the bottom outlet of the storage vessel and the other by means of a stainless steel container attached to a long rod, via the top. In most cases excellent agreement was found between the two samples. A mean was taken in case of difference. The column was then filled with the continuous water phase and the rotor speed adjusted to the required value. The continuous phase inlet and outlet valves were then opened to the required level allowing continuous phase flow through the column. Dispersed phase was then introduced and this displaced the interface level at the top of the column. This level was maintained by adjustment of the continuous outlet phase valve.

After steady state conditions were reached, which usually required 20 minutes depending on the flow rates and concentration of the initial solutions, duplicate samples were withdrawn from the outlets of the two phases. Drop size and hold-up were measured as described earlier in section 9.2.2 and 9.2.1.

9.2.3.2 Time to Reach Steady State

Some preliminary runs were carried out in order to find the time to reach steady state. These involved the collection of samples from the respective outlets

at intervals of three minutes. These samples were then analysed using the method described in para.8.4.3 and the results checked by a mass balance.

Initially results suggested that steady state was not attained even after 45 minutes operation with a total displacement of liquid through the column exceeding 6 times the column volume. This did not agree with other published estimates of 2 to 3 times the equipment displacement being required, and therefore a theoretical study was made on the basis of the mathematical model presented by Jenson and Jeffreys (216). The assumptions made and application of this model are summarised in Appendix 4, together with the computer program written for it. Analysis using the experimental operating data, summarised in Appendix 4, confirmed that the system should have reached 95% steady state in about 15 minutes, i.e. after a total displacement of about 2.5 times the column volume. As a result the experimental sampling and analysis procedure were re-examined.

It was found that the sample collected at the water outlet was covered by a kerosene film. When this sample was poured into the absorbance measurement cell the kerosene entered first, contaminated the aqueous phase and because of its higher absorbance, resulted in spurious readings. This was avoided by pouring the complete sample into a separating funnel first and then quickly with-

drawing a sample of aqueous phase from the bottom for absorbance measurement. The concentration values then obtained and used in the mass balances gave results showing that steady state was reached in about 15 minutes. The mass balance on the two phases checked within + 5%

Using the computer program and later from experimentation it was discovered that the time to reach steady state decreased with,

- (1) Increasing in the ratio of continuous phase flow rate to the dispersed phase flowrate.
- (2) Increase in the total flowrate through the column.
- (3) Decrease in the concentration of acetone in the dispersed phase.

The results obtained were found to be in agreement with the findings of Salem and other workers (11, 37, 38, 217). A displacement of 6 times the column volume as found by Coggan (206) for a pulsed plate column was found to be excessive, and would have been expensive.

The experimental results showing the variation of concentration against time is reproduced in Fig. 9.22.

9.2.3.3 Results

Runs were performed at equivalent rotor speeds in both columns with the exception of the lowest speed, because limitations on the solvent inventory precluded

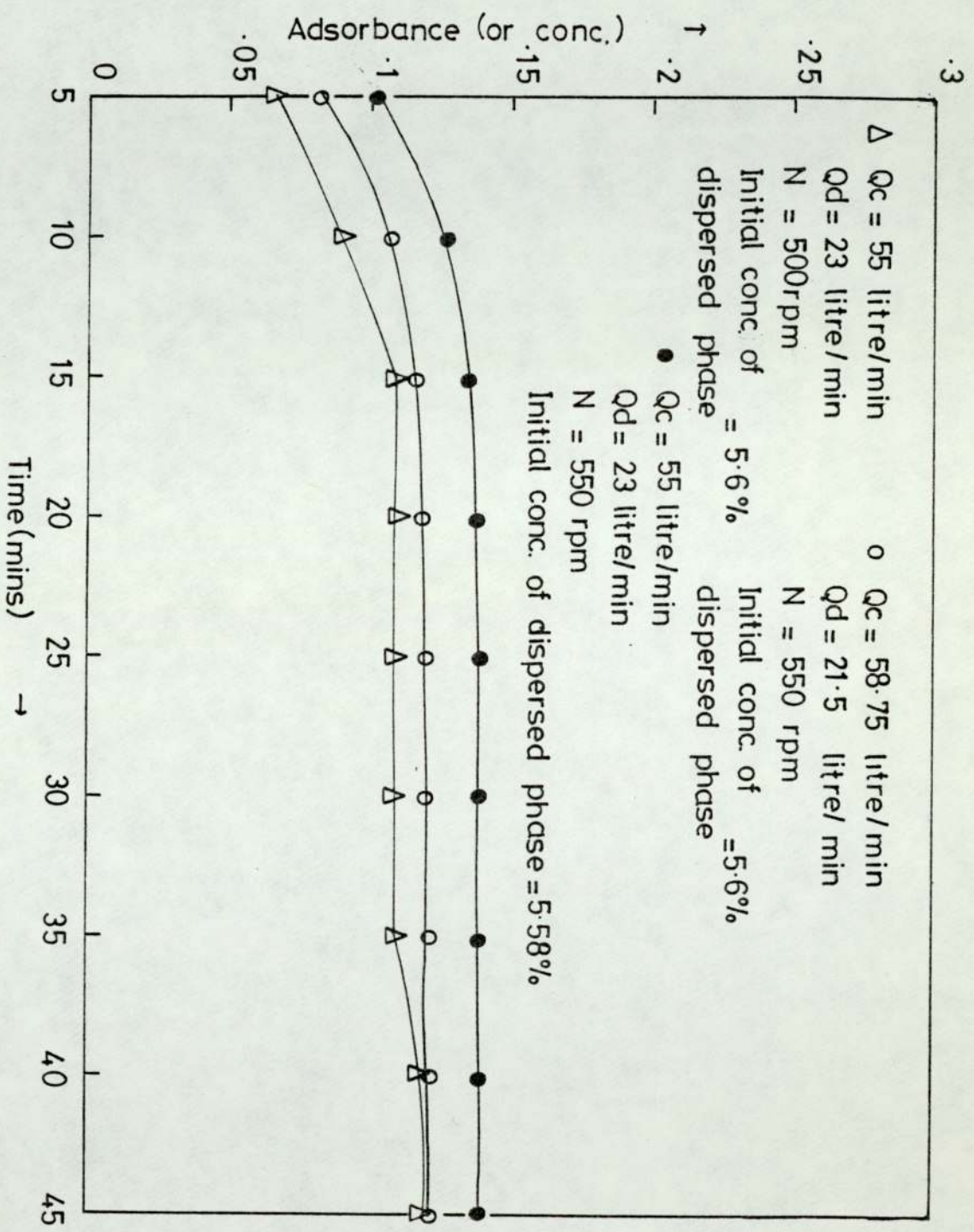


FIG. 9.22 VARIATION OF CONCENTRATION AT THE CONTINUOUS PHASE OUTLET WITH TIME SYSTEM.

the attainment of steady state in the large column. The phase flowrates used in the small column were first chosen to correspond to below 70% of flooding; the flowrates in the large column were then scaled up on the basis of superficial velocity. As discussed later in Chapter 10, this is not an accurate method of scale-up but all that was required was operation at less than 70% of flooding.

The mass transfer coefficient under each set of operating conditions was calculated using equation 1.1 and 1.3. The concentration driving force ΔC was calculated as a log mean concentration driving force, using the exit and inlet concentration of the two phase according to

$$\Delta C_{\ell m} = \frac{\Delta C_1 - \Delta C_2}{\ln \frac{\Delta C_1}{\Delta C_2}} \quad (9.1)$$

where the symbols are as defined in the Nomenclature.

The results of mass transfer experiments on the 450 mm. diameter and 101 mm. diameter columns are summarised in Table 9.1 and 9.2 respectively.

10. MATHEMATICAL MODELS

Because of the limitations outlined in Section 5.8., it is doubtful whether an industrial R.D.C. can be designed from single drop mass transfer data. Therefore design generally necessitates experimentation on a pilot plant. These results are then scaled up. However, the limitations of existing scale-up methods are outlined in Section 7.3.

Two mathematical models are proposed in this work to determine,

- (a) Column diameter,
- (b) Column height,

from data obtained on a pilot plant for a specific duty.

10.1 Scale-up of Column Diameter

10.1.1 Special Case for Identical Systems at Two Different Scales of Operation

For the design of industrial scale columns it is necessary to determine the column diameter for a specific duty. The method proposed by Thornton and co-workers (9) involves determination of the flooding velocities on a pilot scale and extrapolation of the results to an industrial size column. This method assumes that flooding occurs at equal superficial velocities at equivalent rotor speeds in the two columns. The limitation of this approach is that flooding does not always occur at equal superficial velocities in practice. Therefore correlations are proposed for the determination of the diameter of an industrial scale column


from data obtained on a pilot scale column to give a final relationship between the volumetric flowrates, the ratio of column diameter and flooding hold-ups.

The following assumptions are made in the derivation,

- (1) That the flooding velocity and characteristic velocity equations proposed by Thornton et al (9) and modified by Kung and Beckmann (43) are applicable to all size columns.
- (2) That a specific relationship exists between the column diameter, rotor diameter, stator opening and height of the compartment.
- (3) Drop size in the column depends on the system properties and the energy per unit mass, as proposed by Hinze (76).
- (4) The columns are operated with identical systems.

This is a special case but a general correlation can then be developed to predict the diameter of an industrial scale column from data obtained on a pilot scale operating with any system. This involves consideration of not only energy/unit mass but also the system properties.

The derivation for the special case is as follows:-



In an R.D.C. the hold-up of dispersed phase is given by,

$$\frac{V_d}{x} + \frac{V_c}{1-x} = \bar{V}_N (1-x) \quad (10.1)$$

On flooding at a fixed rotor speed each phase flowrate reaches its corresponding maximum value. Hence differentiating and setting $\frac{dV_d}{dx}$ and $\frac{dV_c}{dx} = 0$ gives,

$$V_{dF} = 2\bar{V}_N x_F^2 (1-x_F) \quad (10.2)$$

and

$$V_{cF} = \bar{V}_N (1-x_F)^2 (1-2x_F) \quad (10.3)$$

The characteristic velocity is given by (43)

$$\bar{V}_N = K \frac{\sigma_i}{\mu_c} \cdot \left(\frac{\Delta\rho}{\rho_c}\right)^{0.9} \cdot \left(\frac{g}{RN^2}\right) \cdot \left(\frac{S}{R}\right)^{2.3} \cdot \left(\frac{h}{R}\right)^{0.9} \cdot \left(\frac{R}{D}\right)^{2.6} \quad (10.4)$$

where $K = .0225$ at $\frac{S-R}{D} \leq \frac{1}{24}$

and $= 0.012$ for $\frac{S-R}{D} > \frac{1}{24}$

From the work of Kung and Beckmann (43), Strand et al (8) and Misek (10) a definite relationship should exist between the column diameter and the other relevant column dimensions. The following relationships are assumed to exist in the proposed columns, where the subscripts B and S refer to the large and small columns respectively,

$$R_B = a_1 D_B \quad (10.5a)$$

$$S_B = a_2 D_B \quad (10.6a)$$

$$h_B = a_3 D_B \quad (10.7a)$$

and

$$R_S = b_1 D_S \quad (10.5b)$$

$$S_S = b_2 D_S \quad (10.6b)$$

$$h_S = b_3 D_S \quad (10.7b)$$

Putting the values from 10.5a, 10.6a and 10.7a, into Equation 10.4, gives,

$$\bar{V}_N = K_B \cdot \left(\frac{\sigma_i}{\mu_c}\right) \cdot \left(\frac{\Delta\rho}{\rho_c}\right)^{0.9} \cdot \left(\frac{g}{DN^2}\right)^{1.0} \cdot \left(\frac{a_2 D_B}{a_1 D_B}\right)^{2.3} \cdot \left(\frac{a_3 D_B}{a_1 D_B}\right)^{0.9} \cdot \left(\frac{a_1 D_B}{D_B}\right)^{2.6} \quad (10.8)$$

or

$$\bar{V}_{NB} = K_B \cdot \left(\frac{\sigma_i}{\mu_c}\right) \cdot \left(\frac{\Delta\rho}{\rho_c}\right)^{0.9} \cdot \left(\frac{g}{DN^2}\right)^{1.0} \cdot \left(\frac{a_2}{a_1}\right)^{2.3} \cdot \left(\frac{a_3}{a_1}\right)^{0.9} \cdot (a_1)^{2.6} \quad (10.9a)$$

and

$$\bar{V}_{NS} = K_S \cdot \left(\frac{\sigma_i}{\mu_c}\right) \cdot \left(\frac{\Delta\rho}{\rho_c}\right)^{0.9} \cdot \left(\frac{g}{DN^2}\right)^{1.0} \cdot \left(\frac{b_2}{b_1}\right)^{2.3} \cdot \left(\frac{b_3}{b_1}\right)^{0.9} \cdot (b_1)^{2.6} \quad (10.9b)$$

The flooding velocity in the small column will be given by,

$$V_{dFS} = 2\bar{V}_{NS} x_{FS}^2 (1 - x_{FS}) \quad (10.10)$$

Substitution of the value of \bar{V}_{NS} in Equation 10.10 from 10.9b gives,

$$V_{dFS} = 2x_{FS}^2 (1 - x_{FS}) \cdot K_{S\mu_c} \frac{\sigma_i}{\rho_c} (\frac{\Delta\rho}{\rho_c})^{0.9} \cdot (\frac{g}{D_S N_S^2})^{1.0} \cdot (\frac{b_2}{b_1})^{2.3} \cdot (\frac{b_3}{b_1})^{0.9} \cdot (b_1)^{2.6} \quad (10.11)$$

Similarly, the flooding velocity in the large column will be given by,

$$V_{dFB} = 2 \cdot x_{FB}^2 (1 - x_{FB}) \cdot K_B \frac{\sigma_i}{\mu_c} (\frac{\Delta\rho}{\mu_c})^{0.9} \cdot (\frac{g}{D_B N_B^2})^{1.0} \cdot (\frac{a_2}{a_1})^{2.3} \cdot (\frac{a_3}{a_1})^{0.9} \cdot (a_1)^{2.6} \quad (10.12)$$

Dividing equation 10.11 by equation 10.12 gives

$$\frac{V_{dFS}}{V_{dFB}} = \frac{2x_{FS}^2 (1 - x_{FS})}{2x_{FB}^2 (1 - x_{FB})} \cdot \frac{K_S}{K_B} \cdot \frac{g}{D_S N_S^2} \cdot \frac{D_B N_B^2}{g} \cdot \frac{(\frac{b_2}{b_1})^{2.3} (\frac{b_3}{b_1})^{0.9} (b_1)^{2.6}}{(\frac{a_2}{a_1})^{2.3} (\frac{d_3}{d_1})^{0.9} (a_1)^{2.6}} \quad (10.13)$$

If Q_{dS} and Q_{dB} are the volumetric flowrates of the dispersed phase in the small and large columns respectively under normal operating conditions and Q_{dFS} and Q_{dFB} the flowrates under flooding conditions, then,

$$Q_{dS} = K_{1S} Q_{dFS} \quad (10.14)$$

$$Q_{dB} = K_{2B} Q_{dFB} \quad (10.15)$$

or
$$\frac{Q_{dS}}{Q_{dB}} = \frac{K_{1S}}{K_{2B}} \frac{Q_{dFS}}{Q_{dFB}} \quad (10.16)$$

Also,

$$Q_{dFS} = V_{dFS} \cdot \pi D_S^2 \quad (10.17)$$

$$Q_{dFB} = V_{dFB} \cdot \pi D_B^2 \quad (10.18)$$

Dividing 10.17 by 10.18 gives,

$$\frac{Q_{dFS}}{Q_{dFB}} = \frac{V_{dFS}}{V_{dFB}} \cdot \frac{D_S^2}{D_B^2} \quad (10.19)$$

or

$$\frac{V_{dFS}}{V_{dFB}} = \frac{Q_{dFS}}{Q_{dFB}} \cdot \frac{D_B^2}{D_S^2} \quad (10.20)$$

Substituting the value of $\frac{Q_{dFS}}{Q_{dFB}}$ from equation 10.16 in equation 10.20 gives,

$$\frac{V_{dFS}}{V_{dFB}} = \frac{Q_{dS}}{Q_{dB}} \cdot \frac{K_{2B}}{K_{1S}} \cdot \frac{D_B^2}{D_S^2} \quad (10.21)$$

Substituting the value of $\frac{V_{dFS}}{V_{dFB}}$ from 10.21 into 10.13 gives,

$$\frac{Q_{dS}}{Q_{dB}} \cdot \frac{K_{2B}}{K_{1S}} \cdot \frac{D_B^2}{D_S^2} = \frac{x_{FS}^2 (1-x_{FS})}{x_{FB}^2 (1-x_{FB})} \cdot \frac{K_S}{K_B} \cdot \frac{D_B}{D_S} \cdot \frac{N_B^2}{N_S^2}$$

$$\cdot \frac{\left(\frac{b_2}{b_1}\right)^{2.3} \left(\frac{b_3}{b_1}\right)^{.9} (b_1)^{2.6}}{\left(\frac{a_2}{a_1}\right)^{2.3} \left(\frac{a_3}{a_1}\right)^{.9} (a_1)^{2.6}} \quad (10.22)$$

On rearrangement,

$$\frac{D_B}{D_S} = \frac{x_{FS}^2 (1-x_{FS})}{x_{FB}^2 (1-x_{FB})} \cdot \frac{K_S}{K_B} \cdot \frac{N_B^2}{N_S^2} \cdot \frac{K_{1S}}{K_{2B}} \cdot \frac{Q_{dB}}{Q_{dS}}$$

$$\cdot \frac{\left(\frac{b_2}{b_1}\right)^{2.3} \left(\frac{b_3}{b_1}\right)^{0.9} (b_1)^{2.6}}{\left(\frac{a_2}{a_1}\right)^{2.3} \left(\frac{a_3}{a_1}\right)^{0.9} (a_1)^{2.6}} \quad (10.23)$$

Equation 10.23 can be used to determine the required diameter of the column for a specific duty (i.e. processing Q_{dB} volumetric flow rate of feed) provided the corresponding rotor speed N_B and the hold-up x_{FB} in the large column at flooding is known. However, equation 10.23 can be further simplified by assuming that, under certain conditions of operation, equal mean drop size exists in the two columns. As discussed in Chapter 4, Hinze proposed the equation for maximum stable drop size based on the assumption of an isotropic homogeneous turbulence with

the microscale of turbulence smaller than the drop size. Under such circumstances,

$$d_m = c_1 \left(\frac{g_c \sigma}{\rho_c} \right)^{3/5} (E)^{-2/5} \quad (10.24)$$

Hinze reported the constant c_1 to be approximately 0.72 based on an analysis of data for a rotating cylinder obtained by Clay (218). However, neither an exponent of $-2/5$ on E or a value of $c_1 = 0.72$ provides the best fit of Clay's data (219). Nevertheless, the Hinze equation, with adjustment of constant c_1 as necessary, has been used with some success to predict d_{max} in certain devices such as glove valves, stirred tanks, and rotating cylinders. The explanation may be that the conditions for local isotropy are met approximately. Moreover, Vermeulen et al (78), Calderbank (126), and Kafarov and Babanov (82) successfully correlated mean drop sizes in stirred tanks using equations of this form. Further, the data of Clay (218) suggests that, as a first approximation, the ratio of mean drop size/maximum drop size may be taken as constant.

$$\text{or } d_{(\text{mean dia.})} = K d_{max}. \quad (10.25)$$

Substitution of d_{max} from 10.24 into equation 10.25 gives,

$$d_{(\text{mean dia.})} = K c_1 \left(\frac{g_c \sigma}{\rho_c} \right)^{3/5} (E)^{-2.5} \quad (10.26)$$

where $E = \frac{4}{\pi} c_2 \frac{N^3 R^5}{HD^2}$ (10.27)

Substituting for E in equation 10.26 gives

$$d(\text{mean}) = Kc_1 \left(\frac{g_c \sigma}{\rho_c} \right)^{3/5} \left(\frac{4}{\pi} c_2 \frac{N^3 R^5}{HD^2} \right)^{-2/5}$$
 (10.28)

If d_S and d_B are the mean drop diameters in the small and large columns respectively then

$$d_S = Kc_1 \left(g_c \frac{\sigma}{\rho_c} \right)^{3/5} \left(\frac{4}{\pi} c_2 \frac{N^3 R^5}{hD^2} \right)_S^{-2/5}$$
 (10.29)

and

$$d_B = Kc_1 \left(g_c \frac{\sigma}{\rho_c} \right)^{3/5} \left(\frac{4}{\pi} c_2 \frac{N^3 R^5}{hD^2} \right)_B^{-2/5}$$
 (10.30)

The value of constant c_1 is assumed to be identical in the two cases, provided the same system is used.

For the condition of equal mean drop size in both columns a combination of equations 10.29 and 10.30 gives,

$$\left(\frac{N^3 R^5}{hD^2} \right)_B = \left(\frac{N^3 R^5}{hD^2} \right)_S$$
 (10.31)

Substituting the values of R and h from equation 10.5a,b into equation 10.31 gives,

$$\frac{N^3 (a_1 D)^5}{(a_3 D) D^2} \Big|_B = \frac{N^3 (b_1 D)^5}{(b_3 D) D^2} \Big|_S$$

or $N_B^3 D_B^2 \cdot \left(\frac{a_1}{a_3} \right)^5 = N_S^3 D_S^2 \cdot \left(\frac{b_1}{b_3} \right)^5$ (10.32)

$$\text{or } \left(\frac{N_B}{N_S}\right)^3 = \left(\frac{D_S}{D_B}\right)^2 \cdot \left(\frac{b_1}{a_1}\right)^5 \cdot \left(\frac{a_3}{b_3}\right)$$

$$\text{or } \left(\frac{N_B}{N_S}\right)^2 = \left(\frac{D_S}{D_B}\right)^{2.2/3} \cdot \left(\frac{b_1}{a_1}\right)^{5.2/3} \left(\frac{a_3}{b_3}\right)^{2/3} \quad (10.33)$$

Putting $\left(\frac{N_B}{N_S}\right)$ from (10.33) into equation (10.23),

$$\frac{D_B}{D_S} = \frac{x_{FS} (1-x_{FS})}{x_{FB} (1-x_{FB})} \cdot \frac{K_S}{K_B} \cdot \frac{Q_{dB}}{Q_{dS}} \cdot \frac{\left(\frac{b_2}{b_1}\right)^{2.3} \left(\frac{b_3}{b_1}\right)^{0.9} (b_1)^{2.6}}{\left(\frac{a_2}{a_1}\right)^{2.3} \left(\frac{a_3}{a_1}\right)^{0.9} (a_1)^{2.6}}$$

$$\frac{K_{LS}}{K_{2B}} \cdot \left(\frac{D_S}{D_B}\right)^{4/3} \cdot \left(\frac{b_1}{a_1}\right)^{10/3} \cdot \left(\frac{a_3}{b_3}\right)^{2/3}$$

$$\text{or } \left(\frac{D_B}{D_S}\right)^{7/3} = \frac{x_{FS}^2 (1-x_{FS})}{x_{FB}^2 (1-x_{FB})} \cdot \frac{K_S}{K_B} \cdot \frac{K_{LS}}{K_{2B}} \cdot \frac{Q_{dB}}{Q_{dS}}$$

$$\cdot \frac{\left(\frac{b_2}{b_1}\right)^{2.3} \left(\frac{b_3}{b_1}\right)^{0.9} (b_1)^{2.6}}{\left(\frac{a_2}{a_1}\right)^{2.3} \left(\frac{a_3}{a_1}\right)^{0.9} (a_1)^{2.6}} \cdot \left(\frac{b_1}{a_1}\right)^{10/3} \cdot \left(\frac{a_3}{b_3}\right)^{2/3} \quad (10.34)$$

Equation 10.34 can be used for the prediction of column diameter using data obtained from a pilot scale column, provided the flooding hold up in the large column can be estimated. Flooding hold up in the large column can, in theory, be estimated using Thornton et al's (9) equation,

$$x_{FB} = \left| \frac{(L^2 + 8L)^{0.5} - 3L}{4(1-L)} \right|_B \quad (10.35)$$

where $L = \frac{V_{dF}}{V_{cF}} = \frac{K_{1B} |V_d|_B}{K_{3B} |V_c|_B}$

or $L = \frac{K_{1B} |Q_d|_B}{K_{3B} |Q_c|_B}$

$$= \frac{K_{1B} |Q_d|_B}{K_{3B} |Q_c|_B} \quad (10.36)$$

10.1.2 Scale-up of Column Diameter

General Case - Dissimilar Systems

A generalisation of the mathematical model given in section 10.1 will now be proposed to enable a first estimate to be made of the diameter of an industrial column from a knowledge of the system properties and data obtained in a specific pilot scale column operated with a different system of known properties. The mathematical model is as follows:

Rewriting equation 10.11 and equation 10.12 for large and small columns respectively,

$$\bar{V}_{NB} = K_B \frac{\sigma_B}{\mu_{cB}} \left(\frac{\Delta\rho_B}{\rho_{cB}} \right)^{0.9} \left(\frac{g}{D_B N_B} \right) \left(\frac{a_2}{a_1} \right)^{2.3} \left(\frac{a_3}{a_1} \right)^{0.9} (a_1)^{2.6} \quad (10.11)$$

$$\bar{V}_{NS} = K_S \frac{\sigma_S}{\mu_{CS}} \left(\frac{\Delta\rho_S}{\rho_{CS}}\right)^{0.9} \left(\frac{g}{D_S N_S^2}\right) \left(\frac{b_2}{b_1}\right)^{2.3} \left(\frac{b_3}{b_1}\right)^{0.9} (b_1)^{2.6} \quad (10.12)$$

where K_S or $K_B = .0225$ at $\frac{S-R}{D} \leq \frac{1}{24}$

and $= 0.012$ at $\frac{S-R}{D} > \frac{1}{24}$

Substitution of equation 10.11 and equation 10.12 into equation 10.10 and division, gives

$$\frac{V_{dFS}}{V_{dFB}} = \frac{x_{FS}^2 (1-x_{FS})}{x_{FB}^2 (1-x_{FB})} \cdot \frac{K_S}{K_B} x \frac{D_B N_B^2}{D_S N_S^2} \cdot \left(\frac{\Delta\rho_S}{\rho_{CS}}\right) \cdot \frac{\rho_{CB}^{0.9}}{\Delta\rho_B} \cdot \left(\frac{\sigma_S}{\mu_{CS}}\right) \cdot \frac{\mu_{CB}}{\sigma_B} \cdot \frac{(b_2/b_1)^{2.3} (b_3/b_1)^{0.9} (b_1)^{2.6}}{\left(\frac{a_2}{a_1}\right)^{2.3} \left(\frac{a_3}{a_1}\right)^{0.9} (a_1)^{2.6}} \quad (10.37)$$

Substituting the value of V_{dFS}/V_{dFB} from equation 10.21 and rearranging,

$$\frac{D_B}{D_S} = \frac{x_{FS}^2 (1-x_{FS})}{x_{FB}^2 (1-x_{FB})} \cdot \frac{K_S}{K_B} \cdot \frac{N_B^2}{N_S^2} \cdot \frac{K_{1S}}{K_{2B}} \cdot \frac{Q_{dB}}{Q_{dS}} \cdot \left(\frac{\Delta\rho_S}{\rho_{CS}}\right) \cdot \frac{\rho_{CB}^{0.9}}{\Delta\rho_B} \cdot \left(\frac{\sigma_S}{\mu_{CS}}\right) \cdot \frac{\mu_{CB}}{\sigma_B} \cdot \frac{(b_2/b_1)^{2.3} (b_3/b_1)^{0.9} (b_1)^{2.6}}{\left(\frac{a_2}{a_1}\right)^{2.3} \left(\frac{a_3}{a_1}\right)^{0.9} (a_1)^{2.6}} \quad (10.38)$$

Equation (10.38) contains the expression $\frac{N_B^2}{N_S^2}$.

To eliminate this equation 10.28 can be rewritten for large and small columns,

$$d_S = KC_1 \left(\frac{g_c \sigma_S}{\rho_{cS}} \right)^{3/5} \left(\frac{4}{\pi} C_2 \frac{N_S^3 R_S^5}{H_S D_S^2} \right)^{-2/5} \quad (10.39)$$

$$d_B = KC_1 \left(\frac{g_c \sigma_B}{\rho_{cB}} \right)^{3/5} \left(\frac{4}{\pi} C_2 \frac{N_B^3 R_B^5}{H_B D_B^2} \right)^{-2/5} \quad (10.40)$$

$$\text{If } d_S = d_B \quad (10.41)$$

And assuming conditions of local isotropy are met approximately then,

$$\left(\frac{\sigma_S}{\rho_{cS}} \right)^{3/5} \left(\frac{N_S^3 R_S^5}{H_S D_S^2} \right)^{-2/5} = \left(\frac{\sigma_B}{\rho_{cB}} \right)^{3/5} \left(\frac{N_B^3 R_B^5}{H_B D_B^2} \right)^{-2/5}$$

$$\text{or } \left(\frac{N_S^3 R_S^5}{H_S D_S^2} \right)^{-2/5} = \left(\frac{\sigma_B \rho_{cS}}{\sigma_S \rho_{cB}} \right)^{3/5} \left(\frac{N_B^3 R_B^5}{H_B D_B^2} \right)^{-2/5}$$

$$\text{or } \frac{N_S^3 R_S^5}{H_S D_S^2} = \left(\frac{\sigma_B \rho_{cS}}{\sigma_S \rho_{cB}} \right)^{3/5} \cdot \frac{N_B^3 R_B^5}{H_B D_B^2} \quad (10.42)$$

Substitution of the relationships defined in Equations 10.5a, b, 10.6 a, b and 10.7 a, b and rearrangement yields,

$$\left(\frac{N_B}{N_S} \right)^2 = \left(\frac{\sigma_B \cdot \rho_{cS}}{\sigma_S \cdot \rho_{cB}} \right) \left(\frac{D_S}{D_B} \right)^{4/3} \left(\frac{b_1}{a_1} \right)^{10/3} \left(\frac{a_3}{b_3} \right)^{2/3} \quad (10.43)$$

Equation 10.43 is the requisite condition for scale up, i.e. if the column diameter D_B of an industrial column is to be determined for an operating rotor speed of N_B then the flooding data should be determined at N_S in the small column as defined by equation 10.43.

Substitution from Equation 10.43 for $\frac{N_B}{N_S}$ in Equation 10.38 and rearrangement gives the final expression,

$$\left(\frac{D_B}{D_S}\right)^{7/3} = \frac{x_{FS}^2 (1 - x_{FS})}{x_{FB}^2 (1 - x_{FB})} \cdot \frac{K_S}{K_B} \cdot \frac{\rho_{cS}}{\rho_{cB}} \cdot \frac{\mu_{cB}}{\mu_{cS}} \cdot \frac{K_{1S}}{K_{2B}}$$

$$\cdot \frac{Q_{dB}}{Q_{dS}} \cdot \left(\frac{\Delta\rho_S}{\rho_{cS}} \cdot \frac{\rho_{cB}}{\Delta\rho_B}\right)^{0.9} \cdot \frac{\left(\frac{b_2}{b_1}\right)^{2.3} \cdot \left(\frac{b_3}{b_1}\right)^{0.9}}{\left(\frac{a_2}{a_1}\right)^{2.3} \cdot \left(\frac{a_3}{a_1}\right)^{0.9}}$$

$$\cdot \left(\frac{b_1}{a_1}\right)^{2.6} \cdot \left(\frac{b_1}{a_1}\right)^{10/3} \cdot \left(\frac{a_3}{b_3}\right)^{2/3} \quad (10.49)$$

Equation 10.49 is a general expression which could be used for the preliminary estimation of the diameter of an industrial scale column provided the column geometry, physical properties of the two systems and flooding data for the small scale column are known.

The accuracy of this equation is unlikely to approach that of equation 10.34 because of the assumptions inherent in eliminating C_1 , C_2 from Equations 10.39 and 10.40. Also

trace impurities and surfactants may significantly effect physical properties of a system. Therefore the special case which is based on the use of exactly the same system in both columns is preferable.

10.2 Scale-up of Column Height

In the past liquid-liquid extraction columns have been designed using the same principle as for the design of gas-liquid contacting equipment. This involves evaluation of,

- (a) The number of transfer units for the required separation,
- (b) The height of a transfer unit, and
- (c) The volumetric capacity of the column.

The number of transfer units was estimated from mathematical or graphical material balances (57). The H.T.U. was frequently determined from pilot plant experimental work or from previous plant experience. However, experience with packed distillation and gas absorption columns has shown that this method is fundamentally unsound, since it applies a procedure involving stepwise changes in concentration to an operation in which the concentration actually changes differentially with height. Furthermore, this method does not take back mixing into account. Back mixing is present in most cases and

further analysis is required for the estimation of the increased column height, due to reduced concentration driving force which results from it.

Hence a method is proposed for scale-up from laboratory data for the determination of industrial size of column height from basic considerations.

As discussed in Chapter 1, the rate of mass transfer in a solvent extractor depends on the overall mass transfer coefficient, the interfacial area, and the driving force, i.e.

$$N = K A \Delta C_m \quad (1.1)$$

where ΔC_m is the log mean concentration driving force, which could be determined from Simpson's rule.

Let subscripts B and S denote the large column and the small column respectively, then from equation 1.1 we have,

$$N_B = (K A \Delta C_m)_B \quad (10.45)$$

$$\text{and } N_S = (K A \Delta C_m)_S \quad (10.46)$$

Division of equation 10.45 by equation 10.46 gives,

$$\frac{N_B}{N_S} = \frac{K_B A_B \Delta C_{mB}}{K_S A_S \Delta C_{mS}} \quad (10.47)$$

If a is the surface area per unit volume of column then the total surface area in any column is given by:-

$A = a$ column cross sectional area x effective column height

$$A = a \cdot \frac{\pi}{4} D^2 \cdot H \quad (10.48)$$

Substitution of the value of A from 10.41 into equation 10.40 yields,

$$\begin{aligned} \frac{N_B}{N_S} &= \frac{K_B}{K_S} \cdot \frac{a_B}{a_S} \cdot \frac{D_B^2}{D_S^2} \cdot \frac{H_B}{H_S} \cdot \frac{\Delta C_{mB}}{\Delta C_{mS}} \\ &= \frac{K_B}{K_S} \cdot \frac{a_B}{a_S} \cdot \frac{D_B^2}{D_S^2} \cdot \frac{H_B}{H_S} \cdot \frac{\Delta C_{mB}}{\Delta C_{mS}} \end{aligned} \quad (10.49)$$

Now on the assumption that the drops are spherical and of equal size, it can be expressed by equation 1.2 as,

$$a = \frac{6x}{d_{32}} \quad (1.2)$$

This assumption is often accepted and applied in the design of extraction equipment but a careful assessment of each situation is required before applying it (52). Substituting the value of a from equation 1.2 into 10.49 and rearranging,

$$\begin{aligned} \frac{H_B}{H_S} &= \frac{K_S}{K_B} \cdot \frac{D_S^2}{D_B^2} \cdot \frac{\Delta C_{mS}}{\Delta C_{mB}} \cdot \frac{N_B}{N_S} \cdot \frac{x_S}{d_{32S}} \cdot \frac{d_{32B}}{x_B} \\ \text{or} \quad \frac{H_B}{H_S} &= \frac{K_S}{K_B} \cdot \frac{D_S^2}{D_B^2} \cdot \frac{\Delta C_{mS}}{\Delta C_{mB}} \cdot \frac{N_B}{N_S} \cdot \frac{x_S}{x_B} \cdot \frac{d_{32B}}{d_{32S}} \end{aligned} \quad (10.50)$$

In order to estimate the effective height of the larger industrial column using equation 10.50 it is necessary to predict the overall mass transfer coefficient in it. The overall mass transfer coefficient depends on the inside, outside and interfacial resistance in the system. The latter is usually neglected but recent studies described in para. 5.7.1 have shown that it plays a very important role with some selected systems (56).

As discussed in para. 5.3.2 the coefficient of mass transfer inside the drop depends on the velocity of circulation of liquid within the drop. It is known to increase with the droplet diameter along with favourable system properties.

Therefore to obtain equivalent overall mass transfer coefficients requires equal drop side and equal continuous phase side coefficients in the two units.

A critical examination of the correlation proposed in section 5.4 indicates that while the drop side coefficient depends on the drop diameter the continuous phase side coefficient depends on the characteristic drop velocity. Many workers (76, 60) have shown that equal drop sizes will be produced in two units if a condition of equal energy per unit mass ($\frac{N^3 R^5}{HD^2}$) is satisfied. Conversely, the condition of equal characteristic velocity would require from Kung and Beckmann's (43) correlation for characteristic velocity, $\frac{1}{RN^2}$ to be equal in two

geometrically similar units. It is clearly impossible to meet both of these criteria. However in the majority of industrial systems one of the two resistances is controlling (57), i.e. either the continuous phase or dispersed phase.

If the continuous phase resistance is controlling, as discussed in section 5.6, then equal overall mass transfer coefficients could be obtained by maintaining the group $(\frac{1}{RN^2})$ equal in the two units. The drop size in this case could be calculated using the Hinze (76) correlation given in Chapter 4. If the drop side resistance is controlling then equal drop sizes, and thus equal overall mass transfer coefficients could be obtained by maintaining the energy per unit mass $(\frac{N^3R^5}{HD^2})$ equal in the two units.

To predict the drop side coefficient it is necessary to know the mode of mass transfer which depends upon the size of the drops. This is rendered difficult in an R.D.C. because a drop size distribution exists at any particular rotor speed; this results in differences in the modes of mass transfer between size fractions. However, the drop size distribution in an R.D.C. is normally distributed (52). Therefore a similar distribution should be obtained in the two units at equal energy per unit mass. This would result in equal drop side coefficient in the two units.

If the system is of the type where both the resistances are significant, the power to which N should be raised would lie between 2 and 3. Reman has suggested a figure of 2.8 (7).

10.3 Experimental Verification of Column Diameter Model

10.3.1 Special case - Identical Systems

To test the validity of equation 10.34 the flooding runs described in para. 9.1.1 were conducted under non-mass transfer conditions and at equal energy input per unit mass ($\frac{N^3 R^5}{HD^2}$) in the two columns. Four rotor speeds and several different flowrates of continuous and dispersed phase were used. The respective hold ups at flooding were calculated by insertion of the flooding rates into equations 10.36 and 10.35. The hold-ups were then used to predict the column diameter using equation 10.34 developed in section 10.1. The calculated values of column diameter are plotted against the energy per unit mass group ($\frac{N^3 R^5}{HD^2}$) in Fig. 10.1. Good agreement was obtained especially at ($\frac{N^3 R^5}{HD^2}$) = $29.3 \frac{m^2}{sec^3}$. Of the 64 points plotted 62.5% lie within an accuracy limit of $\pm 5\%$, 95.4% lie within $\pm 10\%$, and all lie within $\pm 15\%$. The agreement was best at ($\frac{N^3 R^5}{HD^2}$) $29.2 \frac{m^2}{sec^3}$ and may be attributed to the fact that at that particular energy input the flow pattern developed was as shown in Fig. 2.3, and behaviour of the units was most typical of R.D.C.

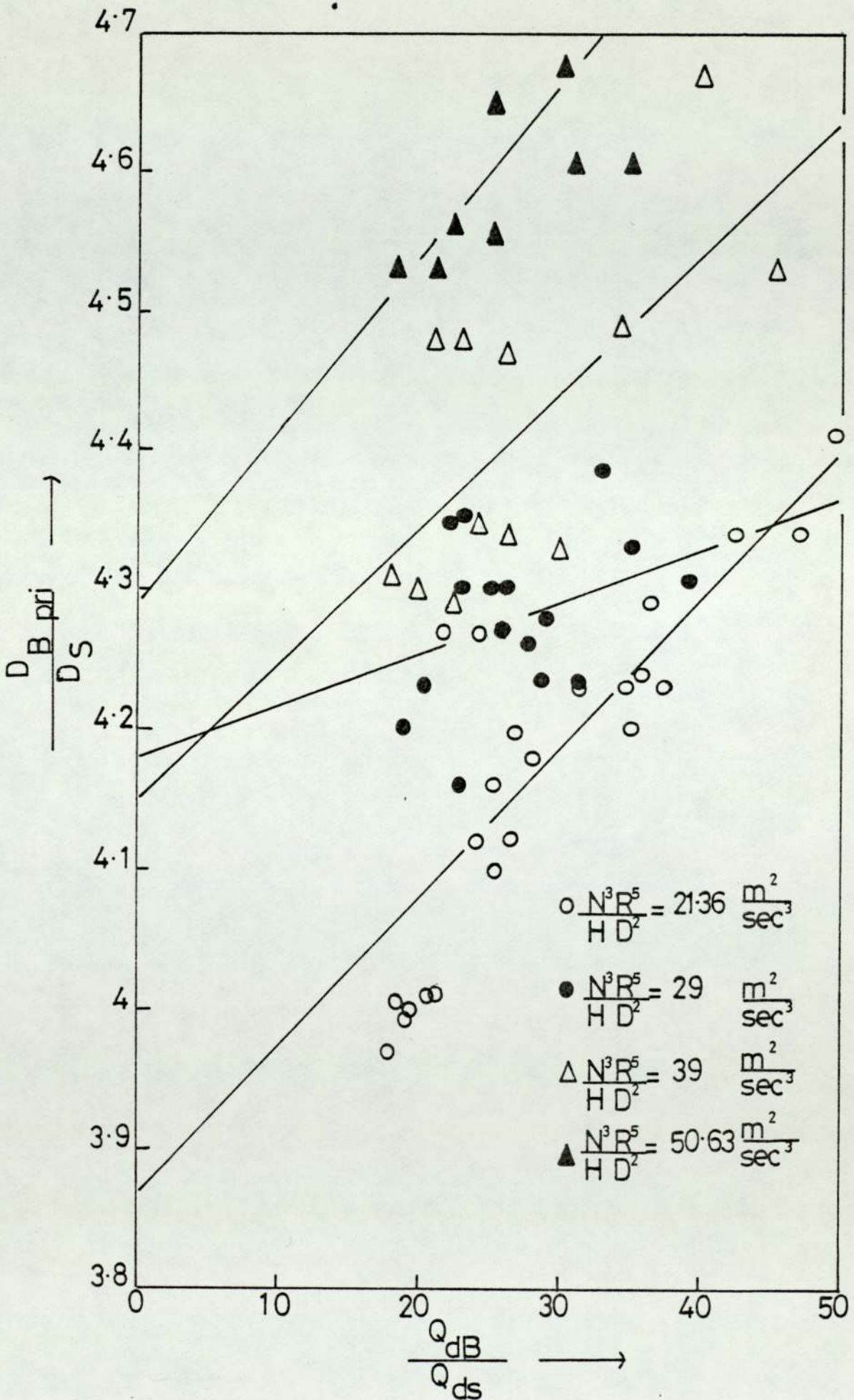


FIG. 10.1 CORRELATION OF EQUATION 10.34.

operation.

To check the validity of equation 10.35 separate experiments were performed to determine the actual flooding hold-up in the 450 mm. diameter R.D.C. column, as discussed in para. 9.1.3.1. A finite time, approximately 15-20 minutes was found to be required for the column to flood. During this time the hold-up continuously increased until the maximum was reached at the flooding point. Typical results are plotted in Figs. 10.2 and 10.3. These suggest that Equation 10.35 gives a reasonable approximation for practical purposes.

10.3.2 Tentative Verification of General Case - Dissimilar Systems

The model described in para. 10.1.1 was tentatively tested with the limited data available from the work of Sarkar (38) and Al-Hemiri (37) with the system toluene-water. Substitution of their data into equation 10.44, yielded the results given in Table 10.1 and 10.2.

The data shows that the predicted diameter is within an accuracy limit of $\pm 15\%$. A better fit would have been achieved if the data had been available at precisely equivalent rotor speeds, defined by equation 10.43, which would have been 391 r.p.m. in the 450 mm diameter column instead of data at 450 r.p.m. as calculated in Table 10.3.

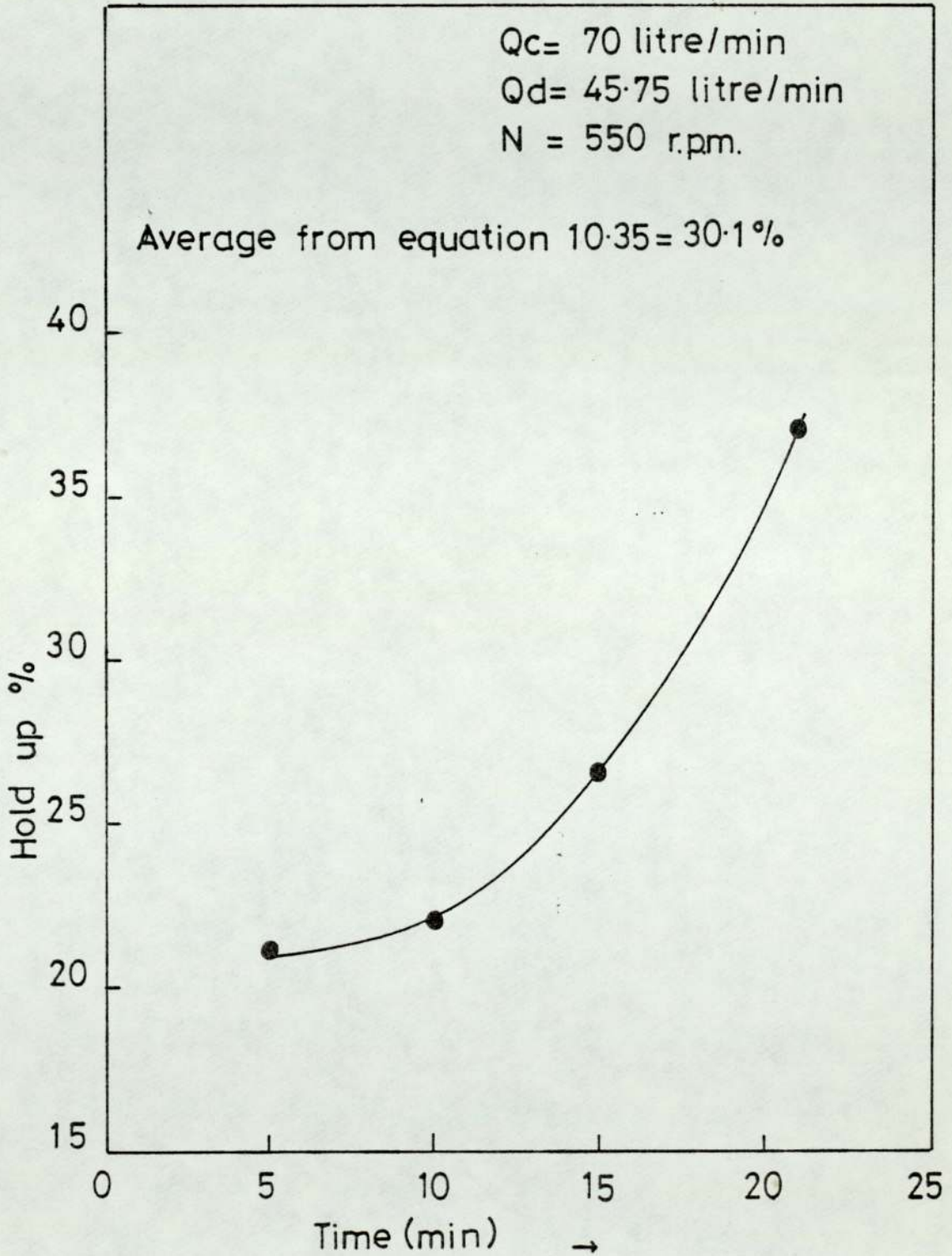


FIG. 10.2 VARIATION OF HOLD-UP WITH TIME AT FLOODING CONDITIONS.

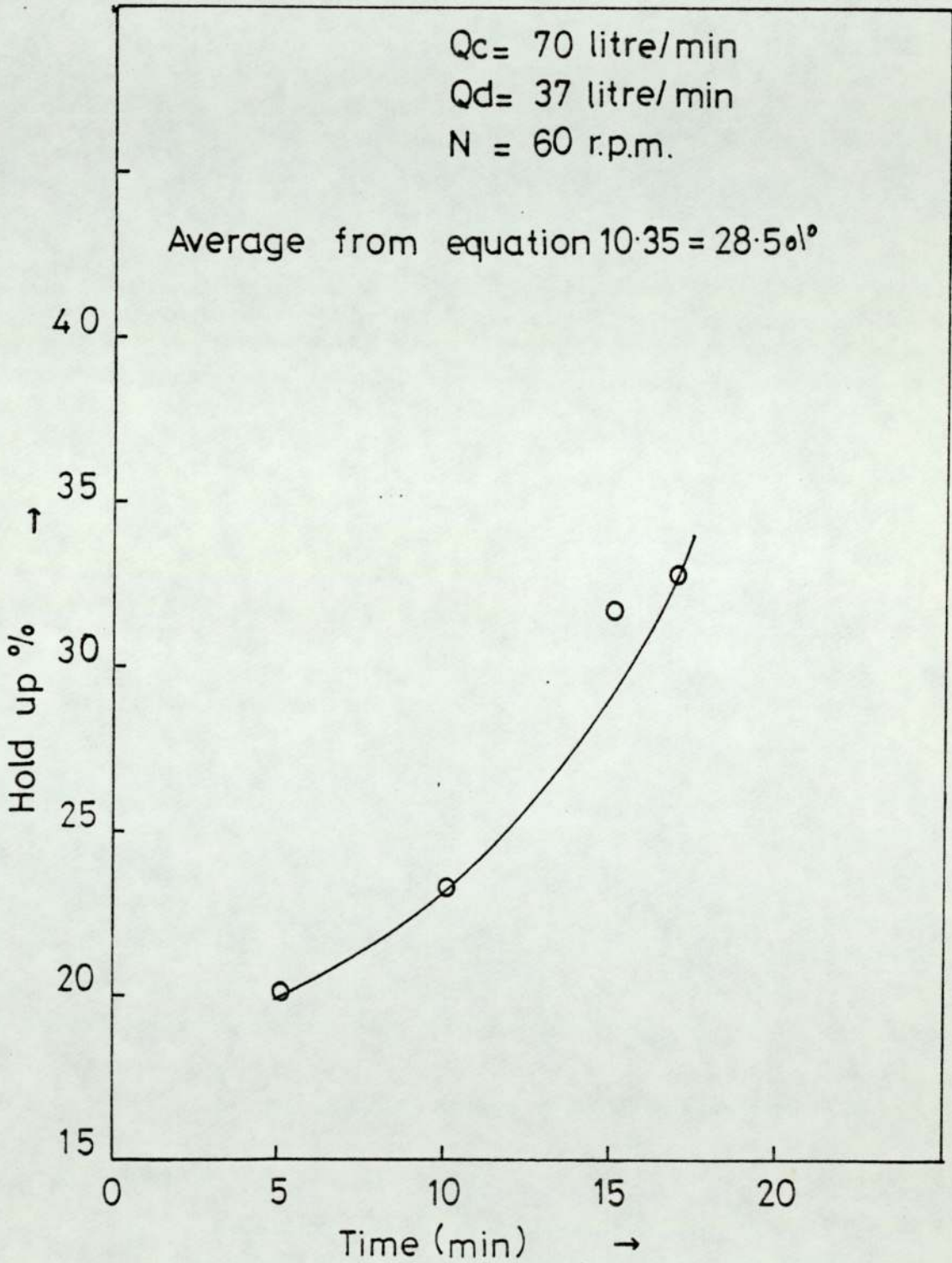


FIG. 10.3 VARIATION OF HOLD-UP WITH TIME AT FLOODING CONDITIONS.

TABLE 10.1

System Kero-water
450 mm. R.D.C.

System - Toluene-water Sarkar (38)
101 mm. R.D.C.

Q_{DS} lit/min	Q_{CS} lit/min	$L = \frac{Q_{DS}}{Q_{CS}}$	x_{FS}	N_S	$x_{FS}^2 (1 - K_{FS})$	Q_{DB} lit/min	Q_{CB} lit/min	N_B	$x_{FB}^2 (1 - x_{FB})$	D_B Predicted mm.
.52	2.91	.180	.20	1000	.033	69.25	70.0	450	.074	440.3
.94	2.26	.41	.26	1000	.052	77	58.75	450	.080	418.4
1.30	1.36	1.01	.33	1000	.074	80.6	55	450	.083	417.2
2.15	.72	2.94	.40	1000	.097	57.0	81.25	450	.065	370.7

System - Toluene-water / Al-Hemiri (37)

TABLE 10.2

System - Kerosene-water

101 mm. R.D.C.

450 mm. R.D.C.

Q_{DS}	Q_{CS}	$L = \frac{Q_{DS}}{Q_{CS}}$	x_{FS}	N_S	$x_{FS} (1-x_{FS})$	Q_{DB} Lit/min	Q_{CB} Lit/min	N_B	$x_{FB} (1-x_{FS})$	D_B Predicted mm
.7	2.85	.24	.24	1000	.045	69.25	70.00	450	.074	442.3
1.66	1.86	.89	.32	1000	.071	77.00	58.75	450	.080	375.7
2.0	1.49	1.34	.35	1000	.081	80.6	55.00	450	.083	368.7
2.5	.49	5.10	.51	1000	.129	57.00	81.25	450	.065	392.2

Variation in results may also be attributed to,

- (1) The use of a slightly different column, i.e. with a bearing support in the middle, by Al-Hemiri (37).
- (2) The use of distilled water as continuous phase by both Sarkar (38) and Al-Hemiri (37). With distilled water there would be less likelihood of interfacial scum and thus less change in system properties, consequently, slightly different flooding results would therefore be obtained, compared with tap water.

Despite these inaccuracies, the results obtained were encouraging, and the procedure appears promising for preliminary sizing of industrial columns for use with systems for which no pilot scale data are available.

The 'equivalent' rotor speeds at which the 450 mm diameter column should be operated, for comparison of the flooding data, can be calculated using equation 10.43. For system toluene-water in the 101 mm diameter and kerosene-water in the 450 mm. diameter column the respective values are as outlined in Table 10.3.

TABLE 10.3

N_S (r.p.m.)	N_B (r.p.m.)
500	195
700	274
800	313
1000	391
1250	489
1500	587

11. DISCUSSION OF RESULTS

11.1 Non-Mass Transfer Studies

11.1.1 Hold-up

The variation of average hold up, with dispersed phase flow velocity in the 450 mm. diameter R.D.C. is illustrated in Fig. 9.13. In general, at a fixed rotor speed and continuous phase velocity, the average hold-up increased with increasing dispersed phase velocity. The rate of increase was greater at higher rotor speeds.

Unlike in other studies (11, 37, 38) the continuous phase velocity had a significant effect on the dispersed phase hold-up. Although only two flows were used the effect was found to be greatest at the highest rotor speed as illustrated in Fig. 9.14. Clearly the effect of continuous phase flow was due to the increase in the drop mean residence times. At the highest speed the drop sizes decreased, and they would therefore tend to be more easily entrained by the countercurrent flow.

Because of the effect of continuous phase flow, average hold up and hold-up profile studies were carried out under countercurrent flow conditions.

The axial hold-up profiles with the sample tube extended to midway between the stator and rotor, i.e. $(\frac{S-R}{2})$ in the 450 mm. diameter R.D.C. are shown in Fig. 9.8. The axial profiles obtained with samples drawn from near the column

walls in both columns are shown in Fig. 9.6 and Fig. 9.7 respectively. Contrary to the results of Strand et al (8), very erratic data were obtained in the 450 mm. diameter column while studying the axial hold-up profiles. This may be explained by the difference in the vertical location of the sample tube. In this study the extended tubes were located in line with the disc, where, as in Strand's study, they were 57 mm. away from the rotating discs (8).

In any future studies it would be worthwhile locating the sample point differently since it appears, from the flow patterns shown earlier in Fig. 3.4, that the hold-up in the high velocity zone in line with any disc is both difficult to sample and not representative of the compartment.

The axial hold-up profiles determined with the sample tube located at the wall of the column were similar to those reported by other workers (8, 37, 38, 39) only at low rotor speeds of the order of 150 and 300 r.p.m. in the 450 mm. diameter column and 404 and 808 r.p.m. in the 101 mm. diameter column. At these rotor speeds, the hold-up increased gradually to a maximum value at a point approximately mid-way up the column and subsequently decreased. At the highest speed studied, i.e. 600 r.p.m., in the 450 mm. diameter column the hold up was found to decrease, then increase and finally decrease again. This would be expected from the drop size analysis for similar conditions

in the column. In theory since smaller drops have lower settling velocities and are more susceptible to backmixing, the hold-up profile should be the inverse of the drop size profile, i.e. the characteristic drop size first decreases to a minimum value at a point corresponding to maximum hold-up value and then increases towards the exit.

In the 450 mm. diameter column, during the point hold-up studies with the sampling tubes positioned at $\frac{S-R}{2}$, a partial vacuum was detected at points moving up the column. Despite the hydrostatic head this prevented samples from being withdrawn from sample taps above compartment 9. Opening a tap above this position resulted in air being sucked into the column at most flowrates and rotor speeds. The suction was found to increase with increase in rotor speed and dispersed phase flowrate. As a result axial hold-up profiles are only reported up to compartment 9, i.e. just above mid-way up the column. An attempt was made to use a hypodermic syringe with a needle to obtain the samples above compartment 9, but consistent results could not be obtained. Clearly a syringe does not provide the best means of collecting two phase samples from a system in which drop sizes are several times larger than the needle size.

The radial hold-up profiles using various types of sampling tube, located in different planes are shown in Figs. 9.9, 9.11 and 9.12. As shown in Fig. 9.9 with a 3mm. bore stainless steel tube located in the same plane as the rotating discs, the hold up was found to increase in moving

away from the wall until it reached a maximum at almost midway between the disc and stator edge, and then decrease sharply near the tip of the rotating disc. The average hold up in the radial direction, found using Simpson's rule (216), lay very near to the position $\frac{S-R}{2}$ as found by Strand et al (8), and was close to both, the average hold up calculated by equation 3.7 and 3.8 and that found by experiment. The hold ups were 7.65%, 7.1% and 5.5% respectively at a continuous and dispersed phase flow rates of 28.5 and 30.5 lit./min. and rotor speeds of 450 r.p.m. The slight variation in the average hold-up from the radial profile compared to the theoretical and experimental values, can be attributed to the fact that compartment 3, in which the hold-up profile was estimated may not be truly representative compartment. As shown in Fig. 9.9, the radial hold-up profile in compartment number 5 followed a similar pattern to that in compartment 3 under similar flow conditions, and rotor speed. Although as shown in Fig. 9.9, the radial hold-up profiles were similar, changes are likely with change in flow velocities and rotor speed. The sharp change in average hold up with change in rotor speeds in the 101 mm. diameter R.D.C. is shown in Fig. 9.15.

The effect of change in the position of sample tube plane was studied using special tubes constructed as shown in Fig. 9.10a, b. The results are shown in Fig. 9.11 and

9.12. During this study, contrary to the results of other workers, only very small hold ups were found near the rotor shaft (8). The hold up decreased towards the rotor shaft and remained fairly small compared to the average hold up in the column. A low hold up near the shaft would be expected, providing wetting effects were absent (37), because of the flow pattern illustrated in Fig. 3.4 associated with centrifugal action. Hence there are probably pockets of very poorly mixed fluid, usually in the area just above the disc, in the 450 mm. diameter column. This is also illustrated in Fig. 9.56.

To ascertain the effect of material of construction of the sampling tube upon hold-up measurement in the 450 mm. diameter column the sampling tube shown in Fig. 9.10b was constructed and used. The results are reproduced in Fig. 9.12. With this tube located as shown, the sample hold ups were generally much higher than those using the stainless steel tube. Two factors may account for the high hold-up values. Firstly the tube was almost in line with the edge of the stator ring, a position of high drop aggregation. Secondly, the high affinity of kerosene towards polypropylene would tend to promote coalescence. Although the stainless steel wire was expected to contribute some affinity towards water, it would be small, due to its relatively small surface area/unit volume, i.e. 1.98 mm^{-1} compared to 7.91 mm^{-1} for the plastic tube. Therefore to

obtain a representative sample requires ideally a sampling tube and tap of material with equal affinity for both phases. Some low surface energy metals exhibit this property (37). However, the feasibility of using these depends on the liquid-liquid system.

In summary the experimentation confirmed that the hold up of the dispersed phase in an R.D.C. varies in both the axial and radial directions. Attempts to measure point or representative compartment hold ups depend on the correct positioning of the sample tube, upon its material of construction, size, and on the flow conditions.

Thus, any error in choosing the correct location, material and size for sampling, a complex, spirally moving, dispersed phase may give highly misleading results. Therefore for practical purposes, even with its limitations (8, 46), the method of measuring average hold up is to be preferred.

11.1.2 Flooding

Two types of flooding were observed; bottom flooding and top flooding, depending upon the method used to approach the flooding condition. Either type of flooding led eventually to the complete rejection of the two phases near to their respective entry points, thus causing 'complete' flooding.

These two types of flooding can be explained on the

basis of the gravitational and buoyancy forces existing under any particular flow condition in the column. If the flooding point is approached by increasing the dispersed phase flow-rate, at constant flow rate of continuous phase and rotor speed, the increased number of drops in a unit cross-sectional area will have increased force in the direction opposite to the flow of continuous phase. Hence, some of it will initially be trapped between the drops and flow out of the dispersed phase outlet at the top, thus flooding the column at the top. The effect is then slowly transmitted throughout the column resulting in 'complete' flooding. The opposite effect occurs when the continuous phase flow-rate is increased slowly at constant flow rate of dispersed phase and rotor speed.

A converse mechanism can also occur depending on the force balances in the column. The increase in flowrate of dispersed phase at the bottom may produce more drops than the column can accept, leading to the drops being rejected at the bottom causing 'bottom' flooding.

The correlation of flooding data, using the characteristic velocity approach, discussed in section 3.2.2, is shown in Fig. 11.1. Excellent straight lines were obtained in the 101 mm. diameter R.D.C. With the large scale column there is some divergence of results, particularly at higher rotor speeds. This is due to increased backmixing of drops at higher rotor speeds, thus giving flooding flowrates

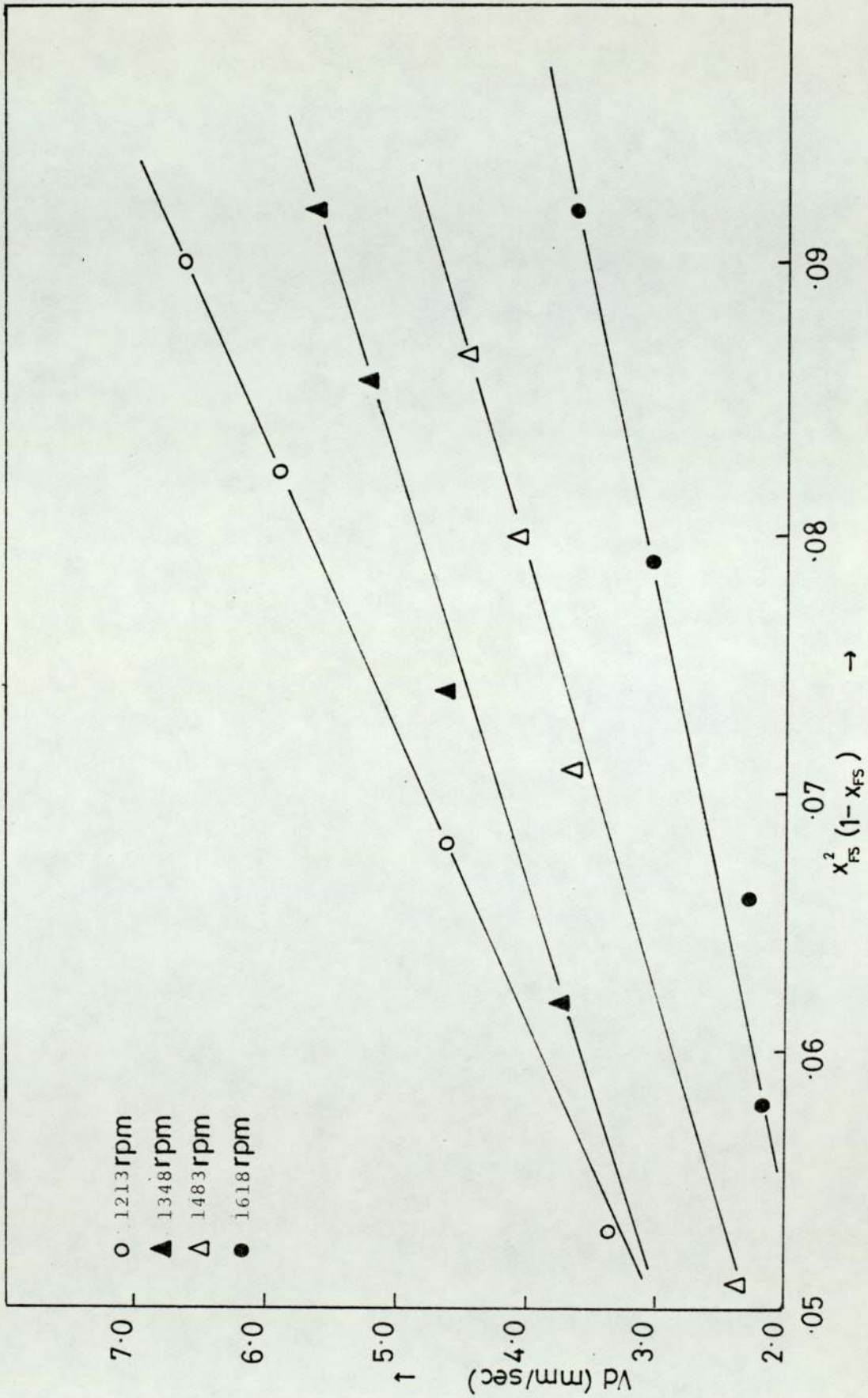


FIG. 11.1 CORRELATION OF FLOODING DATA 101 mm. DIAMETER R.D.C.

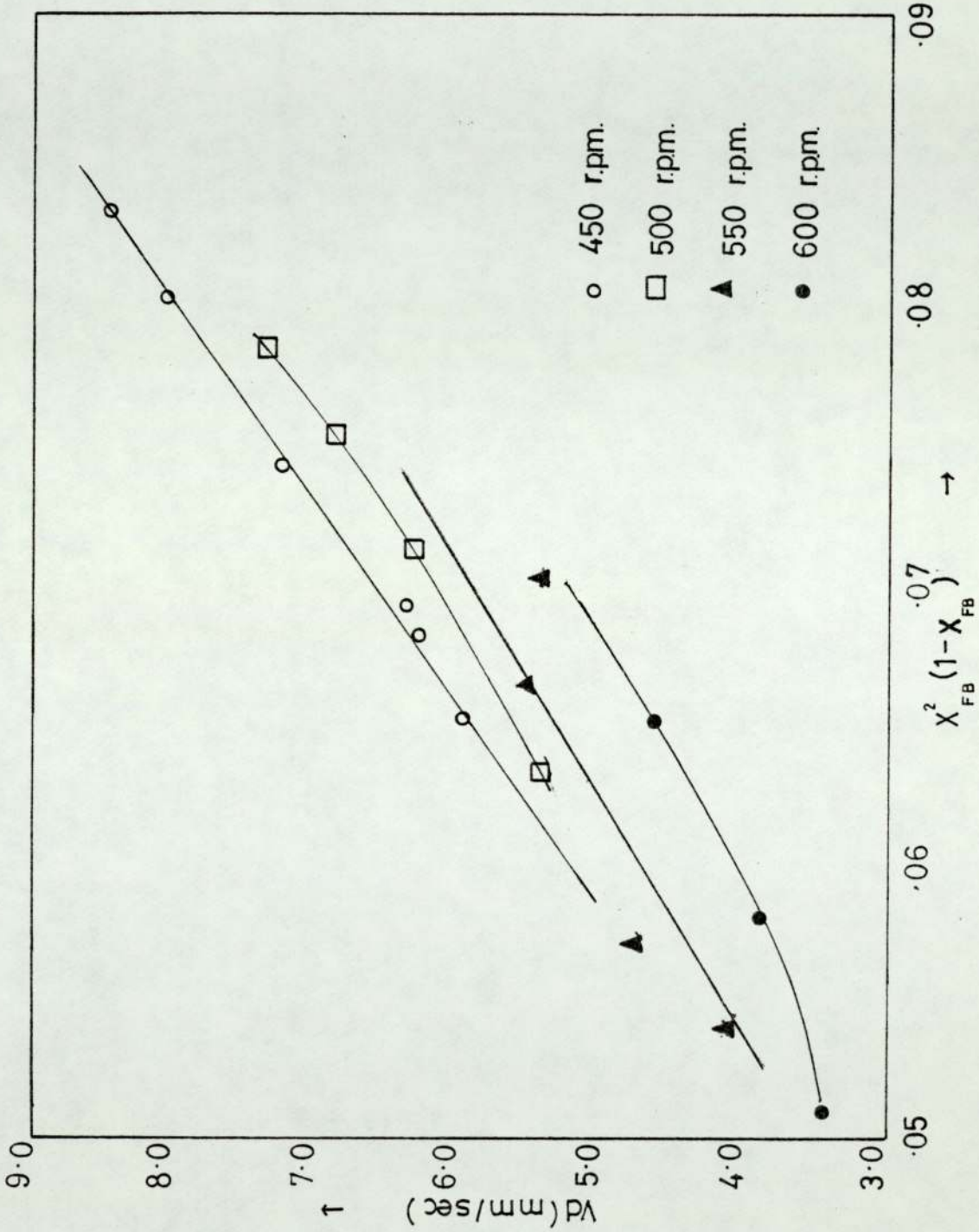


FIG. 11.2 CORRELATION OF FLOODING DATA IN 450 mm DIAMETER R.D.C.

slightly below those anticipated in the absence of back-mixing.

As found earlier in small columns (37,38) flooding was not an instantaneous phenomena in the large column. The time for the column to reach flooding usually depended on the flowrates and rotor speeds; it increased with increase in rotor speed. This may again be due to back-mixing of drops. In fact, it took some time, i.e. 10-20 minutes for enough small drops of 0.1 - 1 mm. size to accumulate in the column to affect normal operation near flooding and eventually flood the column prematurely. Throughout this period the hold up was found to vary as shown in Fig. 10.2 and 10.3. However, equations 3.21 and 3.20 appear satisfactory for calculating hold up at flooding since the values calculated using them usually lay near to the experimental values. Therefore use of equations 3.20 and 3.21 is justified in the prediction of flooding hold ups.

11.1.3 Drop Size

Data for the Sauter mean drop size, as a function of the energy input per unit volume, in the 450 mm. and 101 mm. columns are shown in Fig. 9.5a. In general the drop size increased with any increase in either continuous or dispersed phase velocity. This would be expected since any increase in the velocity of either phase is likely to increase the hold up of the dispersed phase, and thus

enhance drop-drop coalescence (220).

Deviations may be explained by the errors in the method of calculation of Sauter mean drop diameter which is statistical. From Fig. 9.5a, the best correlation of Sauter mean drop data was obtained at an energy per unit volume ($\frac{N^3 R^5}{HD}$) equal to $6.33 \frac{m^2}{sec^3}$. This could be because at that particular energy input, droplet break up is due mainly to the shear force generated by the rotors, and the wall effects are minimal.

To explain the different break up mechanisms in the pilot and industrial scale R.D.C.'s involves consideration of the three parameters involved in drop break-up namely,

- (1) The shear force generated by the rotors,
- (2) The residence time of the drops in the high shear zone beneath the rotors, and
- (3) The velocity of drops in the retarding viscous field in a radial direction and the distance between the swarms of drops travelling in a helical path and the column wall. If the distance is small, the velocity in a radial direction high, and the retarding force low, the wall may have a significant effect on the drop size. Such effects will be termed 'wall effects'.

In an R.D.C. the drop moves away from the rotors towards the column wall in a retarding viscous field. If a drop's energy is absorbed by the counter currently flowing

continuous phase, either it does not reach the wall or it hits the wall below a certain critical speed and rebounds. However, if the drop velocity surpasses the critical speed, then rupture takes place at the column wall. The speed with which the drop is projected from the rotor towards the column wall is a function of the rotor tip speed. At equal energy inputs, in geometrically similar units, the tip speed is different in the two cases, and so is the viscous drag and the distance between the rotating disc and the column wall. In small columns this distance is relatively small and therefore wall effects may be quite significant. Conversely, no drops were observed to rupture at the wall in the large column until a very high rotor speed of the order of 600 r.p.m. was reached. A slightly different drop size can therefore result in two different sized, geometrically similar units, even when they are operated at equal phase velocities and equal energy per unit mass. This was found experimentally, i.e. the drops in the 101 mm. R.D.C. were smaller than in the 450 mm. R.D.C. at comparable rotor speeds. The exception was at energy input of $0.791 \frac{\text{m}^2}{\text{sec}^3}$; this occurred since at this low energy input little break up was due to turbulence and the drop sizes in the column depended on the drop size produced at the distributor.

Generally, when wall effects are negligible droplet break up is due to the combined effect of factors 1 and 2. Therefore, when the combined effect of these two

factors is equal in the two columns, drops of equal sizes will be generated.

Therefore the best correlation of drop size data at an energy input per unit mass of $(\frac{N^3 R^5}{HD^2}) 6.33 \frac{m^2}{sec^3}$ was presumably due to the wall effects being negligible and the combined effect of factor 1 and 2 producing equal drop shearing conditions.

At all rotor speeds in both columns the distribution of drop sizes, throughout the column was usually normal, but sometimes a skewed distribution was present. The width of the distribution generally depended on the rotor speed and was found to be small, i.e. between 2 mm. and 5 mm. at low energy input ($.791 \frac{m^2}{sec^3}$), when turbulent break-up was small and between 1 and 3 mm. at very high ($50.6 \frac{m^2}{sec^3}$) energy inputs.

At intermediate energy inputs, the distribution was fairly wide, i.e. between 1 and 5 mm. This distribution is attributable to the scale of turbulence not being uniform throughout the column cross section and height, but varying with distance in both a radial and an axial direction. At very high energy input the energy distribution throughout the length and width becomes fairly uniform and therefore a small distribution is achieved. The range of drop sizes observed was between 1 mm and 5 mm which is characteristic of those commonly found in an R.D.C. under normal

operating conditions (37, 38). Drops < 1 mm. were not present except at rotor speeds above 600 r.p.m.

The Sauter mean drop sizes were compared with predicted values using the correlations of Misek (10), outlined in chapter 3. Drop sizes were predicted using the appropriate correlations for all three regions; namely laminar (Re No. < 10^4) transition (Re No. < 6×10^4) and turbulent (Re No. > 6.5×10^4). In fact both columns were operated in either the transition or turbulent range but the correlation for laminar conditions was tested to obtain an order of magnitude value. In all cases the predicted drop sizes were less than the actual values by a factor of 3 to 10 times. Moreover, the applicability of these correlations is questionable because they take no account of the dispersed phase hold up and the column height.

The accuracy of the drop size correlation of Al-Hemiri (37) was also tested. Results obtained in the 101 mm. R.D.C. deviated by 30 - 40% from predicted values except at the lowest rotor speed of 404 r.p.m., where the deviation was of the order of 100%. The correlation proved completely unsuitable for the prediction of drop size in the 450 mm. R.D.C. when operated under 'equivalent' conditions as outlined in Table 11.1. This was undoubtedly due to the fact that this correlation was based upon dimensionless Reynolds number and Weber number, whereas the power group $\left(\frac{N^3 R^5}{HD^2}\right)$

TABLE 11.1

450 mm. R.D.C.				101 mm. R.D.C.			
N r.p.m.	Disc Re No.	Tip Speed m/sec	$\frac{N^3 R^5}{HD^2} \frac{m^2}{sec^3}$	N r.p.m.	Disc Re No.	Tip Speed m/sec.	$\frac{N^3 R^5}{HD^2} \frac{m^2}{sec^3}$
150	126322	1.767	0.791	404	17343	1.075	0.791
300	252645	3.534	6.328	808	34686	2.15	6.328
450	378975	5.301	21.36	1213	52030	3.22	21.36
600	505297	7.068	50.625	1616	69373	4.29	50.625

defines the drop size in an R.D.C. more accurately. For example at equal energy per unit volume, $(\frac{N^3 R^5}{HD^2})$, the Reynolds number in the two columns used in this study differed by a factor of 7.27 and predicted drop sizes were found to be 4-5 times less than actual values.

In conclusion, since the prediction of drop size from pilot plant data is an essential factor in scale up, it should, despite the limitations, be based upon equal energy per unit mass in the two units.

11.2 Mass Transfer Studies

11.2.1 Hold-up

As discussed in para. 9.1.3.3 average hold-up was used throughout in the interpretation of mass transfer data. Values of average hold up increased with the increase in either of the phase flowrates and rotor speed. Under

equivalent operating conditions, i.e. equal flowrates and rotor speeds, the values of average hold up under mass transfer conditions were lower than under non-mass transfer conditions. This was in agreement with the observations of drop size, that is with mass transfer taking place from the dispersed phase to the continuous phase, the Sauter mean drop sizes were much larger due to the Marangoni effect, resulting in higher settling velocities and thus lower hold up values. The values obtained with mass transfer taking place were found to be 20-30% lower compared to those in the absence of mass transfer. In a previous study (37) the values reported were sometimes lower by 50%, but this is clearly due to the fact that the concentration levels in this study were generally 5-6% compared to 10% in that work. In addition, the system used in the previous study (37) was toluene-acetone-water for which the interfacial tension variation, and thus the drop size and hold up due to the variation of solute concentration, is different to that of the kerosene-acetone-water system.

11.2.2 Drop Size

As shown in Figs. 9.18 and 9.19 the variation of drop size distribution with column height generally followed a similar pattern despite the different operating conditions and concentrations. This indicates that the average drop size could be defined approximately by evaluating it in a carefully selected compartment.

With mass transfer taking place from the dispersed phase to the continuous phase, the Sauter mean drop size was much greater than under non-mass transfer conditions. This may be attributed to the fact that the presence of acetone during mass transfer runs changes the system properties favourably to produce bigger drops at equal turbulence. Moreover, the transfer of acetone from a kerosene-acetone mixture into water promotes coalescence and this increases the drop size.

11.2.3 Mass Transfer Calculation

The overall mass transfer coefficient was calculated for each experiment using equation 1.1, i.e.

$$N = K a \Delta C_m \quad (1.1)$$

The log mean concentration driving force ΔC_m was calculated from terminal concentrations and the equilibrium data given in Appendix 3. The results are tabulated in Table 9.1 and 9.2.

The rate of mass transfer increased with either phase flowrate as well as rotor speed. To check the reason for this, since the general belief is that increase in rotor speed decreases the mass transfer coefficient thus giving eventually a reduced overall mass transfer rate, the three drop side mass transfer models outlined in Chapter 5 were tested. These calculations revealed that drops as large as 3-6 mm. behaved almost as rigid spheres, that is mass transfer coefficients predicted using the stagnant drop model gave results only 25-50% lower than the experimental values. The deviations from the circulating and oscillating

drop models were of the order of 5 - 10 and 15 to 25 times respectively. Stagnant drop behaviour in this study was probably due to the use of filtered tap water, industrial grade solvents and the scale of operation. The deposition of interfacial scum has been described earlier.

This demonstrates that because of inevitable system 'contaminants' it cannot be assumed that drops oscillate or circulate in an industrial contactor, even though single drop models predict it. The best results as to their behaviour can only be predicted from pilot scale runs with recirculated liquids of the same purity. Furthermore a variable speed agitator is a prerequisite in column design to obtain the flexibility required to overcome the shortcomings in design data.

12. CONCLUSIONS

12.1 General Conclusions

The following general conclusions may be drawn from this work,

1. The 450 mm. diameter column design proved satisfactory for the study of hydrodynamics and mass transfer. Hydrodynamic behaviour was typical of that of an R.D.C. The minimum speed, below which drops became trapped beneath the rotors and stators was 1.77 m/sec. for the 450 mm. and 1.07 m/sec. for the 101 mm. columns. These differ slightly from the published value of 1.52 m/sec. (43).

The main observable differences in behaviour between the large and small columns were as follows.

- (i) There were more 'dead zones' in the 450 mm. diameter column compared with the small one, particularly at low rotor speeds, of the order of 150 to 300 r.p.m. in the large column. The 'dead zones', i.e. zones containing very few or no droplets, in the large column were due to shielded volumes down stream for the rotors and stators which were poorly fed when the rotor speed was low.
- (ii) The large column was less sensitive to fluctuations than the smaller column, which needed more attention during operation. Similarly it was more difficult

to maintain the interface in the smaller column.

This was due to the easier transmittance of disturbance in a short column length, with less volume, compared to a longer length and larger volume.

- (iii) The heights of flocculation and coalescence bands were similar at 'equivalent' operating conditions in the two columns. This suggests that wall effects were not significant in the coalescing section.
- (iv) The time from the onset of flooding to 'complete' flooding was less by a factor of 10 in the small column, compared to the large one. This was due to the extra 'sensitivity' of the small column because of its shorter length. Otherwise, the flooding phenomena in the two glass columns were similar. Identical flooding phenomena, and flooding flowrates would be expected in columns with steel walls provided the organic phase is dispersed. 'Wetting effects' with an organic continuous phase (37) would be less significant in large columns due to the decreased ratio of wall area/flow area.

2. Non-Mass Transfer Studies

- (i) Hold-up - The method of determining point hold-ups, although theoretically preferable, suffers from severe practical limitations. Therefore, in view of uncertainties, average hold-up measurements are adequate for scale-up purposes.

- (ii) Drop Size - No correlations in the literature are appropriate for the prediction of the drop size in both the laboratory scale and industrial scale units. This is because the drop break-up mechanisms differ. The closest agreement in drop size between the two units was under conditions of equal energy per unit mass ($\frac{N^3 R^5}{HD^2}$). The study of drop size in a pilot scale unit thus forms an essential part of any scale up method.
- (iii) Hold-up Profile - Hold-up profiles exist in both the axial and radial directions. However the precise determination of hold-up profiles would require an external technique, e.g. the use of radio active tracers, since the samples withdrawn usually depend on, the material of construction of the sample tube, its position compared with the stator and the rotating discs and its diameter.
- (iv) Scale-up of column diameter can be achieved using equation 10.34, and flooding data obtained on the pilot scale column with the same system, provided the condition of equal energy per unit mass is maintained.
- (v) A first estimate of industrial scale column diameter can be made using equation 10.44 and flooding data obtained on the pilot scale column using a different

system, provided the condition expressed by equation 10.43 is maintained and the interfacial tension and the density difference are not widely different.

3. Mass Transfer Studies

- (i) Both drop size and hold-up are different when mass transfer is occurring compared with non-mass transfer conditions. Therefore data obtained under non-mass transfer conditions must be applied with caution in column design.
- (ii) Limiting Capacity. The limiting capacity of the contactor is also likely to be different under mass transfer since it depends on the drop size in the contactor. However, if the limiting capacity increases with mass transfer in the laboratory scale column, this effect will be repeated on an industrial scale. Therefore the model given for scale up of column diameter based on limiting capacity data, is still applicable. The model can also be used in cases where phase inversion rather than flooding, defines the limiting capacity since the same mathematical treatment has been shown to be applicable (37).
- (iii) The time for the column to reach steady state varied with phase flowrates, concentration of inlet streams and rotor speed. However, it was approximately equal to the time taken for a total displacement of two and a half times the column volume.

(iv) The scale-up of column height is best achieved from a consideration of overall mass transfer coefficient which is independent of the column diameter.

The single drop mass transfer models, derived from results with pure solvents under ideal conditions, cannot be used for the prediction of the overall mass transfer coefficient in an industrial contactor involving swarms of drops containing impurities and surface active agents.

Equal mass transfer coefficients can be achieved in two different scale units with the same system provided equivalence is obtained between the factors affecting the coefficients. As outlined in chapter 5, the overall mass transfer coefficient, in the absence of interfacial resistance, is made up of two resistances, i.e. the continuous phase side resistance and the dispersed phase side resistance. While the dispersed side coefficient depends on the drop size the continuous phase side depends on the characteristic velocity with which the drops rise in a column. In most industrial systems, either of the above two resistances is controlling (57). If the dispersed phase side resistance is controlling then drops of equal size must be generated in the two units to obtain equal mass transfer coefficients. This could be achieved fairly accurately by arranging for equal energy per unit volume ($\frac{N^3 R^5}{HD^2}$) in the two units. Conversely, if the continuous phase resistance is controlling, to obtain equal characteristic

velocities in geometrically similar units requires an equal value of $(\frac{1}{RN^2})$ in the two units. This follows from equation 3.6 by comparing characteristic velocities in two geometrically similar units operating with identical systems. In cases where neither resistance is controlling the numerical value of the power to which rotor speed is raised would lie between 2 and 3. The exact value would however, depend on the relative magnitudes of the two resistances. Equation 10.50 developed in chapter 10 could then be used, provided the relative importance of the resistances is known.

12.2 Recommended Design Procedure

The range of physical properties and conditions for which an R.D.C. may be preferred to other extractor designs were described in chapter 2. Due to its versatility, low cost and ease of operation it may also be preferable as an alternative to packed towers for a low interfacial tension system, with the rotors running below the 'critical' speed.

It is also recommended when solids are present in either phase and where the feed composition may vary, since step changes in the rotor speed provides extra flexibility.

To design an industrial scale R.D.C. for a given system and degree of extraction, it is necessary to evaluate,

- (i) Diameter of the column.
- (ii) Internal geometry of the column.
- (iii) Height of the column, comprising a dispersed phase input/continuous phase de-entrainment section, the agitated section, and a dispersed phase flocculation and coalescence section.

The present study provides a basis for the following recommendations.

12.2.1 Column Diameter

The diameter of an industrial scale R.D.C. can be estimated using equations 10.34, 10.35 and 10.36 developed in chapter 10. This necessitates the performance of limiting capacity experiments using the same system, including any industrial contaminants, in a laboratory scale column. The laboratory column should be designed in such a way that its geometry is within the range given in chapter 3. An infinitely variable drive is preferable and experiments should be performed to cover the range anticipated in the large scale under 'equivalent' operating conditions. For example, the design of distributor for a laboratory column should be based on the mean of expected velocities of dispersed phase in the large column, so that equal size drops will be produced initially. In very large columns the perforated distributor may be omitted but even then some means of coarse dispersion, e.g. multi-inlet pipe, is preferable.

12.2.2 Internal Geometry

Based on the column diameter evaluated from equation 10.34, the internal geometry of a compartment can be determined using the nomograph presented in Fig. 3.6. The best geometry of the R.D.C. for a specific application, however, depends on whether 'high capacity-low efficiency' or 'low capacity - high efficiency' is required. This may depend on whether the system is 'easy' or 'difficult' to extract. If the system is easy to extract then a high capacity low efficiency criteria would be chosen in determining the internal geometry of the column. In this case the ratio of the column dimensions would be, $(\frac{S}{D}) = .75$, $(\frac{R}{D}) = .5$ and $(\frac{H}{D}) = .5$. Conversely for low capacity-high efficiency, the ratios should be approximately, $(\frac{S}{D}) = .66$, $(\frac{R}{D}) = .66$ and $(\frac{H}{D}) = .33$.

12.2.3 Design Procedure for the Distributor

The drop sizes produced from the distributors in the two columns, were close to the values predicted by Treybal's empirical correlation (65). However, the correlation proposed by Meister and Scheele (67) is recommended for general use.

Since the system used in this study, kerosene-water, was similar in physical properties to that studied by Treybal, erroneous results could arise with different systems and Meister and Scheele's correlation is preferable for the reasons outlined in chapter 4.

The rotor had a significant effect on drops produced at the distributor in the 101 mm. R.D.C., where the distance between the distributor and first rotor was only 200 mm. compared with 225 mm. in the 450 mm. column. The distance between distributor and rotor should increase with column diameter to minimise the effect of turbulence from the rotor; as a first estimate the distance should be approximately $D/2$, subject to an upper limit of 1 m.

A free column cross section area as large as possible or in other words a distributor plate as small as possible would be recommended to minimise the effects of continuous phase flow on the drops produced at the distributor. The size of this can then be calculated by keeping the minimum pitch as 1.5 times the expected drop diameter.

Finally, the material of construction must be chosen so that it is not wetted by the dispersed phase and the nozzles should be sharp, upward projected and equi-size. This could be obtained by employing the procedure described in Chapter 8.

12.2.4 Column Height

The total column height required is the sum of three heights, i.e.

$$h = h_{\text{eff}} + h_c + h_s \quad (12.1)$$

The effective height of the column, h_{eff} , can be calculated using equation 10.50 developed in Chapter 10,

based upon results for overall mass transfer coefficients in pilot scale experiments.

Assuming phase separation occurs within the column, the height of the flocculation and coalescence zone in a large column should confirm approximately to that in a laboratory scale column operated under 'equivalent' conditions with the same system. However, to predict the height more accurately the correlations of Hittit (96) may be used. Some deviations may occur if different materials of construction are used for the column walls. Normally for industrial sized columns one to two compartment heights should be adequate depending on the system properties; a reduction in height may be achieved by the use of coalescing aids.

Alternatively an external settler may be used. This may be sized according to the normal procedure for horizontal mixer settlers (221). Again a decrease in size may be obtained with knitted mesh coalescer aids (222).

The height of the bottom disengagement section can be found by analysing the drop size distribution in the pilot scale and evaluating the drop settling velocity for the last 5% or 1% of the bottom end of the drop size distribution data.

Since the drop size in the industrial unit would be slightly higher than that in the pilot scale units the values that will be obtained for h_c and h_s will be slightly

higher than required.

The distributor plate in an industrial unit should be approximately $D/2$ distance away from the bottom rotor. This is however, subject to a maximum distance of 1 m.

12.2.5 Miscellaneous Design Features

In addition to the above the following design features require consideration,

(i) Selection of Suitable Motor

The procedure proposed by Reman (31) and summarised in Chapter 3 is preferred to that of Misek (10) to predict motor power, since it is based on the results obtained in an industrial scale R.D.C. It therefore includes the loss of power due to bearings and friction. It is likely to give slightly higher values than required, which is preferable. On new applications the motor speed should be variable. However, this will be expensive for an industrial R.D.C., therefore provision can usefully be made for a step-wise variation within $\pm 15\%$ of the design speeds.

Only if significant fluctuations may occur in the composition of the feed or the phase flowrate should provision for speed variation be necessary over and above this allowance.

(ii) Bearing and Seal Arrangements

The use of bearings is generally limited in small laboratory columns to avoid extraneous hydrodynamic effects.

For industrial units a thrust and a self-aligning, self-lubricating bearing or a roller bearing may be used at the top, out of contact with liquids. P.T.F.E. bushes in bearing brackets may be used inside the column.

For minimum cost it is preferable to avoid a seal at the top of the column. In columns operated at atmospheric pressure, this is usually achieved by locating the light phase outlet well below the top of the column thus leaving a vapour space. However, such an arrangement is not adequate when,

- (a) The total flow into the column exceeds the total outflow. This can be avoided by increasing the size of the phase outlets, which should in any case be larger than the inlets; consideration must be given to the change in the phase flowrates due to mass transfer.
- (b) When the liquids used are highly volatile and the extraction is carried out at temperatures generating excessive vapour.
- (c) When the column is operated at high pressure.

In the last two cases a mechanical seal is required.

(iii) Shaft Diameter

The shaft diameter should be kept to a minimum in case of laboratory units, to avoid any extraneous hydrodynamic effects. In industrial units the shaft diameter

depends on the diameter and weight of discs and the overall unsupported length will also be kept to a minimum to conserve column volume and to avoid the column behaving as a rotary annular contactor.

(iv) Coalescing Aids

With difficult coalescing systems a knitted mesh pad may be inserted above (or below) the agitated zone. This will also serve to isolate the coalescence zone from the turbulence in the agitated section in the column.

(v) Size of the Reservoirs

For an experimental column of whatever size, the minimum volume of the reservoirs should be approximately three times the column volume. In an industrial process the extract and raffinate reservoirs or surge drums, could be calculated by first estimating the time to reach steady state, using the computer program developed and given in Appendix 4, and then finding the volumes. Material produced in this unsteady state period will differ from that during normal continuous operation.

Finally a slight over design is recommended in the case of an industrial unit, since accumulation of impurities over a period of time may change the wetting characteristics of the column, thus giving lower efficiencies.

RECOMMENDATIONS FOR THE FUTURE WORK

Several interesting areas for further research arose as a result of this study. For some of these phenomena only qualitative, or limited quantitative data, were obtained, and more detailed studies appear worthwhile.

The following is recommended:

- (1) The mathematical model developed to predict the column diameter was tested only for a system for which flooding defined the limiting capacity. It would be useful to test the model with other systems for which phase inversion instead of flooding defines the limiting capacity. Based on the observations of Sarkar (38) and Al-Hemiri (37) on a laboratory scale, practical systems would be butyl acetate-water and toluene-water. There would however be safety and economic constraints upon their use.
- (2) The mathematical model for the prediction of column diameter was only tested for non-mass transfer conditions. The limiting capacity of an R.D.C. would be expected to change with the extent and direction of mass transfer. Whilst this change would be expected to be of equal magnitude in laboratory and industrial extractors, it would be of interest to check how accurately the model applies for extractions involving different systems, e.g. where coalescence is enhanced/retarded, interfacial tension

raised/lowered by solute transfer.

- (3) The theory presented for the difference between drop break up in the large scale and laboratory scale contactors was based upon visual observations and examination of the cine film described in Appendix 1. Further quantification taking into account wall effects in laboratory scale columns, is necessary for the accurate prediction of drop sizes in an industrial unit from data obtained in a laboratory scale.
- (4) Extensive experimentation is required to test further the validity of the model for the scale up of agitated column section height, and the associated theory. This experimentation should involve various systems, namely,
 - (i) One for which the drop side resistance is controlling. A possible system would be toluene acetone-water with mass transfer taking place from the dispersed to the continuous phase.
 - (ii) One for which the continuous phase side resistance is controlling. The system which would meet this requirement is sod. iodide water-isobutanol.
 - (iii) One for which both resistances have equal importance.

Since differing effects are associated with the direction of transfer, as discussed in Chapter 10,

it would be interesting to see which model for scale-up of height would fit with reversal of direction of transfer.

APPENDIX 1

Description of Cine Film

System: Kerosene (dispersed) - water-(continuous)
450 mm. diameter column.

1st Sequence

The column is operating with an agitator speed of 150 r.p.m. generating a hold-up of 5.2%.

2nd Sequence

This follows the first sequence with the rotor speed increased to 300 r.p.m. Droplet break up at this speed is mainly due to the turbulence created by the rotor. Poor mixing is evident, at this rotor speed.

3rd Sequence

The rotor speed is 450 r.p.m. The break up is still mainly due to agitation by the rotor. Although the drops travel as far as the column wall the extent of the rupture at the wall is minimal.

4th Sequence

The column is operating at 600 r.p.m. Break up is due to both agitation of the rotor and impact on the column wall.

APPENDIX 2

SYSTEM PROPERTIES

Kerosene - purchased as the industrial grade with the following properties,

Density 0.7825 gm/c.c.

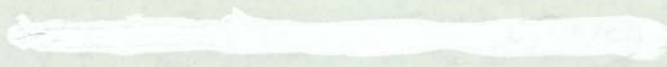
at 20° C

B.Pt. 195° C

Flash Pt. 70° C

Kinematic Viscosity 2.3 cs

Refractive Index. 1.4373 at 20° C



The interfacial tension with filtered tap water as determined in the laboratory using a torsion balance was 35.7 dyne/cm at 20°C.

TABLE 1
SYSTEM PURITY CHECKS

Date	Column size mm	Density gm/cc	Kinematic Viscosity cs	Interfacial Tension dynes/cm
14.5.76	450	.7825	2.3	35.7
10.8.76	450	.78	2.3	35.7
10.8.76	101	.74	2.35	36.0
8.11.76	450	.7850	2.4	35.9
8.11.76	101	.7820	2.38	35.8
5.1. 77	450	.7815	2.3	35.7
5.1. 77	101	.7815	2.3	36.8

APPENDIX 3

CONTENTS

- Fig. 1 Concentration vs Absorbance for
Kerosene-Acetone Solution.
- Fig. 2a,b Concentration vs Absorbance for Water-
Acetone Solution.
- Fig. 3 Equilibrium Diagram for Kerosene Acetone-
Water System.
- Fig. 4 Density vs Concentration of Acetone in
Kerosene.
- Fig. 5 Viscosity vs Concentration of Acetone in
Kerosene.

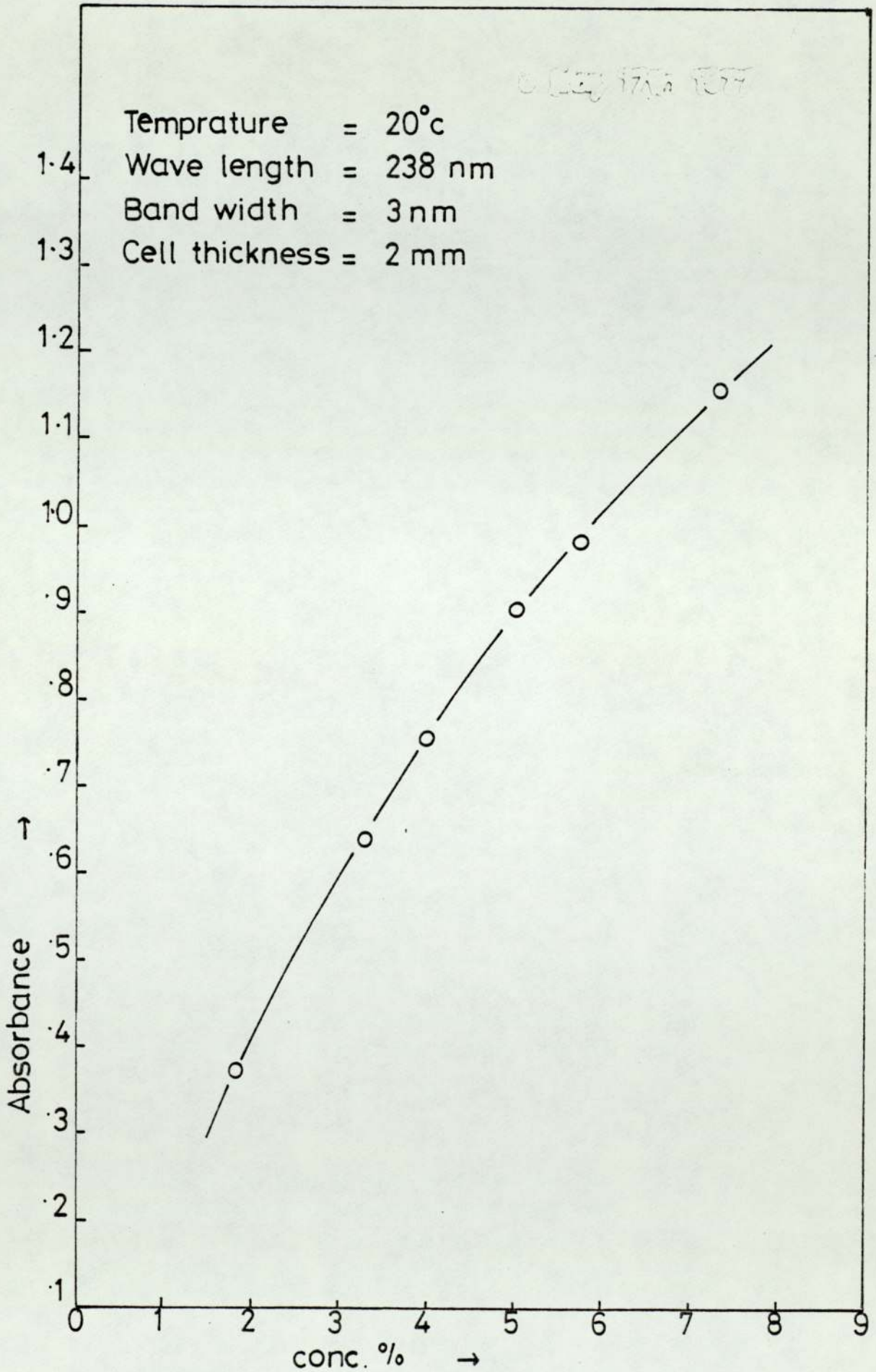


FIG. 1

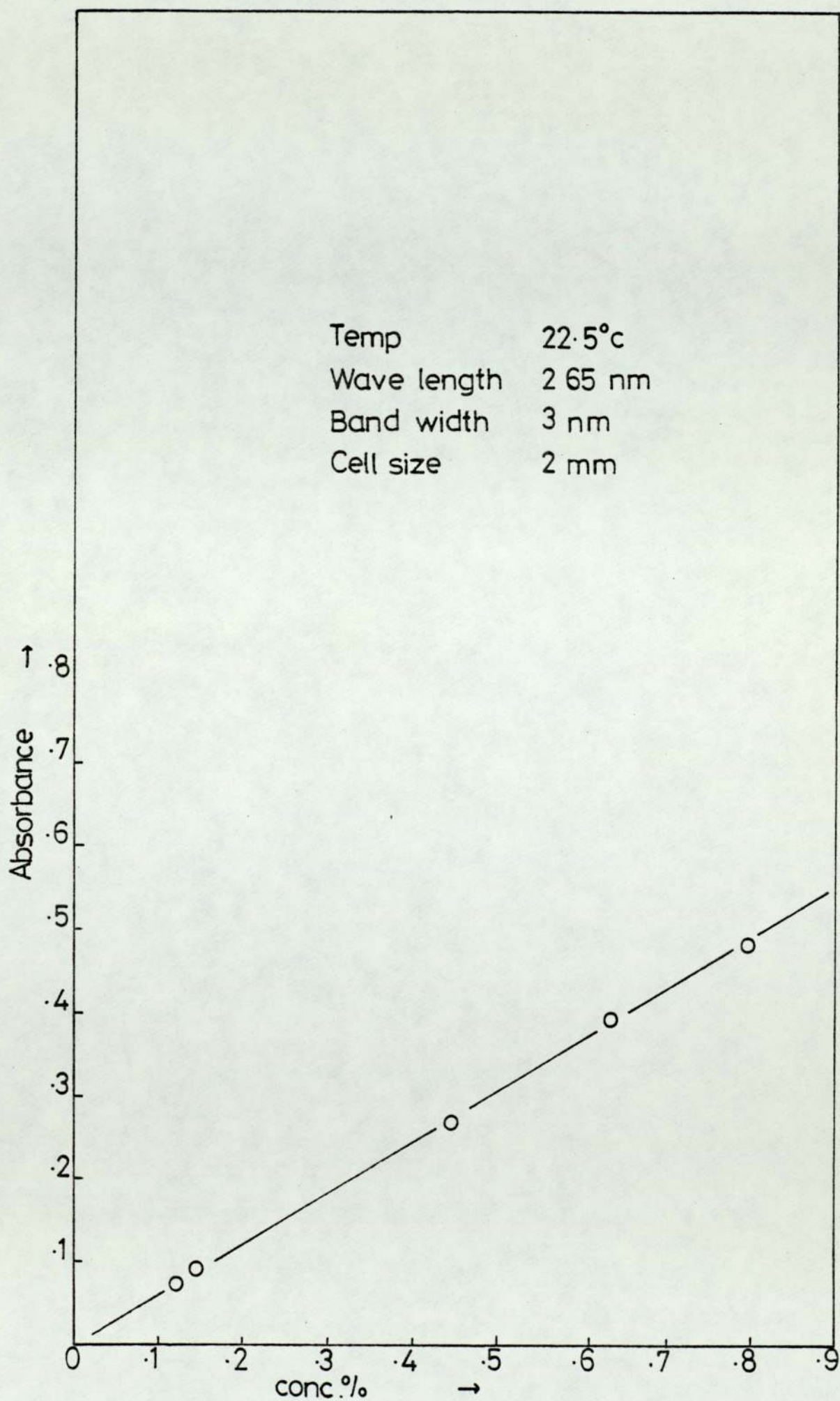


FIG. 2a

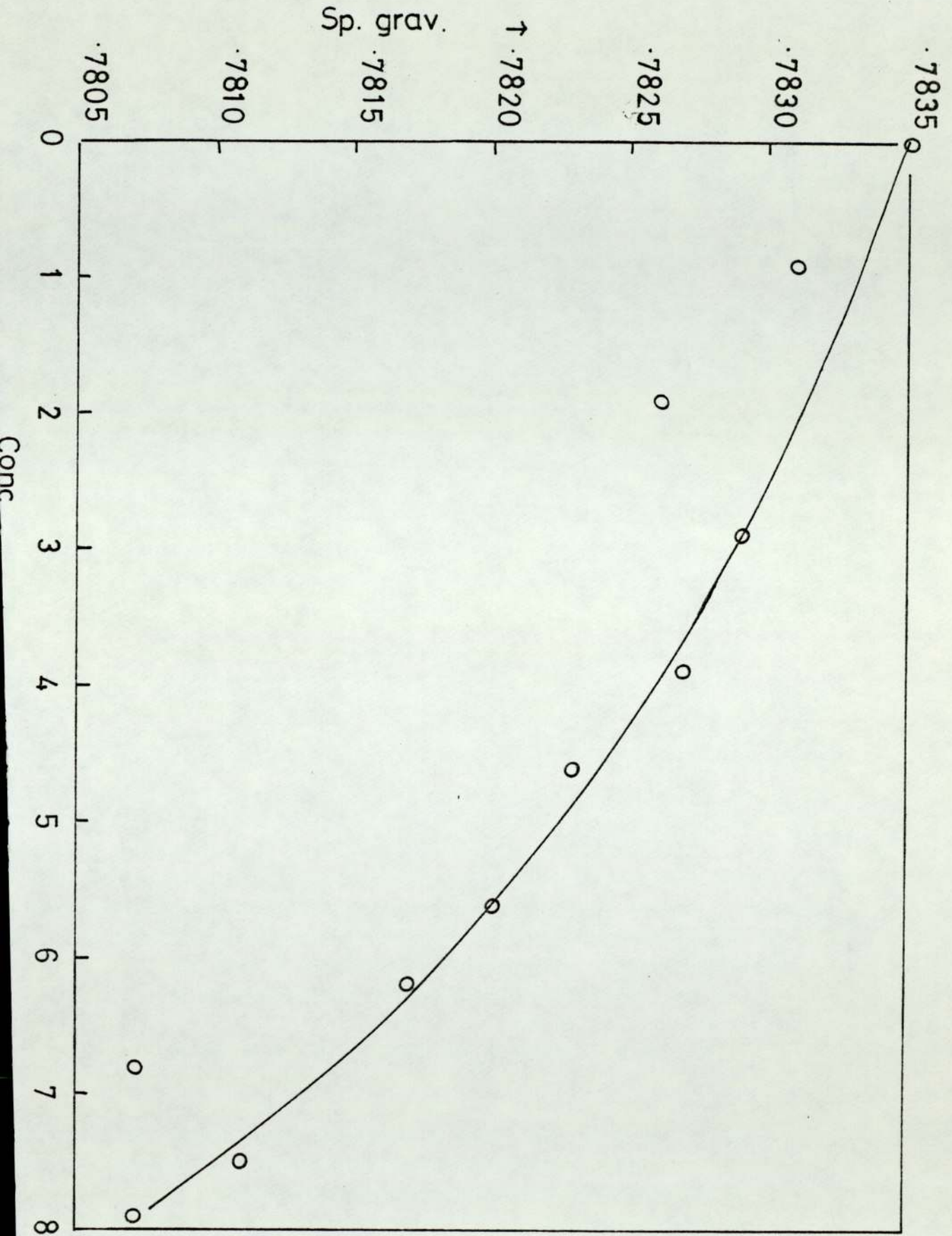


FIG. 4.

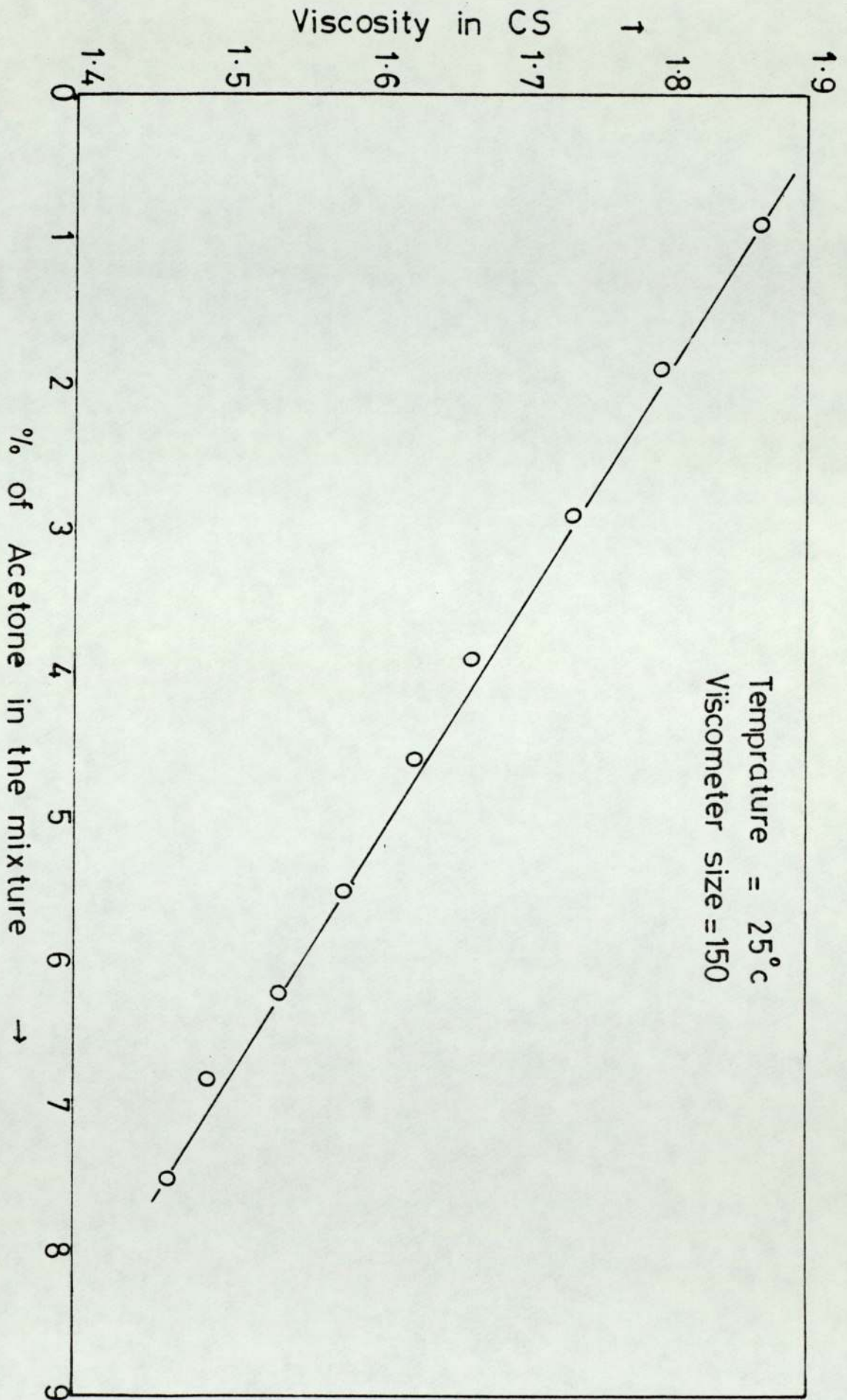


FIG. 5

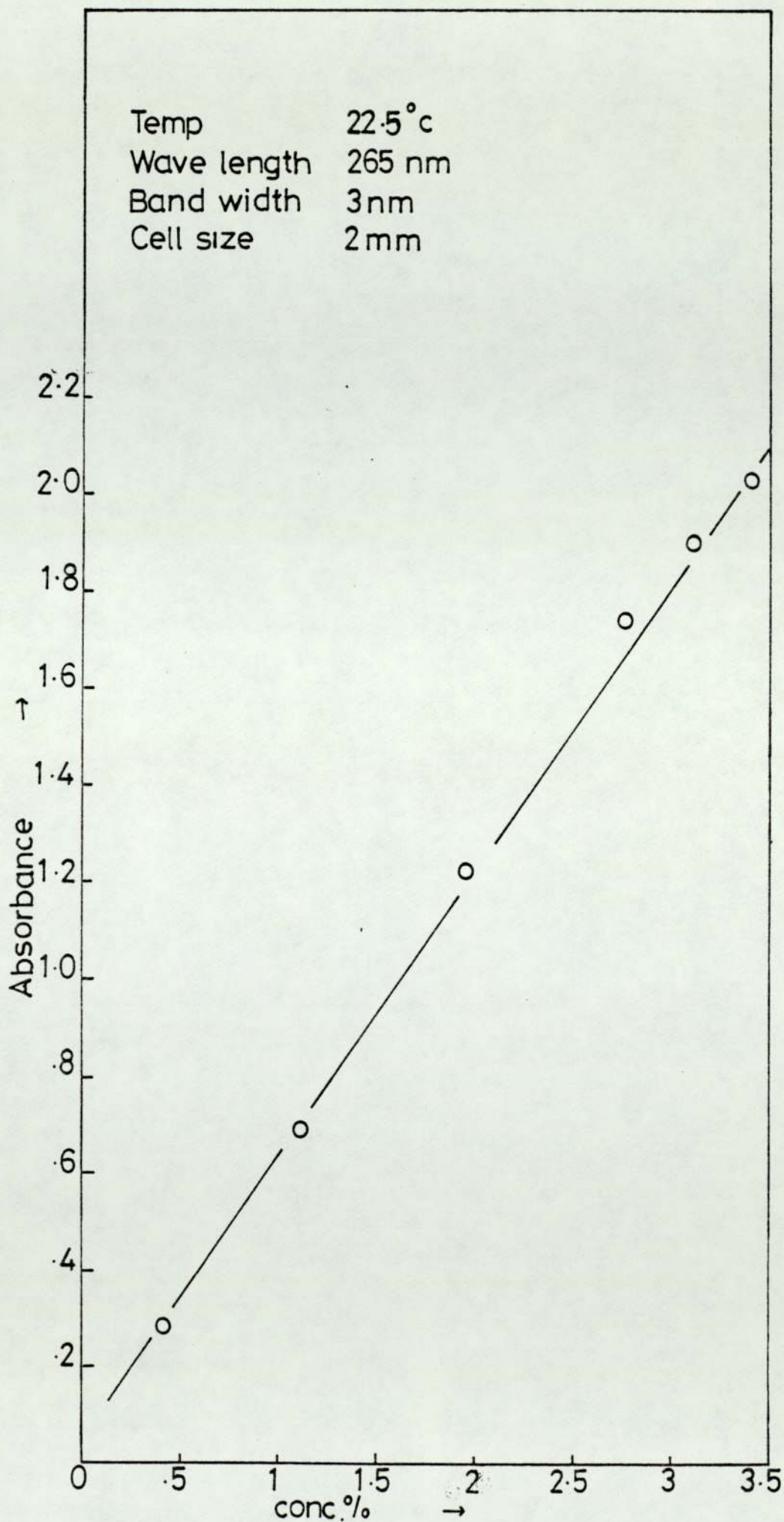


FIG. 2b

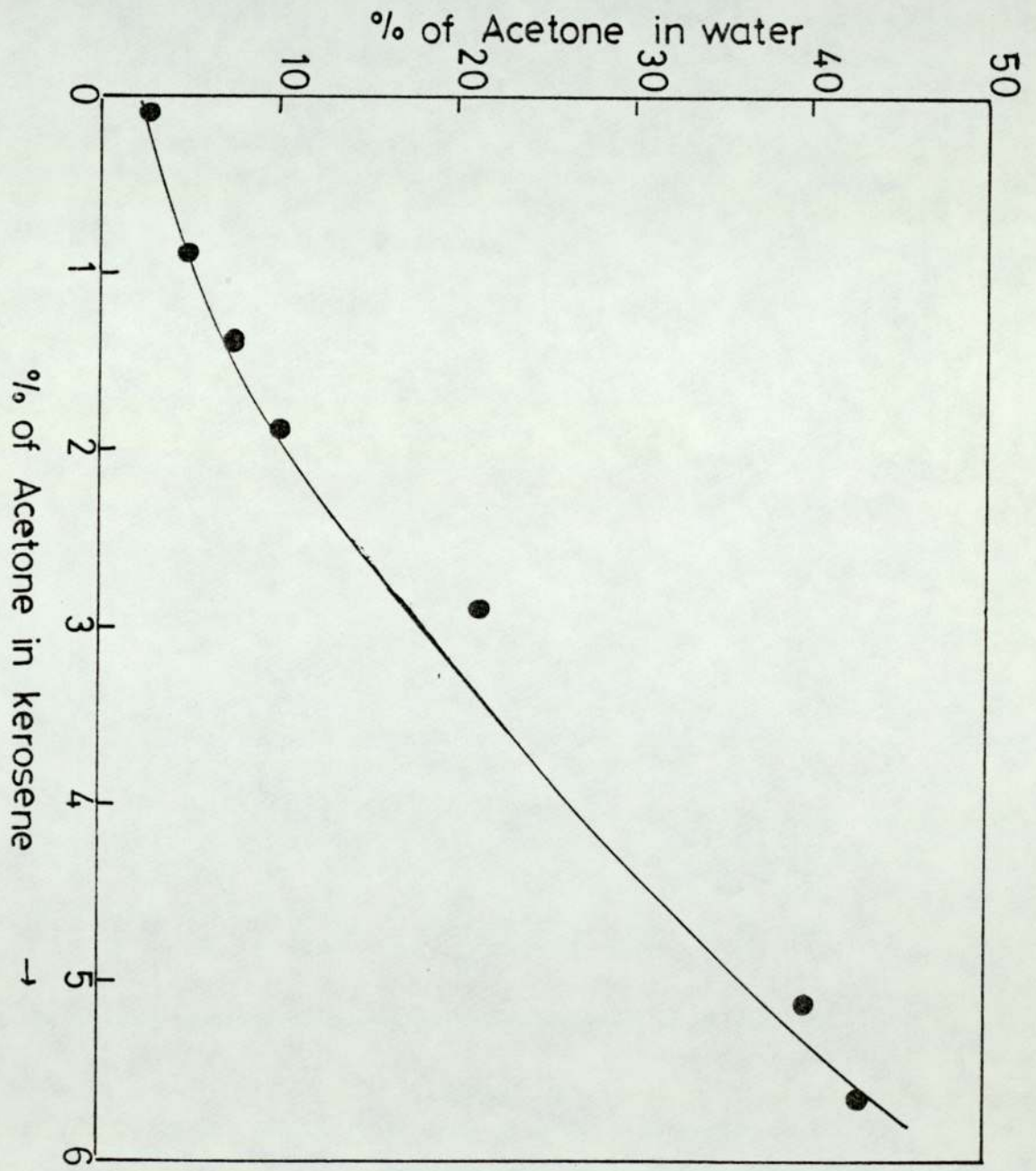


FIG. 3

APPENDIX 4

Computer programs for,

1. Calculation of drop size d_{32} .
2. Estimation for time to reach steady state.

The Sauter mean drop size was calculated using program 1.

PROGRAM 1

1. MASTER
2. REAL MF, ND1, ND2, ND3
3. INTEGER K, I
C MAGNEFING FACTER, MF
4. 5 READ (1,200) I, B, K, MF
5. 200 FORMAT(15, F5, 0, 15, F10, 3)
6. WRITE(2, 201) I, 8
7. 201 FORMAT(1H1, 5X, 'SERIALNO= ', 15, 5X, 'PHOT, NO= ', F5, 0)
8. WRITE(2, 111)
9. 111 FORMAT(1H0, 36X, 'SAUTER MEAN DIAMETER AND ST.DEVIATION
CALCULATION' 1)
10. WRITE(2, 112)
11. 112 FORMAT(24X, 'DM', 8X, 'D', 9X, 'N', 9X, 'D2', 8X, 'D3', 7X,
'Nd1', 7X, 'Nd2', 17X, 'ND3')
12. SUMD=0
13. SUMN=0
14. SUMND1=0
15. SUMND2=0
16. SUMND3=0


```
C  DROP MEAN DIAMETER, DM
C  NUMBER OF DROP, N
17.  DO 20J=1,K
18.  READ(1,114)DM,F
19. 114 FORMAT(F10,2,F10,0)
20.  D=DM/MF
21.  D2=D**2
22.  D3=D**3
23.  ND1=F*D
24.  ND2=F*D2
25.  ND3=F*D3
26.  SUMD=SUMD+F
27.  SUMN=SUMN+F
28.  SUMND1=SUMND1+ND1
29.  SUMND2=SUMND2+ND2
30.  SUMND3=SUMND3+ND3
31. 20 WRITE(2,115)DM,D,F,D2,D3,ND1,ND2,ND3
32. 115 FORMAT(22X,F5.2,3X,F9.5,4X,F3.0,4X,F9.5,1X,F8.4,
      2X,F9.4,2X,F9.4,11X,F9.4)
33.  GO TO 21
34. 21 WRITE(2,116)
35. 116,FORMAT(30X,'-----',4X,'----',24X,'-----',
      1X,'-----',2X1,'-----')
36.  WRITE(2,117)SUMD,SUMN,SUMND1,SUMND2,SUMND3
37. 117 FORMAT(30X,F9.5,3X,F4.0,22X,F9.4,2X,F9.4,1X,F9.4)
38.  WRITE(2,116)
```

```

C ARITHMETIC MEAN DIAMETER, AMD
C SAUTER MEAN DIAMETER ,SMD
C ST.DEVIATION ,SD
39. AMD=SUMND1/SUMN
40. SMD=SUMND3/SUMND2
41. SD=SQRT((SUMND2-(SUMN*AMD**2))/(SUMN-1))
42. WRITE(2,118)AMD
43. 118 FORMAT(20X,'ARITHMETIC MEAN DIA= ',F10.5)
44. WRITE(2,119)SMD
45. 119 FORMAT(20X,'SAUTER MEAN DIA= ',F10.5)
46. WRITE(2,120)SD
47. 120 FORMAT(20X,'STD.DEV= ',F10.6)
48. 1F(I-77)25,26,26
49. I=I+1
50. 25 GO TO 5
51. 26 STOP
52. END

1. FINISH

```

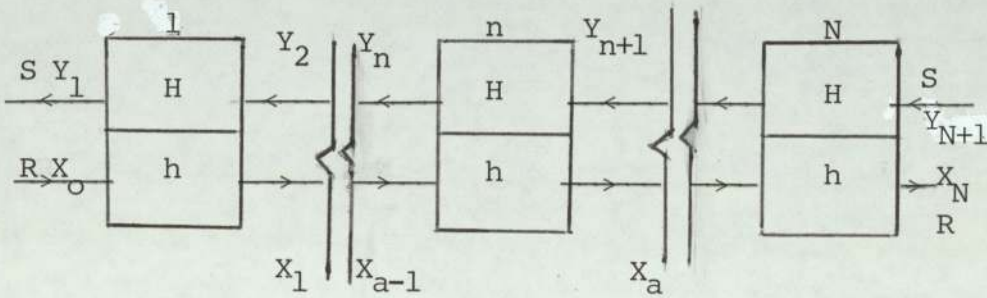
PRINT OUT SERIAL NO= 68 PHOT.NO= *14009

SAUTER MEAN DIAMETER AND ST. DEVIATION CALCULATION

DM	D	N	D2	D3	ND1	ND2	ND3
1.49	1.56842	77.	2.45994	3.8582	120.7684	189.4157	297.0836
2.04	2.14737	55.	4.61119	9.9019	118.1053	253.6155	544.6059
2.59	2.72632	63.	7.43280	20.2642	171.7579	468.2663	1276.6417
3.14	3.30526	56.	10.92476	36.1092	185.0947	611.7868	2022.1164
3.70	3.89474	26.	15.16898	59.0792	101.2632	394.3934	1536.0583
4.25	4.47368	15.	20.01385	89.5356	67.1053	300.2078	1343.0347
4.80	5.05263	3.	25.52909	128.9891	15.1579	76.5873	386.9672
5.35	5.63158	5.	31.71468	178.6037	28.1579	158.5734	893.0187
6.46	6.0000	1.	46.24000	314.4320	6.8000	46.2400	314.4320
	<u>35.60000</u>	<u>301.</u>			<u>814.2105</u>	<u>2499.0861</u>	<u>6813.9586</u>

ARITHMETIC MEAN DIA= 2.70502
 SAUTER MEAN DIA= 3.44684
 STD.DEV= 0.994370

Program 2, written for the determination of time to reach steady state was based on the following mathematical model (216)



Stage Wise Counter Flow System

- Let R Flowrate of continuous phase
- S Flowrate of dispersed phase
- N Total number of stages
- x_n Solute conc. in the continuous phase nth stage
- y_n Solute conc. in the dispersed phase nth stage
- m Distribution ratio
- h Hold-up of dispersed phase per stage
- H Hold-up of continuous phase per stage
- X'_0 Original feed concentration
- X_F New feed concentration.

A solute balance over nth stage gives,

$$R X_{n-1} + S Y_{n+1} - R X_n - S Y_n = h \frac{dx_n}{dt} + H \frac{dy_n}{dt} \quad (1)$$

Assuming equilibrium relationship is,

$$Y_n = mX_n \quad (2)$$

Eliminating Y_n, Y_{n+1} between equation 1 and 2 and rearranging,

$$\alpha X_{n+1} - (\alpha + 1)X_n + X_{n-1} = \beta \frac{dX_n}{dt} \quad (3)$$

$$\text{where } \alpha = mS/R \text{ and } \beta = (h + mH)/R \quad (4)$$

Equation 3 on solving yields,

$$X_n = X_F \left| \frac{\alpha^{N+1-n} - 1}{\alpha^{N+1} - 1} \right| + (X_F - X'_O) \sum \frac{2(-1)^k \alpha^{-(n-1)/2} \text{Sin} \theta \text{Sin} (N+1-n) \theta e^{st}}{(N+1) (\alpha + 1 - 2\sqrt{\alpha} \text{Cos} \theta)} \quad (5)$$

$$\text{where } s = \frac{-\alpha + 1 - 2\sqrt{\alpha} \text{Cos} |k\pi / (N+1)|}{\beta} \quad (6)$$

PROGRAM 2

1. MASTER
- C PROGRAM TO FIND STEADY STATE
2. READ(1,50) DISCOF, S1, R, H1, H2, YF, YO, N1, N2
3. ALPHA=DISCOF*S1/R
4. BETA=(H1+DISCOF*H2)/R
5. B=((ALPHA**(N2+1-N1))-1)/((ALPHA**(N2+1))-1)
6. T=0.0
7. YC=0.0
8. 5 K=1

```
9.    SS=0
10.10 THETA=(K*180)/(N2+1)
11.    S=- (ALPHA+1-2*(SQRT(ALPHA)) *COS (THETA)) /BETA
12.    A=((2*((-1)**K) * (ALPHA**((-N1-1)/2)) *SIN (THETA) *
      CSIN((N2+1-N1)*THETA)) *EXP
      C(S*T))/((N2+1)*(ALPHA+1)-(2*(SQRT(ALPHA)) *COS (THETA)))
13.    SS=SS+A
14.    K=K+1
15.    IF(K.LE.N2) GO TO 10
16.20 YN=YF*B+(YF-YO)*SS
17.40 WRITE(2,60)T,YN
18.    T=T+0.08333
19.    IF(T.LE.11.0) GO TO 30
20.    IF(ABS(YN-YC).LE..0001)GO TO 90
21.30 YC=YN
22.    GO TO 5
23.50 FORMAT(7F0.0,2I0)
24.60 FORMAT(1X,E8.4,E12.5)
25.90 STOP
26.    END
      FINISH
```

PRINT OUT FOR PROGRAM 2

<u>TIME HOUR</u>	<u>CONC. OF THE ACETONE IN THE EXTRACT PHASE AT THE OUTLET</u>
0 (0 min)	.59524E-02
.0333 (2 min)	.13201E-01
.0666 (4 min)	.15495E-01
.0999 (6 min)	.16222E-01
.1333 (8 min)	.16452E-01
.1667 (10 min)	.16525E-01
.200 (12 min)	.16548E-01
.2333 (14 min)	.16555E-01
.2666 (16 min)	.16557E-01
.300 (18 min)	.16558E-01
.333 (20 min)	.16558E-01
.3666 (22 min)	.16557E-01
.400 (24 min)	.16559E-01

DATA 5.26 ∇ 6607.9295 ∇ 3180.79 ∇ 1199.8303
∇ 32.8941 ∇ 0.1975 ∇ 0.0 ∇ 1 ∇ 1

APPENDIX 5

COLUMN OPERATING PROCEDURE

The column was first filled with continuous phase by operating valve V3 and switching on pump No. P1. When the column was full of continuous phase valves V8 and V7 were opened slowly to maintain the level of continuous phase in the column. The agitator motor was then started and the speed adjusted using the infinite gear box on the motor to give the appropriate tachometer reading. The dispersed phase was then slowly allowed to enter into the column through the distributor by opening valves V18, V17, and V11, and starting pump P2. During this period careful control was necessary over valves V8, V4 and V5, to maintain the interface level in the column. The reverse procedure was followed when shutting down the column.

A similar procedure was used for start-up and shut-down off the 101 mm. diameter column.

NOMENCLATURE

A, a	Interfacial area, constant
A_R	Surface area of the rest drop
a_o	Initial radius
a_p	Amplitude
B	Proportionality constant
ΔC	Concentration driving force
ΔC_m	Log mean concentration driving force
C	Constant
C, c	Solute concentration
C_{Rav}	$(C_{RM_1} + C_{RM_2})/2$, where C refers to total concentration of all substances present
D	Column diameter, disc diameter, drop size, diameter of agitator, diffusion coefficient
D_i	Stator diameter
D_k	Column diameter
D_c	Contactore diameter
D_E	Equivalent diffusivity
D_N	Nozzle diameter
D_T	Tower diameter
d_{vs}	Average surface volume drop diameter
d_o, d	Drop size
d_{32}	Sauter mean drop diameter
d_{12}	Hydraulic mean drop diameter
d_m	Maximum stable drop size
d_{95}	Drop diameter below which 95% of drop exist
d_5	Drop diameter below which 5% of drop exist

d_{50}	Drop diameter below which 50% of drop exist
d_p	Diameter of a sphere of volume equal to that of a drop
E	Extract phase flowrate, energy of dissipation per unit mass, dispersion coefficient, eddy diffusivity
E_F	Efficiency during the drop formation
e	Dispersion coefficient
F	Constant in Equation 5.1, Harkins and Brown correction factor
F_B	Continuous phase axial diffusivity
F_C	Average liquid velocity
Fr	Froude number
f_i	Fraction of hold-up of ith fraction
G	Mass flowrate
g	Acceleration due to gravity
H, h_c	Height of contactor, height of coalescence section, effective column height
H_s	Height equivalent of theoretical stage
H, H.T.U.	Height of transfer unit
H_{tor}	Height of transfer unit
H, h_c, h_m	Height of compartment
hs	Height of settling section
I	Intercept on the ϕ axis
i	ith stage
K	Overall mass transfer coefficient
K_1	Constant in Equation 3.7
K_{df}	Mass transfer coefficient during formation

K_{dc}	Mass transfer during coalescence
K_{HB}	Mass transfer coefficient calculated by means of Handlos and Baron
K_B	Constant in Equation 10.9a for large column
K_S	Constant in Equation 10.9b for small column
k	Individual mass transfer coefficient
L	Column height, micro scale of turbulence
m	Equilibrium constant, mass of the drop
N	Moles per unit time, rate of mass transfer, r.p.m.
N.T.U.	Number of transfer unit
N_p	Power number
N_{Pe}	Peclet number
N_{Vi}	Viscosity group
N_{Pe}	Modified Peclet number
N_{Sh}	Sherwood number = kdp/D for drops
N_{tor}	Number of transfer unit
n	Compartment number
P	Power
ΔP	Pressure drop
Pe	Peclet number
Q, q	Volumetric flowrate
Q_o	Initial solute concentration
Q_t	Concentration at time t
R	Disc diameter, radius of capillary, raffinate phase flowrate
ΔR	Distance between agitator and column wall, equal to $(D-R)/2$
Re	Reynolds number

r	drop radius
s	Stator opening
Sc	Schmidt number ($\mu/\rho D_d$)
S_{drc}	Solute transferred per drop
T	Number of transfer unit
t	Time variable during the rise period
t_{coal}	Time taken for coalescence
t_F	Time of formation
U	Superficial velocity, sphere velocity in tower diameter D_T
\bar{U}_O	Characteristic velocity
U_{CD}	Sphere velocity in an infinite space
$(U_O)_{ST}$	Stroke settling velocity
V	Superficial velocity, drop volume
\bar{V}_N	Characteristic velocity, i.e. the mean vertical drop velocity at substantially zero flowrates and rotor speed N .
V_{rl}	Volume added during the release
V_t	Drop terminal velocity
V_F	Drop volume after break off from the nozzle
V_{dr}	Volume of released drop
v	Coalescence frequency
We	Weber number
w^*	Critical approach velocity
w	Oscillation frequency
X, x	Dispersed phase hold up phase concentration
x	Distance
x_i	Hold-up at phase inversion

$$(1-x_R)_{om} = |(1-x_R^*) - (1-x_R)| / \ln |(1-x_R^*) / (1-x_R)|$$

- Y,y Y phase concentration
Z Coalescence coefficient

GREEK LETTERS

- α Major axis of an oscillating drop, velocity
 exponent, back flowrates
 β Minor axis of an oscillating drop
 γ Surface tension, kinematic viscosity, interfacial
 tension
 ϵ Extraction factor, amplitude of oscillation, energy,
 fraction of uncontracted solute
 ϵ_o $\epsilon + (3/\delta)\epsilon^2$
 η Kolmogoroffs length
 θ Time
 λ Eigen value, constant
 μ Viscosity
 ρ Density
 $\Delta\rho$ Density difference
 σ Interfacial tension
 τ Dimensionless time
 ν Kinematic viscosity
 ϕ Hold-up
 ψ A function

SUBSCRIPTS

- A Refers to phase A
Av Average
B,b Big or large
c,C Continuous, coalescence column

$C_{D,c}$	Circulating drop
C'	Capillary
Crit	Critical
d,D	Dispersed
e,E	Extract, efficiency
exp.	Experimental
F	Formation, flooding
f	Flooding, final feed, formation
i	Initial, inside, Ith stage, interface
k	Kinetic
m	Mean
Min.	Minimum
Max.	Maximum
N	Nozzle
n	nth stage
O	Out, outside
O.C.	Overall values with respect to continuous phase
O.F.	Overall values with respect to feed phase
O.m.	Overall mean
P	Plug flow
R	Raffinate
RL,R	Release
S	Solute, solvent, stagnant, slip, small,
SD,S	Stagnant drop, static, small
T	Top
x	Refers to X-phase
Y	Refers to Y-phase
O	Refers to conditions at zero hold-up

- 1 That end of the column where solutions are concentrated
- 2 That end of the column where solutions are dilute

SUPERSCRIPTS

- 0 Initial
- * At equilibrium

REFERENCES

1. Coleby, R., Chap. 4, 'Recent Advances in Liquid Liquid Extraction', Edited by Hanson, C., Pergamon Press, Oxford (1971).
2. British Patent 993, 394.
3. Blumberg, R., et al., Chap. 3, 'Recent Advances in Liquid Liquid Extraction'. Ed. by Hanson, C., Pergamon Press, Oxford (1971).
4. Newman, A.B., Trans. Am. Inst. Chem. Engrs., 27, 127 (1957).
5. Kronig, R. and J.C. Brink, Appl. Scient. Res., A2, 142 (1960).
6. Rose, P.M. and R.C. Kintner, A.J. Ch. E. Jnl. 12, 530 (1966).
7. Reman, G.H., Int. Symp. of Scaling-up, Inst. of Chem. Engrs. (1957), London.
8. Strand, C.P., Olney, R.B. and Ackerman, G.H., A.I.Ch.E. Jnl., 8, 252 (1962).
9. Logsdail, D.H., Thornton, J.D., Pratt, H.R.C., Trans. Inst. Chem. Eng. 35, 301, (1957).
10. Misek, T., Rotacni Diskove Extractory, Statni Nakadelstri Literatury, Prague, (1964).
11. Arnold, D.R., Ph.D. Thesis, University of Aston in Birmingham, (1974).
12. Reman, G.H., Proceeds. 3rd World Pet. Cong. den Haag (1951), Section 3, 121.
13. Misek, T., Chem. Eng. 68, 58 (1961).
14. Marek, J., Misek, T. and Windmer, F., Soc. Chem. Eng., Symp. University of Bradford, U.K., 31st Oct. (1967).

15. Marek, J., Misek, T., Soc. Chem. Eng. Conf. on Solvent Extraction, London, March (1969).
16. Old-shue, J.Y., and Rushton, J.H., Chem. Eng. Prog. 48, 297 (1952).
17. Simonis, H., Process Eng., Nov. 110 (1972).
18. Scheibel, E.G., U.S. Pat., 2,493,265 (1950).
19. Kuhni, A.G., Verfarheus Technik and Apparateban, CH-4123, Aleschwuil-Basel, Schweiz.
20. Treybal, R.E., 'Liquid Extraction', Mc Graw Hill, New York, 2nd Edition, (1963).
21. Thornton, J.D., Trans. Instn. Chem. Engrs. 35, 316 (1957).
22. Coggan, G.C., Instn. Chem. Engrs., 35, 316 (1957).
23. Mumford, C.J., Brit. Chem. Eng., 13, 901 (1968).
24. Todd, D.B., Chem. Engng., 69, 156, (1962).
25. Logsdail, D.H., et al., Chap. 5, 'Recent Advances in Liquid Extraction', Pergamon, London 1971.
26. Kagan, S.Z., Trukhanov, U.G., Kostin, P.A., Kudryanstev, E.W. Int. Chem. Eng. 4, 473 (1964).
27. Reman, G.H., Olney, R.B., Chem. Eng. Prog., 51, 141 (1955).
28. Theyze, U.G., Wall, R.J., Train, K.E., Olney, R.B., Oil Gas Jnl., 59, 70 (1961).
29. Anon. Pet. Processes, 10, 230 (1955).
30. Misek, T. and Rozkos, B., International Chem. Eng. 6, 130 (1966).
31. Reman, G.H., Van der Vusse, J.G., Pet. Refiner 9, 128 (1955).

32. Reman, G.H., *Pet. refiner*, 36, 269 (1957).
33. Reman, G.H., Van der Vusse, J.G., *Genie Chemie*, 74, 106 (1956).
34. Cronan, C.S., *Chem. Eng.*, 65, 54 (1958).
35. Marple, S., Train, K.E., Foster, P.D., *Chem. Eng. Prog.*, 57, 44 (1961).
36. Westerterp, K.R. and Landsman, P., *Chem. Eng. Sci.*, 3, 55 (1954).
37. Al-Hemiri, A.A.A., Ph.D. Thesis, University of Aston in Birmingham (1973).
38. Sarkar, S., Ph.D. Thesis, University of Aston in Birmingham (1976).
39. Rod, U., *Bri. Chem. Eng.*, 16, 617 (1971).
40. Mumford, C.J., Ph.D. Thesis, University of Aston in Birmingham (1970).
41. Davies, J.T., Ritchie, J.M. and Southward, D.C., *Trans. Instn. Chem. Engrs.*, 38, 331 (1960).
42. Reman, G.H., *Chem. Eng. Prog.*, 62, 56 (1966).
43. Kung, K.Y. and Beckmann, R.B., *A.I.Ch.E. Jnl.*, 7, 319 (1961).
44. Reman, G.H., *U.S. Pat.*, 2,601,674.
45. Misek, T., *Coll. Czech. Chem. Comm.* 27, 1767 (1964).
46. Vermijis, H.J.A. and Kramers, H., *Chem. Eng. Sci.* 3, 55 (1954).
47. Gayler, R., Roberts, M.W. and Pratt, H.R.C., *Trans. Instn. Chem. Engrs.* 31, 57 (1953).
48. Thornton, J.D., *Chem. Eng. Sci.*, 5, 201 (1956).
49. Thornton, J.D., and Pratt, H.R.C., *Trans. Instn. Chem. Engrs.*, 31, 289 (1953).

50. Misek, T., Coll. Czech. Chem. Comm. 28, 426, 570, 1631 (1963).
51. Stainthorpe, F.P. and Suddall, M., Trans. Instn. Chem. Engrs., 42, 7 198 (1964).
52. Olney, R.B., A.I.Ch.E. Jnl., 10, 827, (1964).
53. Misek, T., Coll. Czech. Chem. Comm., 29, 2086, (1964).
54. Mumford, C.J. and Jeffreys, G.V., Paper presented to 3rd CHISA Congress, Marianske Lazne, September 1969.
55. Sherwood, T.K., and J.C. Wei, Ind. Eng. Chem., 49, 1030 (1957).
56. Sternling, C.V. and Scriven, L.E., A.I.Ch.E. Jnl., 5, 574 (1959).
57. Cremer, H.W. and Watkins, S.B. (Eds.) Chem. Eng. Practice, Volume 5, Sections 8 and 12, Butterworths, London (1958).
58. Sleicher, C.A., A.I.Ch.E. Jnl., 5, 145 (1959).
59. Johnstone, R.E. and Thring, M.W., 'Pilot Plants, Models, and Scale-up Methods in Chemical Engineering,' Mc Graw-Hill Book Company, Inc. N.Y. (1957).
- + 60. Nagata, S., 'Mixing Principles and Applications', 1st edition, Halsted Press Book, Tokyo (1975).
61. Rosen, A.M. and Krylov, U.S., Chem. Eng. Sci., 22, 407 (1967).
62. Rosen, A.M. and Krylov, U.S., The Chem. Eng. Jnl., 7, 85 (1974).
63. Thornton, J.D. and Bouyatistis, B.A., Ind. Chemist., 42, 1174 (1950).

64. Jeffreys, G.V., and Ellis, E.M.R., CHISA (1962).
65. Hayworth, C.B. and Treybal, R.E., Ind. Eng. Chem.,
42, 1174 (1950).
66. Null, R. and Johnson, H.E., A.I.Ch.E., Jnl., 4,
273 (1958).
67. Scheele, G.F. and Meister, B.J., A.I.Ch.E., 14, 5,
(1968).
68. Harkins, W.D. and Brown, F.E., Am. Chem. Soc. Jnl.,
41, 499 (1919).
69. Ryan, J.T., Thesis Missouri (1966).
70. Rao, E.V.L.N., Kumar, R. and Kuloor, N.R., Chem.
Eng. Sci., 21, 867 (1966).
71. Heertjes, P.M., de Nie, L.H. and de Vries, Chem.
Eng. Sci., 26, 441 and 755 (1971).
72. Dixon, B.E. and Russell, A.A.W., J. Soc. Chem. Ind.,
London, 69, 284 (1950).
73. Nodberg, S., Dechema Monogr, 41, 257 (1962).
74. Angelo, J.B., Lightfoot, E.M. and Howard, D.W.,
A.I.Ch.E. Jnl., 12, 751 (1966).
75. Kolmogoroff, A.N., Doklady Acad. Nank, U.S.S.R.,
30, 301 (1941; 31, 538 (1941).
76. Hinze, J.O., A.I.Ch.E. Jnl., 1, 289 (1955).
77. Rushton, J.H., Rodger, W.A. and Trice, V.G., Chem.
Eng. Prog., 52, 515 (1956).
78. Vermeulen, T., et al, Chem. Eng. Prog., 51, 85 (1955).
79. Skinner, R. and Church, J.M., Ind. Eng. Chem., 52,
253 (1960).

80. Levich, V.G., 'Physico Chemical Hydrodynamics',
Prentice-Hall N.J. (U.S.A.) (1962).
81. Endoh, K., and Oyama, Y., Jnl. Sci. Research
Inst. (Tokyo) 52, 253 (1966).
82. Kafanov, V.V. and Babanov, D.M., Zh. Prikl. Khim.,
32, 789 (1959).
83. Calderbank, P.H., Trans. Instn. Chem. Engrs.,
36, 443 (1958).
84. Sprow, F.B., A.I.Ch.E. Jnl., 13, 995 (1967).
85. Chen, H.T. and Middleman, S., A.I.Ch.E. Jnl.,
989 (1967).
86. Brown, D.E. and Pitt, K., Proc. Chemica, 70,
Butterworth, Australia (1970).
87. Pebalk, V.L. and Mishev, V.M., Teor. Osnovy. Khim.
Tekhnol., 3, 418 (1969).
88. Giles, J.G., Hanson, C. and Marsland, J.H., Proc.
I.S.E.C. 74, The Hague.
89. Mugele, R.A. and Evans, H.D., Ind. Eng. Chem.,
43, 1317 (1951).
90. Sleicher, C.A., A.I. Ch.E. Jnl., 5, 145 (1959).
91. Howarth, W.J., Chem. Eng. Sci., 19, 33 (1964).
92. Madden, A.J. and Damarell, G.C., A.I.Ch.E. Jnl.,
8, 233 (1962).
93. Gillespie, T. and Rideal, E.K., Trans. Faraday
Soc., 52, 1736 (1956).
94. Jeffreys, G.V. and Hawksley, J.L., J. Appl. Chem.
12, 329 (1962).

95. Cockbain, E.G. and Mc Roberts, T.S., *J. Coll. Sci.*, 8, 440 (1953).
96. Hitit, A., Ph.D. Thesis, University of Aston in Birmingham (1972).
97. Jeffreys, G.V. and Lawson, G., *Trans. Instn. Chem. Engrs.*, 43, 294, (1965).
98. Smith, D.V. and Davies, G.A., *Can. Ins. Chem. Eng.*, 48, 628 (1970).
99. Sawistowski, H., Chap. 9. 'Recent Advances in Liquid-Liquid Extraction', edited by Hanson, C., Pergamon Press, Oxford (1971).
100. Sherwood, T.K., et al., *Ind. Eng. Chem.*, 31, 1144 (1939).
101. West, F.P., et al., *Ind. Eng. Chem.*, 43, 234, (1951); 44, 625, (1952).
102. Licht, W. and Pensing, W.F., *Ind. Eng. Chem.*, 45, 1885 (1953).
103. Angelo, J.B., Lightfoot, E.N. and Howard, O.W., *A.I.Ch.E., Jnl.*, 12, 751 (1966).
104. Heertjes, P.M. and Howe, W.A., *Chem. Eng. Sci.*, 3, 122 (1954).
105. Sawistowski, H. and G.B. Goltz, *Trans. Instn. Chem. Engrs.* 41, 174 (1963).
106. Groothuis, H. and Kramers, H., *Chem. Eng. Sci.*, 4, 17 (1955).
107. Coulson, J.H. and Skinner, S.J., *Chem. Eng. Sci.*, 1, 1976 (1951).
108. Heertjes, P.M. and de Nie, L.H., *Chem. Eng. Sci.*, 21, 755 (1966).

109. Ilkovic, D., Colln. Czech. Comm. 6, 498 (1934).
110. Mc Gillavry, D. and Rideal, E.K., Recl. Trav.
Chim. Pays-Bas 56, 1013 (1937).
111. Baird, M.H.I., Chem. Eng. Sci., 9, 267, (1959)
112. Popovich, A.T., Jervis, R.E., and Trass O.,
Chem. Eng. Sci., 19, 357 (1969).
113. Michels, H.H., Thesis, Delaware (1960).
114. Skelland, A.H.P. and S.S. Minhas, A.I.Ch.E. Jnl.
17, 1316 (1971).
115. Russell, A.A.W. and Dixon, B.E., J. Soc. Chem. Ind.,
London, 69, 284 (1950)
116. Kida, H. and Ueyama, K., Kagaku Kikai, 21, 188, (1957).
117. Licht, W., and Conway, J.B., Ind. Engng. Chem.,
47, 1151, (1950).
118. Marsh, B.D. and W.J. Heideger, Ind. Eng. Chem.
Fundamentals, 4, 129, (1965).
119. Hadamand, C.R. and Rybezynski, A., Acad. Sci. Paris,
152, 1735 (1911).
120. Levich, V., Shur. Obstrch. Khim. 19, 18, (1949).
121. Garner, F.H. and Skelland, A.H.P., I.E.C., 48,
51, (1956).
122. Linton, M. and Sutherland, K.I., Proc. 2nd
International Conference of Surface Activity.
123. Newman, A.B., Trans. Am. Inst. Chem. Engrs., 27,
310, (1937).
124. Vermeulen, T., Ind. Eng. Chem. 45, 1664, (1953).
125. Huges, R.R. and Gilliland, E.R., Chem. Eng. Prog.,
48, 497, (1952).

126. Calderbank, P.H. and Korchinski, I.J.B., Chem. Eng. Sci. 6, 65, (1956).
127. Handlos, A.E. and Baron, T., A.I.Ch.E. Jnl., 3, 127, (1957).
128. Skelland, A.H.P., and Wellek, R.H., A.I.Ch.E. Jnl., 10, 491, (1964).
129. Johnson, A.I. and Hamielec, A.E., A.I. Ch.E. Jnl., 6, 145, (1960).
130. Olander, O.R., A.I.Ch.E. Jnl., 12, 1018, (1966).
131. Elzinga, E.R. and Banchemo, J.T., A.I.Ch.E. Jnl. 7, 394, (1961).
132. Garner, F.H. and Tayeban, M., Anal. Renl. Soc. Estan. Fis. Quinn (Madrid, 1356, 479, (1960).
133. Garner, F.H. and Haycock, P.J., Pro. Roy. Soc., A252, 457, (1959).
134. Garner, F.H. and Skelland, A.H.P., Chem. Eng. Sci., 14, 149, (1955).
135. Conkie, W.R. and Savik, P., M.R.C. (Canada) Report M.7, 23, (1953).
136. Ruckenstein, E., Chem. Eng. Sci., 10, 22, (1959).
137. Garner, F.H., Hale, A.R., Chem. Eng. Sci., 2, 157, (1953)
138. Garner, F.H. and Suckling, R.D., A.I.Ch.E. Jnl. 4, 114, (1958).
139. Garner, F.H., Jenson, V.C., Keey, R., T.I.C.E., 37, 197, (1957).
140. Boussinesqu, J.J., Math. Puresappl. 60, 285, (1965).

141. Harriott, P., *Can. J. Chem. Engng.* 40, 60 (1962).
142. Kinard, G.E., Manning, F.S. and Manning, W.P., *British Chem. Eng.*, 8, 326, (1963).
143. White, R.R., and Churchill, S.W., *A.I.Ch.E. Jnl.*, 5, 354, (1959).
144. Cavers, et al., Paper presented to I.S.E.C., 74 S.C.I., Lyon, (1974).
145. Heertjes, P.M. and de Nie, L.H., 'Mass Transfer to Drops' Hanson, C. (ed.), 'Recent Advances in Liquid-Liquid Extraction', Pergamon (1971).
146. Thorsen, G., et al., *Chem. Eng. Sci.*, 23, 413, (1968).
147. Garner, F.H., Foord, A., Tayeban, M., *Jnl. App. Chem.* 9, 315, (1959).
148. Ruby, C.L., and Elgin, J.C., *Chem. Engng. Prog. Symp. Ser.*, 51(16), 17, (1955).
149. Heertjes, P.M., Howe, W.A., and Talsma, H., *Chem. Engng. Sci.*, 3, 122, (1954).
150. Gal-or, B., and Hoelscher, H.E., *A.I.Ch.E. Jnl.*, 12, 499, (1966).
151. Hughmark, G.A., *Ind. Engng. Chem. Funds.*, 6, 408, (1967).
152. Linton, M. and Sutherland, K.L., *Chem. Eng. Sci.*, 12, 214, (1960).
153. Rowe, P.N. et al., *Trans. Inst. Chem. Engrs.*, 43, 14, (1965).
154. Heertjes, P.M. and de Nie, L.H., *Chem. Eng. Sci.*, 26, 697, (1971).
155. Crank, V., 'Mathematics of Diffusion', Oxford University Press, London (1956).

156. Davies, J.T. and Rideal, E.K., 'Interfacial Phenomena', Academic Press, New York, 1961.
157. Orell, A., and Westwater, J.W., A.I.Ch.E. Jnl., 8, 350, (1962).
158. James, B.R., Ph.D. Thesis, University of London, (1963).
159. Sawistowski, H., and Goltz, G.E., Trans. Instn. Chem. Engrs., 41, 174, (1963).
160. Sawistowski, H. and James, B.R., Chemie-Ingr-Tech., 35, 175, (1963).
161. Sawistowski, H. and James, B.R., Proc. IIIrd International Conf. on Surface Active Materials, Akademie Verlag, Berlin, 1967.
162. Austin, L.J., Ph.D. Thesis, University of London, 1966.
163. Maroudas, H.G., and Sawistowski, H., Chem. Eng. Sci., 19, 919, (1964).
164. Marsh, B.D., Sleicher, C.A. and Heideger, W.J., Paper presented at 57th Annual Meeting of the American Inst. of Chem. Engrs., Philadelphia, (1965).
165. Quinn, J.A. and Sigloh, D.B., Can. J. Chem. Eng., 41, 15 (1963).
166. Ladenburg, R., Ann. Physik (4) 23, 447, (1907).
167. Happel, J., and Byrne, B.J., Ind. Eng. Chem., 46, 1181, (1954).
168. Haberman, W.L., and Sayre, R.M., David Taylor Model Basin, (Navy Dept., Washington, D.C.), Rept. No. 1143 (1958).
169. Strom, J.R., and Kintner, R.C., A.I.Ch.E. Jnl., 5, 514, (1959).

170. Edge, R.M., and Grant, C.D., Chem. Eng. Sci., 27, 1709, (1972).
171. Skelland, A.H.P. and Caenepeel, C.L., A.I.Ch.E. Jnl., 18, 1154, (1972).
172. Olney, R.B. and Miller, R.S., 'Modern Chemical Engineering', Vol. 1, p.108, Ed. Acrivos, A., Rheinhold, (1963).
173. Taylor, G.I., Proc. Roy. Soc. (London), A219, 186, (1953).
174. Misek, T., and Rod, V., Chapter 7 in 'Recent Advances in Liquid-Liquid Extraction', Hanson, C. (Ed.), Pergamon (1971)
175. Young, E.F., Chem. Eng., 64, 241, (1957).
176. Miyauchi, T., and Vermeulen, T., Ind. Engng. Chem. Funds., 2, 113, (1963).
177. Hartland, S., and J.C. Mechlenburgh, Chem. Eng. Science, 21, 1209, (1966).
178. Rod, V., Bri. Chem. Eng., 9, 300, (1964).
179. Danckwerts, P.V., Chem. Eng., 2, 1, (1953).
180. Eguchi, W., and Nagata, S., Chem. Engng., Tokyo, 22, 218, (1958).
181. Eguchi, W., and Nagata, S., Mem. Fac. Eng., Kyoto Univ., 21, 70, (1959).
182. Schleicher, C.A., A.I.Ch.E., Jnl.6, 529, (1960).
183. Miyauchi, T. and Vermeulen, T., Ind. Eng. Chem. Fund., 2, 304, (1957).
184. Misek, T., and Rod, V., Paper presented on CHISA, II Congress, Marienbad, Czechoslovakia, (1965).

185. Rod, V., *Por. Chem. Engng.*, 11, 483, (1966).
186. Prochazka, J. and Landau, J., *Coll. Czech. Chem. Chommun.*, 28, 1927, (1963).
187. Aris, R., *Chem. Eng. Sci.*, 9, 266, (1959).
188. Bischoff, K.G., *Chem. Eng. Sci.*, 12, 69, (1960).
189. Bischoff, K.B., and Levenspiel, O., *Chem. Eng. Sci.*, 17, 245, 257, (1962).
190. Miyauchi, T., Mitsutabe, H. and Harase, I., *A.I.Ch.E., Jnl.*, 12, 508, (1966).
191. Sinhrada, F., Prochazka, J. and Landau, J., *Coll. Czech. Chem. Comm.* 31, 1695, (1966).
192. Ingham, J., Chap. 8, 'Recent Advances in Liquid-Liquid Extraction', Pergamon (1971).
193. Westerterp, K.R., and Landsman, P., *Chem. Eng. Sci.*, 17, 363, (1962).
194. Nagata, S., Eguchi, W., Kasai, H., and Mosino, J., *Chem. Engng., Tokyo*, 21, 784, (1957).
195. Westerterp, K.R. and Meyberg, W.H., *Chem. Engng., Sci.*, 17, 373, (1962).
196. Stemerding, S., Lumb, E.C. and Lips., J., *Chemie- Ingr-Tech.*, 35, 844, (1963).
197. Sudall, M., Ph.D. Thesis, University of Manchester, U.K., (1962).
198. Stainthorp, F.P., and Sudall, N., *Trans. Inst. Chem. Engrs.*, 42, T198, (1964).
199. Misek, T., Paper presented at CHISA II Congress, Marienbad, Czechoslovakia, (1965).
200. Rushton, J.H., et al., *Chem. Eng. Prog.*, 46, 467 (1950).

201. Adamson, A.W., 'Physical Chemistry of Surfaces', Interscience Publishers, Inc., (1960).
202. Osipou, L.I., 'Surface Chemistry', Rheinhold Publishing Corp., (1962).
203. Garner, F.H., Ellis, S.R.M., and Hill, J.W., A.I.Ch.E. Jnl., 1, 185, (1955) and Trans. Instn. Chem. Engrs., 34, 223, (1956).
204. Sobolic, R.H. and Himmelblan, D.M., A.I.Ch.E. Jnl., 6, 619, (1960).
205. Treybal, R.E., Ind. Eng. Chem., 51, 262, (1960).
206. Coggan, G.C., Instn. of Chem. Engrs. Symp., on Liquid-Liquid Extraction, April (1967).
207. Sege, G., and Woodfield, F.M., Chem. Eng. Progr. 50, 396, (1954).
208. Haynes, L.G., Himmelblau, D.M., and Schechter, R.S., I and E.C. Process Design and Development, 7, 508 (1968).
209. Misek, T., Coll. Czech. Chem. Comm., 28, 163 (1963).
210. Luhnig, R.W. and Sawistowski, Paper presented at I.S.E.C., The Hague (1971).
211. Quinn, J.A. and Sigloh, D.B., Can. J. Chem. Eng., 298, Dec. (1963).
212. Maskati, A., M.Sc. Thesis, University of Aston(1977)
213. Reman, G.H. and Olney, R.B., Chem. Eng. Prog. 51, 141, (1955).

214. Sitaramayya, T. and Laddha, G.S., The Madras University Journal, 29, 187, (1959).
215. King, P.J. and Rhodes, P., Manufacturing Chem., June, 51, (1964).
216. Jeffreys, G.V. and Jenson, V.G., Mathematical Methods in Chemical Engineering, Academic Press (1962).
217. Salem, A.B.S.H., Ph.D. Thesis, University of Aston in Birmingham (1974).
218. Clay, P.H., Proc. Roy. Acad. Sci. (Amsterdam), 43, 852, 979, (1940).
218. Sleicher, C.A., A.I.Ch.E. Jnl., 8, 471, (1962).
220. Thornton, J.B., and Bonyatitos, B.A., Ind. Chemist., 39, 298, (1963).
221. Jeffreys, G.V. and Davies, G.A., Chapter 14, 'Advances in Liquid-Liquid Extraction', Edited by Hanson, C., Pergamon Press, Oxford, (1971).
222. Shalhoub, N.G., Ph.D. Thesis, University of Aston in Birmingham, (1975).